

# **Method Development in Automated Mineralogy**

Von der Fakultät für Geowissenschaften, Geotechnik und Bergbau  
der Technischen Universität Bergakademie Freiberg

genehmigte

## **DISSERTATION**

zur Erlangung des akademischen Grades

doctor rerum naturalium

Dr. rer. nat.

vorgelegt

von Diplom-Geologe Dirk Sandmann

geboren am 06.11.1973 in Finsterwalde/Niederlausitz

Gutachter: Prof. Dr. (PhD ZA) Jens Gutzmer (Freiberg)

Univ. Prof. Dr. Johann G. Raith (Leoben, Österreich)

Tag der Verleihung: 30.10.2015

„Der Grundgedanke der vorgeschlagenen Anordnung besteht darin, daß eine durch mehrere elektronenoptische Verkleinerungsstufen hergestellte Elektronensonde äußerster Feinheit, deren Spitze mit der abzubildenden Ebene des Objektes zusammenfällt, über das Objekt geführt wird. Je nach der Struktur des Objektes an der Auftreffstelle der Elektronensonde wird die Elektronenenergie oder ihre räumliche Verteilung mehr oder weniger beeinflußt. Wird diese Modulation zur Steuerung der Helligkeit oder Schwärzung eines Schreibfleckes benutzt, der seinerseits synchron zur Sondenbewegung auf dem Objekt eine Schreibfläche abrastert, so gelingt es, die Feinstruktur der abgetasteten Objektbereiche sichtbar zu machen. Da zur bildmäßigen Wiedergabe Sonde und Schreibfleck, wie bei einem Fernsehraster, in untereinanderliegenden Zeilen über Objekt und Bildfläche geführt werden, wurde dem neuen Instrument der Name „Elektronen-Rastermikroskop“ gegeben.“  
(aus v. Ardenne, M. (1938): *Das Elektronen-Rastermikroskop. Praktische Ausführung. Zeitschrift für technische Physik*, 19(11): 407-416.)

Manfred von Ardenne (1907-1997), German research and applied physicist and inventor

Inventor of the ‚Elektronen-Rastermikroskop‘ (the first high-resolution scanning electron microscope), German patent number 765083 (von Ardenne 1937)

---

## Abstract

The underlying research that resulted in this doctoral dissertation was performed at the Division of Economic Geology and Petrology of the Department of Mineralogy, TU Bergakademie Freiberg between 2011 and 2014. It was the primary aim of this thesis to develop and test novel applications for the technology of ‘Automated Mineralogy’ in the field of economic geology and geometallurgy. A “Mineral Liberation Analyser” (MLA) instrument of FEI Company was used to conduct most analytical studies. This automated system is an image analysis system based on scanning electron microscopy (SEM) image acquisition and energy dispersive X-ray spectrometry which can be used to determine both quantitative mineralogical data and mineral processing-relevant parameters. The analyses can be conducted with unconsolidated and solid rocks but also with ores and products of the mineral processing and recycling industry.

In consequence of a first-time broadly-based and comprehensive literature review of more than 1,700 publications related to all types of automated SEM-based image analysis systems several trends in the publication chronicle were observed. Publications related to mineral processing lead the field of automated mineralogy-related publications. However, this is with a somewhat smaller proportion than expected and with a significant decrease in share between around 2000 and 2014. The latter is caused by a gradual but continuous introduction of new areas of application for automated mineralogical analysis such as the petroleum industry, petrology or environmental sciences. Furthermore, the quantity of automated mineralogy systems over time was carefully assessed. It is shown that the market developed from many individual developments in the 1970s and 1980s, often conducted from research institutes, e.g., CSIRO and JKMRRC, or universities, to a duopoly - Intellection Pty Ltd and JKTech MLA - in the 1990s and 2000s and finally to a monopoly by FEI Company since 2009. However, the number of FEI’s competitors, such as Zeiss, TESCAN, Oxford Instruments, and Robertson CGG, and their competing systems are increasing since 2011.

Particular focus of this study, published in three research articles in peer-reviewed international journals, was the development of suitable methodological approaches to deploy MLA to new materials and in new contexts. Data generated are then compared with data obtained by established analytical techniques to enable critical assessment and validation of the methods developed. These include both quantitative mineralogical analysis as well as methods of particle characterisation.

The first scientific paper “Use of Mineral Liberation Analysis (MLA) in the Characterization of Lithium-Bearing Micaceous Minerals” deals with the field of mineral processing and describes the characterisation of lithium-bearing zinnwaldite mica - as potential natural resource for lithium - by MLA as well as the achievement of mineralogical association data for zinnwaldite and associated minerals. Two different approaches were studied to comminute the samples for this work, conventional comminution by crusher as well as high-voltage pulse selective fragmentation. By this study it is shown that the MLA can provide mineral data of high quality from silicate mineral resources and results very comparable to established analytical methods. Furthermore, MLA yields additional relevant information - such as particle and grain sizes as well as liberation and grade-

recovery data. This combination of quantitative data cannot be attained with any other single analytical method.

The second article “Characterisation of graphite by automated mineral liberation analysis” is also located in the field of mineral processing. This research article is the first published contribution on the characterisation of graphite, an important industrial mineral, by MLA respectively an automated mineralogy-related analytical method. During this study graphite feeds and concentrates were analysed. By this study it is shown that it is possible to gather statistically relevant data of graphite samples by MLA. Furthermore, the MLA results are validated by quantitative X-ray powder diffraction as well as particle size determinations by laser diffraction and sieve analysis.

The third research paper “Nature and distribution of PGE mineralisation in gabbroic rocks of the Lusatian Block, Saxony, Germany” deals with the scientific field of geoscience. In this study it is shown that it is possible to obtain a significant body of novel mineralogical information by applying MLA analysis in a region previously regarded as being well-studied. The complex nature and relatively large distribution of the occurring platinum group minerals (PGM) is well illustrated by this contribution. During previous light microscopic studies and infrequent electron microprobe measurements only a handful isolated PGM grains were identified and characterised. In this investigation, using the samples of previous studies, 7 groups of PGM and 6 groups of associated tellurides as well as in total more than 1,300 mineral grains of both mineral groups were identified. Based on the data obtained, important insight regarding mineral associations, mineral paragenesis and the potential genesis of the PGM is obtained. Within this context, the value of MLA studies for petrological research focused on trace minerals is documented. MLA yields results that are both comprehensive and unbiased, thus permitting novel insight into the distribution and characteristics of trace minerals. This, in turn, is immensely useful when developing new concepts on the genesis of trace minerals, but may also give rise to the development of a novel generation of exploration tools, i.e., mineralogical vectors towards exploration akin to currently used geochemical vectors.

The present dissertation shows that automated mineralogy by using a Mineral Liberation Analyser is able to deliver a unique combination of quantitative data on mineralogy and several physical attributes that are relevant for ore geology and mineral processing alike. It is in particular the automation and unbiasedness of data, as well as the availability of textural data, size and shape information for particles and mineral grains, as well as mineral association and mineral liberation data that define major advantages of MLA analyses - compared to other analytical methods. Despite the fact that results are obtained only on 2-D polished surfaces, quantitative results obtained compare well/very well to results obtained by other analytical methods. This is attributed mainly due to the fact that a very large and statistically sound number of mineral grains/particles are analysed. Similar advantages are documented when using the MLA as an efficient tool to search for and characterise trace minerals of petrological or economic significance.

## Zusammenfassung

Die Forschung die der vorliegenden kumulativen Dissertation („Publikationsdissertation“) zugrunde liegt wurde im Zeitraum 2011-2014 am Lehrstuhl für Lagerstättenlehre und Petrologie des Institutes für Mineralogie der TU Bergakademie Freiberg durchgeführt. Das primäre Ziel dieser Arbeit war es neue Einsatzmöglichkeiten für die Technik der Automatisierten Mineralogie im Gebiet der Lagerstättenkunde und Geometallurgie zu entwickeln und zu testen. Im Mittelpunkt der wissenschaftlichen Studien stand die analytische Nutzung des Großgerätes „Mineral Liberation Analyser“ (MLA) der Firma FEI Company. Dieses automatisierte System ist ein Bildanalysesystem und basiert auf der Erfassung von Rasterelektronenmikroskopiebildern und energiedispersiver Röntgenspektroskopie. Mit Hilfe der MLA-Analysetechnik lassen sich sowohl statistisch gesichert quantitative mineralogisch relevante als auch Aufbereitungsprozess-relevante Parameter ermitteln. Die Analysen können sowohl an Locker- und Festgesteinen als auch an Erzen und Produkten der Aufbereitungs- und Recyclingindustrie durchgeführt werden.

Infolge einer erstmaligen, breit angelegten und umfassenden Literaturrecherche von mehr als 1.700 Publikationen im Zusammenhang mit allen Arten von automatisierten REM-basierten Bildanalysesystemen konnten verschiedene Trends in der Publikationshistorie beobachtet werden. Publikationen mit Bezug auf die Aufbereitung mineralischer Rohstoffe führen das Gebiet der Automatisierte Mineralogie-bezogenen Publikationen an. Der Anteil der Aufbereitungs-bezogenen Publikationen an der Gesamtheit der relevanten Publikationen ist jedoch geringer als erwartet und zeigt eine signifikante Abnahme des prozentualen Anteils zwischen den Jahren 2000 und 2014. Letzteres wird durch eine kontinuierliche Einführung neuer Anwendungsbereiche für die automatisierte mineralogische Analyse, wie zum Beispiel in der Öl- und Gasindustrie, der Petrologie sowie den Umweltwissenschaften verursacht. Weiterhin wurde die Anzahl der Systeme der Automatisierten Mineralogie über die Zeit sorgfältig bewertet. Es wird gezeigt, dass sich der Markt von vielen einzelnen Entwicklungen in den 1970er und 1980er Jahren, die oft von Forschungsinstituten, wie z. B. CSIRO und JKMRRC, oder Universitäten ausgeführt wurden, zu einem Duopol - Intellection Pty Ltd und JKTech MLA - in den 1990er und 2000er Jahren und schließlich seit 2009 zu einem Monopol der FEI Company entwickelte. Allerdings steigt die Anzahl der FEI-Konkurrenten, wie Zeiss, TESCAN, Oxford Instruments und Robertson CGG, und deren Konkurrenzsysteme seit 2011.

Ein Schwerpunkt der drei von Experten begutachteten und in internationalen Fachzeitschriften publizierten Artikel dieser Studie war die Entwicklung eines geeigneten methodischen Ansatzes um die MLA-Technik für neue Materialien und in neuem Kontext zu verwenden. Die erzeugten Daten wurden mit Daten die von etablierten analytischen Techniken gewonnen wurden verglichen, um eine kritische Bewertung und Validierung der entwickelten Methoden zu ermöglichen. Dazu gehören sowohl quantitative mineralogische Analysen als auch Methoden der Partikelcharakterisierung.

Der Schwerpunkt der Studie zum ersten Fachartikel „Use of Mineral Liberation Analysis (MLA) in the Characterization of Lithium-Bearing Micas“ liegt im Gebiet der Aufbereitung mineralischer Rohstoffe. Er beschreibt die Charakterisierung von Zinnwaldit-Glimmer - einem potentiellen Lithium-Rohstoff - durch die MLA-Technik

sowie das Erringen von Mineralverwachungsdaten für Zinnwaldit und assoziierter Minerale. Dabei wurden zwei unterschiedliche Wege der Probenzerkleinerung des Rohstoffes untersucht. Zum einen erfolgte eine konventionelle Zerkleinerung der Proben mittels Brecher und Mühle, zum anderen eine selektive Zerkleinerung durch Hochspannungsimpulse. Es konnte aufgezeigt werden, dass die automatisierte Rasterelektronenmikroskopie-basierte Bildanalyse mittels MLA von silikatischen Rohstoffen Mineralinformationen von hoher Güte zur Verfügung stellen kann und die Ergebnisse gut vergleichbar mit etablierten analytischen Methoden sind. Zusätzlich liefert die MLA weitere wertvolle Informationen wie zum Beispiel Partikel-/Mineralkorngrößen, Aussagen zum Mineralfreisetzungsgrad sowie Gehalt-Ausbring-Kurven des Wertstoffes. Diese Kombination von quantitativen Daten kann mit keiner anderen analytischen Einzelmethode erreicht werden.

Der zweite Fachartikel „Characterisation of graphite by automated mineral liberation analysis“ ist ebenfalls im Fachgebiet der Aufbereitung mineralischer Rohstoffe angesiedelt. Während dieser Studie wurden Edukte und Produkte der Aufbereitung von Graphit-Erzen untersucht. Der vorliegende Artikel ist der erste in einer internationalen Fachzeitschrift publizierte Beitrag zur Charakterisierung des Industrieminerals Graphit mittels MLA-Technik bzw. einer Analysenmethode der Automatisierten Mineralogie. Mit der Studie konnte gezeigt werden, dass es möglich ist, auch mit der MLA statistisch relevante Daten von Graphitproben zu erfassen. Darüber hinaus wurden die Ergebnisse der MLA-Analysen durch quantitative Röntgenpulverdiffraktometrie sowie Partikelgrößenbestimmungen durch Laserbeugung und Siebanalyse validiert.

Der dritte Fachartikel „Nature and distribution of PGE mineralisation in gabbroic rocks of the Lusatian Block, Saxony, Germany“ ist im Gegensatz zu den ersten beiden Artikeln im Gebiet der Geowissenschaften angesiedelt. In dieser Studie wird gezeigt, dass es möglich ist mittels MLA-Analyse eine signifikante Anzahl neuer Daten von einem eigentlich schon gut untersuchten Arbeitsgebiet zu gewinnen. So konnte erst mit der MLA die komplexe Natur und relativ große Verbreitung der auftretenden Platingruppenelement-führenden Minerale (PGM) geklärt werden. Während früherer lichtmikroskopischer Analysen und einzelner Elektronenstrahlmikrosonden-Messungen konnten nur eine Handvoll weniger, isolierter PGM-Körner nachgewiesen und halbquantitativ charakterisiert werden. In der vorliegenden Studie konnten nun, an den von früheren Studien übernommenen Proben, 7 PGM-Gruppen und 6 assoziierte Telluridmineral-Gruppen mit insgesamt mehr als 1.300 Mineralkörnern beider Mineralgruppen nachgewiesen werden. Auf der Grundlage der gewonnenen Daten wurden wichtige Erkenntnisse in Bezug auf Mineralassoziationen, Mineralparagenese und zur möglichen Genese der PGM erreicht. In diesem Zusammenhang wurde der Wert der MLA-Studien für petrologische Forschung mit dem Fokus auf Spurenminerale dokumentiert. Die MLA liefert Ergebnisse, die sowohl umfassend und unvoreingenommen sind, wodurch neue Einblicke in die Verteilung und Charakteristika der Spurenminerale erlaubt werden. Dies wiederum ist ungemein nützlich für die Entwicklung neuer Konzepte zur Genese von Spurenmineralen, kann aber auch zur Entwicklung einer neuen Generation von Explorationswerkzeugen führen, wie zum Beispiel mineralogische Vektoren zur Rohstofferkundung ähnlich wie derzeit verwendete geochemische Vektoren.

Mit der vorliegenden Dissertationsschrift wird aufgezeigt, dass Automatisierte Mineralogie mittels Mineral Liberation Analyser eine einzigartige Kombination an quantitativen Daten zur Mineralogie und verschiedene physikalische Attribute, relevant sowohl für die Lagerstättenforschung als auch für die Aufbereitung mineralischer Rohstoffe, liefern kann. Im Vergleich zu anderen etablierten analytischen Methoden sind es insbesondere die Automatisierung und Unvoreingenommenheit der Daten sowie die Verfügbarkeit von Gefügedaten, Größen- und Forminformationen für Partikel und Mineralkörner, Daten zu Mineralassoziationen und Mineralfreisetzen welche die großen Vorteile der MLA-Analysen definieren. Trotz der Tatsache, dass die Ergebnisse nur von polierten 2-D Oberflächen erhalten werden, lassen sich die quantitativen Ergebnisse gut/sehr gut mit Ergebnissen anderer Analysemethoden vergleichen. Dies kann vor allem der Tatsache zugeschrieben werden, dass eine sehr große und statistisch solide Anzahl von Mineralkörnern/Partikeln analysiert wird. Ähnliche Vorteile sind bei der Verwendung der MLA als effizientes Werkzeug für die Suche und Charakterisierung von Spurenmineralen von petrologischer oder wirtschaftlicher Bedeutung dokumentiert.

## Versicherung

Hiermit versichere ich, dass ich die vorliegende Arbeit ohne unzulässige Hilfe Dritter und ohne Benutzung anderer als der angegebenen Hilfsmittel angefertigt habe. Die aus fremden Quellen direkt oder indirekt übernommenen Gedanken sind als solche kenntlich gemacht. Bei der Auswahl und Auswertung des Probenmaterials der Studien zu dieser Arbeit sowie bei der Erarbeitung der Manuskripte zu den in Fachzeitschriften veröffentlichten Artikeln dieser kumulativen Arbeit habe ich Unterstützungsleistungen von folgenden Personen erhalten:

Jens Gutzmer (Betreuer, Koautor Paper 1-3),

Sabine Haser (Koautorin Paper 2).

Weitere Personen waren an der geistigen Herstellung der vorliegenden Arbeit nicht beteiligt. Die Hilfe eines Promotionsberaters habe ich nicht in Anspruch genommen. Weitere Personen haben von mir keine geldwerten Leistungen für Arbeiten erhalten, die nicht als solche kenntlich gemacht worden sind.

Die Arbeit wurde bisher weder im Inland noch im Ausland in gleicher oder ähnlicher Form einer anderen Prüfungsbehörde vorgelegt.

Freiberg, den 23.06.2015



## Acknowledgements

In addition to everyone gratefully acknowledged in the research articles of this doctoral dissertation, I would like to express my deep gratitude to the two supervisors of my dissertation, Professor Jens Gutzmer and Professor Bernhard Schulz, for precise guidance and advice, active support, constructive criticism, and valuable suggestions. All colleagues of the Division of Economic Geology and Petrology of the TU Bergakademie Freiberg and the Resource Analytics Group of the Helmholtz Institute Freiberg for Resource Technology are thanked for their support and fruitful discussions. They are too many to list them individually. I acknowledge Paul Gottlieb (former Principal Technologist at FEI Company, Natural Resources Business Unit) for helpful information regarding the history and development of automated mineralogy. I am deeply grateful to FEI Company for a three-year PhD bursary as well as the twelve-month internship at FEI's Natural Resources Business Unit in Brisbane, Australia. Last but not least I am most grateful to my family for their never-ending support.

## Preface

This doctoral dissertation, supervised by Prof. Dr. (PhD ZA) Jens Gutzmer and Prof. Dr. Bernhard Schulz, is a dissertation by publication and includes a comprehensive introduction, three peer-reviewed articles submitted to international journals and a summary and conclusions section. All three of the research articles were published between 2013 and 2015. Prof. Jens Gutzmer conceived the three research projects. My contribution was the data collection, processing and analysis of the data, and the writing of the manuscripts. Prof. Jens Gutzmer contributed largely to the discussion of the interpretation of the results, and comprehensively revised the manuscript drafts.

The research articles are presented in the following chapters:

Chapter 3: Sandmann, D., Gutzmer, J. (2013). Use of Mineral Liberation Analysis (MLA) in the Characterisation of Lithium-Bearing Micas. *Journal of Minerals and Materials Characterization and Engineering*, 1 (6): 285-292.

The samples for this study were provided by Prof. Jens Gutzmer and colleagues of the Department of Mineralogy, TU Bergakademie Freiberg. Thomas Zschoge (Department of Mechanical Process Engineering and Mineral Processing, TU Bergakademie Freiberg) performed the conventional sample comminution. Peter Segler (Department of Geology, TU Bergakademie Freiberg) provided guidance during the Selfrag high voltage pulse power fragmentation that I carried out. Samples for MLA analysis were prepared by Sabine Haser and Prof. Bernhard Schulz (Department of Mineralogy, TU Bergakademie Freiberg). Dr. Thomas Mütze and Dr. Thomas Leistner (Department of Mechanical Process Engineering and Mineral Processing, TU Bergakademie Freiberg) supported the study by discussions and suggestions. One figure for the article was provided by Petya Atanasova (Helmholtz Institute Freiberg for Resource Technology). The research was supported by the Nordic Researcher Network on Process Mineralogy and Geometallurgy (ProMinNET) and the study was carried as part of a BMBF-funded research project (Hybride Lithiumgewinnung, Project No. 030203009). The open access article was published in the *Journal of Minerals and Materials Characterization and Engineering* (received 17 September 2013; revised 20 October 2013; accepted 2 November 2013).

Chapter 4: Sandmann, D., Haser, S., Gutzmer, J. (2014). Characterisation of graphite by automated mineral liberation analysis. *Mineral Processing and Extractive Metallurgy (Trans. Inst. Min. Metall. C)*, 123 (3): 184-189.

All samples for the study were provided by the AMG Mining AG (formerly Graphit Kropfmühl AG) Hauzenberg. Prof. Jens Gutzmer advised in the sample preparation procedure. The initial sample preparation and experimental work was shared with Sabine Haser. In addition, services were received from AMG Mining AG (Loss-on-ignition (LOI) analytical method and dry sieve classification), Dr. Robert Möckel from the Helmholtz Institute Freiberg for Resource Technology (quantitative XRD analysis) as well as Dr. Martin Rudolph (Helmholtz Institute Freiberg for Resource Technology) and Annet Kästner (Department of Mechanical Process Engineering and Mineral Processing, TU

---

Bergakademie Freiberg) (laser diffraction analysis). Prof. Bernhard Schulz (Department of Mineralogy, TU Bergakademie Freiberg) as well as researchers of the Nordic Researcher Network on Process Mineralogy and Geometallurgy (ProMinNET) supported the study by discussions about data analysis and interpretation. The article was published in *Mineral Processing and Extractive Metallurgy (Trans. Inst. Min. Metall. C)* (received 26 November 2013; accepted 12 June 2014).

Chapter 5: Sandmann, D., Gutzmer, J. (2015). Nature and distribution of PGE mineralisation in gabbroic rocks of the Lusatian Block, Saxony, Germany. *Zeitschrift der Deutschen Gesellschaft für Geowissenschaften (German J. Geol.)*, 166 (1): 35-53.

The polished thin sections and four round blocks for this study were provided by Dr. Andreas Kindermann (Treibacher Schleifmittel Zschornowitz GmbH). All other round blocks, part of a student education collection, were provided by Prof. Thomas Seifert (Department of Mineralogy, TU Bergakademie Freiberg). No additional services were received. The article was published in *Zeitschrift der Deutschen Gesellschaft für Geowissenschaften (German J. Geol.)* (received 30 March 2014; accepted 6 October 2014).

## Contents

Abstract .....	III
Zusammenfassung .....	V
Versicherung.....	VIII
Acknowledgements .....	IX
Preface .....	X
Contents .....	XII
List of Figures.....	XIV
List of Tables.....	XIX
List of Abbreviations .....	XXI
Chapter 1: Introduction.....	1
1.1 Motivation and Approach .....	29
Chapter 2: Methodology.....	30
2.1 Functional Principle of the FEI Mineral Liberation Analyser .....	30
2.1.1 Hardware and Instrument Conditions.....	30
2.1.2 EDS Spectrometer, BSE Image and Probe Current Calibration.....	35
2.1.3 MLA Measurement – Comprehensive Description.....	38
2.1.4 MLA Measurement Modes.....	42
2.2 Sampling and Sample Preparation .....	49
2.3 Reproducibility of Measurements and Possible Sources of Error .....	54
2.4 Method Development.....	67
Published Papers.....	71
Chapter 3: Use of Mineral Liberation Analysis (MLA) in the Characterisation of Lithium-Bearing Micaceous Minerals (Sandmann and Gutzmer, 2013) .....	72
3.1 Abstract .....	72
3.2 Introduction.....	72
3.2.1 Synopsis of the Zinnwald Deposit.....	73
3.3 Methods.....	74
3.3.1 Conventional Comminution Procedure .....	74
3.3.2 High Voltage Pulse Power Technology.....	74
3.3.3 Mineralogical and Microfabric Analysis.....	75
3.4 Results and Discussion .....	75
3.4.1 Particle Size Distribution/Mineral Grain Size Distribution.....	75
3.4.2 Modal Mineralogy .....	76
3.4.3 Mineral Locking and Mineral Association.....	77
3.4.4 Mineral Liberation.....	79
3.4.5 Theoretical Grade Recovery .....	79
3.5 Conclusions.....	80
3.6 Acknowledgements.....	81
Chapter 4: Characterisation of graphite by automated mineral liberation analysis (Sandmann <i>et al.</i> , 2014).....	82
4.1 Abstract .....	82
4.2 Introduction.....	82
4.3 Sample preparation and analytical methods.....	83
4.4 Results and discussion .....	85
4.5 Conclusions.....	90
4.6 Acknowledgements.....	90

---

Chapter 5: Nature and distribution of PGE mineralisation in gabbroic rocks of the Lusatian Block, Saxony, Germany (Sandmann and Gutzmer, 2015).....	93
5.1 Abstract .....	93
5.2 Kurzfassung .....	93
5.3 Introduction.....	94
5.3.1 Geological setting.....	95
5.4 Approach and analytical methods.....	98
5.5 Results.....	99
5.5.1 Modal mineralogy .....	99
5.5.2 Base metal sulphide mineralogy.....	101
5.5.3 PGE mineralogy .....	102
5.5.4 PGM mineralisation and base metal sulphide mineralogy .....	104
5.5.5 PGM mineralisation and alteration.....	107
5.5.6 Mineral grain sizes.....	109
5.5.7 Mineral association.....	109
5.5.8 Palladium and platinum elemental deportment .....	113
5.5.9 Calculated bulk-rock PGE content .....	114
5.6 Discussion .....	115
5.6.1 Comparison of calculated PGE content with assay data .....	117
5.7 Conclusions.....	118
5.8 Acknowledgments.....	118
Chapter 6: Summary and Conclusions .....	119
Bibliography .....	126

## List of Figures

<b>Fig. 1:</b> Consolidated time series of the most important ‘Automated Mineralogy’ systems of Table 1 (1 - Geoscan-Minic, 2 - CESEMI, 3 - QEMSCAN, 4 - CCSEM, 5 - MP-SEM-IPS, 6 - ASPEX, 7 - MLA, 8 - RoqSCAN, 9 - INCAMineral, 10 - TIMA, 11 - Mineralogic Mining/Mineralogic Reservoir).....	3
<b>Fig. 2:</b> Condensed time line of the development of the QEMSCAN and MLA technology and overview of their proprietaries (dark blue – CSIRO, light blue – Intellection, dark green – JKMRC, light green – JKTech, FEI Company – purple). Note: Scale of time line is non-linear. ....	6
<b>Fig. 3:</b> Time series (1982-2014) of the total number of commercial automated mineralogy systems worldwide. Note: Numbers for 1982-2008 consists of MLA and QEMSCAN systems (now both FEI Company). The column for 2014 includes about 250 FEI systems and estimated 35 systems of FEIs competitors. For the years 2006/2007 and 2009-2013 no cumulative year end numbers were found. Hence, for these particular years the numbers of systems are roughly estimated (grey bars). It is likely that the error in estimating is about 5%. ....	12
<b>Fig. 4:</b> Comparison of the number of globally installed MLA and QEMSCAN systems over time (1982-2014). Note: For the years 2006/2007 and 2009-2013 it was not possible to calculate reliable cumulative year end numbers. See text for sources of information. The numbers for the period of time until 2008 are audited, whereas for 2014 an error of about 5% is likely. ....	12
<b>Fig. 5: a)</b> Time series (1982-2014) of total globally installed QEMSCAN systems, <b>b)</b> time series (1997-2014) of total globally installed MLA systems. Note: For the years 2006/2007 (QEMSCAN) and 2009-2013 (both system types) no cumulative year end numbers are publically available. ....	13
<b>Fig. 6:</b> Overview of total QEMSCAN systems by country (for 2008 and 2014). ....	14
<b>Fig. 7:</b> Overview of total MLA systems by country (for 2008 and 2014). ....	15
<b>Fig. 8:</b> Overview of total automated mineralogy systems of FEI Company (QEMSCAN + MLA) by country (for 2008 and 2014). ....	15
<b>Fig. 9:</b> Distribution of worldwide QEMSCAN systems by groups of users, <b>a)</b> for 2008, <b>b)</b> for 2014. ....	17
<b>Fig. 10:</b> Distribution of worldwide MLA systems by groups of users, <b>a)</b> for 2008, <b>b)</b> for 2014. ....	18
<b>Fig. 11:</b> Distribution of worldwide automated mineralogy systems (QEMSCAN + MLA) by groups of users, <b>a)</b> for 2008, <b>b)</b> for 2014. ....	19
<b>Fig. 12:</b> Time series (1968-2014) of publications related to automated mineralogy (all system types). ....	20
<b>Fig. 13:</b> Time series (1975-2014) of publications related to the QEMSCAN and MLA technologies. ....	21
<b>Fig. 14:</b> Cumulative distribution of publications related to automated mineralogy (by system type, end date 31 <sup>st</sup> December 2014). Note: Other* includes also publications where multiple systems were mentioned or publications with an unknown (not named in detail) automated mineralogy system type. ....	22
<b>Fig. 15:</b> Time series (1968-2014) of publications related to automated mineralogy by area of application, <b>a)</b> absolute data, <b>b)</b> normalised data. ....	23
<b>Fig. 16:</b> MLA 650 FEG system in the Geometallurgy Laboratory at the Department of Mineralogy, TU Bergakademie Freiberg. ....	30

<b>Fig. 17:</b> Greatly simplified overview of the external and internal parts of the Quanta SEM (IGP – Ion Getter Pump, PVP – Pre-Vacuum Pump, TMP – Turbo Molecular Pump, USP – Uninterruptible Power Supply).....	31
<b>Fig. 18:</b> Schematic overview of the general components of the Quanta SEM instrument.....	32
<b>Fig. 19:</b> Functional principle of the raster scanning of the electron beam across a specimen surface (grey).....	33
<b>Fig. 20:</b> Schematic overview of the electron scattering processes beneath a specimens surface (modified after Molhave (2006)).....	33
<b>Fig. 21:</b> Schematic relationship between backscattering coefficient $\eta$ , atomic number $Z$ and BSE grey value (modified after Reed (2005) and FEI Company (2011a)). .....	34
<b>Fig. 22:</b> Flowchart of calibrations to be performed prior to the start of MLA measurements and respective software/hardware needs to be used. ....	36
<b>Fig. 23:</b> Sketch of standards block for X-ray and BSE image calibration consisting of three metals and three minerals.....	37
<b>Fig. 24:</b> Schematic overview of the relationship between beam energy and interaction volume (modified after (Egerton 2005)). .....	37
<b>Fig. 25:</b> Flowchart of the functional principle of the BSE image processing during the MLA measurement. ....	39
<b>Fig. 26:</b> Steps of the particulation feature, <b>a)</b> acquired BSE image, <b>b)</b> background (epoxy resin) is removed, <b>c)</b> touching particles are separated (compare circle in b) and c)), <b>d)</b> image is cleaned from undersized particles and image artefacts (compare rectangle in c) and d)). .....	40
<b>Fig. 27:</b> Exemplary particle showing the segmentation feature behaviour of the MLA measurement, <b>a)</b> BSE image after background removal, <b>b)</b> BSE grey value histogram showing three main grey levels, <b>c)</b> segmented image showing the three main phases plus 3 minor phases. Note: The segmented image is based on the grey level value information exclusively and does not contain any mineral information.....	41
<b>Fig. 28:</b> Definition of particles and grains, <b>a)</b> particle consists of various grains, <b>b)</b> particle consists of one grain. ....	41
<b>Fig. 29:</b> Schematic overview of X-ray measuring points, <b>a)</b> centroid method, <b>b)</b> grid method.....	42
<b>Fig. 30:</b> Example of a XMOD measurement mode grid. ....	44
<b>Fig. 31:</b> Example for the procedure of the SPL measurement mode, <b>a)</b> BSE image, <b>b)</b> particle including a mineral phase matching the search criteria. ....	45
<b>Fig. 32:</b> Example for the procedure of the SPL_Lt measurement mode showing interleaved boxes surrounding phases of interest, <b>a)</b> BSE image, <b>b)</b> processed image. ....	46
<b>Fig. 33:</b> Flowchart of the sample preparation procedure for MLA analysis (modified after FEI Company (2011d)).....	50
<b>Fig. 34:</b> Simplified sample preparation procedure for thin sections (modified after Hirsch (2012)). ....	52
<b>Fig. 35:</b> Flowchart of MLA analysis workflow. ....	67
<b>Fig. 36:</b> Flowchart of the sample processing during this study (Note: sieve fractions are given in $\mu\text{m}$ and the related cumulative distribution $Q3(x)$ in %). .....	74
<b>Fig. 37:</b> Particle size distribution <b>(a)</b> and zinnwaldite mineral grain size distribution <b>(b)</b> of the combined data for all size fractions for the conventional comminution subsample and the high voltage pulse power fragmentation subsample. ....	76

<b>Fig. 38:</b> Modal mineralogy of MLA measurements for the subsample from (a) conventional comminution and (b) high voltage pulse power fragmentation. The diagram shows as well the data of the educt ('combined') as the data for the different sieve fractions. ....	77
<b>Fig. 39:</b> Mineral association for zinnwaldite mineral grains in the different sieve fractions (a) from conventional comminution and (b) high voltage pulse power fragmentation. ....	77
<b>Fig. 40:</b> Line-up of three groups of different zinnwaldite locking characteristics (Row 1 – liberated zinnwaldite grains; Row 2 – binary (with only one other phase) locked zinnwaldite grains; Row 3 – ternary and higher (with more than one phase) locked zinnwaldite grains) from the conventional comminution subsample. ....	78
<b>Fig. 41:</b> Intense overgrowth and replacement of zinnwaldite (light grey; elongated) by muscovite (medium grey) in a younger greisenisation stage (BSE image from Atanasova (2012)). ....	78
<b>Fig. 42:</b> Mineral liberation by particle composition for zinnwaldite mineral grains in different sieve fractions from (a) conventional comminution and (b) high voltage pulse power fragmentation subsamples. ....	79
<b>Fig. 43:</b> Theoretical grade recovery curve for zinnwaldite mineral grains in different sieve fractions from (a) conventional comminution and (b) high voltage pulse power fragmentation subsamples. ....	80
<b>Fig. 44:</b> (A) Backscatter electron (BSE) image of a MLA measurement frame of concentrate sample LynxConc90 mounted in carnauba wax (black - matrix of carnauba wax; dark grey - graphite; brighter grey tones - silicates) and (B) associated false colour image after background extraction and classification of minerals (graphite - black; quartz - blue; clay-minerals - brown; pyrite – red; muscovite - yellow) (size of frame: 500 x 500 pixels = 1.5 x 1.5 mm). ....	85
<b>Fig. 45:</b> Modal mineralogy of the five graphite samples studied based on MLA measurements and results of Rietveld analysis for comparison. ....	86
<b>Fig. 46:</b> (A) Cumulative particle size distribution and (B) cumulative graphite mineral grain size distribution. ....	87
<b>Fig. 47:</b> Comparison of particle size distributions as determined by sieve classification, wet laser diffraction (WLD) and MLA for sample FeedSB (Note: comparative data for all samples are included in the supplementary data). ....	87
<b>Fig. 48:</b> Mineral association for graphite mineral grains. ....	89
<b>Fig. 49:</b> Mineral liberation by free surface curve for graphite. ....	89
<b>Fig. 50:</b> Calculated mineral grade recovery curve for graphite. ....	90
<b>Fig. 51:</b> Generalised geological map of the southern section of the Lusatian Block including position of sample localities (modified after Leonhardt (1995); numbers refer to Table 13; note: sample locality 10 is about 40 km east of this map section) and major municipalities (inset shows the position of the study area in eastern Germany). ....	96
<b>Fig. 52:</b> MLA XMOD false colour mineral images of characteristic gabbroic rocks and base metal mineralisation (all scale bars are 10.000 µm in width). (a) Pyroxene-hornblende-orthopyroxene-gabbro with incipient amphibole-chlorite-serpentine alteration (amphibole - green, chlorite - pink, serpentine - light slate grey) showing typical plagioclase laths (brownish) surrounded by pyroxene crystals (light bluish) and olivine (dark blue) (sample SS11, Kunratice). (b) Sulphide-bearing gabbroic-rock with highly intense chlorite-sericite-talc alteration (chlorite - pink, sericite - yellow, talc - bluish grey) showing relictic pyroxene (light bluish) and plagioclase	



(brownish) as well as partly remobilised sulphide mineralisation with pyrrhotite (red), chalcopyrite (blue violet) and Ni-Fe sulphide (dark brown) (sample HG3B, Grenzland). **(c)** Massive sulphide sample showing pyrrhotite (red), Ni-Fe sulphide (dark brown), magnetite (indian red), pyrite (flesh tones) and rare silicates (sample ESoh1-5, Sohland-Rožany). **(d)** Massive sulphide ore with pyrrhotite (red) and Ni-Fe sulphide (dark brown) as well as alkali feldspar (pale ochre), plagioclase (brownish) and quartz (blue). Pyrite (flesh tones) of younger origin fills a fissure in pyrrhotite. Chalcopyrite (blue violet) is remobilised and replaced next to the silicates (sample ESoh2-2, Sohland-Rožany). **(e)** Sulphide-bearing gabbroic-rock with intense chlorite-amphibole alteration (chlorite - pink, amphibole - green) showing relictic pyroxene (light bluish). Pyrrhotite (red) shows a semi-massive to scaffold texture. Ni-Fe sulphide (dark brown) is directly associated with pyrrhotite whereas younger-stage chalcopyrite (blue violet) cross-cut pyrrhotite (red) and gangue (sample ESoh5, Sohland-Rožany). **(f)** Sulphide-bearing pyroxene-hornblende-orthopyroxene-gabbro with intense serpentine-amphibole-chlorite-sericite alteration (serpentine - light slate grey, amphibole - green, chlorite - pink, sericite - yellow) shows a triangular-acute angle ore texture to scaffold ore texture. The base metal sulphides consist of pyrrhotite (red), chalcopyrite (blue violet) and Ni-Fe sulphide (dark brown) (sample ESoh4, Sohland-Rožany). **(g)** Sulphide-bearing pyroxene-hornblende-orthopyroxene-gabbro with intense chlorite-amphibole-serpentine-sericite alteration (chlorite - pink, amphibole - green, serpentine - light slate grey, sericite - yellow) shows a blebby to disseminated ore texture with pyrrhotite (red), Ni-Fe sulphide (dark brown), pyrite (flesh tones) and chalcopyrite (blue violet) (sample ESoh12, Sohland-Rožany). ..... 101

**Fig. 53:** Examples of high-resolution BSE images illustrating important characteristics of PGM, native gold and telluride grains (scale bars 10  $\mu\text{m}$  in width, except (b) and (g) 5  $\mu\text{m}$ , (k) and (l) 20  $\mu\text{m}$ ). **(a)** Four sperrylite grains (white, about 2-4  $\mu\text{m}$  in size) found by MLA measurement plus three grains (< 1  $\mu\text{m}$ ) too small for MLA SPL\_Lt measurement in pyrrhotite next to a magnetite grain (left) (sample ESoh1-3, locality Sohland-Rožany). **(b)** Sperrylite grain (white) at the contact between pyrrhotite (medium grey) and albite (dark grey) (sample ESoh2-2, locality Sohland-Rožany). **(c)** Two palladium-bearing melonite grains (white) in stilpnomelane (dark grey) next to pyrrhotite (medium grey) (sample ESoh1-1, locality Sohland-Rožany). **(d)** Testibiopalladite grain (middle right; bright grey adjacent to native gold) and native gold (middle right, white) as well as nickeline (middle left medium grey) in a cobaltite-gersdorffite series grain in a pyrrhotite matrix; silicates on the left edge are titanite (dark grey) and chlorite (darkest grey) (sample Sohld02, locality Sohland-Rožany). **(e)** Pd antimonide (possibly sudburyite; brightest grey) associated with testibiopalladite (somewhat darker) and nickeline (medium grey) in an alloclasite grain in a pyrrhotite matrix. In pyrrhotite several pentlandite “flames” occur. Darkest grey (left edge) is K-feldspar (sample Sohld09, locality Sohland-Rožany). **(f)** Native gold (white) associated with nickeline (medium grey) in a cobaltite-gersdorffite series grain in a pyrrhotite matrix. In pyrrhotite a pentlandite “flame” and chlorite (darkest grey) occur (sample Sohld07, locality Sohland-Rožany). **(g)** Idiomorph altaite grain (white) in pyrrhotite (grey) next to chlorite (dark grey) (sample Sohld04, locality Sohland-Rožany). **(h)** Two coloradoite grains (white) associated with melonite (medium grey) in pyrrhotite next to a small chamosite grain (dark grey) (sample Sohld13, locality Sohland-Rožany). **(i)** Idiomorph Bi telluride grain (possibly tsumoite; white) in

pyrrhotite (grey) (sample ESoh2-5, locality Sohland-Rožany). <b>(j)</b> Melonite grain (light grey) in a pyrrhotite matrix with pentlandite “flames”. Silicates are chlorite (dark grey) and stilpnomelane (darkest grey) (sample Sohld08, locality Sohland-Rožany). <b>(k)</b> Two vavřínite grains (light grey) in a pyrrhotite matrix (grey) with pentlandite “flames” (sample Sohld04, locality Sohland-Rožany). <b>(l)</b> Vavřínite grain (light grey) associated with pentlandite (left and top; medium grey), stilpnomelane (top right; darkest grey) and chlorite (bottom right; dark grey). Areas somewhat darker than pentlandite (bottom middle and top middle) are pyrrhotite (sample Sohld04, locality Sohland-Rožany). .....	105
<b>Fig. 54:</b> <b>(a)</b> Comparison of base metal sulphide (BMS) content and number of PGM grains per sample. <b>(b)</b> Comparison of base metal sulphide (BMS) content and number of non-PGE-bearing telluride grains per sample.....	106
<b>Fig. 55:</b> <b>(a)</b> Comparison of total alteration (chlorite, serpentine, talc, sericite, stilpnomelane, amphibole, epidote, and carbonates) and number of PGM grains per sample. <b>(b)</b> Comparison of total alteration (chlorite, serpentine, talc, sericite, stilpnomelane, amphibole, epidote, and carbonates) and number of non-PGE-bearing telluride grains per sample. Alteration mineral content is calculated from MLA XMOD modal mineralogy normalised to 100% non-sulphides. ....	107

## List of Tables

<b>Table 1:</b> Types of ‘Automated Mineralogy’ systems and their appearance in the course of time (as of November 2014). Note: For some systems, sometimes contradictory information was found. In the column ‘System’ the country of development is given, which can differ from the country of current production. If no launch time were found the year of first mention in a publication or news is given. If no termination time were found the last year of mention in a publication or news is given. For some systems just one publication/ news could be found. A more consolidated view of these automated systems can be seen in Fig. 1. ....	2
<b>Table 2:</b> Purchasable ‘Automated Mineralogy’ solutions of FEI, CGG, TESCAN, Oxford Instruments, and Zeiss (by end of 2014) (sources: <a href="http://www.fei.com/products/sem/">http://www.fei.com/products/sem/</a> , <a href="http://robertson.cgg.com/roqscan">http://robertson.cgg.com/roqscan</a> , <a href="http://www.tescan.com/en/products/tima">http://www.tescan.com/en/products/tima</a> , <a href="http://www.oxford-instruments.com/products/microanalysis/energy-dispersive-x-ray-systems-eds-edx/eds-for-sem/mineral-liberation">http://www.oxford-instruments.com/products/microanalysis/energy-dispersive-x-ray-systems-eds-edx/eds-for-sem/mineral-liberation</a> , <a href="http://www.zeiss.com/microscopy/en_de/products/scanning-electron-microscopes/mineralogic-systems.html">http://www.zeiss.com/microscopy/en_de/products/scanning-electron-microscopes/mineralogic-systems.html</a> ). ....	10
<b>Table 3:</b> Common areas of application for the automated mineralogy technology, usable materials, and leading references. ....	26
<b>Table 4:</b> Detector types available for the Quanta SEM series and areas of application (after FEI Company (2009c, d)). ....	35
<b>Table 5:</b> Available MLA measurement modes. ....	43
<b>Table 6:</b> Measurement outcomes of the MLA software, definitions of parameters and benefits (compiled after FEI Company (2011a)). ....	47
<b>Table 7:</b> List of sample types, purpose of analyses, attributes studied and common MLA measurement modes. ....	48
<b>Table 8:</b> Potential sources of error and possibilities of error reduction related to the MLA technique (significantly modified after Barbery (1992)). ....	56
<b>Table 9:</b> Analysis of vulnerabilities of the MLA technique and suggested solutions. ....	68
<b>Table 10:</b> List of samples. ....	83
<b>Table 11:</b> Results of calculated elemental assay by MLA and carbon measurement with LOI method (all values are given in wt.%). ....	86
<b>Table 12:</b> P-values of the three different size distribution measurements for all five samples (MLA - mineral liberation analyser, WLD - wet laser diffraction, SC - dry sieve classification). ....	88
<b>Table 13:</b> Sample localities and number of samples (note: geographic coordinates are sourced from <a href="http://www.openstreetmap.org">http://www.openstreetmap.org</a> ). ....	98
<b>Table 14:</b> Measurement settings (note: number of frames per thin section varies due to different sample sizes on the microscope slides; total measurement area varies therefore from about 700 mm <sup>2</sup> to about 1.200 mm <sup>2</sup> ). ....	99
<b>Table 15:</b> PGE- and/or Te-bearing minerals identified and their association with mineral groups, with mineral formula and elemental composition based on SEM analyses (note: <sup>#</sup> - elemental composition calculated from mineral formula; <sup>A</sup> potentially sudburyite ((Pd,Ni)Sb); * ‘formulas’ in square brackets show only main the main elements of the particular mineral phase). ....	103
<b>Table 16:</b> Number of mineral grains found with SPL_Lt_MAP measurement mode and their relative modal abundance (RMA) per locality. ....	104
<b>Table 17:</b> Mineral grain sizes (in µm) of the different mineral groups in total and per locality (note: the size calculation is based on the measured 2D surface area of	

the grains and calculated using the equivalent circle diameter; min. = minimum, percentile P50 $\hat{=}$ median, max. = maximum).....	108
<b>Table 18:</b> Mineral association (expressed as % association) of PGM, native Au, telluride and native bismuth grains found by MLA measurement. ....	110
<b>Table 19:</b> Relative deportment of (A) palladium, (B) platinum, and (C) rhodium to mineral groups. ....	113
<b>Table 20:</b> Pt, Pd and Au bulk-rock estimates (in ppb) calculated by the MLA software per locality (note: min. = sample minimum, max. = sample maximum, mean = arithmetic mean, s.d. = standard deviation).....	114
<b>Table 21:</b> Comparison of Pt, Pd, Au values calculated by MLA analysis in this study and values given from Uhlig et al. (2001) (NiS Fire Assay-ICP/MS) as well as calculated relative difference (Uhlig et al. 2001 = 100%). For evaluation the BMS content as well as the number of Pt, Pd and Au-bearing mineral grains for each sample are given (note: b.d.l. – below detection limit, # estimated detection limit is 0.4 ppb; * bulk sample ESoh2/98). ....	116

## List of Abbreviations

AAN	Average Atomic Number
AARL	Anglo American Research Laboratories
ALS	an Australian analytical services provider (formerly Australian Laboratory Services)
AMA	Automated Mineral Analysis
AMCA	Analysis of Mineral and Coal Associations
AMIRA	Australian Mineral Industries Research Association
ANSTO	Australian Nuclear Science and Technology Organisation
ASPEX	a former American producer of scientific and technical instruments (acronym for Application Specific Products Employing Electron Beam and X-ray Technology)
AWE	Atomic Weapons Establishment (Scientific research facility, UK)
BGR	German Federal Institute for Geosciences and Natural Resources (Bundesanstalt für Geowissenschaften und Rohstoffe)
BMS	Base Metal Sulphide
BSE	Backscattered Electrons
BRGM	Bureau de Recherches Géologiques et Minières (French government geological survey)
CANMET	Canada Centre for Mineral and Energy Technology
CBS	Concentric Backscattered Detector
CCPI	Chlorite-Carbonate-Pyrite Index
CCSEM	Computer-Controlled Scanning Electron Microscopy/Microscope
CESEMI	Computer Evaluation of SEM Images
CGG	a French geophysical services company (formerly Compagnie Générale de Géophysique)
CMM-REDEMAT	Centro Mínero Metalúrgico-Rede Temática em Engenharia de Materiais (Brazilian Network in Materials Engineering)
CSIRO	Commonwealth Scientific and Industrial Research Organisation (Australian federal government agency for scientific research)
DTA/TG	Differential Thermal Analysis/Thermo-Gravimetry
EBSD	Electron Backscatter Diffraction
EDAX	a US scientific instruments producer
EDS/EDX	Energy-Dispersive X-ray Spectroscopy
EIT+	Wroclaw Research Centre, Poland
EMPA	Electron Micro Probe Analyser
EPMA	Electron Probe Microanalyser
ETD	Everhart-Thornley Detector
FEI	a US scientific instruments producer (formerly Field Emission Inc.)
FEG	Field Emission Gun
FIB	Focused Ion Beam
FORTRAN	programming language (derived from Formula Translating System)
GXMAP	a MLA measurement mode
HIF	Helmholtz Institute Freiberg for Resource Technology, Germany
IA	Image Analysis
ICAM	International Council for Applied Mineralogy
ICP	Inductively Coupled Plasma
ICP-MS	Inductively Coupled Plasma Mass Spectrometry

---

IGP	Ion Getter Pump
INAA	Instrumental Neutron Activation Analysis
ISI	a former US producer of scientific instruments (International Scientific Instruments, Inc.)
IUGS	International Union of Geological Sciences
JEOL	a Japanese scientific instruments producer (formerly Japan Electron Optics Laboratory Company, Limited)
JKMRC	Julius Kruttschnitt Mineral Research Centre (research centre within the SMI)
JKTech	a technology transfer company (for the SMI)
LA-ICP-MS	Laser Ablation Inductively Coupled Plasma Mass Spectrometry
LEO	a SEM series of company Leica
LFD	Large Field Detector
LOI	Loss on Ignition
MINCLASS	a mineral classification program
MLA	Mineral Liberation Analyzer/Analyser
MMIA	Minerals and Metallurgical Image Analyser
MP-SEM-IPS	MicroProbe–Scanning Electron Microscope–Induced Photoelectron Spectroscopy
NiS Fire Assay	Nickel Sulphide Fire Assay
NTNU	Norwegian University of Science and Technology, Trondheim (Norges teknisk-naturvitenskapelige universitet)
PE	Primary Electrons
PGE	Platinum Group Elements
PGM	Platinum Group Minerals
PSEM	"personalized" SEM
PTA	Particle Texture Analysis
PVP	Pre-Vacuum Pump
QAPF diagram	Quartz, Alkali Feldspar, Plagioclase, Feldspathoid diagram
QCAT	Queensland Centre for Advanced Technologies, Australia
QEM*SEM/ QEMSCAN	Quantitative Evaluation of Minerals by Scanning Electron Microscopy
QMA	Quantitative Mineral Analysis
QUANTAX	EDS system of company Bruker
QXRD	Quantitative X-ray Diffraction Analysis
RMA	Relative Modal Abundance
RPS	a MLA measurement mode
RWTH Aachen	German University of Technology, Aachen (Rheinisch-Westfälische Technische Hochschule Aachen)
SC	Sieve Classification
SDD	Silicon Drift Detector
SE	Secondary Electrons
SEFRAG	Selective Fragmentation (by High Voltage Pulse Power Technologies)
SEM	Scanning Electron Microscope/Microscopy
SEMPC	SEM Point-Count Routine
SGS	a Swiss analytical services provider (formerly Société Générale de Surveillance)
SIMS	Secondary Ion Mass Spectrometry
SMI	Sustainable Minerals Institute (Australian resources research institute)

---

SPL,	
SPL_Lt,	
SPL_Lt_MAP,	
SPL_XBSE,	
SPL_GXMAP,	
SPL_DZ	MLA measurement modes
SXBSE	a MLA measurement mode
TESCAN	a Czech scientific instruments producer
TIMA	TESCAN Integrated Mineral Analyser
TMP	Turbo Molecular Pump
USP	Uninterruptible Power Supply
UVR-FIA	a German services provider (environmental engineering, processing, recycling, refining)
WDS/WDX	Wavelength-Dispersive X-ray Spectroscopy
WLD	Wet Laser Diffraction
XBSE,	
XBSE_STD	MLA measurement modes
XMOD,	
XMOD_STD	MLA measurement modes
XRD	X-ray Diffraction
XRF	X-ray Fluorescence
XSPL	a MLA measurement mode
μCT	Micro-X-ray Tomography





## Chapter 1: Introduction

Automated Mineralogy may be considered as a subsection of the science of Applied Mineralogy / Process Mineralogy. According to Petruk (2000) “applied mineralogy in the mining industry is the application of mineralogical information to understanding and solving problems encountered during exploration and mining, and during processing of ores, concentrates, smelter products and related materials”. The constitution of the International Council for Applied Mineralogy (ICAM 2000) states: “Applied mineralogy covers the complete spectrum of mineralogical activity in 1) the exploration for, and exploitation of, base metals, precious metals, base minerals, industrial minerals, building and construction materials, and carbonaceous materials, in mining, extractive metallurgy, and economic geology, as well as in 2) the investigation and development of refractories, ceramics, cements, alloys and other industrial materials, including ancient material, and 3) the study and protection of the environment.” Accurate mineralogical information is required to develop solutions for efficient mineral processing. It may comprise of the mineral composition data of ores and mineral particles, size and shape data of particles and mineral grains, as well as mineral association, locking, and liberation data and textural information. Such mineralogical information is crucial for a resource-, energy- and cost-efficient and thus sustainable performance of the processing technology. For example, quantitative information regarding liberation and characteristics of particles during beneficiation is of great importance. Locked particles are a major source of inefficiencies either in concentrates (dilution) or in tailings (loss of metals). Here, a rapid and quantitative characterisation of the beneficiation products can lead to valuable improvements. ‘Automated Mineralogy’ was established as a result of the need for an automated fast and reliable control of the process mineralogy. This was driven in particular by the need for an automated mineral identification system (Gottlieb 2008).

Automated Mineralogy can be regarded as the usage of diverse analytical systems (mainly based on Scanning Electron Microscopy) for the quantitative analysis of solid natural substances and artificial materials. These systems measure samples in a largely automated manner but still require manual data processing and assessment. However, a proper definition for the term ‘Automated Mineralogy’ was never determined and thus can be rather seen as an elastic term.

### Early Developments of ‘Automated Mineralogy’ Systems

During the late 1960s and 1970s a range of semi-automated and automated computer-controlled SEM and electron microprobe-based systems have been developed in several countries. This includes among others the Geoscan-Minic system of the Royal School of Mines (London, UK) (Jones & Gavrilovic 1968, Jones & Shaw 1974, Jones & Barbery 1976, Jones 1977), the CESEMI system (Computer Evaluation of SEM images) of the Pennsylvania State University (State College, USA) (White et al. 1968, White et al. 1970, White et al. 1972, Lebedzik et al. 1973, Troutman et al. 1974, Dinger & White 1976), an automated JEOL JSM U3 SEM at the BRGM (France) (Jeanrot et al. 1978, Jeanrot 1980, Barbery 1985), and other systems. An overview of such systems as documented in the literature study can be seen in Table 1. Unfortunately, the investigation of the early

automated systems must remain incomplete because literature is scant for several of these developments. However, it is safe to say that none of the early system developments reached maturity required for commercialisation. A more comprehensive bibliography on “SEM image measurement of ... particles” is given in the PhD thesis of Hall (1977) but includes also numerous non-automated systems. In addition, also several automated “television based analysing instruments” (e.g., Imanco Quantimet, Bausch and Lomb Omnicon, Leitz Texture Analysis System, Zeiss Micro-Videomat) were developed but did use optical microscope and camera images only (Henley 1983).

**Table 1:** Types of ‘Automated Mineralogy’ systems and their appearance in the course of time (as of November 2014). Note: For some systems, sometimes contradictory information was found. In the column ‘System’ the country of development is given, which can differ from the country of current production. If no launch time were found the year of first mention in a publication or news is given. If no termination time were found the last year of mention in a publication or news is given. For some systems just one publication/news could be found. A more consolidated view of these automated systems can be seen in Fig. 1.

System	Launch	First News or Publication	Last News or Publication	Termination	Commercialised
Geoscan-Minic (UK)	?	1968	1977	?	no
CESEMI (USA)	?	1968	1982 (1987)	?	no
QEMSCAN (MINSCAN, QEM*SEM) (Australia)	1976 (1982)	-	-	available	yes
BRGM system (France)	1977	-		?	no
modified electron microprobe of Falconbridge (Canada)	?	1982		?	no
CCSEM (USA)	?	1983	2012	available	yes
computer-controlled SEM of Schlumberger-Doll Research (USA)	?	1984		?	no
MP-SEM-IPS image analyser (Canada)	?	1987	-	available?	yes?
Areal Analysis Program of the University of Adelaide (Australia)	?	1987		?	no
automated electron beam analytical instrument of the University of Calgary (Canada)	?	1987		?	no
SEM/MINID (?)	?	1990		?	no
Leica Cambridge morpho-chemical analysis system (UK)	1990	-	2001	?	yes
ASPEX systems (USA)	1992	-	-	available	yes
MMIA (Minerals and Metallurgical Image Analyser) (USA)	1993	-	2004	?	no
QMA and AMCA (USA)	?	1993		?	no
MINCLASS/SEMP (USA)	?	1994		?	no
MLA (Australia)	1997	-	-	available	yes
AutoGeoSEM (Australia)	?	2000	2014	available?	no
Ascan (South Africa)	?	2001	2007	?	no
PTA system (Norway)	2001	2006	-	available	no

**Table 1:** (continued).

System	Launch	First News or Publication	Last News or Publication	Termination	commercialised
AMA (Automated Mineral Analysis) (Australia)	?	2009	2010	?	no
Identiplat (part of the SmartPI™ automated particle analysis system) (South Africa)	?	2011		?	no
RoqSCAN (USA)	2011	-	-	available	yes
INCAMineral (UK)	2012	-	-	available	yes
TESCAN Integrated Mineral Analyser (TIMA) (Czech Republic)	2012	-	-	available	yes
Mineralogic Mining/Mineralogic Reservoir (Germany)	2014	-	-	available	yes

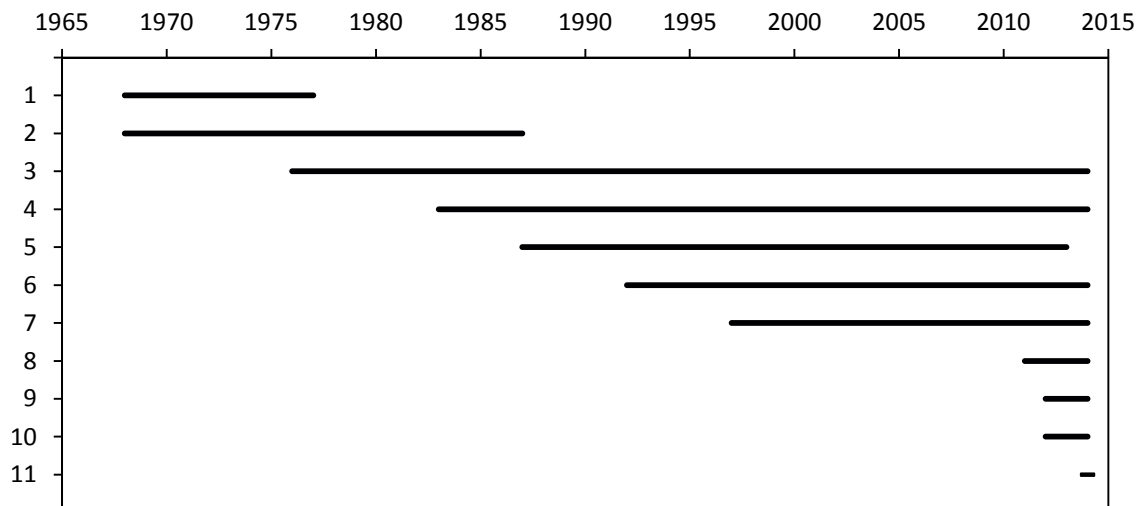


**Fig. 1:** Consolidated time series of the most important 'Automated Mineralogy' systems of Table 1 (1 - Geoscan-Minic, 2 - CESEMI, 3 - QEMSCAN, 4 - CCSEM, 5 - MP-SEM-IPS, 6 - ASPEX, 7 - MLA, 8 - RoqSCAN, 9 - INCAMineral, 10 - TIMA, 11 - Mineralogic Mining/Mineralogic Reservoir).

From 1974 to the end of 1976 John Sydney Hall and scientists of the Commonwealth Scientific and Industrial Research Organisation (CSIRO, Port Melbourne, Victoria), Australia's national science agency, used an electron microprobe to develop a technique (called 'MINSCAN') to outline the surfaces of minerals in composite particles. During this period of time John Sydney Hall was a PhD student at the Julius Kruttschnitt Mineral Research Centre (JKMRC), Australia and involved in the AMIRA (Australian Mineral Industries Research Association) P9 project 'Simulation and Automatic Control of Mineral Treatment Processes' (Lynch 2011). The primary MINSCAN system comprised of a minicomputer-controlled (Interdata 70 computer, 16 bit architecture, 64 Kbytes of core memory, 1  $\mu$ s cycle time, 16 general purpose registers) electron microprobe JEOL JXA-50 equipped with an electron beam step generator (allowing to measure a sample block

stepwise, from point to point), signal discriminators and a nDOS operating system software as well as an off-line FORTRAN image analysis program (Hall 1977, Frost et al. 1976). Allen Forrest Reid (Chief of the Division of Mineral Engineering in CSIRO) was responsible for the development of the MINSCAN system (which was renamed to QEM\*SEM [Quantitative Evaluation of Minerals by Scanning Electron Microscopy] after 1977) for automated characterisation of ores and minerals by scanning electron microscope imaging and X-ray analysis. He and his working group published numerous articles which addressed the new technology (Reid & Zuiderwyk 1975, Grant et al. 1976, Grant et al. 1977, Grant et al. 1979, Grant & Reid 1980, Grant et al. 1981, Grant & Reid 1981). It has to be noted that this first MINSCAN system, with a JEOL electron microprobe JXA-50 as the hardware platform, was termed by the authors (incorrectly) as a “computer controlled on-line scanning electron microscope image analyser” (Grant et al. 1977). In general, the scientific instruments manufacturing company JEOL labels their electron probe microanalyser product series with the model designation ‘JXA’ and scanning electron microscopes with ‘JSM’ (JEOL Ltd. 2014).

### **First Market-ready Systems**

The first papers dealing with a more general description of the QEM\*SEM technique were published by Miller et al. (1982), Reid & Zuiderwyk (1983), and Reid et al. (1985). In 1982 the first “real SEM-based” (see above) QEM\*SEM system (QS#0, analogue prototype) was installed at the CSIRO in Melbourne, Australia. The machine type of this system was a JEOL JSM-35C SEM equipped with one EDS detector (Laukkanen & Lehtinen 2005). In the same year the trademark QEM\*SEM was registered (trademark numbers 381005 and 381006). However, this trademark numbers were removed from the register in early 2014 (IP Australia 2014). 1983 a fully computer-controlled and completely redesigned digital QEM\*SEM prototype (QS#1) was installed at CSIRO (Melbourne, Australia). The platform of this system was an ISI 100B SEM with 4 Tracor EDS detectors. 1984 the digital production model QS#2, based on an ISI SX30 SEM, with 4 Tracor EDS detectors was installed at CSIRO (Laukkanen & Lehtinen 2005). In 1985 the first commercial sold QEM\*SEM system (QS#3, ISI SX40 SEM with 2 Gresham and 2 Tracor EDS detectors) was installed outside CSIRO at the University of Minnesota, USA and in 1987 the first industrial QEM\*SEM (QS#5, ISI SX40 SEM with 4 Gresham EDS detectors) was installed at Johannesburg Consolidated Investment Co. Ltd. (now Anglo Platinum) in Johannesburg, South Africa (Laukkanen & Lehtinen 2005).

In the 1980s another automated system, referred to as MP-SEM-IPS [MicroProbe–Scanning Electron Microscope–Induced Photoelectron Spectroscopy] image analyser, was established at CANMET (Canada) (Petruk 1986, Mainwaring & Petruk 1987, Petruk 1988a). This system consisted of a JEOL JXA-733 electron microprobe which was interfaced with a Tracor Northern energy-dispersive X-ray analyser and a Kontron SEM-IPS image analyser (Mainwaring & Petruk 1987, Petruk 1988a). This powerful combination allowed using the MP-SEM-IPS system for diverse applications such as mineral beneficiation analysis, search for specific phases, analysis of unbroken ore and much more (Mainwaring & Petruk 1987, Petruk 1988a, Lastra et al. 1998, Petruk & Lastra 2008, Lastra & Petruk 2014).

Also with the beginning of the 1980s automated systems called CCSEM (computer-controlled scanning electron microscopy) initially constructed by RJ Lee Group, Inc. (USA) were used (Casuccio et al. 1983, Schwoeble et al. 1988, Schwoeble et al. 1990, Galbreath et al. 1996, Gupta et al. 1998, Langmi & Watt 2003, Keulen et al. 2008, Keulen et al. 2012). However, the usage of this terminology is not consistent in the literature. Sometimes CCSEM was used as a synonym for ‘Automated Mineralogy’ in general and sometimes the term was used for the specific instruments for particle characterisation of the RJ Lee Group. In addition the meaning ‘coal characterisation scanning electron microscope’ can be found for CCSEM (van Alphen 2005). Furthermore terms in the literature appeared such as ‘automated image analysis’, ‘automated mineral analysis’, ‘SEM/Image-Analysis’, ‘SEM-based automated image analysis’, or ‘SEM-EDS-IA’. Here, without a proper system or platform description, an exact assignment is impossible. Some automated systems appeared only for a short period of time in the literature or only in subordinate clauses of articles such as the ‘areal analysis program’ (on a JEOL 733 microprobe) of the University of Adelaide, Australia, a modified electron microprobe (Cambridge Scientific Instruments, Model Mark V) at Falconbridge, Canada, a computer-controlled SEM “automatically measuring the relative content and distribution of minerals in rock samples”, at Schlumberger-Doll Research, USA, or an automated electron beam analytical instrument at the University of Calgary, Canada (Springer 1982, Minnis 1984, Nicholls & Stout 1986, Both & Stumpfl 1987). A commercial system for automatic quantitative metallography developed by US Steel Research Laboratory and Tracor Northern has been marketed by Tracor Northern, USA (Tracor Northern 1981, Henley 1989).

The term ‘Automated Mineralogy’ made its first appearance as keyword in an article of Sutherland et al. (1988) of CSIRO and in the article titles of Sutherland et al. (1991) and Sutherland & Gottlieb (1991). In 1992 ASPEX (a division of RJ Lee Group, Inc.) started the production of "personalized" SEMs (or PSEM), among others for automated particle analysis and materials characterisation (ASPEX Corporation 2006).

### **Breakthrough of ‘Automated Mineralogy’**

In 1994 the first modern SEM and image analysis-based mineral analysis system (with a Philips XL40 SEM platform) – precursor to MLA – was installed at the WMC’s Kambalda Nickel Mines (Gu & Sugden 1995). In 1995 CSIRO scientists, led by Paul Gottlieb, developed a PC-controlled new generation QEM\*SEM system equipped with digital SEM, light element detectors, which was re-branded as QEMSCAN (Quantitative Evaluation of Minerals by SCANning Electron Microscopy; the spelling ‘QemSCAN’ was used at the beginning, but soon changed to ‘QEMSCAN’). For this propose the SEM platform of the system was changed to a LEO 440 SEM and the first QEMSCAN system (QS#9) was installed at CSIRO in 1996 (Laukkanen & Lehtinen 2005). From this time on the CSIRO’s systems were called QEMSCAN but the technology for this system still was termed QEM\*SEM (CSIRO 2008).

	1974	1978	1982	1983	1984	1985	1994	1995
QEMSCAN	John Hall starts PhD work on the MINSCAN system	MINSCAN system renamed to QEM*SEM	Analogue QEM*SEM prototype (QS#0)	Digital QEM*SEM prototype (QS#1)	Digital QEM*SEM production model (QS#2)	First commercially sold QEM*SEM system (QS#3)		Next generation of QEM*SEM → QEMSCAN
Proprietor	<hr style="border: 2px solid blue;"/>							
MLA							Precursor to MLA installed at WMC	

**Fig. 2:** Condensed time line of the development of the QEMSCAN and MLA technology and overview of their proprietaries (dark blue – CSIRO, light blue – Intellection, dark green – JKMRRC, light green – JKTech, FEI Company – purple). Note: Scale of time line is non-linear.

Fig. 2: (continued).

	1996	1997	2000	2001	2003	2009	2010	2011	2012/2013
QEMSCAN				JKTech MLA Bureau opened	CSIRO spin- off company Intellection formed	FEI Company acquired Intellection	QEMSCAN available on FEI Quanta 650 SEM platform	QEMSCAN Wellsite solution introduced	2013 QEMSCAN Express launched
Proprietor									
MLA	Development of MLA starts	First MLA delivered to JKMRC from Philips (FEI)	First MLA system sold				FEI Company acquired JKTech's MLA business; MLA 650 launched		2012 MLA Express launched

Dr. Ying Gu joined the JKMRC in 1996 as a Senior Research Fellow to start the development of the JKMRC/Philips Electron Optics Mineral Liberation Analyser (MLA), a competing product to QEMSCAN. Before joining JKMRC, Ying Gu worked (1995-1996) as a Research Scientist with CSIRO's QEM\*SEM group. In 1997 the first MLA development system was delivered to JKMRC from Philips, and in the same year (February 1997) FEI Company (USA) combined its operations with Philips Electron Optics (Netherlands) whereby FEI became the manufacturer of the SEM platforms for the MLA technique (FEI Company 1996, 1997). However, the first MLA system was build up with a Philips XL40 scanning electron microscope (JKTech Pty Ltd 2007).

### **Rapid Innovation and Market Penetration**

In 1999 the JKMRC MLA Bureau in Brisbane, Australia was opened, which was enlarged to the JKTech (Commercial Division of the JKMRC) MLA Bureau in March 2001 (JKMRC 1999, JKTech Pty Ltd 2001). In 2000 the first MLA system was sold to a mining company (Anglo Platinum) (Sustainable Minerals Institute 2006). At the turn of the millennium the breakthrough of the commercialisation of both QEMSCAN and MLA systems was made and the method of 'Automated Mineralogy' succeeded to enter the market. This was mainly based on the competition between CSIRO/LEO/Leica and JKMRC/Philips/FEI with its rival technological platforms. In November 2003 CSIRO spin-off company Intellection Pty Ltd was formed to develop further and enhance the commercialisation of the QEMSCAN technology (Tattam 2003, CSIRO 2004). By the beginning of 2004 the hardware platform of the QEMSCAN systems was changed from the LEO SEMs to the Carl Zeiss EVO50 SEM (Laukkanen & Lehtinen 2005). In 2006 the trade mark QEMSCAN (trademark number 1139670) was registered and expanded in 2008 (trademark number 1227841) (IP Australia 2014). These two trademarks now are owned by FEI Company. A condensed time line of the development of both the QEMSCAN and the MLA technology is shown in Fig. 2.

During the 1990s and 2000s several automated systems of limited importance (short term, single-unit productions, prototypes) were used but the range of printed literature and/or digital information regarding these systems is very limited (Table 1). In the publication of Nitters & Hagelaars (1990) a SEM/MINID system is mentioned, but no detailed information are given. The Leica Cambridge morpho-chemical analysis system, based on the Cambridge Scientific Instruments Stereoscan 360 SEM and the Quantimet 570 image analyser was launched around 1990 and the system was able to obtain "quantitative information on the modal composition of the samples, as well as grain size distributions and mode of occurrence of specific minerals" (Morris 1990, Penberthy & Oosthuyzen 1992, Penberthy 2001). The MMIA (Minerals and Metallurgical Image Analyser) was developed at the Utah Comminution Centre, USA (King & Schneider 1993, Schneider et al. 2004).

Two automated analysis routines, 'Quantitative Mineral Analysis' (QMA) and 'Analysis of Mineral and Coal Associations' (AMCA), were developed at the Brigham Young University, USA (Harb et al. 1993, Yu et al. 1994). At the University of North Dakota, USA a mineral classification program (MINCLASS) using a SEM point-count routine (SEMP) was developed (Folke Dahl et al. 1994). An AutoGeoSEM (Philips XL40



SEM fitted with an EDAX detector) is used at CSIRO, Australia (Robinson et al. 2000, Paine et al. 2005, Stewart & Anand 2014). Anglo American Research Laboratories (Pty) Ltd. (AARL) developed the ASCAN system (Viljoen et al. 2001, van Alphen 2005) and Mintek, South Africa developed Identiplat for automated platinum group metals (PGM) identification as a part of the Zeiss SmartPI automated particle analysis system (Bushell 2011).

The Particle Texture Analysis (PTA) system of the University of Trondheim, Norway (NTNU) was developed between 2001 and 2005 and “is based upon the same main principals as the former known systems” Geoscan, MP-SEM-IPS, QEMSCAN or MLA (Moen et al. 2006, Moen 2006). This technique uses a Hitachi S-4300SE SEM and the Oxford Instruments Analytical Limited Inca Feature software for data acquisition. The particle texture analysis post-processing software was developed at the NTNU. A detailed description of the PTA technology can be found in the PhD thesis of Moen (2006).

### **FEI Dominance**

In 2009 FEI Company acquired both Intellection Pty Ltd (in January; for approximately US\$ 2.8 million) and JKTech MLA (in June; for 5 million AUD) (FEI Company 2009a, b) and from this time on FEI dominated, and still dominates, the market of automated mineralogy systems. The acquisitions led to a SEM platform change in 2009 for both QEMSCAN and MLA. The QEMSCAN platform was changed from the Zeiss EVO 50 SEM (in use since 2004) to the FEI Quanta 650 SEM, which is available in tungsten filament version or FEG version. The MLA platform was changed from the FEI Quanta 600 SEM to the Quanta 650 W (tungsten filament) or Quanta 650 FEG SEM. This results in the fact that now with one SEM platform both techniques can be used. In 2012, FEI acquired ASPEX Corporation (purchase price US\$ 30.5 million), a leading provider of “rugged scanning electron microscopes (SEMs) and related services for environmentally demanding military, industrial and factory floor applications” (FEI Company 2012). As a result of this acquisition the ASPEX EXtreme, EXplorer and EXpress SEMs could be integrated into FEI’s SEM product range (ASPEX Corporation 2011, FEI Company 2014b). By the end of 2014 the following ‘Automated Mineralogy’ products of FEI Company were available: MLA650/650F, QEMSCAN 650/650F, MLA/QEMSCAN Express, and QEMSCAN Wellsite (Table 2).

### **Recent Developments**

Since 2011 four new automated mineralogy solutions were brought to marketability. RoqSCAN was developed by Fugro Robertson Ltd., USA (acquired by CGG in 2013) in collaboration with the Carl Zeiss AG, Germany and launched in April 2011 (Fugro Robertson Ltd 2011, Fugro Robertson 2011). RoqSCAN is a fully portable and ruggedised solution and optimised for the needs of the petroleum industry. Hence, it is the direct and chief competitor of FEI’s QEMSCAN Wellsite technology.

In January 2012 Czech company TESCAN, a.s. (now TESCAN ORSAY HOLDING, a.s.) introduced the TIMA Mineralogy Solution (TESCAN Integrated Mineral Analyser) (TESCAN 2012). This system is a chief competitor of FEI’s MLA technology.

The TESCAN TIMA can be purchased either with a MIRA FEG-SEM or a VEGA SEM platform (TESCAN 2014) and provides three measurement modules – ‘Modal Analysis’, ‘Liberation Analysis’ and ‘Bright Phase Search’ (Králová et al. 2012a). In comparison to FEI’s MLA 650 the TIMA can be equipped with up to 4 integrated EDS detectors (MLA: 2 EDS detectors) but the SEM chamber is significantly smaller. This results in a lower number of samples per sample block holder (TIMA sample holder for 7 blocks of  $\varnothing$  30 mm; MLA sample holder for 14 blocks of  $\varnothing$  30 mm) (FEI Company 2011b, TESCAN 2014). However, the TIMA system is able to support an optional auto sample loader unit for up to 100 blocks either 25 or 30 mm in diameter (AXT Pty Ltd 2014).

**Table 2:** Purchasable ‘Automated Mineralogy’ solutions of FEI, CGG, TESCAN, Oxford Instruments, and Zeiss (by end of 2014) (sources: <http://www.fei.com/products/sem/>, <http://robertson.cgg.com/roqscan>, <http://www.tescan.com/en/products/tima>, <http://www.oxford-instruments.com/products/microanalysis/energy-dispersive-x-ray-systems-eds-edx/eds-for-sem/mineral-liberation>, [http://www.zeiss.com/microscopy/en\\_de/products/scanning-electron-microscopes/mineralogic-systems.html](http://www.zeiss.com/microscopy/en_de/products/scanning-electron-microscopes/mineralogic-systems.html)).

Product	SEM	Notes
FEI MLA 650/ FEI MLA 650F	FEI Quanta 650 W/ FEI Quanta 650 FEG	MLA core product
FEI QEMSCAN 650/ FEI QEMSCAN 650F	FEI Quanta 650 W/ FEI Quanta 650 FEG	QEMSCAN core product
FEI MLA Express	FEI/ASPEX EXpress	low-cost, bench-top, automated mineralogy analyser
FEI QEMSCAN Express	FEI/ASPEX EXpress	low-cost, bench-top, automated mineralogy analyser
<i>FEI MLA Minesite</i>	<i>FEI/ASPEX EXtreme</i>	<i>rugged and portable system for mining industry (development ceased?)</i>
FEI QEMSCAN WellSite	FEI/ASPEX EXtreme	rugged and portable system for petroleum industry (on- and off-shore)
Robertson CGG RoqSCAN	Zeiss (no details provided)	FEI WellSite competitor
TESCAN TIMA	VEGA SEM	thermal emission SEM (tungsten filament)
TESCAN TIMA	MIRA SEM	Schottky field emission (FEG)
Oxford Instruments INCAMineral	compatible with a wide range of SEMs	can be retrofitted to existing SEMs
Zeiss Mineralogic Mining	Zeiss EVO	solution for mining industry, for 24/7 ore process control
Zeiss Mineralogic Mining	Zeiss SIGMA	solution for mining industry, for research into ore processing
Zeiss Mineralogic Mining	Zeiss SIGMA HD	solution for mining industry, for high resolution mineral mapping
Zeiss Mineralogic Reservoir	Zeiss EVO	solution for petroleum industry, for 24/7 operation
Zeiss Mineralogic Reservoir	Zeiss SIGMA HD	solution for petroleum industry, for high speed mineral mapping
Zeiss Mineralogic Reservoir	Zeiss Crossbeam	solution for petroleum industry, for 3D correlation

The automated INCAMineral solution was launched by Oxford Instruments plc, UK in June 2012 (Oxford Instruments plc 2012). This product can be used with a wide range of SEMs and can be retrofitted to existing systems. A detailed description of this technology can be found elsewhere (Oxford Instruments plc 2014).

In 2014 Zeiss, Germany launched the 'Mineralogic Mining' and 'Mineralogic Reservoir' systems (Carl Zeiss AG 2014b, Marketwire L.P. 2014). 'Mineralogic Mining' is intended for the mining industry whereas 'Mineralogic Reservoir' is designed as a petrophysics solution for the petroleum industry. Both systems can be combined with a choice of three SEM platforms, which can be equipped with one to four energy dispersive spectrometers (Carl Zeiss AG 2014a).

### **Market Overview of 'Automated Mineralogy' Systems**

The number of automated mineralogy systems is rather low in comparison to the total number of scanning electron microscopes worldwide. In the next paragraph efforts are being made to create a comprehensive overview of the number of currently existing automated mineralogy instruments (as at end of 2014). Here, only the commercial instruments of the world market leader FEI Company and its competitors CGG, TESCAN, Oxford Instruments, and Zeiss will be considered in detail, as the information regarding the others systems is very poor and often only one prototype was constructed (see above). For the early QEM\*SEM/QEMSCAN and MLA systems the search was relatively easy as very good overviews can be found in the attachments of Laukkanen & Lehtinen (2005) and in the newsletters of Intellection Pty Ltd (newsletter 'sift') and JKTech Pty Ltd (newsletter 'MLA today') (Intellection Pty Ltd 2008, JKTech Pty Ltd 2008). This covers the period of time from the 1980's to 2008/2009 when both systems were acquired by FEI Company. For the period from 2009 to now the information was more difficult to obtain, as FEI Company does not provide statistics related to its sales of automated mineralogy systems. The same applies for the RoqSCAN, INCAMineral, TIMA, and Mineralogic systems. Thus a countless number of information sources were used to try to assess the distribution of automated mineralogy instruments across the globe. This information sources include numerous newsletters from CSIRO, CSIRO's mineral resources group, CSIRO Minerals Down Under Flagship, JKMRC, and JKTech, the annual reports of FEI Company, CSIRO, and QCAT (Queensland Centre for Advanced Technologies), as well as thousands of press releases of CSIRO, JKMRC, JKTech, FEI, CGG, TESCAN, Zeiss, and their several international suppliers. Furthermore automated mineralogy systems were found while investigating more than 1,700 scientific publications, found via Scopus and Google Scholar. Here, the information regarding the automated mineralogy instruments were often found in the methodology section of the publications. In addition the regular Google web search engine was used for the search for automated mineralogy systems.

In total 270-300 commercial automated mineralogy systems were installed by the end of 2014 (Fig. 3). It should be recalled that several new types of systems, such as RoqSCAN, TIMA, INCAMineral, and Mineralogic, have become available to the market since 2011. For these, the number of systems (by the end of 2014) is rather vague. For RoqSCAN systems, exclusively used by the petroleum industry, the total number was estimated to be <10, but could be higher. TESCANs TIMA system was found at

FLSmidth, USA (2 systems), CMM-REDEMAT, Brazil, and CSIRO, Australia. The total number of TIMA systems was estimated to be <10 (by the end of 2014). The same applies for INCAMineral systems. The recently introduced Mineralogic systems were estimated to be <5 at the end of 2014. The total number of systems of FEI company (MLA + QEMSCAN), which dominate the market of automated mineralogy systems (with about 80-90% market share), has been estimated with about 240-250 by the end of 2014, based on the investigations mentioned above.

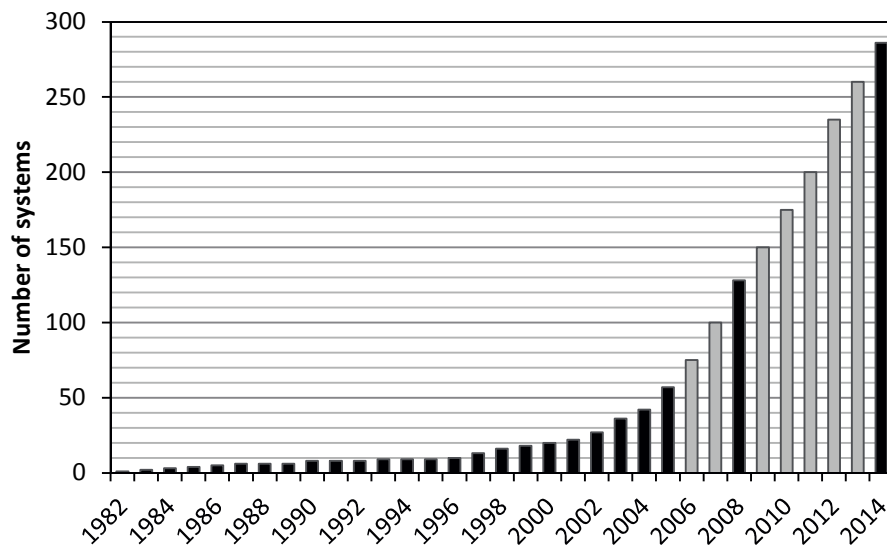


**Fig. 3:** Time series (1982-2014) of the total number of commercial automated mineralogy systems worldwide. Note: Numbers for 1982-2008 consists of MLA and QEMSCAN systems (now both FEI Company). The column for 2014 includes about 250 FEI systems and estimated 35 systems of FEIs competitors. For the years 2006/2007 and 2009-2013 no cumulative year end numbers were found. Hence, for these particular years the numbers of systems are roughly estimated (grey bars). It is likely that the error in estimating is about 5%.

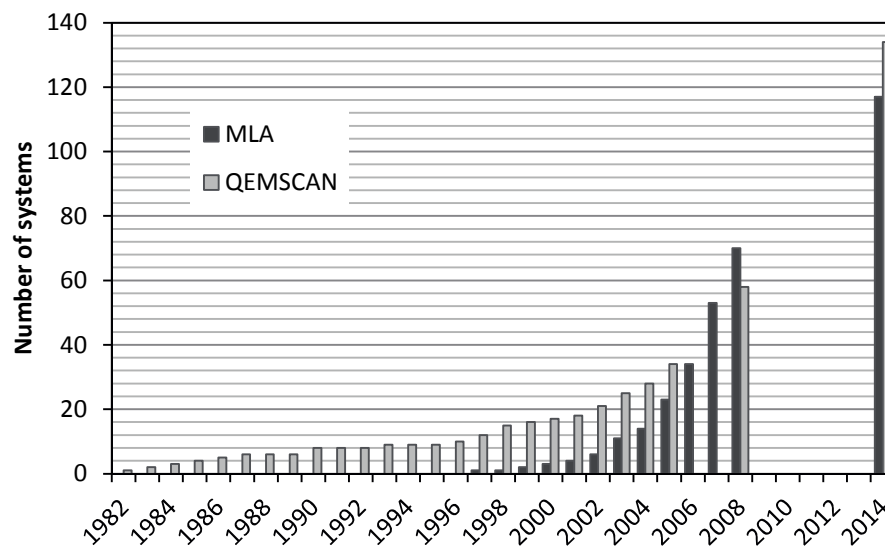


**Fig. 4:** Comparison of the number of globally installed MLA and QEMSCAN systems over time (1982-2014). Note: For the years 2006/2007 and 2009-2013 it was not possible to calculate reliable cumulative year end numbers. See text for sources of information. The numbers for the period of time until 2008 are audited, whereas for 2014 an error of about 5% is likely.

By comparing the number of existing MLA and QEMSCAN (inclusive QEM\*SEM) systems over time it is obvious that the number of sold MLA systems out-competed the number of QEMSCAN systems in 2006/2007, and for 2008 a considerable surplus of MLA systems can be seen (Fig. 4). However, by 2014 this situation changed considerably. Now the number of QEMSCAN systems installed globally is significantly higher than the number of MLA systems. This could be related to the recent global mining crisis (Australian Broadcasting Corporation 2014), as the QEMSCAN systems are also highly useful for the petroleum industry, which commands much greater research funding volume and has been somewhat more stable, than the mining industry, until the significant dropdown of the oil price in mid-2014.

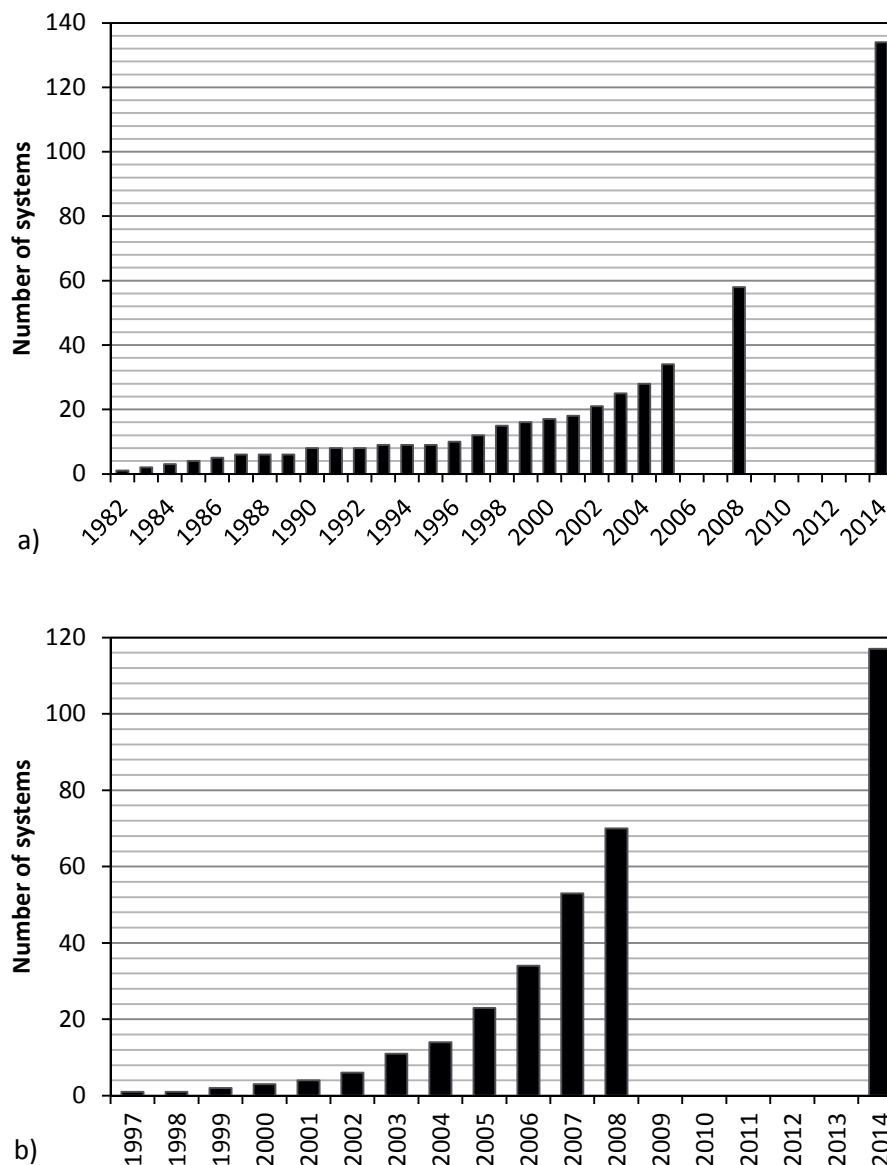


**Fig. 5:** **a)** Time series (1982-2014) of total globally installed QEMSCAN systems, **b)** time series (1997-2014) of total globally installed MLA systems. Note: For the years 2006/2007 (QEMSCAN) and 2009-2013 (both system types) no cumulative year end numbers are publically available.

While comparing the development of installations of MLA and QEMSCAN systems in detail it can be seen that the number of QEMSCAN systems (developed by CSIRO, Australia) increased rather slowly over the first 20 years. Between 1982 and 2002 just 21 systems were installed (Fig. 5a). This resulted in the foundation of the CSIRO spin-off company Intellection Pty Ltd in November 2003, as CSIRO, a federal government agency of Australia, was not able to merchandise these instruments. After this, the number of systems more than doubled in only 6 years (2003-2008). This ratio stayed about the same over the following 6 years (2009-2014). The number of MLA installations stayed low, in contrast to QEMSCAN, just for less than ten years and by 2005 more than 20 MLA systems were installed (Fig. 5b). Between 2005 and 2008 the total number of installed MLA systems increased by 130 to 150% per year respectively 300% for this particular period of time (3 years period). The increase of MLA systems slowed down between 2008 and 2014 (160% increase), whereas the increase of QEMSCAN systems for the same period of time was more than 200%.

### Geographic Distribution of QEMSCAN and MLA Systems

A complete overview of the distribution of QEMSCAN and MLA systems globally for every single year of production would extend the scope of this section too much. Hence, the section is limited to the years 2008 and 2014, which is a good comparison for the time before and after the takeover of both technology platforms by FEI Company. The overview of countries in Fig. 6 in which QEMSCAN systems were installed is clearly dominated by main mining countries, such as Australia, South Africa, Canada, USA, and Chile. The same applies for the list of countries with MLA systems, except for Chile (no MLA system) (Fig. 7).

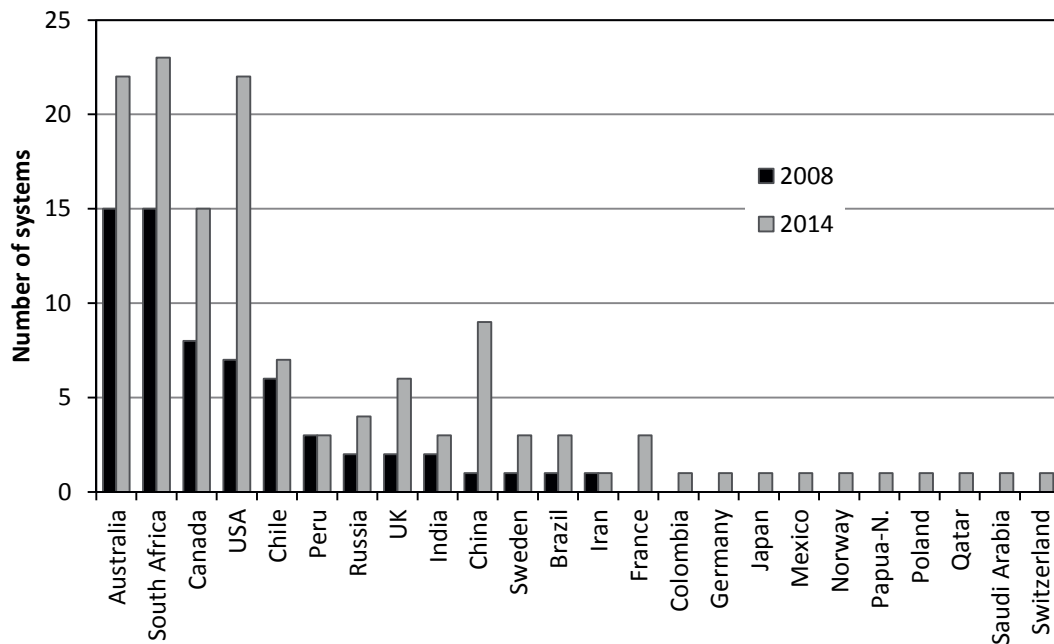


**Fig. 6:** Overview of total QEMSCAN systems by country (for 2008 and 2014).

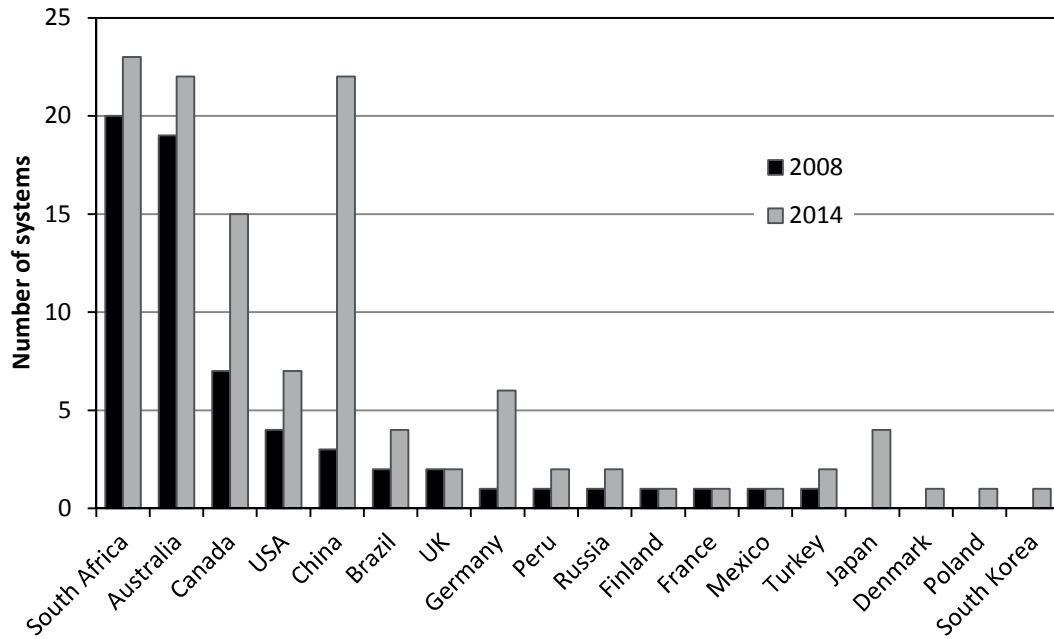


**Fig. 7:** Overview of total MLA systems by country (for 2008 and 2014).

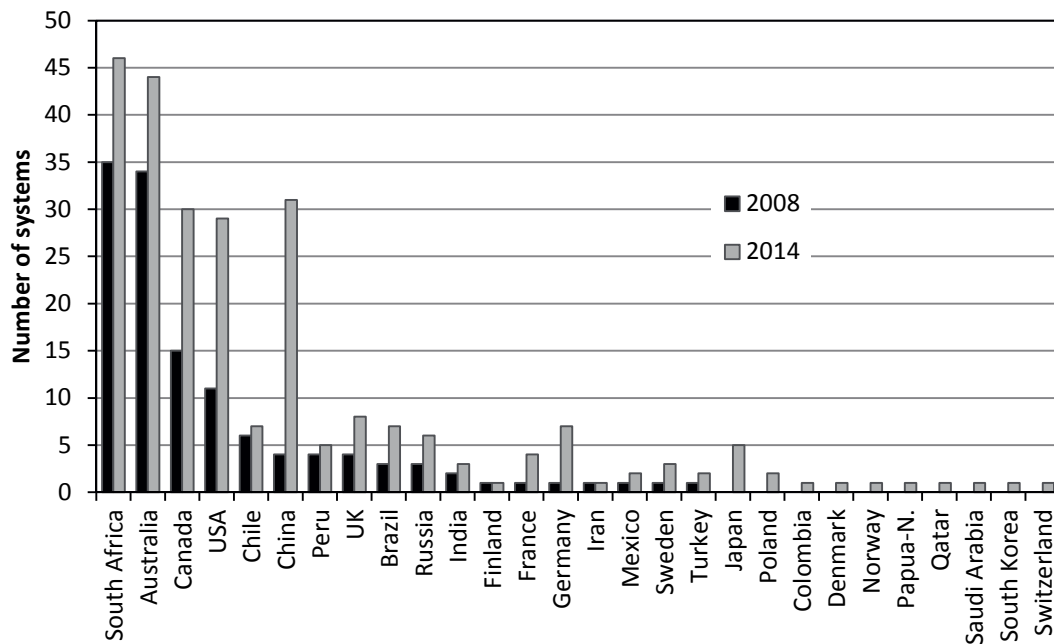


**Fig. 8:** Overview of total automated mineralogy systems of FEI Company (QEMSCAN + MLA) by country (for 2008 and 2014).

From 2008 to 2014 all of the main QEMSCAN-owning countries showed a significant increase in the number of systems (Fig. 6). For the same period of time the increase of MLA systems in the main mining countries in Fig. 7 was much lower, except for Canada which showed about the same increase for both QEMSCAN and MLA. A country with a considerable increase in both QEMSCAN and MLA systems is China. Here, the increase in MLA systems is higher than the increase in QEMSCAN systems (Fig. 6, Fig. 7). It can be noted that the highest number of petroleum industry-related instruments can be found in

China, whereas “classical” oil & gas producing countries such as Saudi-Arabia, Qatar, Norway, France, Russia and Columbia owned often only one or two systems by 2014. In the USA at least four petroleum industry-related systems were found.

The overview of all installed automated mineralogy systems of FEI Company (QEMSCAN + MLA) in Fig. 8 shows that Australia and South Africa are the dominating countries with the highest number of systems in 2008 and in 2014. In total, automated mineralogy systems of FEI are today installed in 28 countries up from 18 countries in 2008. In Fig. 8 it can be seen that “early leaders” in automated mineralogy such as Australia and South Africa had a lower increase in the total number of installed systems than the “followers” such as China, Canada, USA, Germany, and Japan in the years from 2008 to 2014.

The number of automated mineralogy systems of FEI Company installed in Germany increased from one system in 2008 to seven systems in 2014. In 2008 one MLA system was installed at the German Federal Institute for Geosciences and Natural Resources (Bundesanstalt für Geowissenschaften und Rohstoffe, BGR) in Hannover. In 2014 three MLA systems were installed in Freiberg (2x Helmholtz Institute Freiberg for Resource Technology, 1x TU Bergakademie Freiberg), two MLA systems at the BGR in Hannover, one QEMSCAN system at the RWTH Aachen University, and one MLA system at ThyssenKrupp Industrial Solutions (formerly ThyssenKrupp Polysius), Beckum.

### **Application Sectors of ‘Automated Mineralogy’ Systems**

By investigating the groups of users of all installed QEMSCAN systems it can be seen that one third of the systems is used in the commercial services area (Fig. 9). This remained rather constant between 2008 (Fig. 9a) and 2014 (Fig. 9b) and includes service laboratories such as ALS, SGS, FLSmidth, and Actlabs. The proportion of the mining industry sector in the QEMSCAN usage decreased significantly between 2008 and 2014 from more than 40% down to 30%. By the same proportion the petroleum (Oil&Gas) sector increased. The share of the universities in the total number of QEMSCAN systems almost doubled between 2008 and 2014, whereas the share of research institutes, such as CSIRO, ANSTO, AWE, and EIT+, is stable but diversified (Mining + Other) in the same time period.

The groups of users of all installed MLA systems in Fig. 10 are dominated by the mining industry sector (40-50%). However, as with QEMSCAN systems a decrease in the percentage between 2008 (Fig. 10a) and 2014 (Fig. 10b) is undeniable. The proportion for the commercial services area in MLA system ownership is lower than for QEMSCAN systems but shows just a slightly decrease between 2008 (23%) and 2014 (19%). In contrast, the share of the research institutes has more than doubled within this period of time. The percentage of MLA systems installed at universities was relatively constant between 2008 and 2014.

When examining the global distribution of automated mineralogy systems (QEMSCAN + MLA) by groups of users in Fig. 11 the decrease of the proportion of the mining industry between 2008 (Fig. 11a) and 2014 (Fig. 11b) is significant but this sector is still the largest user of automated mineralogy systems. The second largest group of users of such systems are commercial services laboratories (with a relatively stable share between 2008 and 2014) as they often have a number of systems installed in one lab. For



example, ALS Mineralogy (based in Brisbane, Australia) uses nine MLA systems (ALS Limited 2015) at one site. The proportion of the petroleum (O&G) industry increased from 1% in 2008 to 7% in 2014 and is assumed to be an important growth market for automated mineralogy systems in future.

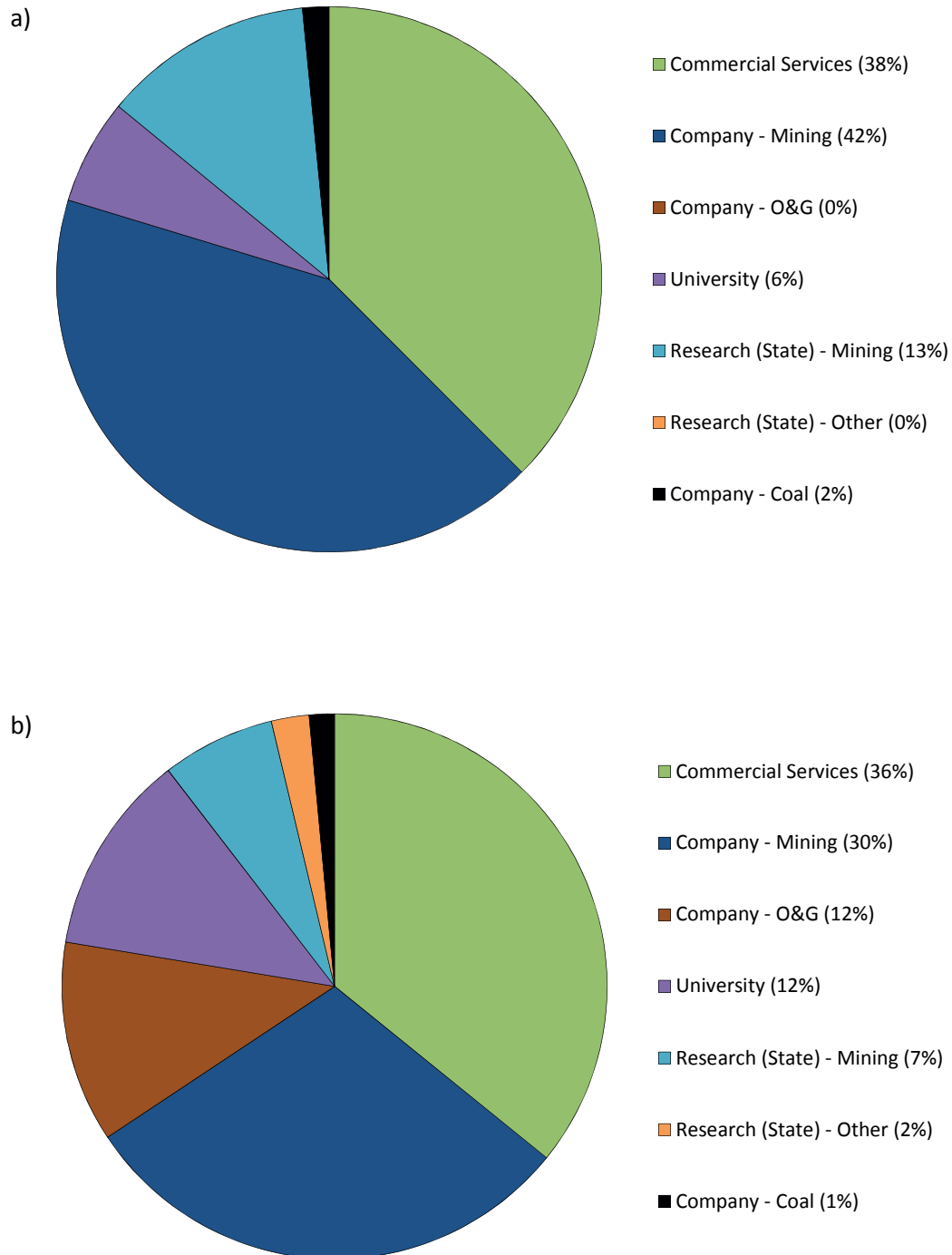


**Fig. 9:** Distribution of worldwide QEMSCAN systems by groups of users, **a)** for 2008, **b)** for 2014.

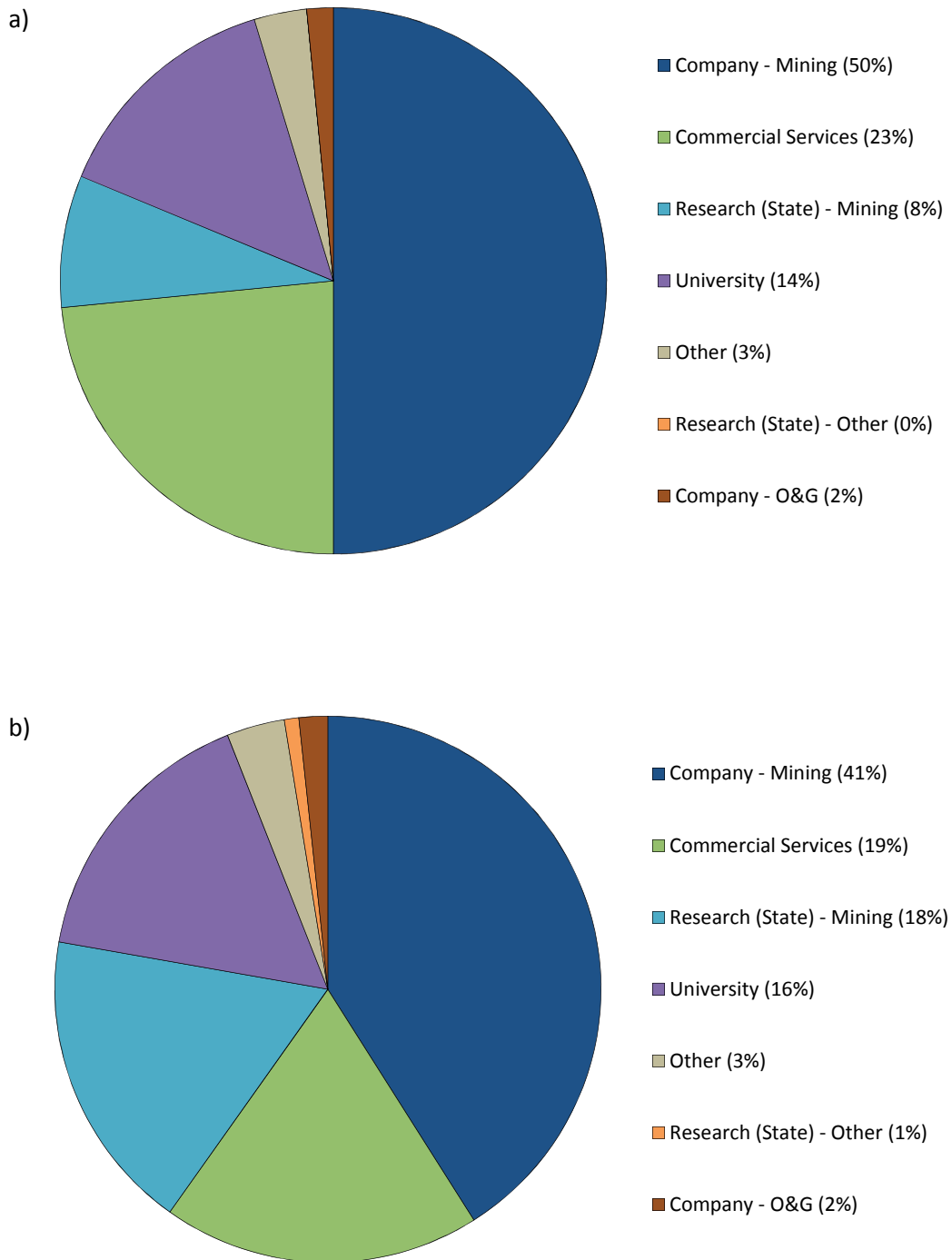


**Fig. 10:** Distribution of worldwide MLA systems by groups of users, **a)** for 2008, **b)** for 2014.

The proportion of universities and research institutes in the global automated mineralogy systems (QEMSCAN + MLA) is relatively similar and is below 20% for both 2008 and 2014 (Fig. 11). By examining the owner of QEMSCAN and MLA systems in the research institutes sector it can be seen that almost all institutes purchased just one system. Exceptions are the Guangzhou Research Institute of Non-ferrous Metals (China) and the Helmholtz Institute Freiberg for Resource Technology (Germany) with two systems each. It is obvious that the vast majority of research institutes owning automated mineralogy systems are related to research fields of minerals engineering and resource technology. In the universities sector the number of system owner with two automated mineralogy

systems is slightly higher than in the research institutes sector. Universities owning two systems are the Camborne School of Mines (UK), the Memorial University of Newfoundland (Canada), the University of Cape Town and the University of Johannesburg (both South Africa). Again, the systems are mainly used in departments related to minerals engineering and resource technology, but also in earth sciences, mineralogy and geology departments.

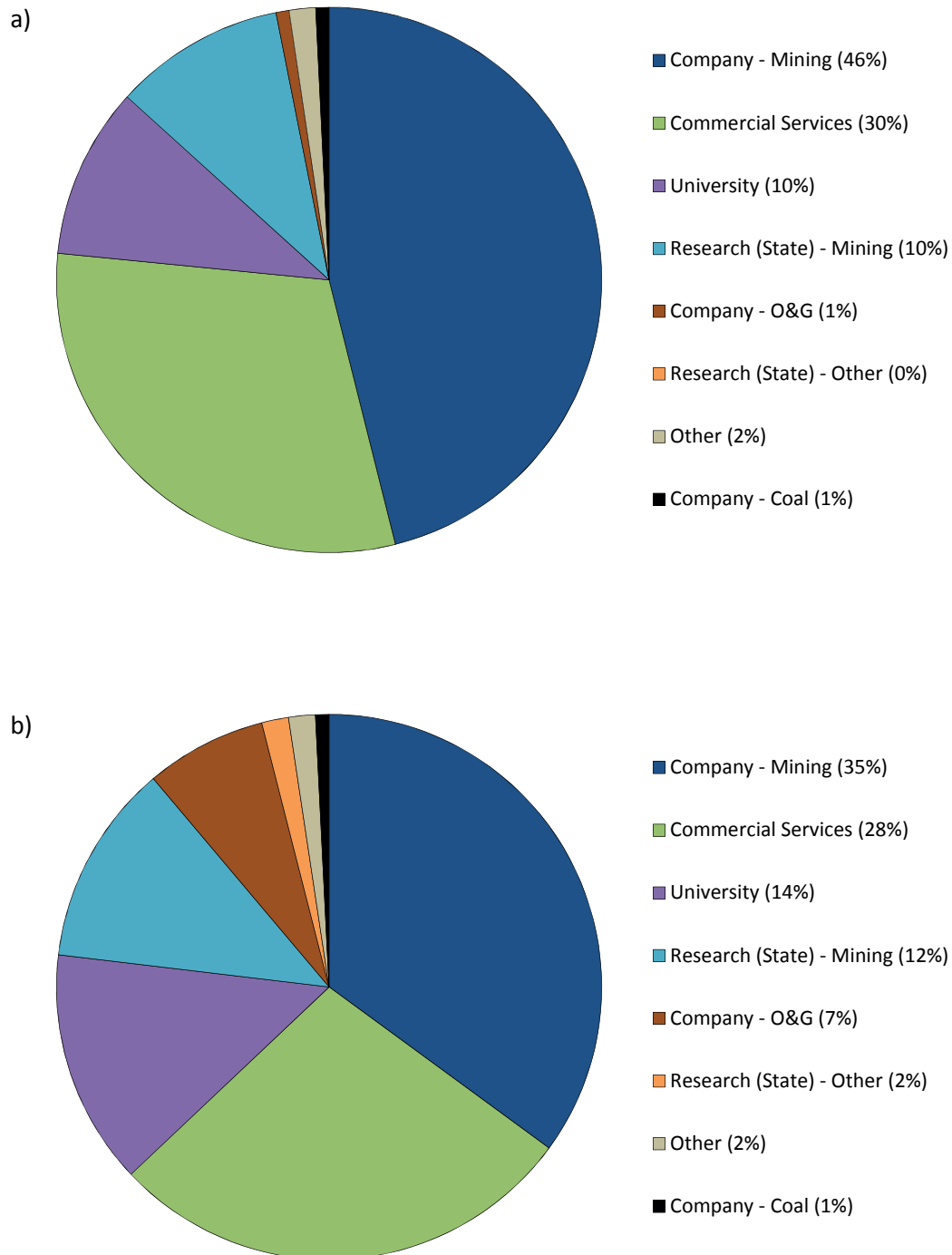


**Fig. 11:** Distribution of worldwide automated mineralogy systems (QEMSCAN + MLA) by groups of users, **a)** for 2008, **b)** for 2014.

### Application of ‘Automated Mineralogy’ in Research

The following section, describing the fields of application of automated mineralogy, is based on the investigation of publications of various sources. Three bibliographic databases were used for this purpose, Google Scholar, Scopus, and GeoRef. In total more than 1,700 publications related to automated mineralogy were found by this search, by end date 31<sup>st</sup> December 2014. When reading this section it should be remembered, that the textual content of an electronic document (e.g., a pdf file) is not searchable if the document pages consist of images which is often true for older volumes of journals as well as not computerised and thus manually scanned older documents (articles, conference abstracts, theses, ...). An unknown number of publications are not electronically available and not cited non-electronic documents can be completely hidden. Hence, a large number of undetected cases can be presumed and the total number of publications dealing with automated mineralogy may be somewhere between 2,000 and 3,000 by end date 31<sup>st</sup> December 2014. The scale in which automated mineralogy contributes to a publication differs enormous, from just one sentence in a publication to a methodological focus that dominates the entire publication.

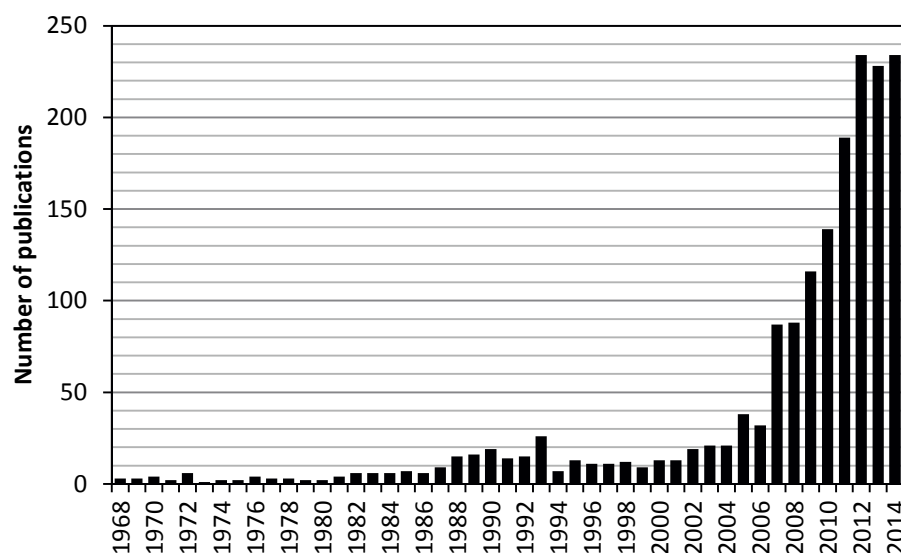


**Fig. 12:** Time series (1968-2014) of publications related to automated mineralogy (all system types).

An overview on the number of publications related to all system types of automated mineralogy in Fig. 12 shows less than 10 publications per year for the early years of system development until 1987. Between 1988 and 1993 a minor peak (up to 26 publications for the year 1993) can be seen which can be correlated with installation of the first QEM\*SEM systems and their initial commercialisation. After this time period the number of publications slightly decreased to 7-13 per year until 2001. From 2002 to 2004 the number is stable at a level of 20 publications per year and includes some of the first peer-reviewed publications related to the MLA technology. The years 2005 and 2006 show more than 30 publications each. This is followed by an abrupt rise to more than 80 publications per year for the time period 2007-2008. In these years the commercialisation of both QEMSCAN and MLA systems was well established and more than 100 automated mineralogy systems installed globally. From 2009 to 2012 each year shows a strong rise in

the number of publications per year (2009 – about 120; 2010 – about 140; 2011 – about 190; 2012 – about 230). For 2013 and 2014 each about 230 publications were found. It should be mentioned again that all numbers stated above are minimum numbers as there is an estimated number of unknown cases.

By comparing the publications relevant to QEMSCAN and MLA instruments it becomes apparent that QEMSCAN has always had the lead (Fig. 13). However, the difference between the numbers of publications based on the two systems varies significantly and is smaller between 2010 and 2012 and larger for 2013 and 2014. Concerning this it must be stated that the search for publications related to QEMSCAN is easier than the search for publications related to MLA. QEMSCAN is a unique and as a trademark registered acronym. Here, not only the previous acronym QEM\*SEM but also mistakes in writing such as QEM\*SCAN, QEMSEM, and QUEMSCAN had to be considered. In contrast, the search for publications related to the MLA technique is more complex as MLA is not a registered trademark and this acronym represents more than one hundred different meanings such as ‘Modern Language Association’, ‘Microlens Array’, ‘Mercury Laser Altimeter’, ‘Methyllycaconitine’, ‘Methyl Lactate’, ‘Multi-layer Absorption’, ‘Mouse Lymphoma Assay’, ‘Minimum Legible Area’, or ‘Machine Learning Algorithm’. However, the search for the full terms ‘Mineral Liberation Analyzer’ and ‘Mineral Liberation Analyser’ is not perfect as in several publications the acronym is used only. Thus it was found that a combination of the search terms “MLA” and "Mineral Liberation" gives the most extensive results. Hence, it can be stated that the difference in the number of publications related to QEMSCAN and MLA seen for 2013 and 2014 is not caused by not optimised search terms but as yet the basic cause could not be clarified. However, one general cause of the dominance of the number of QEMSCAN-related publications towards to MLA-related publications may be the about 10 years earlier development and commercialisation of the QEMSCAN technology.

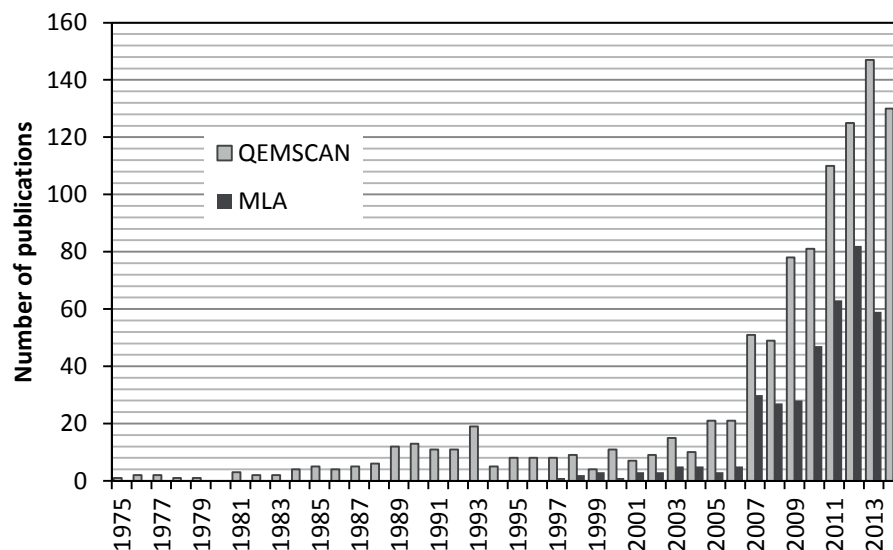


**Fig. 13:** Time series (1975-2014) of publications related to the QEMSCAN and MLA technologies.

The cumulative distribution of publications related to automated mineralogy by system type (end date 31<sup>st</sup> December 2014) shows that publications dealing with the QEMSCAN technology dominate the field by nearly 60% (Fig. 14). This is followed by MLA publications and publications related to other systems (including ‘multiple systems’ and ‘unknown system’). The recently introduced TIMA, RoqSCAN and INCAMineral systems contribute with 1% each.

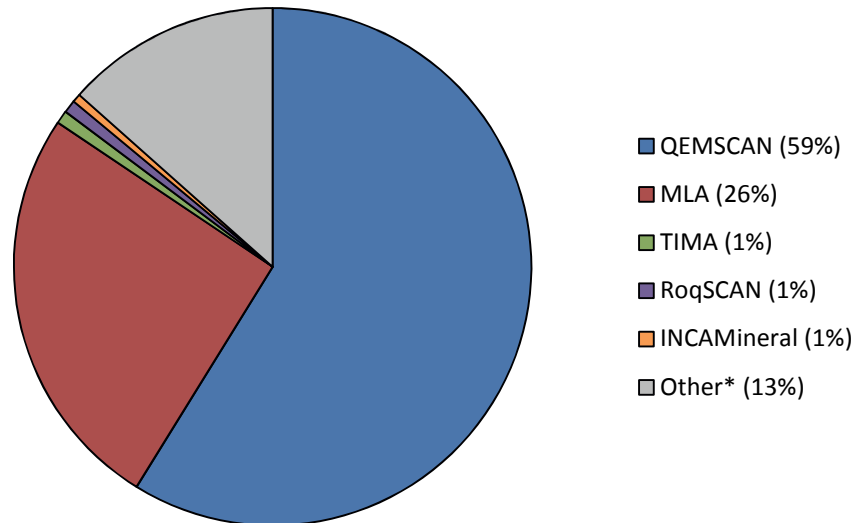


**Fig. 14:** Cumulative distribution of publications related to automated mineralogy (by system type, end date 31<sup>st</sup> December 2014). Note: Other\* includes also publications where multiple systems were mentioned or publications with an unknown (not named in detail) automated mineralogy system type.

The time series of publications related to all types of automated mineralogy shows a comprehensive view of all fields of application (Fig. 15). It should be stated that for a minor percentage of publications the allocation to just one field of application was debatable as some overlaps exist between different areas of application. In such a case the publication was allocated to the dominant area of application. The same is true for publications dealing with more than one area of application.

It was stated by Gottlieb (2008) that automated mineralogy was established to “automate the process needed to acquire process mineralogy information”. However, in Fig. 15b it can be seen that the first years were dominated not by mineral processing-related publications but by publications dealing with the methodology of the new automated mineralogy systems (Jones & Gavrilovic 1968, White et al. 1968, White et al. 1970, Lebedzik et al. 1973, Jones & Shaw 1974, Troutman et al. 1974, Reid & Zuiderwyk 1975, Frost et al. 1976, Grant et al. 1976, Grant et al. 1977, Hall 1977, Jones 1977, Jeanrot et al. 1978, Martens et al. 1978, Grant et al. 1979, Jeanrot 1980, Lee & Fisher 1980) and their physical principles (Reed 1968, Jones & Gavrilovic 1969, Beamond 1970, Matson et al. 1970, Taylor & Gottlieb 1986). It is obvious that methodology papers were common over the entire time series but their percentage decreased over time. The following publications are considered to be one of the most relevant publications for the established automated mineralogy systems: QEM\*SEM/QEMSCAN (Miller et al. 1982, Sutherland et al. 1988, Gottlieb et al. 2000, Pirrie & Rollinson 2011), MLA (Gu 1998, Gu 2003,

Fandrich et al. 2007), TIMA (Králová et al. 2012a, Králová et al. 2012b, Králová & Motl 2014), RoqSCAN (Oliver 2012, Oliver et al. 2013, Ashton et al. 2013a), INCAMineral (Liipo et al. 2012, Lang et al. 2013).

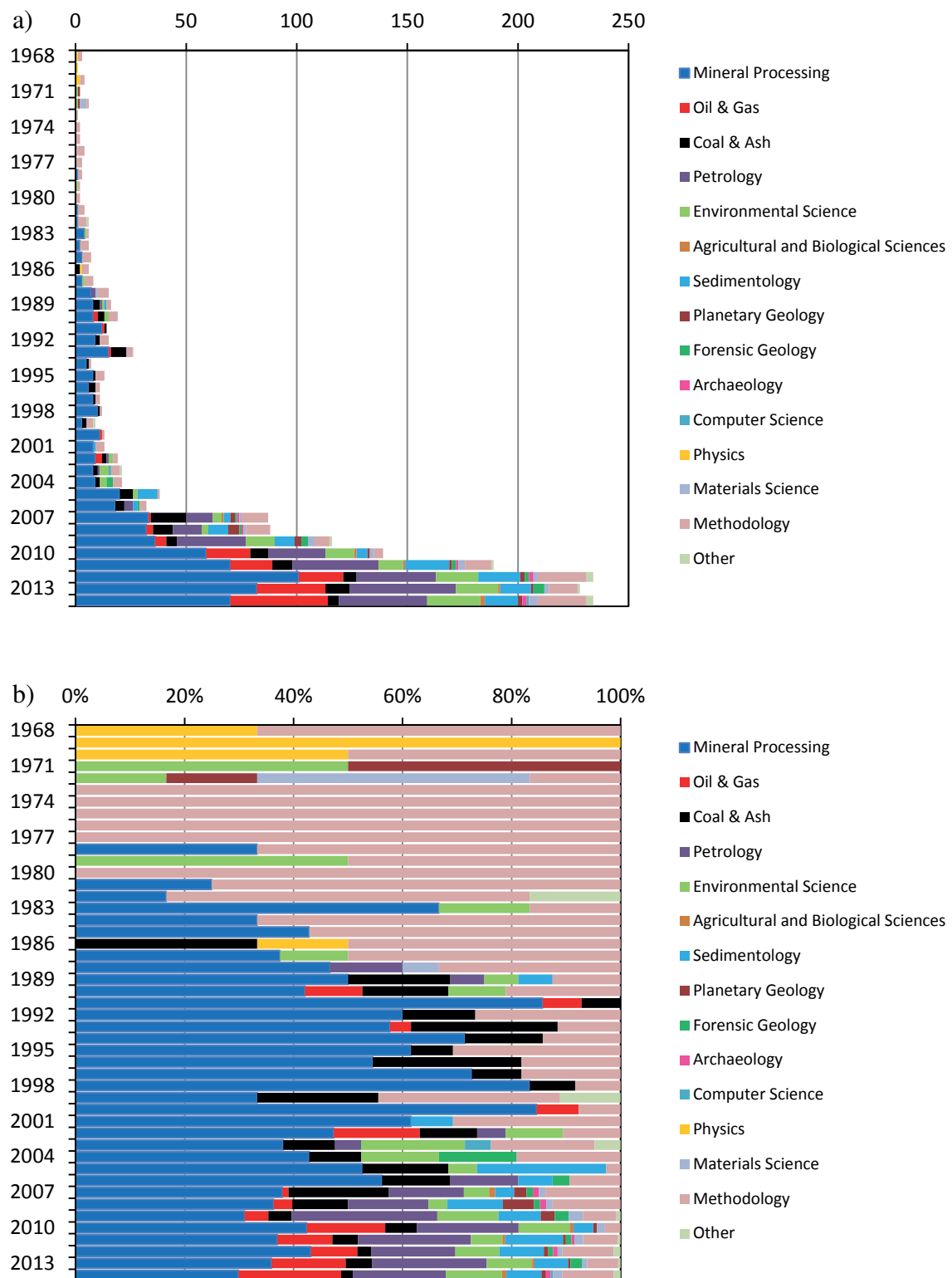


**Fig. 15:** Time series (1968-2014) of publications related to automated mineralogy by area of application, **a)** absolute data, **b)** normalised data.

The first automated mineralogy publication found in this study that has been related to mineral processing was published by Tilyard (1978) and from this point onwards mineral processing publications were the main area for automated mineralogy-related publications. In this sector, automated mineralogy is used to assess industrial products from mineral processing, such as feeds, middlings, concentrates and tailings (Table 3). Prior to the arrival of automated mineralogy this had to be conducted manually by optical reflected and transmitted light microscopy. The automation of such optical systems was under development but limited soon due to several complicating reasons such as the different behaviour of ore minerals and rock-forming minerals in reflected and transmitted light (Gottlieb 2008). This limitation directed further developments towards scanning electron microscopes and electron microprobes to try to improve mineral processing technologies such as comminution, screening, flotation, leaching or grade control. This again gave the possibility to compare ores and plant performance looking for relationships between ore characteristics and concentrate grade and recovery (cf. Gottlieb 2008). In Fig. 15b it can be seen that the peak of the share of publications related to mineral processing was reached in the 1990s and since then the share of such publications has been decreasing. However, it needs to be noted that this decrease is in relative terms mainly, as in absolute numbers the contributions towards mineral processing has still been increasing until 2012 (Fig. 15a). Some of the more relevant of in total more than 600 publications of this area of application were published by Allan & Lynch (1983), Petruk (1988a), Sutherland (1989), Sutherland & Gottlieb (1991), Wen Qi et al. (1992), Austin et al. (1993), Zamalloa et al. (1995), Lätti et al. (2001), Lotter et al. (2002), Lotter et al. (2003), Baum et al. (2004), Goodall et al. (2005), Lastra (2007), Pascoe et al. (2007), Hoal et al. (2009a), Oghazi et al. (2009), Butcher (2010), Ford et al. (2011), Celik et al. (2011), MacDonald et al. (2012), Mwase et al. (2012), and Agorhom et al. (2013).

The analysis of ores and associated gangue in drill cores and coarse-crushed samples from exploration projects and mines to be able to analyse the mineral and textural associations which helped to assess the potential of a deposit has become another typical application of automated mineralogy (Gottlieb 2008). Automated mineralogy is also used to help for the search for rare minerals as native gold or platinum group minerals. At the beginning of the development of automated mineralogy the focus was on sulphides as the EDS detectors were not able to detect light elements such as carbon, oxygen, fluorine and sodium (Gottlieb 2008). The improvement of the detectors allowed to discriminate metal oxides and carbonates and thus to analyse new types of ores, such as copper oxides and carbonates or nickel laterites as well as gangue mineral groups (silicates, oxides, and phosphates) (Sutherland et al. 1999). Recent applications in the field of ore characterisation, which accounts for mineral processing too, include among others base metals (sulphide and non-sulphide), precious metals, iron ores and heavy mineral sands.

The publication of papers dealing with the automated characterisation of primarily rocks and ores started in the late 1980s but were completely discontinued in the 1990s (Harrowfield et al. 1988, Walker et al. 1989) (Fig. 15). However, since 2000 several papers dealing with automated mineralogy related to petrology and/or ore characterisation were published, such as Benvie (2007), Goodall & Butcher (2007), Huminicki et al. (2007), Shaffer & Huminicki (2007), Kormos et al. (2008), Sikazwe et al. (2008), Smith et al.



(2008), Hoal et al. (2009b), Hoal et al. (2009c), Ross et al. (2009), Kelly et al. (2010), Ayling et al. (2011), Gräfe et al. (2011), Grammatikopoulos et al. (2011), Mondillo et al. (2011), Rollinson et al. (2011), Scott et al. (2011), Van der Merwe (2011), Huminicki et al. (2012), Mkhathshwa (2012), Mngoma (2012), Boni et al. (2013), Gregory et al. (2013), Potter-McIntyre (2013), Schmandt et al. (2013), Sciortino et al. (2013), Wilde et al. (2013), Anderson et al. (2014), Garagan (2014), McGladrey (2014), O'Driscoll et al. (2014), Santoro et al. (2014), and Tonžetić et al. (2014).

Since the 1990s samples of the petroleum (oil & gas) industry such as cores, cuttings/chips and related materials are in the focus of automated mineralogy (Fig. 15, Table 3). Automated mineralogy in oil and gas is applied to the characterisation of both conventional and unconventional reservoirs. For the petroleum industry automated mineralogy can not only provide quantitative mineralogical and textural information but also porosity data, on micro and macro scale. Systems with a high-resolution imaging system can even provide quantitative data for the nano-porosity level. Due to the high secrecy in this industry sector the number of relevant publications is limited. In Fig. 15 it can be seen that the publications found for the sector of the petroleum industry are scattered between 1990 and the mid-2000s. Since 2006 a continuous increase in the proportion of petroleum-related automated mineralogy paper is apparent. A list of available publications in this area of application of automated mineralogy includes Butcher et al. (2000), Butcher & Botha (2007), Messent & Farmer (2008), Sliwinski et al. (2009), Fröhlich et al. (2010), Lemmens et al. (2010), Ahmad & Haghghi (2012), Alkuwairan (2012), Koolschijn (2012), Wandler et al. (2012), Ashton et al. (2013b, c), Zijp et al. (2013), Ardila & Clerke (2014), Burtman et al. (2014), Ly et al. (2014), Marquez et al. (2014), and Sjølling et al. (2014).

Since the 1980s the characterisation of coals, their associated minerals and combustion residues has been an area of application of automated mineralogy. However, the share of publications related to this area is relatively erratic over time and ranges from zero to about 20% of all annually published papers in automated mineralogy (Fig. 15). Since the mid-2000s a systematic decrease in the proportion of coal-related automated mineralogy papers can be seen. The most imported publications of this area of application were published by Creelman et al. (1986), Gottlieb et al. (1989), Straszheim & Markuszewski (1989), Ghosal et al. (1993), Schimmoller et al. (1995), Galbreath et al. (1996), Wigley et al. (1997), Cropp et al. (2003), Liu et al. (2005), van Alphen (2007), Vuthaluru & French (2008), French & Ward (2009), Matjie et al. (2011), Klopper et al. (2012), and Rodrigues et al. (2013).

Environmental science is next to mineral processing one of the oldest areas of application of automated mineralogy (Fig. 15). One group of these publications covers the field of atmospheric aerosols/airborne dust such as Byers et al. (1971), Butcher et al. (2005), Hynes et al. (2007), Williamson et al. (2013), and Gasparon et al. (2014). Another group of environmental science-related publications such as Newman et al. (1989), Pirrie et al. (2009b), Simons et al. (2011), Redwan & Rammlmair (2012), Redwan et al. (2012), Kelm et al. (2014), and Rieuwerts et al. (2014) deals with contaminations, mainly caused by abandoned mining, such as waste rocks/tailings (including acid rock drainage and neutral rock drainage) and contaminated soils next to smelters.

**Table 3:** Common areas of application for the automated mineralogy technology, usable materials, and leading references.

Area of Application	Materials	References
Mineral Processing	feeds, concentrates, middlings, tailings from different stages of mineral processing	Allan & Lynch (1983), Petruk (1988a), Sutherland (1989), Sutherland & Gottlieb (1991), Wen Qi et al. (1992), Austin et al. (1993), Zamalloa et al. (1995), Lätti et al. (2001), Lotter et al. (2002), Lotter et al. (2003), Baum et al. (2004), Goodall et al. (2005), Lastra (2007), Pascoe et al. (2007), Hoal et al. (2009a), Oghazi et al. (2009), Butcher (2010), Ford et al. (2011), Celik et al. (2011), MacDonald et al. (2012), Mwase et al. (2012), and Agorhom et al. (2013).
Petrology/Ore Characterisation	primarily minerals, rocks (solid rocks), mineralisation/ores (without any relationship to mineral processing)	Benvie (2007), Goodall & Butcher (2007), Huminicki et al. (2007), Shaffer & Huminicki (2007), Kormos et al. (2008), Sikazwe et al. (2008), Smith et al. (2008), Hoal et al. (2009b), Hoal et al. (2009c), Ross et al. (2009), Kelly et al. (2010), Ayling et al. (2011), Gräfe et al. (2011), Grammatikopoulos et al. (2011), Mondillo et al. (2011), Rollinson et al. (2011), Scott et al. (2011), Van der Merwe (2011), Huminicki et al. (2012), Mkhathshwa (2012), Mngoma (2012), Boni et al. (2013), Gregory et al. (2013), Potter-McIntyre (2013), Schmandt et al. (2013), Sciortino et al. (2013), Wilde et al. (2013), Anderson et al. (2014), Garagan (2014), McGladrey (2014), O'Driscoll et al. (2014), Santoro et al. (2014), and Tonžetić et al. (2014).
Oil & Gas	cores, cuttings and related samples from productive or exploration wells in the petroleum industry	Butcher et al. (2000), Butcher & Botha (2007), Messent & Farmer (2008), Sliwinski et al. (2009), Fröhlich et al. (2010), Lemmens et al. (2010), Ahmad & Haghighi (2012), Alkuwairan (2012), Koolschijn (2012), Wandler et al. (2012), Ashton et al. (2013b, c), Zijp et al. (2013), Ardila & Clerke (2014), Burtman et al. (2014), Ly et al. (2014), Marquez et al. (2014), and Sølling et al. (2014).
Coal & Ash	coals, primarily associated minerals and combustion residues	Creelman et al. (1986), Gottlieb et al. (1989), Straszheim & Markuszewski (1989), Ghosal et al. (1993), Schimmoller et al. (1995), Galbreath et al. (1996), Wigley et al. (1997), Cropp et al. (2003), Liu et al. (2005), van Alphen (2007), Vuthaluru & French (2008), French & Ward (2009), Matjie et al. (2011), Klopper et al. (2012), and Rodrigues et al. (2013).
Environmental Science	atmospheric aerosols/airborne dust, contaminated materials, acid forming waste rock/acid rock drainage, neutral rock drainage, carbon storage/CO <sub>2</sub> injection/sequestration	Byers et al. (1971), Newman et al. (1989), Butcher et al. (2005), Hynes et al. (2007), Pirrie et al. (2009b), Armitage et al. (2010), Armitage et al. (2011), Simons et al. (2011), Redwan & Rammlmair (2012), Redwan et al. (2012), Armitage et al. (2013), Williamson et al. (2013), Gasparon et al. (2014), Kelm et al. (2014), Rieuwerts et al. (2014), and Swift et al. (2014).
Agricultural and Biological Sciences	soil, fertiliser, microbialites, microbes	Hoare (2007), Airo (2010), Lynch et al. (2013), Burne et al. (2014), and Pierson (2014).

**Table 3:** (continued).

Area of Application	Materials	References
Sedimentology	sediments, heavy minerals (without any relationship to mineral processing)	Riley et al. (1989), Frei et al. (2005), Knudsen et al. (2005), Pudmenzky et al. (2007), Paine et al. (2005), Bernstein et al. (2008), Speirs et al. (2008), Haberlah et al. (2010), Haberlah et al. (2011), Tsikouras et al. (2011), Wilton & Winter (2012), and Nie et al. (2013).
Planetary Geology	lunar and other extra-terrestrial materials or simulants, impact melt-related materials	Görz et al. (1971), Görz et al. (1972), Ly et al. (2007), Rickman et al. (2008), Botha et al. (2009), and Young et al. (2012).
Forensic Geology	all kind of materials related to criminological/forensic investigations, historic pharmaceutical materials	Pirrie et al. (2004), Pirrie et al. (2009a), Pirrie (2009), and Pirrie et al. (2013).
Archaeology	pottery, ancient ceramics, stone implements and other ancient artefacts	Knappett et al. (2011), Andersen et al. (2012), and Šegvić et al. (2014).
Materials Science	recent ceramics, refractories, linings, polymers, asphalt	Thaulow & White (1972), White et al. (1972), Stjernberg et al. (2010), Pal et al. (2012), Ulsen et al. (2012), and Kahn et al. (2014).
Other	paleontological relicts	Bishop & Biscaye (1982), Chin et al. (2013), Good & Ekdale (2014), and Gu et al. (2014).

A relatively new application in environmental science pertains to the characterisation of rocks for their CO<sub>2</sub> storage potential. Here automated mineralogy contributes with publications from Armitage et al. (2010), Armitage et al. (2011), Armitage et al. (2013), and Swift et al. (2014).

Agricultural and Biological Sciences are areas of application for the automated mineralogy only in rare exceptional cases (Table 3). Just five publications could be found by this search (Hoare 2007, Airo 2010, Lynch et al. 2013, Burne et al. 2014, Pierson 2014). In all of them automated mineralogy is just an auxiliary technique.

In contrast, sedimentology is an important area of application for automated mineralogy and since the mid-2000s it contributes to the total number of publications by about 10% (Table 3, Fig. 15). The main fields of research are provenance studies, the characterisation of heavy mineral deposits, aeolian and fluvial geomorphology, glaciology and the search for indicator minerals in till and stream sediments. Relevant publications for this area of application were published by Riley et al. (1989), Frei et al. (2005), Knudsen et al. (2005), Pudmenzky et al. (2007), Paine et al. (2005), Bernstein et al. (2008), Speirs et al. (2008), Haberlah et al. (2010), Haberlah et al. (2011), Tsikouras et al. (2011), Wilton & Winter (2012), and Nie et al. (2013).

A further but relatively small field of application for automated mineralogy is planetary geology where the technology is being used to analyse lunar and other extra-terrestrial samples and simulants (Table 3). As early as 1971 and 1972 lunar samples were studied by the CESEMI technology (Görz et al. 1971, Görz et al. 1972). More recent

publications of this area of application include Ly et al. (2007), Rickman et al. (2008), Botha et al. (2009), and Young et al. (2012).

The application of automated mineralogy in forensic geology is a relatively exotic area of application and since 2004 not more than 20 publications related to this subject were published (Fig. 15, Table 3). The vast majority of them are related to the work of Duncan Pirrie and Gavyn K. Rollinson of the Camborne School of Mines, UK (Pirrie et al. 2004, Pirrie et al. 2009a, Pirrie 2009, Pirrie et al. 2013). Also an exotic area of application is the characterisation of archaeological artefacts by automated mineralogy. Here, less than 10 publications were published since 2007. The three most important of these are Knappett et al. (2011), Andersen et al. (2012), and Šegvić et al. (2014).

Materials Science is an area of application for automated mineralogy since the first studies in 1972 (Thaulow & White 1972, White et al. 1972) using the CESEMI technology (Fig. 15, Table 3). Some more recent publications were published by Stjernberg et al. (2010), Pal et al. (2012), Ulsen et al. (2012), and Kahn et al. (2014).

Lastly some publications were published that do not fit in one of the previous categories of application of automated mineralogy and were included into 'Other' (Table 3, Fig. 15). Examples of such publications are Bishop & Biscaye (1982), Chin et al. (2013), Good & Ekdale (2014), and Gu et al. (2014).

In summary, it can be seen that the areas of application for the technology of automated mineralogy were dominated by methodology publications at the beginning and mineral processing-related publications during the 1990s and 2000s. The latter still have the most important share (about 30% in 2014) on the field of automated mineralogy but with a decreasing predominance since about the year 2000 (Fig. 15). These area of application is followed nowadays (by percentage of publications in 2014) by the characterisation of rocks/ores and analyses related to the petroleum (oil & gas) industry (each about 15-20%). Environmental science-related and methodology publications are the next two important areas of application by 2014 (each about 10%). All other areas of application of automated mineralogy mentioned above are of minor importance currently. In Fig. 15 it can be seen that the number of areas of application of automated mineralogy increased in the course of time. Even though some areas of application contribute only to a smaller proportion (and partly erratic) of the total number of publications all of them show an increasing total number of publications in the course of time. Areas of application with a growing share in the near future might be the petroleum industry, petrology, and environmental science, based on the development of the proportions since 2012 (Fig. 15a).

## 1.1 Motivation and Approach

Mineral processing-related studies have been the main field of application for automated mineralogy since the development of the first SEM and electron microprobe-based instruments in the 1970s. As elucidated in the previous section, several other fields of application for automated mineralogy appeared over time. However, here the automated mineralogy instrument were often just used as a supporting instrument for broadly conceived studies so that for example comprehensive MLA studies are less common than would be expected by the total number of automated mineralogy literature (see section above).

Regarding the type of sample material it should be reminded, that various studies were performed using processed (granular) materials but considerably fewer studies used thin sections for their measurements. In the case of studies conducted on granular materials samples containing metal ore dominate by far and non-metallic materials are less common. For the sample preparation of granular material the methodology using epoxy resin as embedding medium predominates by far, since this is the perfect method for almost all types of minerals. Unfortunately this method cannot be used as soon the sample material contains minerals of very low density (e.g., graphite).

The motivation behind the three studies of this thesis was to provide a broader view over the capabilities of the MLA technology beyond the everyday standard analyses. Furthermore, efforts were made to develop and test novel analytical approaches for MLA investigations. The first study approaches the question if silicate raw material containing a valuable mineral that cannot be easily distinguished by its EDS spectrum from gangue minerals, can be analysed as effectively and reliably as a raw material with oxide or sulphide ore minerals. The approach for the second study of this thesis was to increase the understanding of the possibilities for the characterisation of graphite-bearing samples by the MLA technique. This application is entirely novel for automated mineralogy as it needs to resolve the difficulty of suitable sample preparation and independent verification of results obtained by MLA. The third study was conducted to evaluate the benefits of an additional MLA measurement on the (given the possibilities at that time) well-studied samples of a previous research project. A further motivation of this study was to show that it is possible by MLA to detect, quantify and characterise even very small amounts of rare minerals.

## Chapter 2: Methodology

### 2.1 Functional Principle of the FEI Mineral Liberation Analyser

The FEI Mineral Liberation Analyser (MLA) as the sole instrument used for all automated mineralogy measurements for the three research studies of this thesis will be described hereinafter in detail. The MLA solution is based on a scanning electron microscope (SEM) of the FEI Quanta SEM product line. For the particular analyses of this work a Quanta 600 FEG system and a Quanta 650 FEG system were used at the Department of Mineralogy of the TU Bergakademie Freiberg, Germany (Fig. 16).



**Fig. 16:** MLA 650 FEG system in the Geometallurgy Laboratory at the Department of Mineralogy, TU Bergakademie Freiberg.

#### 2.1.1 Hardware and Instrument Conditions

The FEI Quanta SEM product line was introduced in 2001 (FEI Company 2001). This series of SEMs offers a high image resolution and can be used for the widest range of samples. The Quanta SEMs can be operated in high vacuum, low vacuum or ESEM (environmental scanning electron microscope) mode. However, for MLA analyses only the high vacuum mode is convenient, currently. Here, the pressure range should be in the order of  $10^{-5}$  to  $10^{-7}$  Pa. To achieve an excellent high vacuum the Quanta SEM is equipped with a build-in turbo molecular pump (TMP) and two external rotary pre-vacuum pumps (PVP)

(FEI Company 2009d). A general overview of the Quanta SEM instrument and its external parts can be seen in Fig. 17. The specimen chamber/column section of the Quanta is isolated from the gun section so that the latter is still under ultra-high vacuum (normally between  $10^{-8}$  and  $10^{-10}$  Pa) while the chamber door is open. This enables a fast pumping, a short time to stabilise the electron beam and thus a fast analyses start after specimen change. The gun section of the SEM is equipped with two ion getter pumps (IGP) to allow the permanent ultra-high vacuum. External parts of the SEM are a water cooler which is used to cool down parts of the SEMs gun and column sections, a compressor for compressed air (required for valves and SEM levelling) and an uninterruptible power supply unit to supply emergency power if the regular power source fails (FEI Company 2009c, 2011b). In addition, the Geometallurgy Laboratory at the Department of Mineralogy is equipped with an air conditioning to keep the Quanta SEMs at a constant temperature level.

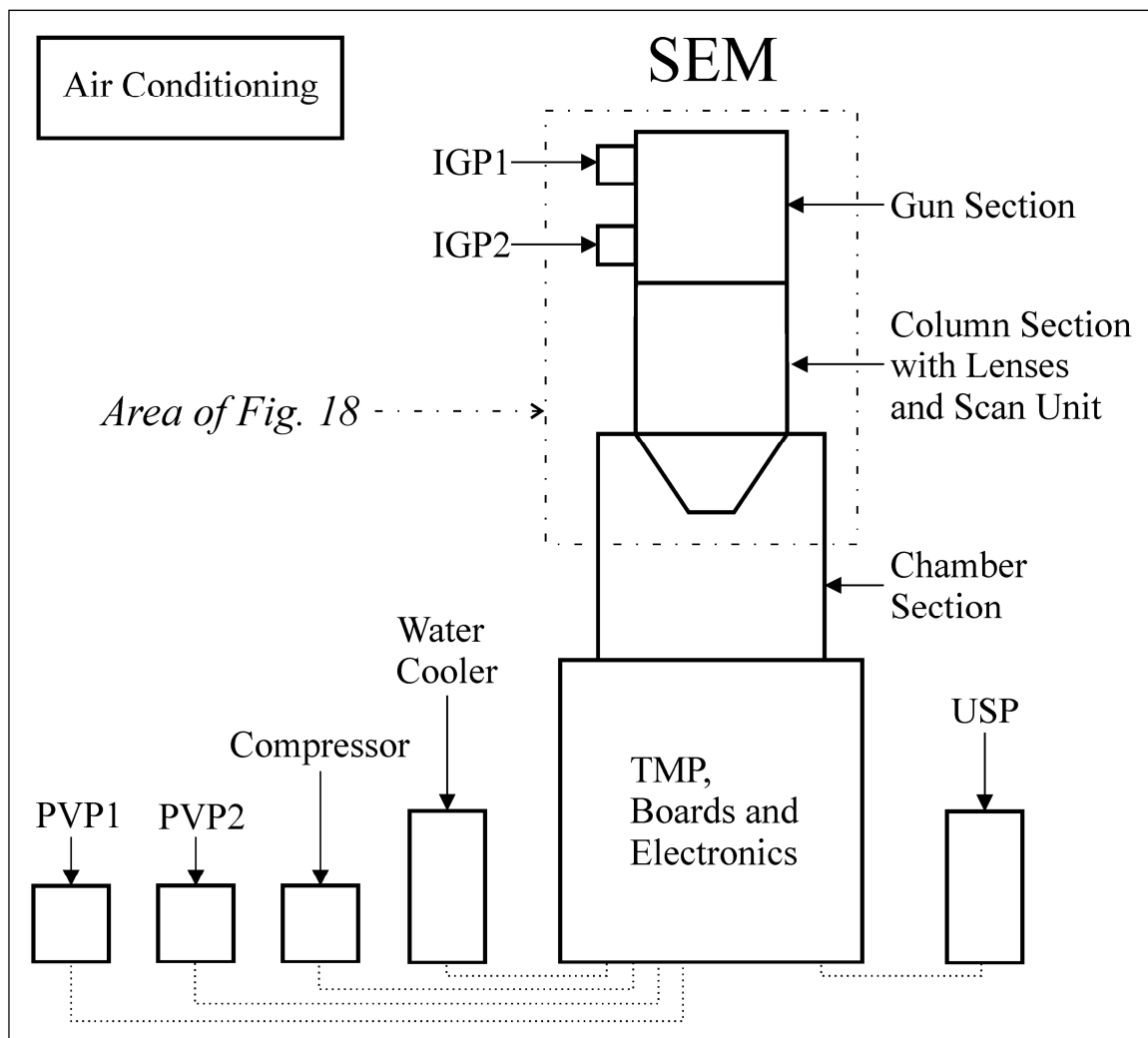


**Fig. 17:** Greatly simplified overview of the external and internal parts of the Quanta SEM (IGP – Ion Getter Pump, PVP – Pre-Vacuum Pump, TMP – Turbo Molecular Pump, USP – Uninterruptible Power Supply).

The Quanta SEMs consist of four main components (Fig. 18) (FEI Company 2009d). The electron source/gun emits the electron beam. The lens system consisting of several electromagnetic lenses is used to focus the electron beam and after passing the lens system

the beam hits the specimen surface. A lens aperture size of 50  $\mu\text{m}$  (position 3 at the final lens aperture strip) was used for all analyses of this study. The scan unit moves the beam in a raster pattern over the specimen. The detection unit collects and converts different types of signals produced by the interaction of the electron beam with the specimen surface such as backscattered electrons, secondary electrons and X-rays.

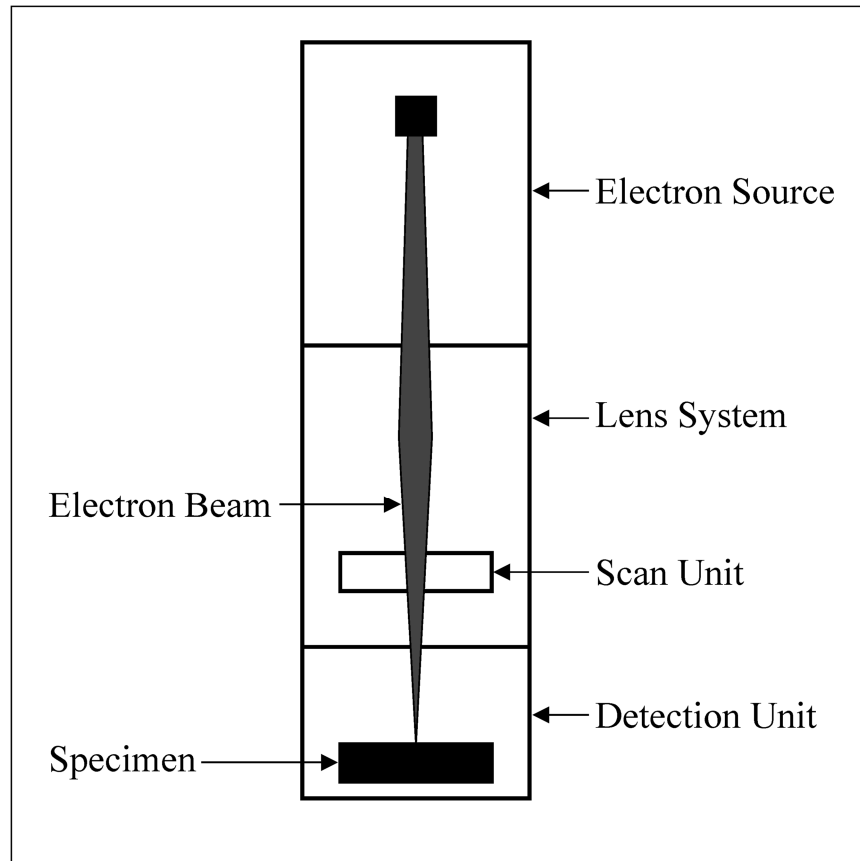


**Fig. 18:** Schematic overview of the general components of the Quanta SEM instrument.

Quanta SEMs can be purchased either with a tungsten filament cathode or with a field emission gun (FEG) (FEI Company 2014a). The two systems used for all measurements of this study are equipped with Schottky type FEGs. These Schottky emitters are made by coating a tungsten crystal with a layer of zirconium oxide (Scheu & Kaplan 2012). In comparison to tungsten cathodes a FEG produces a beam with a smaller diameter, a greater current density and thus a better image brightness, spatial resolution and improved signal-to-noise ratio. A second advantage is a greatly increased emitter lifetime in comparison to tungsten cathodes (Nabity et al. 2007).

The beam of electrons generated by the FEG is focused by the lens system and scanned horizontally across the specimen in two perpendicular (x and y) directions (raster scanning) by the scan unit (Fig. 18). This causes the electron beam to sequentially cover a rectangular area on the specimen (Fig. 19). The primary electrons emitted by the electron emitter impinge on the specimen surface and slow down through inelastic interactions with outer atomic electrons, while elastic deflections by atomic nuclei determine their spatial distribution (Egerton 2005, Reed 2005).



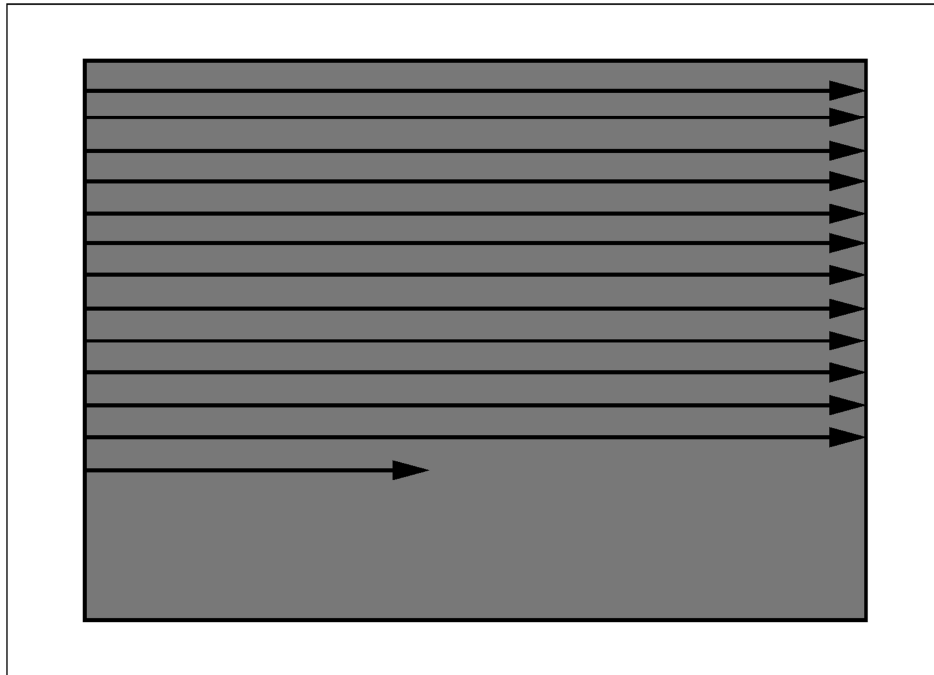


**Fig. 19:** Functional principle of the raster scanning of the electron beam across a specimen surface (grey).

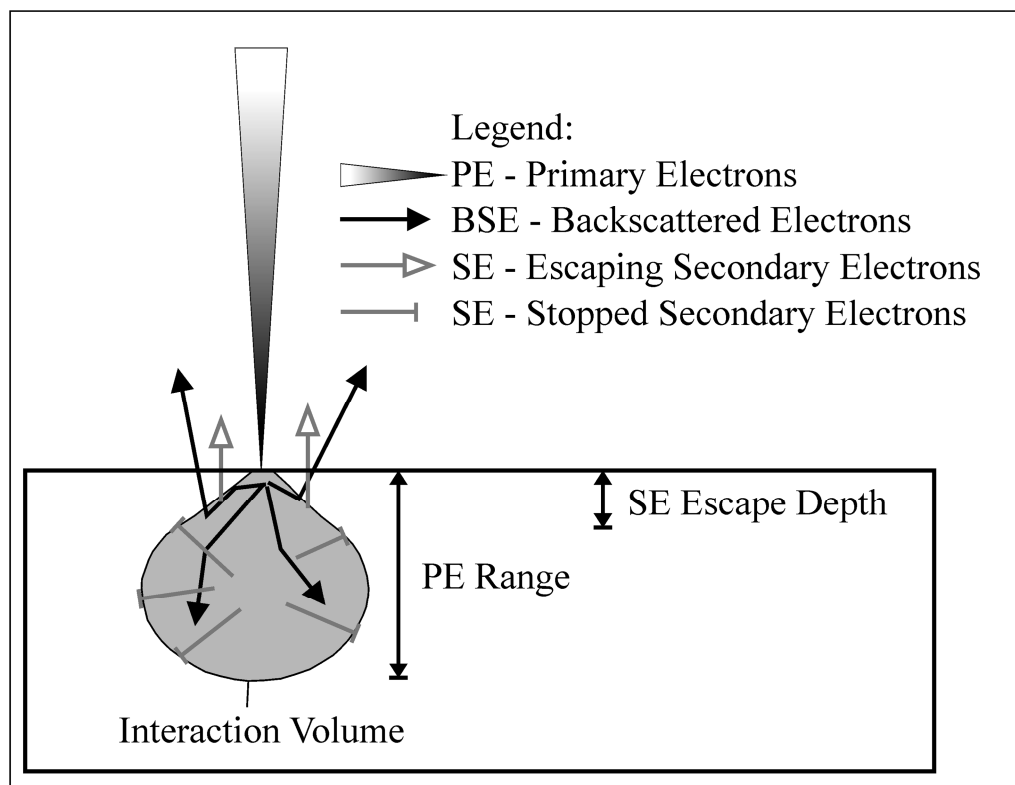


**Fig. 20:** Schematic overview of the electron scattering processes beneath a specimen's surface (modified after Molhave (2006)).

Some of the backscattered electrons leave the specimen and re-enter the surrounding vacuum in which case they can be collected as a backscattered electron (BSE) signal (Fig. 20). This fraction of electrons (backscattering coefficient  $\eta$ ) is strongly dependent on the atomic number  $Z$  of the elements respectively the average atomic number  $Z$  of the mineral

on the spot where the electron beam impinges on the specimen (Fig. 21) (Heinrich 1966, Egerton 2005). According to Heinrich (1966) this dependence can be approximately expressed by the following equation (2.1).

$$\eta(Z) = -0.0254 + 0.016Z - 1.86 \times 10^{-4}Z^2 + 8.31 \times 10^{-7}Z^3 \quad (2.1)$$

However, this is valid only for the energy range from 30 to 5 keV and more complicated for energies below 5 keV (Reichert 2007). In general, the dependence results in BSE images showing variations in chemical composition of a specimen, with minerals having a lower average atomic number (e.g., silicates, carbonates) appear darker and minerals having a higher atomic number (such as oxides, phosphates, sulphides) appear lighter (Reed 2005).

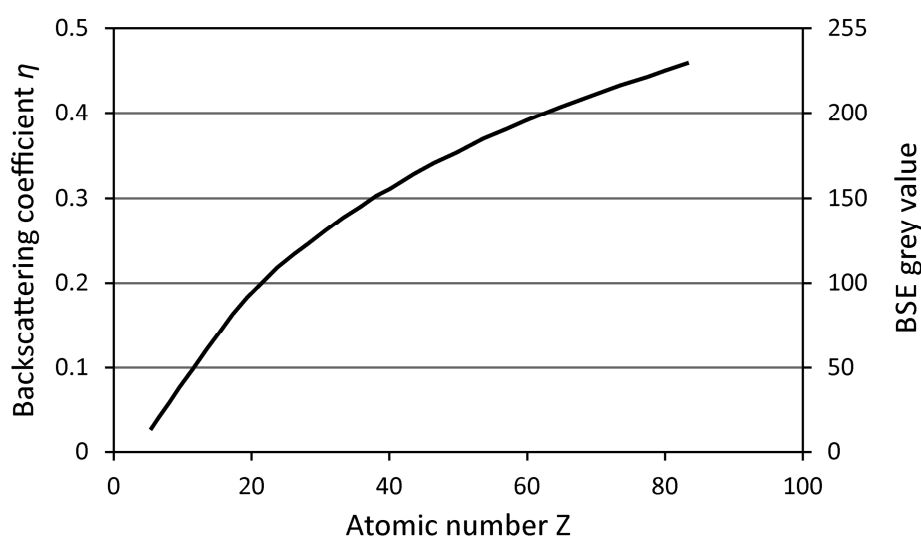


**Fig. 21:** Schematic relationship between backscattering coefficient  $\eta$ , atomic number  $Z$  and BSE grey value (modified after Reed (2005) and FEI Company (2011a)).

In this context, it should be considered that chemically identical minerals, such as calcite and aragonite (both  $\text{CaCO}_3$ ) or rutile, anatase and brookite (all  $\text{TiO}_2$ ) cannot be distinguished by compositional contrast, i.e., BSE grey value, as their atomic number  $Z$  is identical. The same applies to chemically different minerals which have a very similar atomic number (e.g., hematite [ $Z = 20.6$ ] and pyrite [ $Z = 20.7$ ]). A relative difference of about 1% in the BSE coefficient is needed to distinguish between adjacent minerals in BSE images (Reed 2005).

In addition to the interactions of electrons with outer atomic electrons, interactions between entering electrons into the specimen and atomic nuclei give rise to the emission of X-ray photons (Egerton 2005, Reed 2005). These characteristic X-ray photons can be detected by X-ray spectrometers/detectors. The Quanta SEMs at the Department of Mineralogy, TU Bergakademie Freiberg, used for this work, are equipped each with two silicon drift energy dispersive (SDD-EDS) X-ray spectrometers of Bruker Corporation. The Quanta 600 FEG system is equipped with dual XFlash 5010 detectors and the Quanta 650 FEG system with dual XFlash 5030 detectors (Bruker AXS 2010a, b). These SDD X-ray detectors allow high-speed spectra acquisition and communicate with the SEM over

QUANTAX signal processing units and the QUANTAX ESPRIT software. In addition, a number of other detectors are available for the Quanta SEM series. An overview of these detector types and areas of application can be seen in Table 4.

**Table 4:** Detector types available for the Quanta SEM series and areas of application (after FEI Company (2009c, d)).

<b>Detector Type</b>	<b>Area of Application</b>
Concentric Backscattered detector (CBS)	backscattered electrons (BSE) in high and low vacuum mode; required for MLA analysis
Everhart-Thornley detector (ETD)	secondary electrons (SE) in high vacuum mode
Energy Dispersive Spectroscopy detector (EDS)	X-rays/elemental analysis; required for MLA analysis
Infrared CCD camera	sample and stage orientation in specimen chamber
Wavelength Dispersive X-ray Spectrometry detector (WDS)	X-rays/elemental analysis
Electron Backscatter Diffraction detector (EBSD)	electron backscatter diffraction pattern
Cathodoluminescence detector	cathodoluminescence
Large Field detector (LFD)	SE + BSE in low vacuum mode
Gaseous Secondary Electron detector (GSED)	SE in low vacuum mode
Gaseous Backscattered Electron detector (GBSD)	SE + BSE in ESEM mode
Gaseous Secondary Electron detector (GAD)	SE in ESEM mode
Scanning Transmitted Electron Microscopy detector (STEM I)	transmitted electrons in high vacuum mode
Wet Scanning Transmitted Electron Microscopy detector (Wet STEM)	transmitted electrons in ESEM mode
Annular STEM detector (STEM II)	transmitted electrons in high vacuum mode
Low Voltage, High Contrast detector (vCD)	BSE in high and low vacuum mode
Scintillation InColumn detector (ICD)	SE in beam deceleration mode

### 2.1.2 EDS Spectrometer, BSE Image and Probe Current Calibration

The dual Bruker SDD-EDS X-ray spectrometers on both MLA systems at the Geometallurgy Laboratory of the Department of Mineralogy, TU Bergakademie Freiberg allow spectra acquisition times of up to 5 milliseconds and less. In this process 2,000 X-ray photons are acquired at each analysis point. This requires a highly accurate X-ray spectrometer calibration which shall be conducted before each measurement. The fully automatic spectrometer calibration corrects the energy axis of the EDS spectrometer and to perform this calibration a sample of known composition is required - ideal is a single element sample (Bruker Nano GmbH 2011). For this purpose a pin of pure copper metal mounted in a small standard block (see Fig. 23) is used at the Geometallurgy Laboratory. A flowchart of all calibrations to be performed prior to the start of a MLA measurement is shown in Fig. 22.

The BSE image quality depends upon the accelerating voltage, beam current, working distance, and thickness of the carbon coating on the specimen surface. The BSE image quality and especially BSE image stability is a critical factor for MLA analysis as a

perfect and stable BSE image is crucial for an accurate image processing and thus important for reliable data collection. To achieve this, set-up to a fixed working distance (distance of the specimen top surface to the SEM's objective lens) as well as a standardised BSE image calibration has to be conducted to allow measurements with a high accuracy and precision. For the analyses of this study an analytical working distance of 10.9 mm (for the MLA 600 FEG system) and 12.0 mm (for the MLA 650 FEG system) was used, respectively. Prior to the MLA measurement-related BSE image calibration a general BSE image optimisation at the SEM is highly recommended. After focussing, the stigmator control can be used to correct image astigmatism. The source tilt function corrects a potential imaging illumination drop and the lens alignment function minimises the objective imaging shift during focusing (FEI Company 2009d).

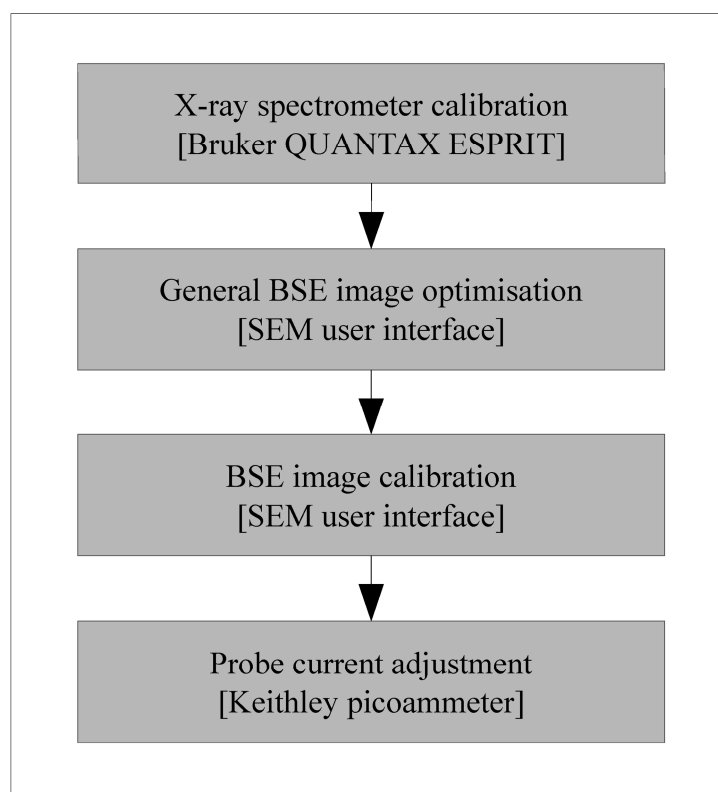


**Fig. 22:** Flowchart of calibrations to be performed prior to the start of MLA measurements and respective software/hardware needs to be used.

To calibrate the BSE image prior the MLA measurements each FEI specimen holder is equipped with a small standards block ( $\varnothing$  10 mm) consisting of three metal pins (gold, silver, and copper) and three homogeneous mineral grains (galena, chalcopyrite, and quartz) (Fig. 23). Depending on the type of sample material a different calibration can be conducted. For sulphidic materials a calibration using the gold pin is recommended as sulphides, in general, have a high mean atomic number. In contrast, for non-sulphidic materials a calibration using the copper pin is suggested to obtain a higher image contrast between the silicates having lower mean atomic numbers. The BSE image calibration for MLA measurement is performed by setting up the BSE grey level of the chosen material in the standards block (e.g., gold) to about 250 (by changing the contrast value in the SEMs user interface) and setting up the BSE grey level of the background material (typically

epoxy resin) to about 20 (by changing the brightness level in the SEMs user interface). As an alternative a Faraday cup (if provided on the specimen holder) can be used to set the background BSE grey level to about 5. It has to be noted that BSE image calibration for MLA can only be performed manually. In contrast, both BSE image calibration and EDS spectrometer calibration is done semi-automatically in the QEMSCAN software (FEI's second automated mineralogy solution).

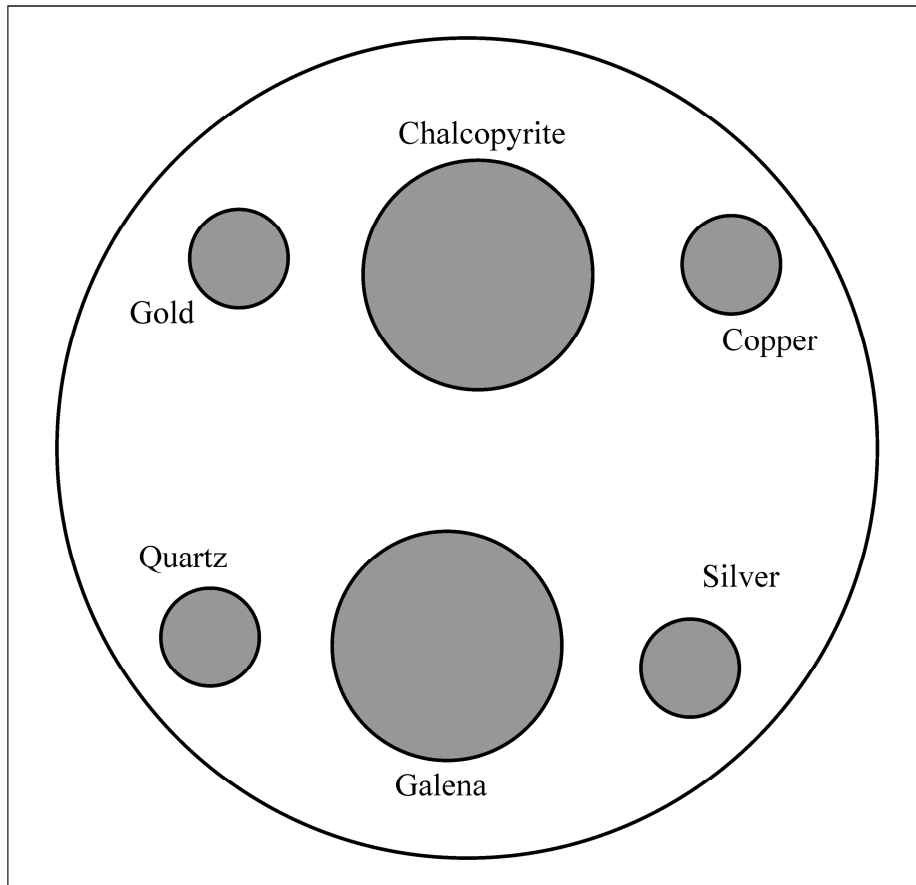


**Fig. 23:** Sketch of standards block for X-ray and BSE image calibration consisting of three metals and three minerals.

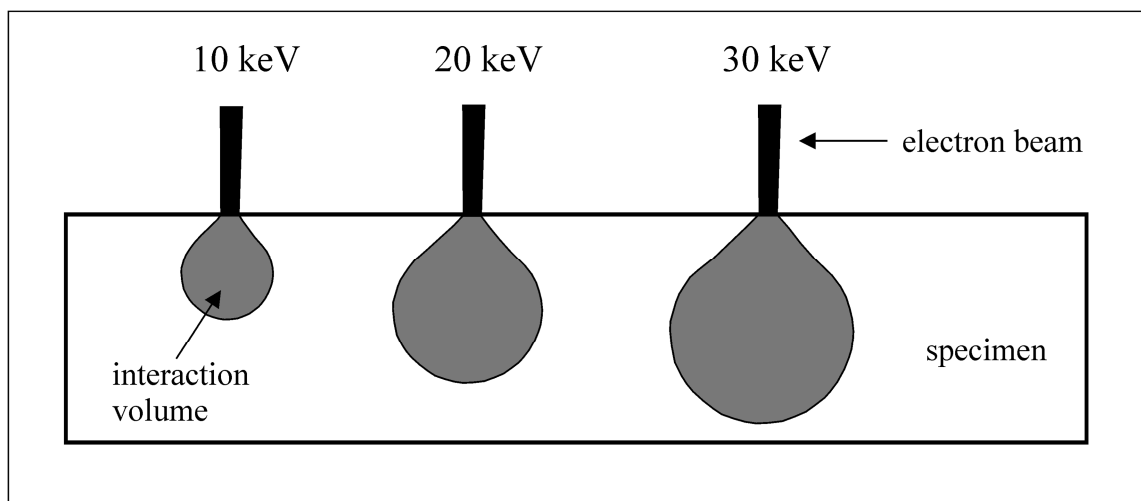


**Fig. 24:** Schematic overview of the relationship between beam energy and interaction volume (modified after (Egerton 2005)).

For SEM-based image analysis with FEIs automated mineralogy instruments two fixed overall electron beam accelerating voltage settings have become the preferred choice. An accelerating voltage of 15 kV is mainly used for sulphide-free specimens (rock sections, sediments, organic matter), whereas for ore-bearing samples and sulphide-rich specimens an accelerating voltage of 25 kV is used. It has to be noted that a higher accelerating voltage causes a larger interaction volume of the electron beam with the specimen than a lower accelerating voltage (Fig. 24) (Egerton 2005).

To allow reliable and repeatable results of the MLA measurement the SEM has to be set-up to a specific fixed probe current which shall be stable during the whole measurement time. For all measurements of this study the probe current was set-up to 10 nA using a Keithley Instruments Model 6485 picoammeter. By adjusting the beam spot size the probe current can be changed. A larger spot size causes a higher probe current and a smaller spot size results in a lower probe current. In general, the spot size number for a 10 nA probe current setup was in the range of 5 and 6 for all measurements of this study. It has to be noted that the spot size number shown by the Quanta user interface is not the spot diameter as the spot diameter depends on spot size number and accelerating voltage. For spot size number 5 and 25 keV accelerating voltage the theoretical spot diameter is about 4-5 nm and for spot size number 6 and 25 keV accelerating voltage the theoretical spot diameter is about 9 nm (FEI Company 2009d).

### **2.1.3 MLA Measurement – Comprehensive Description**

After the SEM has been set-up a MLA measurement can be performed. In the ‘Basic Setup’ of the MLA Measurement software parameters such as measurement modes, BSE image settings, particle feature and separation settings (e.g., specific grey value for the background of the BSE image), X-ray acquisition settings, and measurement finalisation settings can be determined. In the ‘Online Setup’ of the MLA Measurement software the SEM conditions will be recorded and the measurement area can be defined (FEI Company 2011a). To understand the behaviour of the different MLA measurement modes a general description of the MLA measurement functional principle has to be given first. A flowchart of the first part of this functional principle can be seen in Fig. 25.

#### **Functional Principle**

At first a BSE image (a so-called frame) is acquired, followed by particulation and segmentation of this image (Gu 2003, Fandrich et al. 2007, FEI Company 2011a). Considering that, the user has to define a specific grey value for the background of the BSE image (= grey value of the epoxy resin) in the MLA Measurement software if the sample is a grain mount (= consists of granular material). Otherwise the user has to disable the background value in the setup if the specimen is a solid rock or an ore section. The particulation feature consists of three steps (background removal, de-agglomeration, and clean-up) and makes sense only in the case if the sample is a grain mount (Fig. 26) (Gu 2003, Fandrich et al. 2007, FEI Company 2011a).

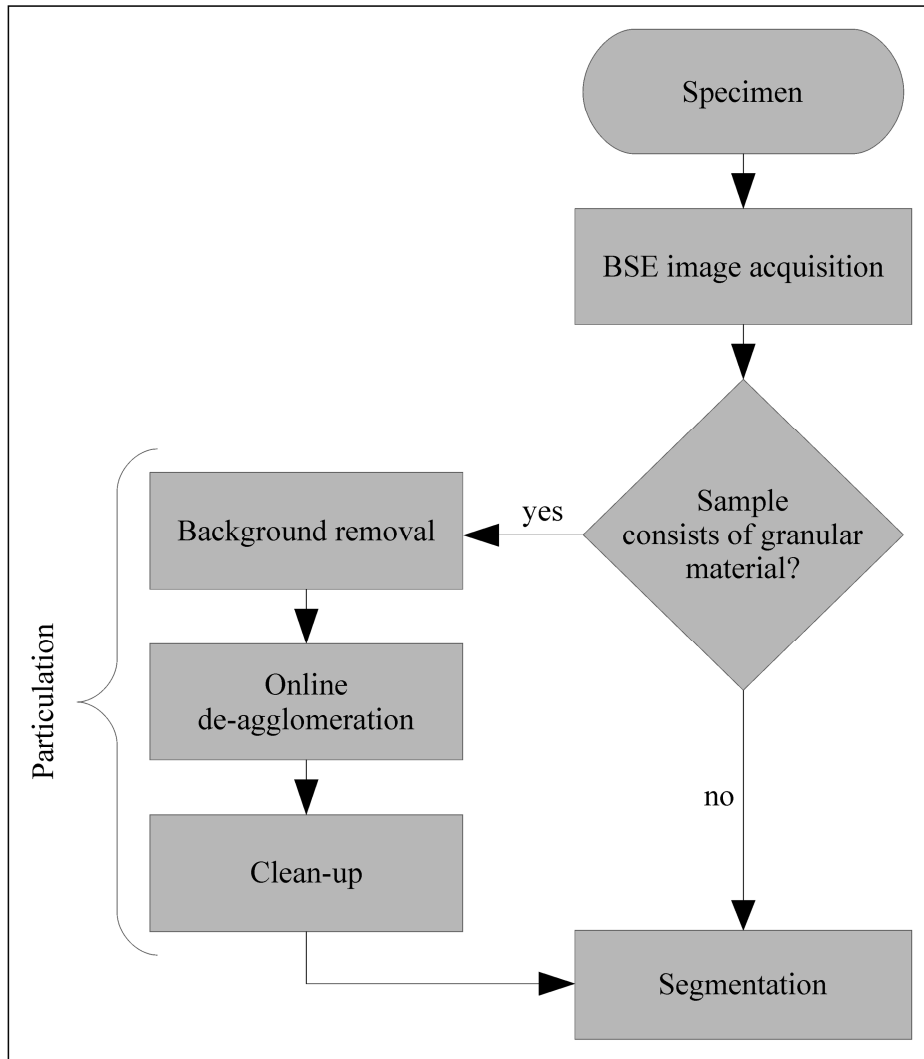


**Fig. 25:** Flowchart of the functional principle of the BSE image processing during the MLA measurement.

### Particulation Feature

The particulation starts by removing the background of the BSE image (Fig. 26b). After background removal any potential touching particles in the image are separated by online de-agglomeration (Fig. 26c). At this, three shape factors (circular ratio, rectangular ratio, and combined ratio) determine if a particle is agglomerated respectively is touching another particle. If the sample is a solid rock or an ore section a de-agglomeration is unnecessary. The de-agglomeration step is followed by a clean-up step (Fig. 26d). Its purpose is to remove any undersize particles generated by sample preparation (e.g., dust in air bubbles) or online de-agglomeration and to remove any particles touching the edge of the frame, if desired. The latter happens only if this feature was selected by the user in the measurement setup. (Gu 2003, Fandrich et al. 2007, FEI Company 2011a)

### Segmentation Feature

The segmentation feature works for both grain mounts and solid sections. It specifies the internal structures of a particle based on its BSE grey level characteristics by delineation of mineral grains within particles and determination of grain boundaries (Fig. 27). In addition

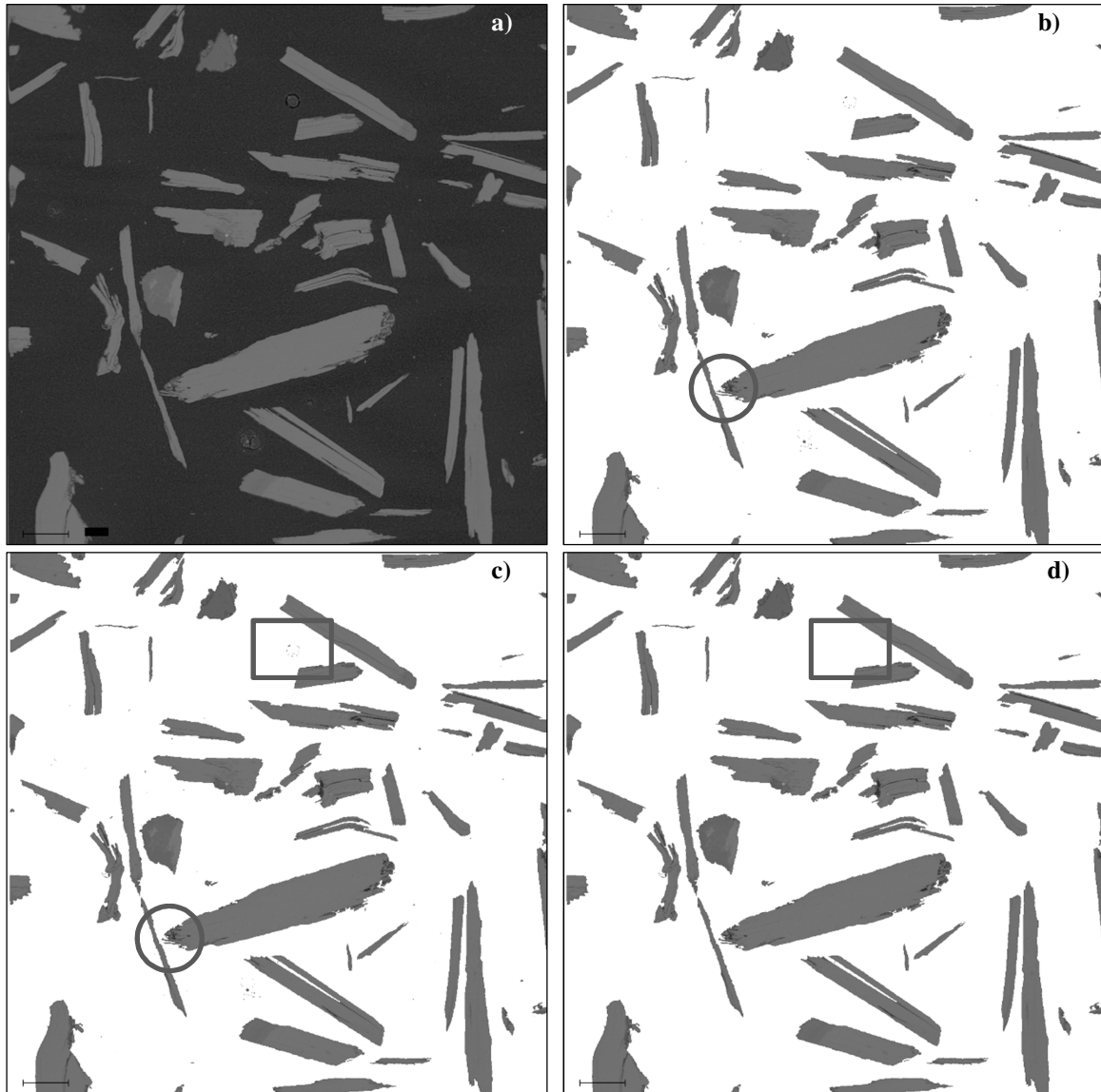


**Fig. 26:** Steps of the particulation feature, **a)** acquired BSE image, **b)** background (epoxy resin) is removed, **c)** touching particles are separated (compare circle in b) and c)), **d)** image is cleaned from undersized particles and image artefacts (compare rectangle in c) and d)).

segmentation removes artefacts on the specimen, such as cracks, holes and relief (Gu 2003, Fandrich et al. 2007, FEI Company 2011a).

The time of the entire procedure of BSE image acquisition, particulation and segmentation shown in Fig. 25 is about 1-10 seconds per frame, depending on the number of particles per frame. It has to be noted that in MLA software the definition of particles and grains are as follows (Fig. 28) (FEI Company 2011a). A particle may consist of one or more grains. A grain is part of one particle or the entire particle itself. A grain can sometimes consist of several mineral grains of the same type (e.g., discrete but touching quartz grains) as they will be seen as an area of consistent grey level in the BSE image.



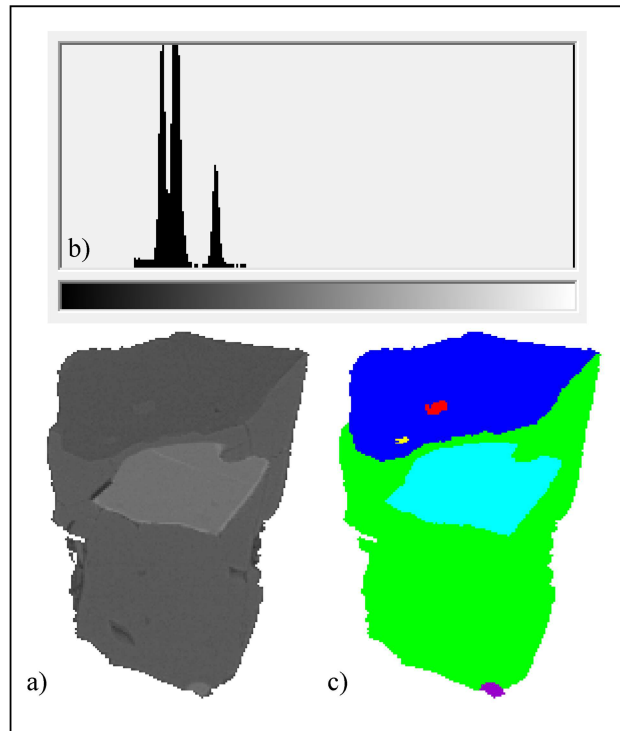


**Fig. 27:** Exemplary particle showing the segmentation feature behaviour of the MLA measurement, **a)** BSE image after background removal, **b)** BSE grey value histogram showing three main grey levels, **c)** segmented image showing the three main phases plus 3 minor phases. Note: The segmented image is based on the grey level value information exclusively and does not contain any mineral information.

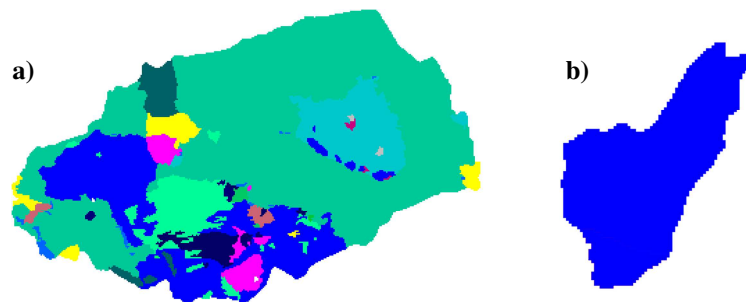


**Fig. 28:** Definition of particles and grains, **a)** particle consists of various grains, **b)** particle consists of one grain.

### X-Ray Acquisition

After the BSE image acquisition, particulation and segmentation steps are finished the X-ray acquisition points in the segmented image will be determined depending on the chosen measurement type. In general, two methods of X-ray acquisition are existent. Either a centroid location for the X-ray analysis in the segmented phase is selected or the entire phase is mapped by a closely spaced grid of X-ray points (Fig. 29). After the X-ray acquisition of all measuring points within a frame is finished the next BSE image will be acquired, particulated, segmented, and analysed. This procedure will be continued until the terminating condition (number of frames, number of particles or time limit) is reached. The resultant group of images/frames can be joined together during MLA offline image processing. The sequence of image acquisition differs between two options. The frames of a rectangle measurement area (e.g., a thin section) will be analysed by horizontal

directional movement (starting frame – bottom left). The frames of a round specimen will be analysed by circular directional movement (starting frame – centre point). (Gu 2003, Fandrich et al. 2007, FEI Company 2011a)

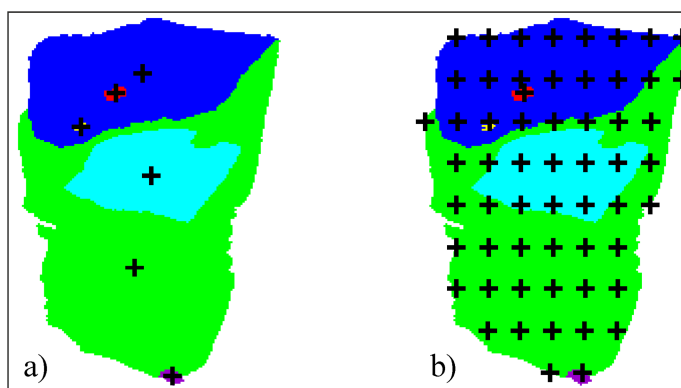


**Fig. 29:** Schematic overview of X-ray measuring points, **a)** centroid method, **b)** grid method.

#### 2.1.4 MLA Measurement Modes

Various measurement modes are available in the MLA Measurement software, each designed for specific applications (Table 5). Even though, only the XBSE, XMOD, GXMAP, and SPL mode were the measurement modes used for the investigations of this study an overview of all selectable modes will be described in the following. This description is mainly based on FEI Company (2010, 2011a) and own observations. The XBSE and XMOD measurement modes are the only ones which allow an automated collection of standards during the measurement. This procedure collects reference X-ray spectra for each mineral phase present in the specimen (Fandrich et al. 2007, FEI Company 2011a).

##### **XBSE Measurement Mode**

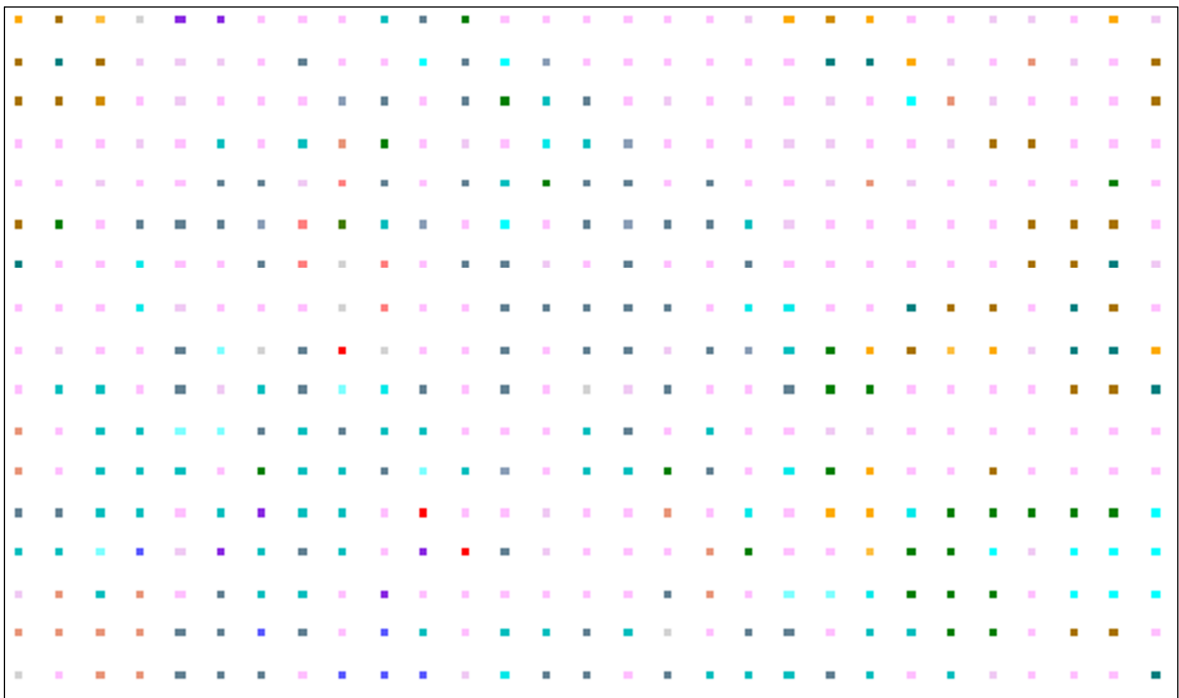
The XBSE measurement mode is the quasi-default as this is the only one which allows BSE image acquisition plus automated reference standard collection. XBSE undergoes the image processing steps (acquisition, particulation, and segmentation), mentioned above, and uses the segmented image to analyse each segmented phase with a single centroid X-ray point (see Fig. 29a as an example). This results in a very fast measurement as it requires only a small number of X-ray analyses per frame. However, the XBSE measurement mode should only be used in exceptional cases. It can be used if a specimen contains phases with sufficient BSE contrast to ensure effective phases segmentation. It is also feasible for granular materials with very small particle sizes as they are not feasible for particle mapping. Whenever minerals of rather similar BSE grey level values can be expected in a specimen the usage of the more exact GXMAP measurement mode shall be preferred. This particularly applies to silicate-bearing, sulphide-bearing or native element-bearing specimens. (Fandrich et al. 2007, FEI Company 2011a)

Table 5: Available MLA measurement modes.

Name	Measurement Mode	Result Types	Typical Applications	Remarks
BSE	BSE	BSE image	image documentation of specimens	no X-ray acquisition
XBSE XBSE_STD	Extended BSE analysis	BSE image + X-ray information (acquisition per centroid mode)	all types of samples (particularly suitable for fine-grained granular material and good discriminable phases)	fast measurement, partly inaccurate (esp. for phases with relatively similar BSE grey level), optional reference standards collection
XMOD XMOD_STD	X-ray modal composition	X-ray map (comparable to point counting)	all types of samples, but suitable only for modal mineralogy information	no BSE image, no size parameters, very fast, optional reference standards collection
GXMAP	Grain X-ray mapping	BSE image + X-ray map	all types of samples (particularly suitable for non-granular materials, complex specimens and zoned minerals)	accurate measurement mode, time-consuming measurement
SPL SPL_XBSE SPL_GXMAP SPL_DZ SPL_Lt	Sparse phase liberation	BSE image + X-ray information of specific phases (not entire sample)	search mode for rare phases such as valuable metals in ores (PGE, Au) or metal losses in tailings	only suitable where mineral of interest is present at low levels, otherwise very time-consuming
SXBSE	Super XBSE analysis	BSE image + X-ray information (acquisition per centroid mode)	suitable for minerals with variable stoichiometry	long count analysis (high quality quantitative EDS analysis), very time-consuming
RPS	Rare phase search	BSE image + X-ray information of specific phases (not entire sample)	suitable for samples with very low concentrations of the mineral of interest	uses an elemental trigger
XSPL	Extended SPL analysis	BSE image + X-ray information of specific phases (not entire sample)	suitable for samples with very low concentrations of the mineral of interest	combines SPL and GXMAP with RPS elemental classification

### XMOD Measurement Mode

The XMOD measurement mode is a point counting method (similar to point counting with an optical light microscope) with a user-defined step size of the grid and collects one X-ray spectrum at each counting point (Fig. 30). It uses the BSE image to discriminate particles from background and collects the X-ray spectra from the particles only. However, it solely produces modal mineralogy information of the sample but not particle shape or mineral association and liberation data. As no image processing steps have to be conducted hundreds of thousands measuring points can be analysed within a few minutes. This results, for example, in measurement times of about half an hour per thin section at a 10x10 µm grid. (Fandrich et al. 2007, FEI Company 2011a)



**Fig. 30:** Example of a XMOD measurement mode grid.

### GXMAP Measurement Mode

The GXMAP measurement mode uses the same point counting method as XMOD but implements all BSE image processing steps of acquisition, particulation, and segmentation prior X-ray spectra collection (Fig. 29b). In contrast to XMOD, custom BSE grey scale triggers or specific X-ray spectrum triggers can be defined for X-ray mapping of phases of interest. Phases outside of these thresholds are analysed by a single centroid X-ray point as in the XBSE mode. It has to be noted that the GXMAP mode has some limitations as a significant amount of mixed spectra, a poor grain boundary definition between minerals with minor BSE contrast differences and significant longer measurement times than the XBSE measurement mode. However, due to the much better discrimination of minerals of rather similar BSE grey level values the GXMAP mode should be the first choice for measurements of full specimens, if feasible. (Fandrich et al. 2007, FEI Company 2011a)

Both XBSE and GXMAP measurement modes provide the same results for the samples: modal mineralogy information, calculated assay data, elemental distribution

information, particle density distribution, mineral association and mineral locking data, mineral grain and particle size distribution, mineral liberation data as well as theoretical grade-recovery data (see Table 6 for parameter definitions) (Fandrich et al. 2007, FEI Company 2011a).

### SPL Measurement Mode and Sub-Modes

The SPL (sparse phase liberation) measurement mode is a search mode and not suited to measure an entire specimen completely. It can be used for samples where the minerals of interest are present in very low amounts (typically < 1 wt.%). Typical examples for areas of application are the search for Au or PGM and the investigation of sulphides in tailings or penalty element-bearing minerals in concentrates. In this measurement mode the user can define BSE thresholds for the minerals of interest search. Only particles containing these particular mineral grains will be analysed but not the entire sample (see Fig. 31). The measurement of the particles can be conducted by either single X-rays (SPL\_XBSE) or X-ray mapping (SPL\_GXMAP). In the majority of cases a SPL measurement uses a higher SEM image magnification than a measurement of the entire sample such as GXMAP since only a small area of the sample is analysed. It has to be noted that the SPL measurement mode does not provide bulk mineral information as only specific parts of the entire specimen are analysed. Calculated elemental assay results, for example, have to be considered in relation to a GXMAP or XBSE measurement of the exactly same total measurement area to be comparable. (Fandrich et al. 2007, FEI Company 2011a)

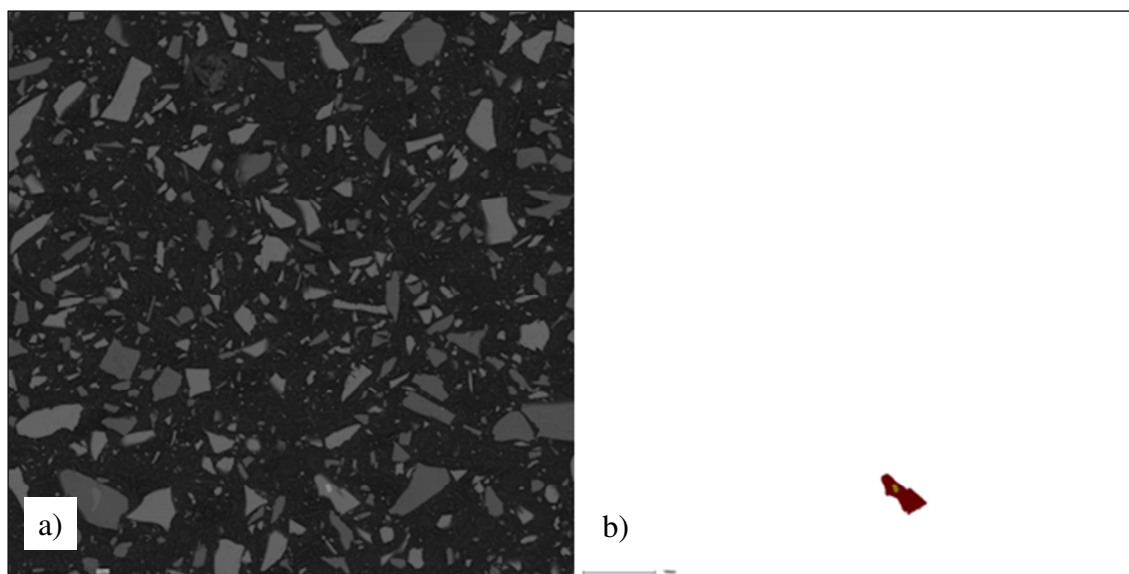


**Fig. 31:** Example for the procedure of the SPL measurement mode, **a)** BSE image, **b)** particle including a mineral phase matching the search criteria.

Two special SPL measurements sub-modes are available for specific applications. The SPL\_DZ (Dual Zoom) mode allows rapid analysis of a sample at a relatively low magnification level but zooms to a higher BSE image resolution as soon a phase of interest is detected and recaptures the BSE image for SPL analysis. The SPL\_Lt (light sparse phase liberation) measurement mode can be used where a regular particle-based SPL mode is not feasible such as for a thin section or a drill core. The standard SPL mode would analyse

here the entire frame as it does not contain of several particles but of one single ‘particle’ (= the entire frame). SPL\_Lt draws a box around the found mineral of interest and measures each grain inside this box (Fig. 32). The size of the box can be defined by the user. In addition, the user can decide whether the entire box (SPL\_Lt\_MAP) will be mapped or only specific mineral phases. (Fandrich et al. 2007, FEI Company 2011a)

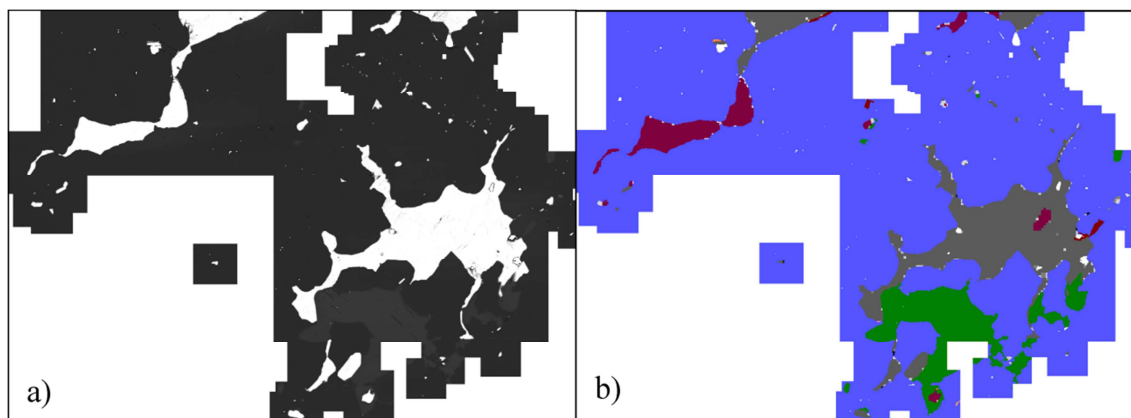


**Fig. 32:** Example for the procedure of the SPL\_Lt measurement mode showing interleaved boxes surrounding phases of interest, a) BSE image, b) processed image.

### **SXBSE Measurement Mode**

The SXBSE (Super XBSE analysis) measurement mode is a special measurement mode and is used only in particular cases. This measurement mode is an adjusted XBSE mode and enables to analyse specific minerals of interest by long count spectra. For those minerals of interest an X-ray trigger can be employed. The X-ray acquisition time of a long count spectrum (over 1,000,000 counts) of one measuring point can be 20 seconds and more. The long count spectra are stored separately for subsequent analysis to obtain accurate elemental quantification for the minerals of interest. This measurement is suitable for minerals with variable stoichiometry, e.g., sphalerite. It should be noted that this measurement mode is not a standard mode, due to the lengthy X-ray spectra acquisition times and thus long measurement times. (Fandrich et al. 2007, FEI Company 2011a)

### **RPS/XSPL Measurement Modes**

The RPS (rare phase search) measurement mode uses elemental triggers to find minerals of interest. In contrast to the newer XSPL measurement mode, which shall replace the RPS mode, the RPS mode requires manual interaction and characterisation after particles of interest were found. In contrast to the standard RPS measurement mode, XSPL uses an automated RPS technique and combines SPL and GXMAP features with the RPS elemental classification. For samples having very low concentrations of the mineral of interest this is a fast and accurate measurement mode. However, this is not a standard MLA measurement mode as for RPS triggers pure element standards are needed which are often expensive or difficult to obtain. (Fandrich et al. 2007, FEI Company 2011a)

## Measurement Outcomes and Sample Types

The various measurement outcomes of the MLA software as well as their definitions and benefits of the parameter can be seen in Table 6. The most diverse samples types can be analysed by the different MLA measurement modes, such as particulate materials (e.g., mineral processing products and drill cuttings (drill bit-induced rock chips)), rock sections, drill cores, hand specimens, sediments, soils, atmospheric dusts, man-made products, etc. (FEI Company 2011a, Pirrie & Rollinson 2011). Each of them will be analysed for different purposes and consequent requires different handling (Table 7).

**Table 6:** Measurement outcomes of the MLA software, definitions of parameters and benefits (compiled after FEI Company (2011a)).

<b>Measurement Outcome</b>	<b>Definition of Parameter</b>	<b>Benefits</b>
Mineral reference	list of minerals and their chemical and physical properties used in the mineral reference database	control of the mineral reference database
Particle and grain properties	compositional and physical parameters as well as shape factors and association data	can be exported for processing in computational statistics software
Modal mineralogy	quantitative modal composition (in area% or wt.%)	statements regarding mineral composition of the sample and occurrence of trace minerals
Calculated assay	calculated elemental composition	statements regarding elemental composition of the sample, possibility to compare calculated and chemical assays to assess the accuracy of the mineral reference database
Elemental distribution	calculated distribution of elements in minerals	statements regarding distribution of valuable elements in their hosting minerals
Elemental and mineral grade recovery	theoretical recovery of selected minerals or elements against the grade for a given particle population	beneficial for mineral processing optimisation
Particle and mineral grain size distribution	relative amount (by wt.%) of particles or mineral grains present according to size ranges	assessment of the efficiency in mineral processing, size information
Particle density distribution	relative amount of particles present according to density ranges	predictions of mineral processing behaviour, assessment of the efficiency in mineral processing
Mineral association and locking	amount of associated (adjacent) minerals and free boundaries, amount of liberated particles	predictions of mineral processing behaviour, assessment of the efficiency in mineral processing
Phase specific surface area (PSSA)	calculated relative mineral boundary to mineral area ratio	predictions of mineral processing behaviour, assessment of the efficiency in mineral processing
Mineral liberation by particle composition and free surface	relative amount of particles present according to liberation classes, mineral liberation can be defined by composition of the particle or surface exposure of the mineral of interest	predictions of mineral processing behaviour, assessment of the efficiency in mineral processing

**Table 7:** List of sample types, purpose of analyses, attributes studied and common MLA measurement modes.

<b>Sample Type</b>	<b>Source</b>	<b>Purpose</b>	<b>Attributes Studied</b>	<b>Common MLA Measurement Modes</b>	<b>Drawbacks</b>
Particulate material (feeds, middlings, concentrates, tailings)	mineral processing industry	plant monitoring, process improvement	mineral liberation, grade/recovery, modal mineralogy, size data, mineral association	XBSE, GXMAP, SPL	just a snapshot of a complex process; time series (costly) would be of great value
Particulate material (drill cuttings/rock chips)	petroleum industry (production and exploration)	lithotyping, clay mineral characterisation, pore assessment, minimise drilling problems	modal mineralogy, size data	XBSE, GXMAP	only macro-porosity identifiable by MLA
Solid rocks and ores (rock sections, drill cores, hand specimens)	mineral exploration, mining	characterisation (mineralogy, associations, (micro-)fabrics, texture), search for valuable minerals	modal mineralogy, size data, mineral association	GXMAP, XMOD, SPL	long measurement times at higher magnifications, potential data overflow
Sediments, soils	exploration, mining, environmental projects	characterisation, identifying the source, search for valuable minerals, study of contaminations, provenance studies	modal mineralogy, size data, mineral association	XBSE, GXMAP, XMOD, SPL	
Atmospheric and industrial dusts	environmental projects, health-care sector	size and mineral characterisation, identifying the source	size data, modal mineralogy	XBSE	minimum particle size limit (~ 1 µm) due to SEM capabilities
Man-made products (ceramics, construction materials, metallurgical products)	industry, archaeology	quality control, search for impurities, assessment of provenance	modal mineralogy, mineral association	XBSE, GXMAP, SPL	



## 2.2 Sampling and Sample Preparation

As the analysis of a total volume of a material is impossible a subset of this volume must be selected. This subset must be representative for the total volume (Jones 1977, 1987c). The fundamental principles to accurate sampling for MLA analysis are not different than for many other analytical techniques (e.g., for chemicals assays) and can be found elsewhere (Gy 1979, Jones 1987c, Whateley & Scott 2006, Morrison & Dunlison 2011, Rossi & Deutsch 2014). According to Whateley & Scott (2006) “correct sampling technique requires a random selection of each sample from the population”.

In general, two fundamentally different types of materials can be distinguished for MLA analysis. Granular materials, such as mineral processing-related samples and sediments, can be sampled by random selection and prepared as described hereinafter. Nongranular materials, such as solid rock samples or ore samples, are difficult to sample in a random and representative manner (Whateley & Scott 2006, Rossi & Deutsch 2014). Here, a large number of samples would be required to be representative for the deposit/study area.

For the vast majority of samples, the volume of material must be reduced after sampling as for sample preparation for MLA analysis only a few grams of material are needed. However, this small amount of material must be representative for the total sample volume too (Jones 1977, 1987c). Hence, the sample has to be split by a random selection. Several methods or instruments such as scoop sampling, coning and quartering, chute splitter (e.g., Jones Riffle), table splitter, and rotary riffler can be used for this purpose (Jones 1987c, Allen 2003, Wills & Napier-Munn 2011).

One of the most important prerequisites in order to achieve precise, reliable, representative and reproducible MLA measurement results is an accurate sample preparation technique as a well-polished planar specimen surface is crucial for each SEM-based quantitative image analysis. This is important due to two main reasons. An uneven specimen surface prevents the optimal analysis of all parts of the specimen because of shadowing effects showing low to minimal X-ray detection (Severin 2004). Secondly, the maximum number of electrons interacts with the sample and produces X-rays when the electron beam is perpendicular to the sample surface. At an angled sample surface the number of X-rays produced in the sample is significantly lower (Severin 2004). Another challenge for sample preparation, particularly with regard to samples consisting of granular materials, is to avoid segregation by density or size (respectively mass) within the sample and to ensure a random dispersion of the particles (Jackson et al. 1984). Two causes of segregation can be observed. A cluster of particles will show density segregation between particles of different modal mineralogy (Jackson et al. 1984). For example, particles consisting of native gold will show segregation to a greater extent than particles consisting of quartz. In addition, segregation can be seen between small (lightweight) and large (heavy) particles (Jackson et al. 1984). This effect concerns in particular un-sized samples and can be neglected in sized samples.

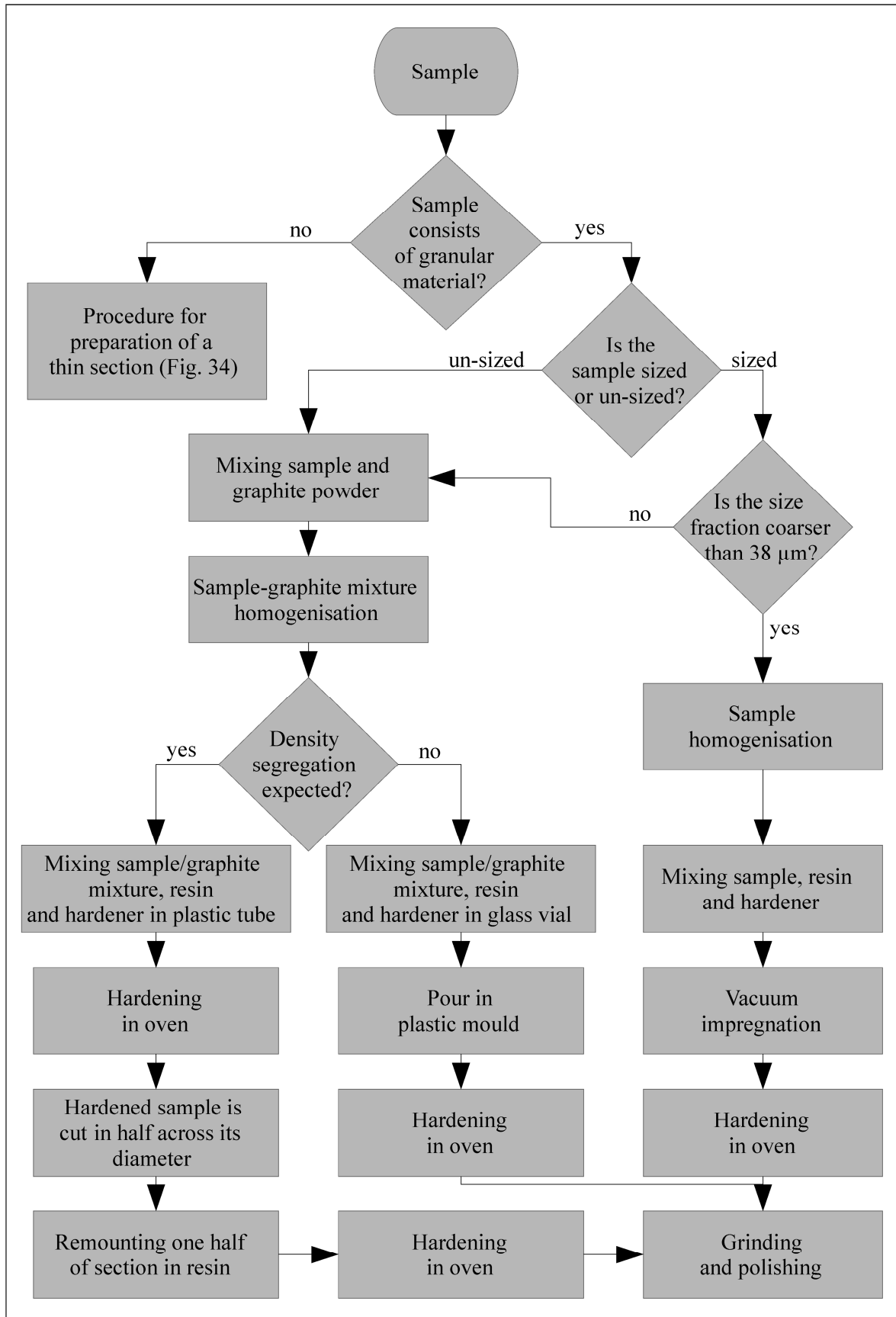


**Fig. 33:** Flowchart of the sample preparation procedure for MLA analysis (modified after FEI Company (2011d)).

Various instructions for best practice sample preparation for automated mineralogy were published by Jackson et al. (1984), Gomez et al. (1988), Hrstka (2008), FEI Company (2011d), Bachmann et al. (2012), and Kwitko-Ribeiro (2012). The suggested method sequence for granular materials starts by mixing the sample material and graphite powder (Fig. 33). Here, graphite works as a filler and separation agent for preventing touching particles and for a better particle de-agglomeration. In general, an agglomeration of particles has to be avoided as this would falsify the results of liberation, locking, and association data. The sample-graphite mixture will be mechanical shaken in cylindrical plastic moulds for homogenisation. If the sample consists of coarse-grained sized material mixing with graphite powder is not needed (FEI Company 2011d). In the case of medium and fine-grained sized materials an admixture of graphite having the same size fraction as the sample material is beneficial (Allen Darveniza, pers. comm. 2014).

According to Jackson et al. (1984) the minimum weight of a dry sample for sample preparation should be 1-2 g and about 20 g as an optimum. If feasible, the fractionation of the sample into single size fractions is preferred, but not mandatory. Jackson et al. (1984) suggest a size range not exceeding a factor of two on sieve size and found that the most suitable size ranges are: -425 +212  $\mu\text{m}$ , -212 +106  $\mu\text{m}$ , -106 +53  $\mu\text{m}$ , -53 +27  $\mu\text{m}$ , -27 +15  $\mu\text{m}$  and -15 +8  $\mu\text{m}$ . The first three ranges can be obtained by screen sieving, whereas for the other three cyclosizing has to be conducted (Jackson et al. 1984).

It has to be noted that studies using sized fractions are more expensive and time-consuming than the analysis of un-sized materials, because of the larger quantity of samples. Lastra & Petruk (2014) compared in a recent case study the comparative liberation of sized and un-sized samples. The study was performed using Pb-Zn-Cu ore from around a processing node (CuPb rougher feed, concentrate, and tailings) from a concentrator plant with one part of samples letting un-sieved and the other part of samples sieved into six size fractions. The analyses were carried out using the MP-SEM-IPS image analyser (Petruk 1988b) and resulted in particle size distribution data, mineral quantities and mineral liberation data. The results of the study by Lastra & Petruk (2014) showed differences between the sized and the un-sized samples for all of them. However, the authors presented that the trends observed for the sieved samples were often similar to that observed for the un-sieved samples. Hence, they concluded that observations relative for the improvement of the studied processing node can be arrived by using either the data from the sieved or the un-sieved samples. Unfortunately, it remains unclear if this conclusion can be assumed for other ore types or different processing plant designs as no further studies dealing with such comparative analyses are published in peer-reviewed journals. In addition it should be noted that the conclusions drawn from the study of Lastra & Petruk (2014) cannot applied to non-mineral processing-related samples as here no trends have to be assessed.

For coarse-grained granular material (which has not to be mixed with graphite powder) the first sample preparation step is to homogenise the sample. This is followed by mixing the sample with a resin and a hardener in a plastic mould (Fig. 33). This is done with the help of vacuum impregnation in a vacuum chamber where the resin can fill all pores in the material and the occurrence of bubbles can be minimised. After this, the sample is placed in an oven for some hours until the resin has hardened (FEI Company

2011d). A sample consisting of a fine-grained granular material which does not expect to show potential density segregation is mixed with graphite and homogenised afterwards. This is followed by stirring the mixture with a resin and a hardener in a glass vial in an ultrasonic bath (Fig. 33). After that the mixture is poured into a plastic mould and put in an oven to allow the resin to harden (FEI Company 2011d). A sample of fine-grained granular material which could be susceptible to density segregation has to be prepared in a somewhat different way. However, the first steps are relatively similar to the method described above. The fine-grained granular material is mixed with graphite and the mixture is homogenised. This is followed by stirring the mixture with a resin and a hardener in a plastic tube in an ultrasonic bath (Fig. 33). Following this, the plastic tube with the mixture is put in an oven to allow the resin to harden. After the sample block is hardened the block is cut in half across its diameter using a diamond saw and remounted afterwards in a normal resin block, so that the full settling area can be analysed (Hiemstra 1985, FEI Company 2011d).

The hardening segregation processes cannot be excluded completely, thus different approaches were tested to neutralise or to prevent these effects. Different attempts were used by Petruk (1976) and Stewart & Jones (1980) but without great success. The former mixed unscreened crushed material with only a few drops of resin to have a mixture where the particles cannot settle. The others used a procedure of mixing sieve-sized particles with a putty-like epoxy that prevents particle settling. A study by Kwitko-Ribeiro (2012) showed that by using a dynamic curing sample preparation process the admixture of graphite can be saved and density segregation can be minimised. However, no other publication related to this method could be found up to now. Hence, the sample preparation procedures described above (Fig. 33) are still the most frequently used methods.

After hardening in the oven the sample blocks are ready for grinding and polishing. This process uses abrasive particles to remove material from the surface of the block. Several rounds of successively finer grinding and polishing are needed to obtain a perfectly polished sample surface. Each type of sample material requires somewhat different grinding and polishing parameters because of different physical properties of minerals such as hardness and cleavage. A grinding and polishing method for quartz, topaz, and mica-bearing greisen-type mineralisation was established by Bachmann et al. (2012).

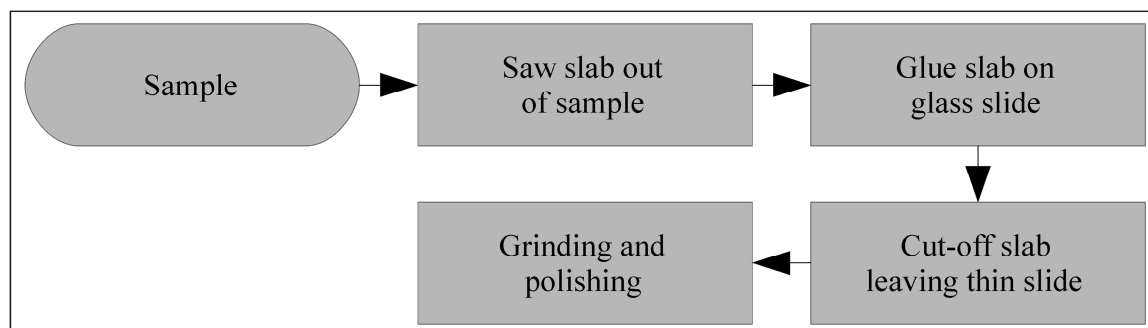


**Fig. 34:** Simplified sample preparation procedure for thin sections (modified after Hirsch (2012)).

For polished thin sections a different sample preparation procedure has to be performed. A detailed description of this procedure can be found at the Geology Departments webpage

---

of the Western Washington University (Hirsch 2012). Briefly summarised, the thin section preparation starts initially by sawing a representative slab out of the sample (Fig. 34). This slab is glued on a glass slide using epoxy resin. After the resin is hardened, the slab is cut off using a cut-off saw leaving a thin slice. Following this, the slice is grinded and polished similar to the procedures for granular material mounted in epoxy resin.

In addition to the traditional sample preparation steps of grinding and polishing, described above, another method was established since the 1990s. Due to its sputtering capability, the focused ion beam (FIB) technique can be used as a micro-machining tool to modify or machine materials at micro- or nano-scales (Mackenzie & Smith 1990, Young 1993). FIB milling can also be used for clay-rich samples (difficult to get a perfect polish), such as shale samples in the petroleum industry (Sok et al. 2010, Lemmens et al. 2011). It should be mentioned that for this method a pre-smoothed surface is necessary as for FIB milling the slice thickness is in the range of nanometres and thus has a long processing time.

## 2.3 Reproducibility of Measurements and Possible Sources of Error

This section gives an overview on the reproducibility of MLA measurement results and an error discussion. Despite MLA analyses result in valuable numerical data for a large series of relevant attributes (quantitative mineralogy, mineral locking and association, particle and grain size, liberation etc.) for which clear criteria of quantification exist (see, for example, Jones (1987a) and Petruk (2000)) the MLA (and similar systems) do only yield quasi quantities. This is, because there is no stringent error assessment in the software available currently and there are no standards of known composition that may be used for calibration. This strictly limits - at present - the use of results from SEM-based image analysis as quantitative data.

### Error Assessment

Unfortunately, only in a few of the long list of automated mineralogy-related publications (about 1,700) examined for this study (see chapter 1) the authors tried to assess the inadequacies mentioned above. These specific publications were often related to specific issues (e.g., mineral liberation) but did not cover the entire spectrum of error assessment. For example, Leigh et al. (1993) established confidence limits for liberation measurements for automatic image analysis systems. A study by Lätti & Adair (2001) evaluated the stereological bias in polished sections of sized fractions of titanium-bearing ore analysed by QEM\*SEM. The authors showed that for the material studied, stereological bias was minimal. Gay & Morrison (2006) also dealt with the field of stereology by the comparison of the three-dimensional properties predicted from measured two-dimensional sections with measured three-dimensional properties. Gu et al. (2012) compared the results of 2-D and 3-D particle size measurements obtained from micro X-ray computed tomography to assess the general correctness of size data obtained by 2-D using SEM-based technology such as MLA and QEMSCAN. The authors showed that the 2-D measurements systematically underestimated the results. However, based on the 2-D particle size calculation parameters (equivalent circle/sphere size, short axis and long axis) different degrees of deviations were observed. Evans & Napier-Munn (2013) used a statistical method based on bootstrap resampling to assess the error in grain size distribution and quantitative mineralogy of automated mineralogy measurements which can be used to estimate a minimum number of particles respectively a measurement area needed to obtain a reliable measurement result. Blaskovich (2013) compiled a list of “automated mineralogy on-going issues” including sampling, stereology, particle statistics, and operator and instrument errors. This author also performed repeated measurements while rotating the samples which resulted only in minor differences to the initial measurements.

An opportunity to assess the quality of an automated mineralogy analysis is the comparison of the measurement results with different analytical techniques such as quantitative X-ray diffraction analysis (QXRD) or chemical assays as they yield an error assessment and the systems can be calibrated. A comparison of MLA measurement results with other automated mineralogy systems may be beneficial for a rough estimation of the accuracy of the results. It should be noted that not all numerical values shall be compared directly between different analytical methods or instruments due to the different analytical

approach of different techniques. In the automated mineralogy-related literature only a small number of such analytical comparisons can be found. A variety of examples is presented in the following. An example for the determination of gold ores by different automated mineralogy techniques was compiled by Goodall & Scales (2007). A conference paper by Brown & Dinham (2007) of Anglo Research, South Africa compared MLA and QEMSCAN analytical results for PGM and base metal sulphide (BMS) analyses. At first, they illustrated that a comparison of the PGM distribution in samples analysed by five MLAs show highly correlated results. A comparison of BMS distributions obtained by five MLAs and three QEMSCANs revealed a relative standard deviation of 4-5% for pyrrhotite, pentlandite, and chalcopyrite as well as 19% for pyrite. Brown & Dinham (2007) concluded that the latter was caused by the low pyrite concentrations in the sample. Finally, the authors compared calculated assays obtained from MLA analyses and chemical assays. The results showed strong positive correlations for Cu, Ni, and Fe. Likewise, a comparison of chemical assays and calculated assays from MLA analysis was presented by Miranda & Seal (2008) for copper ores. Results obtained from chemical and calculated assays were shown to be very similar. The results of a study by Spicer et al. (2008) comparing QXRD and MLA analyses of heavy mineral sands showed similar results for minerals such as rutile, zircon, and ilmenite, but some differences for hematite and magnetite. Kwitko-Ribeiro (2012) used the comparison of assays calculated from QEMSCAN analyses with chemical assays to show the improvements of a sample preparation optimisation study.

### **Sources of Error**

Modified after “an overview of the type of problems encountered in the application of image analysis techniques to mineral processing problems, in particular in the assessment of liberation” compiled by Barbery (1992) the potential sources of error in MLA analyses of granular materials and thin sections can be distinguished as they can be seen in Table 8. In the following paragraphs these sources of error will be discussed in detail. It should be reminded that errors can be distinguished into two types: random errors which can be revealed by repeating the measurements and systematic errors which cannot be revealed by this way (Taylor 1997).

### **Errors brought in by Task Definition and Sampling**

The sources of error are not only limited to the MLA system itself but begin already with the definition of the task of the analysis (Table 8). Here, the opportunities and limitations of the MLA technique need to be considered. A definite task is crucial to the success of the analysis. Sampling in the field/plant and subsampling in the laboratory are applications prior to analysis which require an elaborate sampling strategy. Before the start of the sampling both the required number of samples and the amount of sample material should be defined. Several sampling techniques were presented by different authors such as Gy (1979), Jones (1987c), and François-Bongarçon & Gy (2002). The following sentences of this paragraph are based on their suggestions. The nugget effect should be considered

**Table 8:** Potential sources of error and possibilities of error reduction related to the MLA technique (significantly modified after Barbery (1992)).

Area of MLA Analysis	Potential Sources of Error	Type of Error	Rating/Risk	Possibility of Error Reduction
Definition of task	ignorance of MLA method and capabilities	systematic	low to medium	awareness off MLA capabilities and limitations
Sampling	non representative sampling, nugget effect, to small amount of material, confusion, contamination	systematic / random	medium to high	accurate planning before sampling (sampling strategy), sufficient amount of material, accurate sample labelling, clean equipment
Sample splitting	wrong method, not random splitting, instrument errors, confusion, contamination	systematic / random	low to medium	accurate sample homogenisation prior to splitting, duplicates and replicates, sample series, regular instrument control, labelling, clean splitting equipment
Sample preparation – embedding	preferred orientation, specific gravity effects, agglomeration, residual moisture	systematic / random	low to high	sample preparation adapted for mineral properties (e.g., strong density differences), best practice procedure, mixing sample with separation agent (e.g., graphite), special de-agglomeration procedure, preparation of sized fractions
Sample preparation – grinding and polishing	soluble and swelling minerals, phase removal, selective polishing, contamination, instrument errors	systematic / random	low to high	accurate grinding and polishing procedure adapted for the specific minerals of the sample, tools to detect risk minerals (e.g., XRD), accurate equipment cleaning, labelling, regular instrument control
MLA measurement – preliminary work	carbon coating, mounting sample in sample holder	systematic	low to medium	monitor the thickness of the carbon coating, measurement protocol incl. sample positions on sample holder, double-check correct sample mounting
MLA measurement – general operation	operator errors, instrument errors	systematic / random	medium to high	careful measurement setup, measurement protocol, double-check instrument setup, monitor instrument conditions
MLA measurement – BSE images	BSE calibration, image focus, working distance, instrument errors (e.g., BSE image stability), image resolution	systematic / random	medium to high	accurate calibration, monitor image stability, correct working distance, excellent image focus



Table 8: (continued).

Area of MLA Analysis	Potential Sources of Error	Type of Error	Rating/Risk	Possibility of Error Reduction
MLA measurement – X-ray acquisition	X-ray detector calibration, detector stability, maximum pulse processor throughput, electron beam excitation volume, detection limit, instrument errors	systematic / random	medium to high	double-check calibration directly after the calibration procedure, check detector stability periodically, adjust electron beam current, acceleration voltage and maximum pulse throughput for the specifics of each sample, long count measurement mode if required
MLA mineral reference list	varying mineral chemistry, trace elements in solid solution, peak overlaps, mixed spectra, polymorphs, missing major minerals, type errors, “unknowns”, different acceleration voltages	systematic / random	medium to high	accurate construction of mineral reference list, double-check chemical composition of reference minerals, additional usage of supporting methods (e.g., optical microscopy, XRD, LA-ICP-MS, EMPA), distinguished mineralogical knowledge
MLA image processing software	mineral classification, artefacts, frame boundary issues, duplicate particles, touching particles, software bugs	systematic / random	low to medium	advanced mineral classification routine, accurate image screening and assessment, reanalysis of single mineral grains
Statistical effects	2-D section-based technology, number of particles, shape of particles	systematic / random	low to medium	comparison with other analytical techniques, sufficient number of analysed particles/samples, particle removal filter test
Effects of stereology	2-D section-based image analysis		low to high	stereological models and corrections, other analytical techniques (e.g., micro-X-ray tomography ( $\mu$ CT) or High Resolution X-ray Microtomography (HRXMT))

especially for the sampling of gold or PGE-bearing samples. An accurate sample labelling is needed to minimise the possibility of confusion and slip in of errors. The sample contamination risk can be reduced by keeping the sampling equipment clean. After initial sampling a subsequent potential addition of samples should be avoided due to unclear relationships to the initial samples.

### **Errors brought in by Sample Homogenisation and Sample Splitting**

The next sources of error are the sample splitting process and the sample homogenisation prior the splitting (Table 8). For this a rotary micro riffler (or spinning riffler) is recommended as it provides the lowest standard deviation of several sampling/splitting methods such as cone and quartering, scoop sampling, table sampling, chute riffling, and rotary riffling (Allen 2003). For a test material consisting of 60% coarse-grained and 40% fine-grained sand Allen (2003) found, while comparing different splitting methods, that for the spinning riffling method (rotary riffling) the percentage standard deviation was about 0.1% and the estimated maximum sample error about 0.4%. To achieve best sample splitting results an accurate sample homogenisation prior to splitting must be ensured.

The correct homogenisation of a sample can be tested by preparing and measuring duplicates and replicates. The rotary riffling procedure used at the Department of Mineralogy, TU Bergakademie Freiberg produces eight subsamples. For example, four out of these eight blocks could be used for such tests. However, it should be considered that the additional preparation and measurement of duplicates and replicates will multiply the (often limited) MLA measurement and processing time. In the case of particulate materials (grain mounts) the differences within the measurements of multiple blocks of the same material should be relatively small as long the material is well homogenised and as long as there are no separation effects during sample preparation.

For the sample splitting process the same applies as for sampling. Correct labelling and accurate equipment cleaning are crucial for reliable analysis results. A check of the correct instrument functionality should be done from time to time if the instrument used for splitting consists of moving or rotating parts to ensure early detection of wear-out effects.

A study by Voordouw et al. (2010) dealing with the evaluation of platinum group minerals (PGM) in thin sections by MLA (SPL measurement mode, see section 2.1.4) quantified the reproducibility and significance of the analyses by in-run duplication, out-run duplication, and serial sections. As in-run duplication and out-run duplication were not related to the sample preparation but the MLA measurement itself this will be reviewed a little further down. The measurements of serial sections (five thin sections cut in sequential order from the same core sample) presented by Voordouw et al. (2010) showed that differences in wt.%<sup>PGM</sup> for individual PGM can range up to 32 wt.%. Such differences in the measurement of serial thin sections strongly depend on the heterogeneity of the sample material and the irregular distribution of the PGM. A series of thin section of a very fine-grained material in which the studied components are distributed evenly (i.e., nugget effect absent) will show fewer differences than a series of thin sections of a heterogeneous and/or coarse-grained sample. In the case of heterogeneous thin sections each measurement of a single thin section represents just this particular section but not the entire sample material. For a reliable analysis which shall be representative for the entire sample it is important to

measure a sufficient number of PGM (or other rare minerals of interest). However, it is almost impossible to estimate the number of rare mineral grains (of the mineral of interest) prior the measurement without any tools to achieve a sufficient number of grains. Tools which could be used to roughly estimate this number of mineral grains and thus the number of thin sections needed for a reliable analysis are light microscopic investigations and preliminary investigations using a SEM. Micro-X-ray tomography ( $\mu$ CT) is a potential method to investigate the distribution of precious metals in the sample. It should be noted that the MLA data evaluation software is able to combine several measurements (e.g., thin sections) which helps to evaluate a series of contiguous thin sections as one sample.

### **Errors brought in by Sample Preparation – Embedding**

Despite the fact that the MLA Measurement and MLA Image Processing software is able to de-agglomerate touching particles (to obtain correct shape and size data) to a certain degree it is an advantage to prevent touching particles already during the sample preparation. A common procedure for this is to mix the sample material with graphite powder as filler and separation agent (see section 2.2). It should be ensured that only pure or synthetic graphite is used for this as natural graphite can contain certain amounts of other minerals. It has proved to be beneficial to use a graphite particle size for mixing similar to the sample particle size (Allen Darveniza, pers. comm. 2014). For instance a powder sample ranging in size  $< 50 \mu\text{m}$  should not be mixed with graphite ranging 150 to 300  $\mu\text{m}$  but can be mixed with graphite in a 20-53  $\mu\text{m}$  size range. The mixing with the correct graphite material helps also to avoid agglomeration of particles during the sample mixing. To minimise the effects of agglomeration it should be ensured that the sample material is sufficiently dry. To remove residual moisture the sample material can be placed in an oven at a temperature that ensures that no mineral will be modified. For heavily agglomerated samples a technical application note for de-agglomeration was prepared by FEI Company (2011c). For preventing gravity effects in sample preparation, which can be a significant source of error for specific types of materials, see section 2.2. The same applies for the discussion regarding the differences of preparing sized or un-sized samples.

### **Errors brought in by Sample Preparation – Grinding and Polishing**

For the sample preparation steps of grinding and polishing several potential sources of error can be compiled (Table 8). Among others, it has to be clarified if the sample material consists of water-soluble minerals or other risk minerals such as swelling minerals. Samples with a high content of clay minerals or other minerals with a perfect cleavage can be exposed to phase removal during grinding and polishing. For detection of such minerals tools like X-ray diffraction analysis should be used prior sample preparation. The different polishing properties of different minerals can led to selective polishing. This effect can be minimised by the application of accurate grinding and polishing procedures directly adapted for the specific minerals of the sample. Correct sample labelling, perpetual and accurate equipment cleaning (especially the grinding and polishing disks) as well as a regular instrument control is essential for error reduction. After polishing, each sample should be cleaned in an ultrasonic cleaner to remove displaced particles and other loose

contamination. The results of a study by Hrstka (2008) suggested that sample surface contamination and surface defects caused by sample preparation including bubbles, cracks and pluckouts (break-outs) can play a significant role in the repeatability of QEMSCAN measurements. This is likely for MLA measurements too.

### **MLA Measurement-related Sources of Error – Preliminary Work**

Prior to MLA measurement the sample has to be coated with electrically conductive carbon. An accurate cleaning of the sample surface is required before the coating process as contaminations will generate multiple artefacts. An optimum coating thickness must be ensured for all samples as a too thin carbon coat can cause charging and a too thick carbon coat will lead to a X-ray intensity loss (Kerrick et al. 1973). According to the sample preparation note prepared by FEI Company (2011d) “the optimum thickness is between 200 and 250 Å”. It is recommended to use a brass stub for thickness monitoring, a method that is well established for electron microprobe analysis for decades. A carbon layer of about 250 Å of thickness gives the brass a blue interference colour (Kerrick et al. 1973). Another potential source of error is the mounting of the samples into the sample holder. Here, great care must be taken to mount the sample planar into the sample holder. Furthermore, it is recommended to draw up a measurement protocol for each measurement and outline a sample position scheme for the sample holder to avoid confusion of the sample position.

### **MLA Measurement-related Sources of Error – General Operation**

Very important potential sources of error are operator errors and MLA instrument errors (Table 8). To reduce operator errors while setting up a measurement the operator can be supported by a second MLA user as he can supervise the set-up and detect operator errors. Great care should be taken that the SEM set-up is correct and the right setting was used for the chosen MLA measurement mode. For example, a SPL search mode for tiny mineral grains of interest requires not only the selection of feature size ‘1 pixel’ but also to set the X-ray collection grain size to value ‘1’ and the SPL minimum grain size to value ‘1’. As the latter two have a preset value of ‘4’ the sole adjustment of the feature size value to ‘1’ would lead to a number of mineral grains of interest found but not analysed, as soon their grains size ranges between 1 and 3 pixel. In general, it should be considered that almost all values in the MLA Measurement software are based on pixel unit and not micrometre scale unit.

General instrument errors can be caused by operational factors such as chamber vacuum, gun and column vacuum, and instrument temperature. Here, a constant monitoring is required to reveal such errors. The instrumental reproducibility of a MLA instrument can be evaluated by repeating analyses of one selected sample. In addition, the measurement of one sample in different instruments can be performed to assess the precision of the technique. For example, Hrstka (2008) studied the reproducibility of QEMSCAN measurements by setting up and running standard tests on two different QEMSCAN instruments and found that, in general, the reproducibility of the systems themselves was excellent, ranging between 0.4 and 1.5 per cent relative standard deviation.

For a so-called in-run duplication a MLA study by Voordouw et al. (2010) analysed a thin section twice in the same analytical run. Voordouw et al. (2010) stated that the “in-run analysis of duplicates showed that the wt.%<sup>PGM</sup> of individual PGM measured in the second analysis was within 11 wt.%<sup>PGM</sup> of the first analysis” and “the wt.%<sup>BMS</sup> and wt.%<sup>Silicate</sup> in the second analysis within 2 wt.% of that measured in the first run”. This shows that for minor and trace minerals such as PGM larger differences between duplicate measurement series can be expected (due to the nugget effect) and that major minerals (e.g., silicates) will show smaller differences between duplicate measurement series. As the authors used a search mode (SPL measurement mode) for their measurements it can be assumed that these values will be lower for an in-run duplication using a full sample area measurement mode, such as GXMAP. In general, in-run duplications should give a very good to excellent reproducibility for analyses of both polished sections and particulate materials as long the measurement parameters (esp., the area of analysis) and the instrument conditions remain constant. An out-run duplication of the study by Voordouw et al. (2010), reanalysing a thin section several months after it had been analysed the first time, gave errors for PGM, BMS, and silicates similar to those calculated from their in-run duplication. The samples were removed from the sample holder in between the reanalysis (Jens Gutzmer, pers. comm. 2015). For an absolutely reliable out-run duplication the position of the samples in the sample holder should have to be switched and the samples itself should be rotated somewhat (round blocks) or by 180° (thin sections) towards the initial measurement if an exact identical measurement area can be ensured.

### **MLA Measurement-related Sources of Error – BSE Image**

The BSE image-related errors (Table 8) are crucial with respect to the success of a MLA measurement as the BSE image is the basis of the analysis (see section 2.1.3). The correct working distance of every sample must be ensured as this distance influences the grey level of a BSE image. A different working distance between two samples will cause different BSE grey values for the same mineral in these two samples. A SPL search mode, for example, using a BSE trigger will miss in this case some mineral grains in one of the two samples. Also, the BSE calibration prior the measurement must be performed very accurately (see section 2.1.2). Unfortunately, in some MLA measurements BSE image stability issues can be seen where the source of these issues remains unclear. For the early detection of this instrument error the BSE image stability shall be checked after every measurement. It has to be considered that image resolution is a limiting factor related to MLA analysis as only phases visible in the BSE image can be detected and thus analysed. Lastly, an excellent image focus is required which can be achieved by careful SEM optimisation using stigmator control, source tilt function, and lens alignment function.

### **MLA Measurement-related Sources of Error – X-ray Acquisition**

To achieve reliable X-ray spectra for all mineral phases during a MLA analysis the X-ray detector calibration prior the measurement must be performed very accurately (see section 2.1.2). This potential source of error can be assessed by double-checking the result of calibration on a mineral of known composition. In this case, it is suggested to use the

copper metal pin on which the detector calibration was conducted as control mineral. The X-ray detectors of Bruker Corporation used at both MLA systems of the Geometallurgy Laboratory, TU Bergakademie Freiberg are in general of high stability, so that X-ray detector-related issues (e.g., cooling issues) are very rare. However, it is recommended to check the correct performance periodically. This applies even more for the communicating QUANTAX signal processing units and QUANTAX ESPRIT software as here issues arise more frequently.

An occasional source of error is the selection of the correct maximum pulse throughput of the signal processing unit as for example a setting to a maximum pulse throughput of 90 kcps will preserve the first channels of a spectrum (e.g., the position of the carbon  $K\alpha$  peak) while a setting to 600 kcps will remove the first channels of a spectrum, which is critical for the distinction between carbonates and oxides. Furthermore, it should be considered that, especially for fine-grained materials, the size of the electron beam excitation volume has to be taken into account. The same applies for a thin mineral grain where the electron beam will affect the phase present below this grain too. To reduce this effect two parameters could be changed. As described in section 2.1.2 the beam acceleration voltage influences the excitation volume and thus this volume can be reduced by lowering the voltage. FEI Company (2010) recommends to use an acceleration voltage of 15 keV if the average particle size and/or mineral grain size is below 38  $\mu\text{m}$ . In like manner, the electron beam current has an impact on the excitation volume, but not to the extent as the acceleration voltage. Thus, a decrease of the electron beam current shall be limited to particularly applications in which the exclusive decrease of the acceleration voltage is not sufficient. One last point regarding X-ray-related sources of error is the detection limit of elements which is approximately 0.1% for the EDS technology (Reed 2005). As the spectrum acquisition time per analysis point during a MLA measurement is below 10 milliseconds the “real” detection limit of elements is by far higher. Depending on the type of mineral and other factors such as acceleration voltage and beam current this limit can be assumed to be between 1 and 5%. As soon as a lower detection limit of elements for a specific mineral is required the SXBSE measurement mode, providing X-ray acquisition times of 20 seconds and more, must be chosen.

### **MLA Mineral Reference List-related Sources of Error**

The field of X-ray-related sources of error is strongly linked to the sources of error related to the MLA mineral reference list. Here, an expert knowledge is required that can assess the correct mineral phase chemistry whilst taking into account the limitations of the EDS technology. It should be noted that a MLA measurement just stores X-ray spectra for each analysis point and does not actively quantify the compositional data for each point. Rather, the acquired X-ray spectra are compared with reference spectra stored in the MLA mineral reference list and assigned to a reference mineral by the closest match methodology. Hence, all mineral grains assigned to a specific reference mineral will get the elemental composition stored in the database entry for this reference mineral. Especially for minerals of variable chemical composition the compositional values in the MLA mineral reference list should be chosen very carefully. Supporting analytical techniques such as electron micro probe analyser (EMPA) or laser ablation ICP-MS (LA-ICP-MS) can assist to amend

the values for chemical composition in the MLA mineral reference list. This applies for trace elements and elements in solid solution such as Au in pyrite too, as the SEM is not able to detect minor and trace elements (see section above). For example, after determination of an average of 100 ppm Au in the pyrites of a sample by EMPA this value could be included in the reference pyrite chemical composition for better accuracy.

An advantage in relation to mineral identification is peak overlaps like for the Mo-L $\alpha$ 1, S-K $\alpha$ 1 and Pb-M $\alpha$ 1 peaks. The operator who builds the mineral reference list should use in such case supporting analytical techniques such as optical microscopy if required. A next challenge is the occurrence of mixed spectra (often related to fine-grained materials). Here, it must be balanced carefully whether a mixed reference spectrum has to be included in the MLA mineral reference list as a mix reference or if the mixed reference spectrum has to be rejected as poor spectra easily can corrupt the complete mineral reference list. Unfortunately, directly after a MLA measurement is finished and the initial mineral reference list was collected it remains unclear if one reference spectrum was found only at one particular place or all over the sample. To assess the significance of a mixed spectrum and subsequently to decide if this particular spectrum is needed or not it is recommended to classify the sample with the initial mineral list first and to build-up the proper mineral reference list for the project afterwards. While building up a MLA mineral reference list it should be remembered that a SEM equipped with an EDS detector cannot distinguish polymorph modifications of minerals (e.g., anatase, brookite, and rutile; all TiO<sub>2</sub>). Here, the operator has to decide by his expert knowledge if one or more modifications could be excluded in this particular case or if the reference entry should include the names of all polymorph modifications. The same is true for the discrimination between amorphous and crystalline phases having the same chemical composition.

All minerals/phases without reference spectra in the MLA mineral reference list will be grouped as “unkown”. Missing major minerals is a crucial source of error and will led to significant analysis errors. It has to be noted that for every reference mineral in the MLA reference mineral list its correct density value must be typed in. This density value will be used for the calculation of the proportion by weight in the MLA data evaluation software and thus has to be correct to ensure an accurate analysis result (Jones 1987b). Concerning the entry of the group of “unknowns” (which cannot be deleted) in the MLA reference mineral list it has to be considered that this entry has a default density value of zero. Unfortunately, this point is often ignored and will result in the exclusion of the group of “unknowns” from the analysis result. As the MLA results for modal quantification of both atomic% concentration and wt.% concentration are normalised to 100% this will led to an overestimation of the other mineral phases. However, if a proper mineral reference list is build up and no mineral entry is missing the atomic% of “unknowns” is often below 0.1%. But for a reliable analysis result this issue regarding to the “unknowns” shall be fixed. As the group of “unknowns” can consist of many different phases and/or mixes an optimal average density value should be chosen. This could be related to the sample type or in the most general sense the estimated average crustal density of the 2.8 g/cm<sup>3</sup> (Taylor & McLennan 1995). A last issue which should be mentioned with regard to the MLA mineral reference list is to use the same acceleration voltage for both the measurement and the spectra for mineral reference list. For example, for a MLA measurement which was

conducted by using a setting of 25 keV a reference spectrum collected at 15 keV will cause mineral misidentifications.

### **MLA Image Processing Software-related Sources of Error**

Potential sources of error in the MLA Image Processing software are less common than in the measurement routine. However, based on the type of minerals in the samples some classification issues can be observed. This includes, among other things, minerals having a relative similar chemical composition such as magnetite and hematite. Here, the use of the advanced mineral classification routine is recommended to reduce misclassification. If false classifications of minerals are suspected it is recommended to perform a reanalysis of suspicious mineral grains by using the Bruker QUANTAX ESPRIT software. This is especially recommended if this concerns minerals of interest such as the findings of the SPL search mode. After successful mineral classification the MLA images have to be screened very accurately as every undetected error will falsify the final result of the analysis. Potential errors which should be carefully investigated are artefacts, frame boundary issues, duplicate particles, touching particles. Artefacts can be relicts of the sample preparation such as displaced particles, air bubbles, scratches, and cracks. Another group of artefacts are particles for which, during sample preparation, no planar surface could be made (e.g., due to breaking out of the surface while grinding). These minerals will show false spectra and could mimic other minerals.

Frame boundary issues can be caused by using the XBSE measurement mode at samples containing of minerals having relatively similar BSE grey values. In such a case, it may happen that a particle divided by a frame boundary will show different minerals on its left and right hand side (see section 2.1.4). Another potential source of error related to frame boundaries are duplicate particles as usually the setting of a MLA measurement will produce minimal overlapping frames to avoid gaps within particles after frame merge. The MLA Image Processing software normally will remove duplicates after merging all frames but in rare cases some duplicate particles will be missed and should therefore be removed manually after detection. Another method to prevent duplicates and image merging-related software bugs is an MLA analysis option to remove particles touching the frame boundary during the measurement. The same function is available in the MLA Image Processing software where particles touching the frame boundary can be removed too, but after the measurement. However, the usage of this removal function can only be recommended in the case of sized granular materials. The use of the removal function in the case of a sample consisting of varying particles sizes would lead to the removal of a higher proportion of larger particles and consequently bias the results.

Incorrect results particularly with respect to mineral association, mineral locking, and liberation statistic can be caused by touching particles. Even with the best sample preparation and the most accurate measurement setting some touching particles can occur in every sample. If such a touching particle was found during screening of the MLA images it has to be separated manually. In this context it should be noted that the usage of the de-agglomeration function available in the MLA Measurement software and MLA Image Processing software can cause errors in particular cases. The de-agglomeration function available in both software programs separates touching particles by using the



shape factors circular ratio, rectangular ratio, and combined ratio. If the ratio of two touching particles is higher than the threshold value this touching particles will be separated. As compact single particles have lower and elongated single particles higher ratios, the latter (if very long and slim) can have even higher ratios than two touching compact particles. The de-agglomeration of these two compact particles can sometimes “overreact” and “separate” (slice) elongated single particles too. This issue concerns micas in particular due to their often elongated shape in 2-D sections. To prevent this behaviour the only solution is here to deactivate the de-agglomeration function in the MLA Measurement software and to process touching particles manually in MLA Image Processing. As with any software several other software bugs may occur in the MLA software which could also affect the reliability of the analyses in some cases.

### **Sources of Error Related to Statistical Effects**

A common concern in relation to quantitative automated SEM-based image analysis is the fact that this technology is based on the evaluation of 2-D sections. However, the disadvantage in comparison to a 3-D analytical method can be minimised by analysing a high number of particles. Theoretically, the MLA can analyse more than one million particles per sample. However, the greater the number of particles in a sample the longer is the time for sample preparation, measurement and data processing, and consequently the costs. Hence, an optimum number of particles must be found providing sufficient accurate analysis results within an acceptable handling time. A broad rule is that the general number of particles in a sample consisting of granular material should be about 20,000 (see for example, Taşdemir (2008), Sylvester (2012), and Lastra & Petruk (2014)). This implies that for a coarse-grained sample more than one block has to be prepared to achieve reliable particle statistics. To assess if a statistically representative number of particles was analysed during the MLA measurement a simple test can be conducted after the measurement with help of the MLA Image Processing software. This software provides several filter functions and one of them can remove a random percentage of particles from a sample. The removal of a small percentage of particles (e.g., 5%) of a statistically representative sample would show no significant change in the results whereas a removal of the same percentage of particles of an unrepresentative sample will change the results significantly. When studying a small group of minerals of interest (e.g., trace minerals like PGM) a high particle number cannot be achieved or would be extremely time-consuming and awfully expensive. A study by Hrstka (2008) found by conducting several experiments (measurement of replicates, repeating measurements with one system, repeating measurements using two different systems, sample regrinding and remeasurement) that for an exact quantitative mineralogy the minimum number of particles containing any rare mineral of interest (MOI) should be over 1000, but with more than 100 MOI-containing particles still valid quantitative information can be obtained.

### **Sources of Error Related to Stereology**

A last important field of error related to the MLA technique (and every SEM-based image analysis method) is stereology. Several dozen of studies dealing with the effects of

stereology and stereological models related to image analysis were published since the 1970s. Important examples of such publications may include Barbery (1974, 1985, 1992), Jones & Barbery (1976), King (1978, 1979, 1982, 1994), Barbery et al. (1981), Hill et al. (1987), Meloy et al. (1987), Sutherland et al. (1988), Ferrara et al. (1989), Laslett et al. (1990), Gay (1995, 1999), Leigh et al. (1996), Fandrich et al. (1997), Leigh et al. (1997), Fandrich et al. (1998), King & Schneider (1998a, b), Lin et al. (1999), Spencer & Sutherland (2000), and Lätti & Adair (2001). It has to be noted that the two main areas of application for stereological models are particle/grain size distribution analysis and mineral liberation analysis. Hence, stereological studies were almost always conducted in relation to samples of mineral processing. In general, it is accepted that an analysis of a 2-D section without stereological correction overestimates the extent of liberation. A comparison of 2-D and 3-D particle size measurements by Gu et al. (2012) found a systematically underestimation of the particle size data by 2-D measurements. This is because 2-D sections of particles are always equal or smaller than the 3-D size and the measured 2-D size strongly depends on the particle orientation related to the particle shape. It has to be noted that many publications dealing with the effects of stereology related to size distributions are of a more theoretical nature and practical studies comparing 2-D and 3-D analytical techniques are scarce. A practical study by Lätti & Adair (2001) showed that for some types of ores the stereological bias of the mineral liberation is very small. However, here the same applies as before - theoretical assumptions dominate and practical comparative studies are scarce.

In summary it should be expressly pointed out that many of the errors listed above can be reduced respectively minimised by accurate planning, careful implementation, double check of settings (optimally, by a second person), and careful data processing. Random errors can be evaluated by repeating steps of the analysis, e.g., measurement, and can be reduced by increasing the number of data/observations. Random errors limit the precision of an analysis, whereas the systematic errors reduce the accuracy of an analysis. The latter are rather difficult to detect (Taylor 1997, Exell 2001).

The positioning of a concrete prioritisation of all MLA analysis-related sources of error is rather difficult as this depends on many influencing factors. However, a rough positioning includes the sampling-related sources of error, all measurement-related sources of error and the mineral reference list-related sources of error in a group of higher risk. The rating of the risk of sources of error related to sample preparation and stereology are heavily dependent on the sample type and the properties of the minerals, and thus can range from low to high. Sources of error with a low to medium risk level are those related to the definition of the analysis tasks, the sample splitting process, the carbon coating before measurement, the usage of the MLA Image Processing software, and sources of error related to statistical effects.

## 2.4 Method Development

For each type of sample material to be analysed by MLA a careful consideration has to be applied to take the correct approach to sample preparation, measurement setup, data processing, and data evaluation (Fig. 35). Here, the sources of error prioritised at the end of section 2.3 need to be considered carefully for method development to achieve the optimal analysis results. The current section highlights common problematic issues when using the MLA system with regards to sampling, sample preparation, measurements, image processing, and data assessment and gives suggestions to improve the MLA analytical technique in relation to the addressed issues (Table 9).

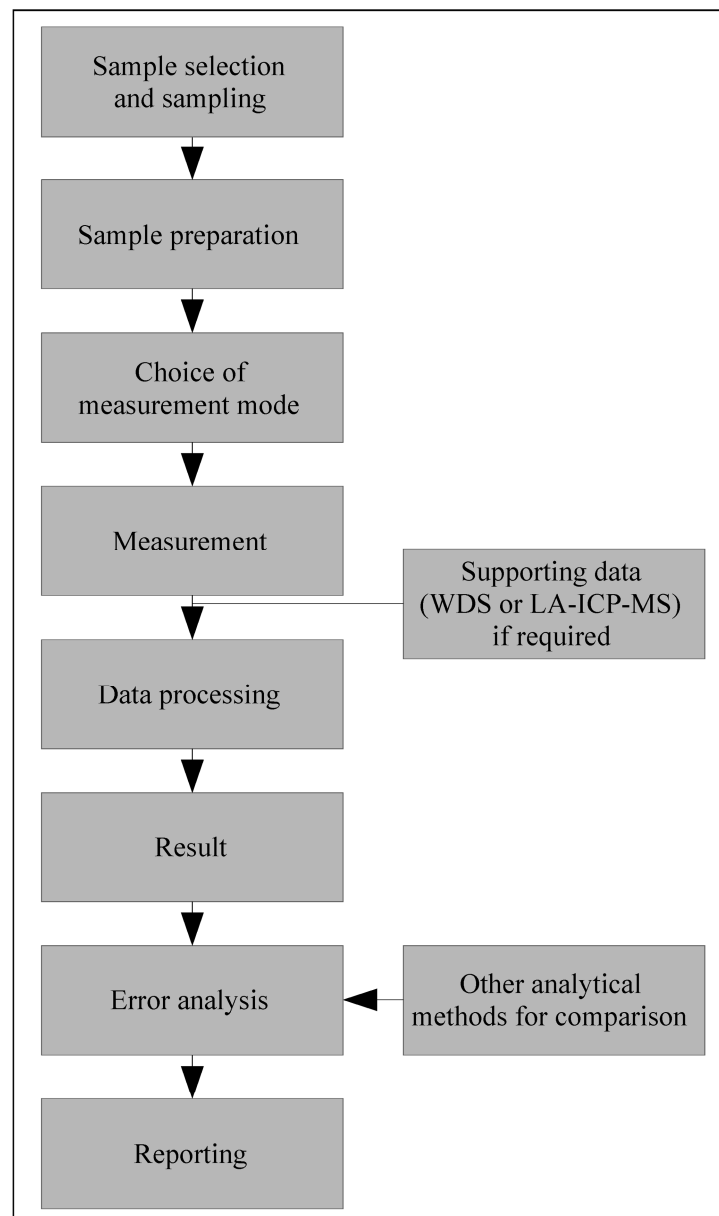


**Fig. 35:** Flowchart of MLA analysis workflow.

The chosen samples must be randomly selected and representative for the population. The amount of sample material must contain a sufficient total number of particles or number of particles containing the minerals of interest. If sample splitting is required the selection has

to be random and representative. For samples of granular materials the nature of the material has to be clarified before sample preparation. For material of rather consistent physical properties (e.g., hardness, density, and others) of its components standard sample preparation methods will suffice (see section 2.2). If, for example, high density differences in a samples are expected gravitational settling may occur during sample preparation. Therefore, it is suggested to prepare a perpendicular section of the first grain mount to assure representativity and to observe possible effects of settling (see Fig. 33). As soon as organic material is expected in a sample type regular epoxy resin having the same BSE grey level value as organic material cannot be used for mounting of the particles. In this case the sample has to be prepared using a binder with a lower (carnauba wax) or higher (chlorinated epoxy, brominated epoxy, iodinated epoxy, barium-doped epoxy) BSE grey level value than the organic material (Gottlieb et al. 1990, Agron-Olshina et al. 1992). Thin sections consisting of minerals having uniform physical properties are less critical in sample preparation but a very well-polished surface is needed to allow fast and accurate analysis. Thin sections consisting of minerals showing strong differences in physical properties such as hardness (e.g., calcite and pyrite) are much more difficult to handle. Here, the sample preparation requires an accurate assessment of the sample surface between the single grinding and polishing steps to prevent significant relief or pluck-outs. For new types of samples often a series of sample preparation tests is required to find the optimum setting for the grinding and polishing process.

**Table 9:** Analysis of vulnerabilities of the MLA technique and suggested solutions.

Area	Weak Spots	Suggested Solutions
Sampling	random selection, representativity, amount of sampled material	accurate planning prior to sampling, confer with supervisor
Sample preparation	sample splitting, physical properties of sample material, organic material	careful assessment of sample material, sample preparation tests, alternative binder
Choice of measurement	type of sample material, objective of the analysis, availability of automated reference mineral collection function	be aware of task of analysis, weight advantages and disadvantages of different measurement modes
Measurement	operator knowledge, SEM setting, measurement mode related limitations, mineral reference list (entries, spectra, reference values), image resolution, electron beam size/excitation volume	expert knowledge required, accurate handling of all steps of measurement set-up, accurate build-up of mineral reference list, support by other analytical data (EMPA, LA-ICP-MS), pure reference minerals
Data processing	mineral classification, de-agglomeration function, image quality	advanced mineral classification if required, eventually manual de-agglomeration, careful image screening
Reporting	error analysis, accuracy and precision of the measurement, number of digits after the decimal point, comparability of data	careful assessment of the analysis results, reporting of duplicate analysis, (reporting of certified reference sample analysis) [unavailable currently], comparability tests using additional analytical methods (chemical assay, QXRD)

As the SEM setting of 25 keV accelerating voltage is almost a default for MLA measurements it is suggested to evaluate the analytical requirements prior to measurement. For silicate-rich and sulphide-poor samples often a setting to an accelerating voltage of 15 keV would be beneficial as it reduces the electron beam excitation volume, improves the electron beam and image resolution, and thus enhances the characterisation of fine-grained materials such as clay minerals. It has to be noted that, in the case of the usage of carnauba wax as mounting media the contamination risk as well for BSE detectors and for EDX detectors is relatively high. Hence, while using carnauba wax as mounting media only a low BSE image magnification should be used during the measurements. In general, MLA measurement methods using a mapping of the entire specimen are preferred against centroid-based measurement modes as the latter tend to have often problems with minerals of relatively similar average atomic numbers respectively BSE grey values. However, there is no image-based MLA mapping mode which is able to collect automated mineral reference standards during the measurement. For this particular purpose only XBSE\_STD (centroid-based X-ray acquisition) and XMOD\_STD (mapping mode, but not image-based) modes can be used. Another pitfall with respect to mineral reference standards occurs in the SPL search modes as they find tiny mineral grains of interest but no reference standards were collected for these grains by XBSE\_STD mode due to their small grain size. Hence, these mineral grains will be classified as 'unknown'. Unfortunately, there is no SPL mode-based mineral reference standard collection up to now. Due to this reason all mineral grains classified as 'unknown', in a SPL measurement mode, should be investigated carefully and verified regarding their EDS spectra.

Unfortunately, directly after a MLA measurement with reference standard collection (e.g., XBSE\_STD) is finished and the initial mineral reference list was collected it remains unclear if a reference spectrum was found only at one particular place or all over the sample. To assess the significance of a (potentially mixed) spectrum and subsequently to decide if this particular spectrum is needed or not it is recommended to classify the sample with the initial mineral list first. As inaccurate and faulty reference spectra can affect the total measurement result such a first classification with the pristine mineral reference list should be conducted prior to the proper handling of the reference list. Afterwards the final mineral reference list for the project can be build-up (including removing of incorrect spectra, naming of minerals, adding of mineral properties). To optimise this procedure an initial automated mineral classification directly after completion of the measurement would be of great value. In addition, it should be considered that a mixed EDS spectrum from the boundary of two minerals can be similar to an EDS spectrum of another mineral. An example for this is the mixed spectrum of albite and chamosite as it is similar to the spectrum of the tourmaline variety schorl. In this case, a retention of this mixed spectrum, named as tourmaline (or schorl) in the mineral reference list, would lead to a disperse grain boundary-based occurrence of "tourmaline grains". Here, the entire sample area must be carefully investigated whether a tourmaline spectrum is required for the particular sample or not. If both mineral phases (schorl and albite-chamosite mixed spectrum) occur in a sample an automated discrimination is impossible and supporting analytical techniques, accurate image investigation and manual image processing are required. For specific purposes actual measured chemical composition

values should be used for the mineral entries in the MLA mineral reference list instead of the calculated compositions based on a simple stoichiometric formula. Here, the minerals can be characterised by the more precise wavelength dispersive X-ray spectrometry (WDS) using an electron micro probe analyser (EMPA). This can be beneficial for minerals with a varying chemical composition (e.g., because of elemental substitution) or for minerals containing specific trace elements (e.g., indium in sphalerite). Similar information could be obtained by using laser ablation inductively coupled plasma mass spectrometry (LA-ICP-MS). If a search mode is conducted for a MLA measurement it is often difficult to obtain the reference spectra for all important minerals. In this case, a stock of pure minerals mounted in a reference block which could be used for reference spectrum acquisition would be beneficial. An example consisting of copper mineral reference particles can be found in a publication by Weißflog et al. (2011).

Sometimes problems can occur with regards to the automated online de-agglomeration function in the MLA Measurement software respectively the de-agglomeration function in the MLA Image Processing software. Here, especially elongated particles such as micas are endangered to be sliced. When expecting this issue for a sample the de-agglomeration function in the MLA Measurement software should be deactivated. Hence, touching particles must be processed manually in the MLA Image Processing software which is time consuming. Due to the functional principle of the de-agglomeration procedure, using the shape factors circular ratio, rectangular ratio, and combined ratio, and the shape of the particles this issue cannot be solved by optimisation of the de-agglomeration setting. To avoid this issue the MLA software could be improved by the addition of an advanced de-agglomeration menu providing more choices in future.

To assess the accuracy of a MLA analysis duplicate measurements would be valuable. Unfortunately, nothing regarding this is included in the MLA software by default. Thus, the user will have to ensure to perform such considerations. If it is allowed by the limitations of the measurement time one duplicate measurement per analysis session is recommend urgently. A procedure to assess the accuracy of a MLA analysis could be to include a reference sample, having a certified mineral composition, mineral liberation and so on, into the measurement series. However, this reference sample should use the same mineral reference list as the regular samples, so that the mineral reference list of the regular measurement will not be distorted. The results of every MLA analysis should be evaluated critically, and if possible, be subjected to a comparison. For MLA result comparability tests additional analytical methods can be used which could include methods with a different analytical approach such as quantitative X-ray powder diffraction (QXRD) analysis or an analytical chemistry technique. Both of them are beneficial due to an accurate calibration using reference standards. In addition, a comparison of MLA results with the results of other automated SEM-based image analysis technologies can eventually be advantageous.

---

## Published Papers

In the following three chapters the fields of application of automated mineralogy used for the scientific papers published for this thesis will be presented. All three papers are based on studies which used the capabilities of the Mineral Liberation Analyser (MLA) of FEI Company. The first paper deals with the characterisation of lithium-bearing zinnwaldite micas in respect to mineralogical and mineral processing-relevant parameters. The second paper shows that methods of automated SEM-based image analysis, such as MLA, can be used in addition to 'traditional' methods to characterise graphite feed and concentrate materials. Whereas the first two papers link the fields of mineralogy and mineral processing the third paper focuses on platinum-group minerals (PGM) in gabbroic dykes of the Lusatian block, Germany. The latter paper demonstrates the possible application of automated mineralogy in the field of petrology - and even in the definition of exploration criteria, a field that has not been covered appropriately in literature. The other two papers, in contrast, contribute to new methods for the application of automated mineralogy in the field of industrial minerals, which is also currently widely underestimated.

It has to be noted that the lists of references, in the three original publications placed at the end of each paper, are moved and merged in this version to one comprehensive reference list at the end of the thesis. This modification to the papers was made to achieve a consistent structure of the thesis and to avoid confusion with regards to the location of the references.

## **Chapter 3: Use of Mineral Liberation Analysis (MLA) in the Characterisation of Lithium-Bearing Micas (Sandmann and Gutzmer, 2013)**

### **3.1 Abstract**

The capabilities and opportunities of the application of automated mineralogy for the characterisation of lithium-bearing zinnwaldite-micas are critically assessed. Samples of a crushed greisen-type ore comprising mostly of quartz, topaz and zinnwaldite (Li-rich mica) were exposed to further comminution by cone crusher and high voltage pulse power fragmentation. Product properties were analysed using a Mineral Liberation Analyser (MLA) and the obtained mineralogical and mineral processing relevant parameters were carefully evaluated with special focus on the characteristics of zinnwaldite. The results illustrate that both samples contain a significant quantity of very fine particles that are product of comminution. The modal mineralogy in the different sieve fractions is characterized by the accumulation of minerals of low hardness in the finest fraction and the enrichment of topaz, having a high hardness, in the somewhat larger fractions. Based on the results of mineral association data for zinnwaldite, a displacement of the muscovite-quartz ratio, in comparison to the results of modal mineralogy, was observed indicating good quartz-zinnwaldite boundary breakage and weak muscovite-zinnwaldite breakage. Liberation as well as mineral grade recovery curves indicate that fraction -1000 to +500  $\mu\text{m}$  is most suitable for beneficiation. The results of this study demonstrate that SEM-based image analysis, such as MLA, can effectively be used to investigate and evaluate phyllosilicate minerals in a fast and precise way. It is shown that the results of MLA investigations, such as modal mineralogy, are in good agreement with other analytical methods such as quantitative X-ray powder diffraction.

### **3.2 Introduction**

Comminution is one of the most energy intensive - and thus most costly - processes in industrial mineral processing. As energy costs continue to rise, comminution can compromise the profitability of a mining operation. Innovative concepts for energy-efficient comminution are therefore of great relevance. Comminution by high voltage pulse power fragmentation is such a novel concept that may be considered. Recent studies by Wang et al. (2011) illustrate that this technology, in certain cases, can be more energy-efficient compared to conventional mechanical comminution.

However, particle size reduction is only one tangible attribute to be achieved by comminution. Liberation of ore minerals is a second parameter that is of equal interest and that cannot be neglected. The present study describes the degree of liberation and particle/mineral grain size distribution achieved from samples treated with high voltage pulse power fragmentation as well as conventional mechanical comminution. Automated mineralogy – using a Mineral Liberation Analyser (Gu 2003, Fandrich et al. 2007) – was



used to quantify liberation and other tangible particle and mineral attributes.

An example of coarse-grained and isotropically textured raw material was selected for the experimental study. This material is originated from the Zinnwald Sn-W-Li greisen deposit and contains of zinnwaldite, next to quartz, topaz as well as minor cassiterite, wolframite, and fluorspar. Zinnwaldite, a Li-rich mica and main commodity of interest in this study (as a potential ore mineral), ranges up to 5 mm in grain size (Atanasova 2012).

Lithium is an emerging commodity because of its importance in energy storage systems (e.g., Li-ion batteries). Future demand for lithium is set to increase rapidly, mainly due to the continuous growth of world automobile market, rising prices for crude oil and the resultant increasing demand for lithium-ion batteries (Goonan 2012). In 2011, about two third of global lithium production came from surface brine deposits (e.g., from Chile, China and Argentina) and one third from hard-rock silicate ores. In the latter case spodumene-bearing pegmatites are the dominant source of Li-bearing hard-rock silicates, with Greenbushes (Australia) and Bikita (Zimbabwe) as prominent examples.

Li-bearing micas, namely lepidolite and zinnwaldite, currently have very limited economic significance in lithium production as they are mined only in Portugal and Zimbabwe. However, due to their wide distribution and abundance such Li-bearing micas may well become an attractive proposition, if the demand for lithium will indeed increase as predicted. It appears thus imperative to define and optimize technological approaches to liberate and concentrate Li-bearing mica (Siame & Pascoe 2011).

### 3.2.1 Synopsis of the Zinnwald Deposit

The historic Zinnwald deposit, located in the Eastern Erzgebirge/Východní Krušné hory, straddles the Saxon (Germany) - Bohemian (Czech Republic) border. Tin mining took place there from the 16th century to the 1940s (German part) resp. 1990 (Czech part). From the mid-19th century tungsten was mined and from 1869 to 1945 lithium-bearing mica concentrates were produced. During this period, Zinnwald was one of the few industrial sources of lithium globally. At present, the German side of the deposit is explored by the Solarworld AG.

The Zinnwald deposit is classified as a greisen-type orebody. This orebody is located in a fluorine-rich granitic stock intruded into Palaeozoic rhyolites. The highly altered granites host a series of lens-like Li-Sn-W-bearing greisen bodies consisting mostly of quartz, zinnwaldite, topaz and minor fluorite as well as vein-style Sn-W mineralisation. (Baumann et al. 2000)

The lithium content of the greisen deposit is solely hosted in a series of mica named zinnwaldite (Formula:  $\text{KLiFe}^{2+}\text{Al}(\text{AlSi}_3\text{O}_{10})(\text{F},\text{OH})_2$ ) extending in composition from the mineral siderophyllite ( $\text{KFe}^{2+}_2\text{Al}(\text{Al}_2\text{Si}_2\text{O}_{10})(\text{OH})_2$ ) to polyolithionite ( $\text{KLi}_2\text{Al}(\text{Si}_4\text{O}_{10})(\text{F},\text{OH})_2$ ). Zinnwaldite from the Zinnwald deposit is available as a candidate reference sample (Zinnwaldite ZW-C), and according to Govindaraju et al. (1994), has an average  $\text{Li}_2\text{O}$  content of 2.43 wt.% (n=44).

### 3.3 Methods

The material for this study was part of a large bulk sample of approximately 4 metric tons that was taken from a greisen body during a pilot project to the current exploration program by Solarworld AG. The entire bulk sample was crushed at the UVR-FIA GmbH, Freiberg, using a jaw crusher with a gap width of 35 mm. The resultant product was homogenized and split up in two representative subsamples at the Department of Mechanical Process Engineering and Mineral Processing of the TU Bergakademie Freiberg. The entire process is illustrated in Fig. 36.

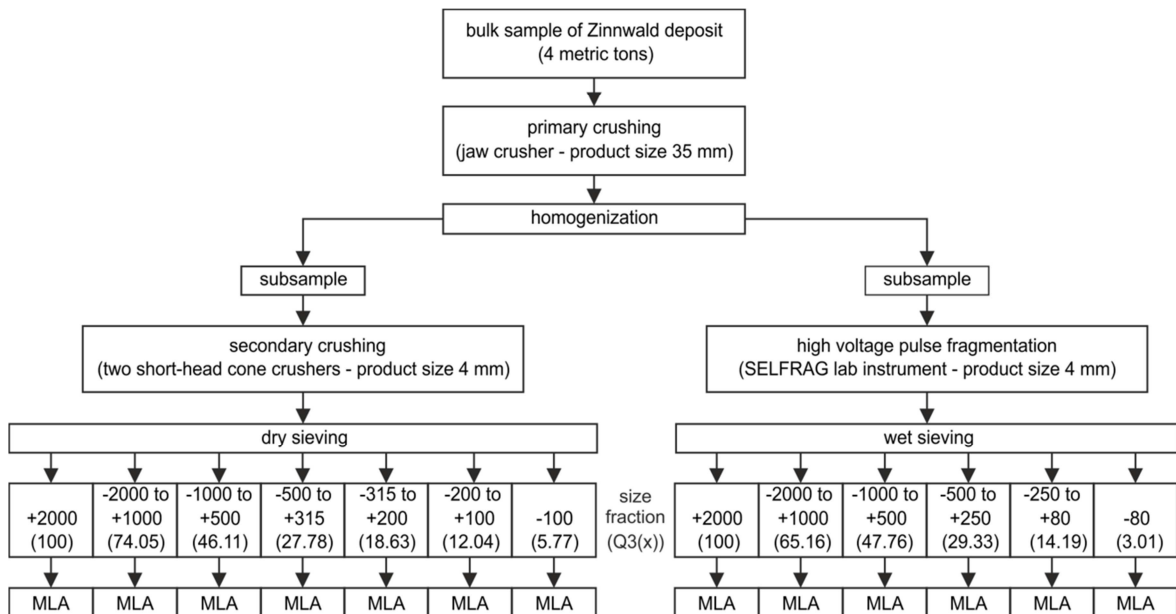


**Fig. 36:** Flowchart of the sample processing during this study (Note: sieve fractions are given in  $\mu\text{m}$  and the related cumulative distribution  $Q3(x)$  in %).

#### 3.3.1 Conventional Comminution Procedure

The first representative subsample was passed through a short-head cone crusher with a product size of 4 mm at the Department of Mechanical Process Engineering and Mineral Processing of the TU Bergakademie Freiberg. A representative subsample was taken and sized into seven sieve fractions (Fig. 36), used for Mineral Liberation Analysis (MLA).

#### 3.3.2 High Voltage Pulse Power Technology

A second subsample of crushed greisen was used as educt for high voltage pulse fragmentation. A SELFRAG lab instrument (Bluhm et al. 2000, Wang et al. 2011, Dal Martello et al. 2012), installed at the Department of Geology, TU Bergakademie Freiberg, was used for this purpose. The following instrument settings were used: voltage of the output impulse generator 150 kV, pulse frequency 3.3 Hz, and working electrode gap 10 to 40 mm. An amount of 2 kg was processed using the SELFRAG instrument feed sieve of 4 mm and on average 200-300 pulses. The product of high voltage pulse fragmentation was classified into six sieve fractions (Fig. 36) for MLA analysis.

### 3.3.3 Mineralogical and Microfabric Analysis

All 13 subsamples were prepared as polished grain mounts at the Department of Mineralogy, TU Bergakademie Freiberg. Great care was taken to avoid preferred orientation of the zinnwaldite mica that tends to form thin plates on fragmentation. Several steps of sample preparation as described by Jackson et al. (1984) were conducted including random subsampling by a rotary riffler, mixing the sample with crushed graphite and mechanical shaking of the mixture in cylindrical plastic moulds.

Quantitative studies of mineralogy and microfabric were performed at the Department of Mineralogy, TU Bergakademie Freiberg, using a FEI MLA 600F system (Gu 2003, Fandrich et al. 2007, MacDonald et al. 2012). The scanning electron microscope FEI Quanta 600F is equipped with a field emission source (FEG) and two SDD-EDS X-ray spectrometers (Bruker X-Flash) combined with Mineral Liberation Analysis (MLA) software. The polished grain mounts were carbon-coated prior to measurement to obtain an electrically conducting surface. The samples were analysed with a grain X-ray mapping measurement mode ('GXMAP') at a magnification of 175 times and a X-ray mapping threshold for back scattered electron (BSE) image grey values of 25. The analytical working distance was 10.9 mm, the emission current 190  $\mu$ A, the probe current 10 nA and the overall electron beam accelerating voltage 25 kV. Standard BSE image calibration was set with epoxy resin as background (BSE grey value <25) and gold as upper limit (BSE grey value >250). See further detail to MLA measurement modes in Fandrich et al. (2007).

## 3.4 Results and Discussion

The results of MLA measurements provide a broad range of mineralogical and processing parameters (Gu 2003, Fandrich et al. 2007). The most relevant parameters for the evaluation of effectiveness of conventional as well as high voltage pulse power treatment are presented hereinafter.

It should be noted that systematic errors can be induced by sample preparation and MLA analysis methods. As it is difficult to quantify them, a precise sample preparation, which comprehends and minimizes preparation problems, is needed to scale down the systematic errors (Bachmann et al. 2012).

### 3.4.1 Particle Size Distribution/Mineral Grain Size Distribution

The results of particle size distribution of the combined data for all size fractions show a minor amount of top sized material and a larger quantity of finest material for both the conventional comminution subsample as well as the high voltage pulse power subsample (Fig. 37a). The same applies to the zinnwaldite grain size distribution which shows nearly the same distribution as the corresponding particle sizes (Fig. 37b). It must be noted that the sizes obtained by the mineral liberation analysis are measured in 2D using the equivalent circle diameter of the particle respectively grain area. These 2D generated size data give in general a smaller size in comparison to 3D data. In spite of

this obvious limitation it has been shown by a recent study that size data measured by image analysis systems are in general in good agreement to other size distribution measurement systems (Vlachos & Chang 2011).

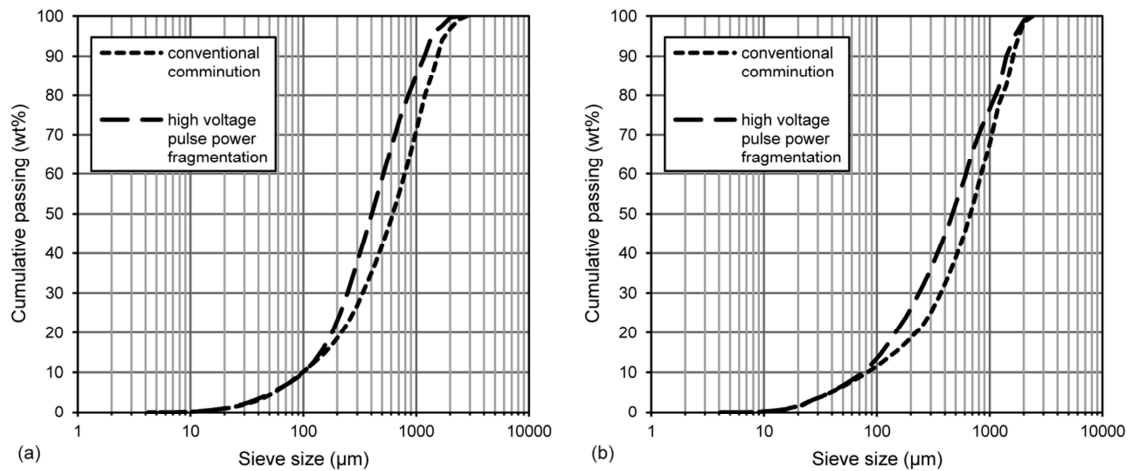


**Fig. 37:** Particle size distribution (a) and zinnwaldite mineral grain size distribution (b) of the combined data for all size fractions for the conventional comminution subsample and the high voltage pulse power fragmentation subsample.

### 3.4.2 Modal Mineralogy

The data of modal mineralogy obtained by this MLA study corroborate previous results of transmitted-light microscopic studies (Bolduan et al. 1967, Seibel 1975, Sala 1999). Light-microscopic observations of polished thin sections showed that zinnwaldite and quartz are usually coarse-grained with mineral grain/aggregate sizes of 5-6 mm. Topaz mineral grains are ordinarily somewhat smaller (up to 1 mm).

Main constituents of the two subsamples analysed here are quartz, zinnwaldite, and topaz. Further minerals in minor portions are muscovite, kaolinite, fluorite, hematite as well as in small quantities (each <0.1 wt.%) barite, crandallite, cassiterite, dolomite, columbite, scheelite, monazite, zircon, xenotime, florencite, siderite, cerphosphorhuttonite, gypsum, apatite, wolframite, ilmenorutile, sphalerite, chernovite, and uraninite. Both subsamples display varying proportions of main minerals in the larger sieve fractions, whereas the amount of zinnwaldite is more consistent in fractions of smaller particle size (-315 μm in the conventional sample and -500 μm in the high voltage pulse power sample). In relation to the combined educt sample there is a concentration of muscovite, kaolinite, fluorite and hematite in the finest fraction as well as a distinct enrichment of topaz in the fraction -500 to +100 μm respectively +80 μm (Fig. 38). This can be interpreted by the different physical properties of the minerals. For example, topaz is much harder (Mohs hardness 8) than the minerals enriched in the smallest fraction (e.g. kaolinite with Mohs hardness 2) and need more specific energy to become comminuted.

It should be mentioned that a test of high-intensity magnetic separation of zinnwaldite ore was conducted with material from both subsamples, but is not part of this paper. In a recent paper by Leißner et al. (2013) the entire mineral processing (comminution and magnetic separation) of the zinnwaldite-bearing greisen-type ore from the Zinnwald

deposit is discussed. The authors show that in all chosen size fractions liberation efficiencies are better than separation efficiencies for zinnwaldite and conclude that the separation process should be improved for process optimisation.

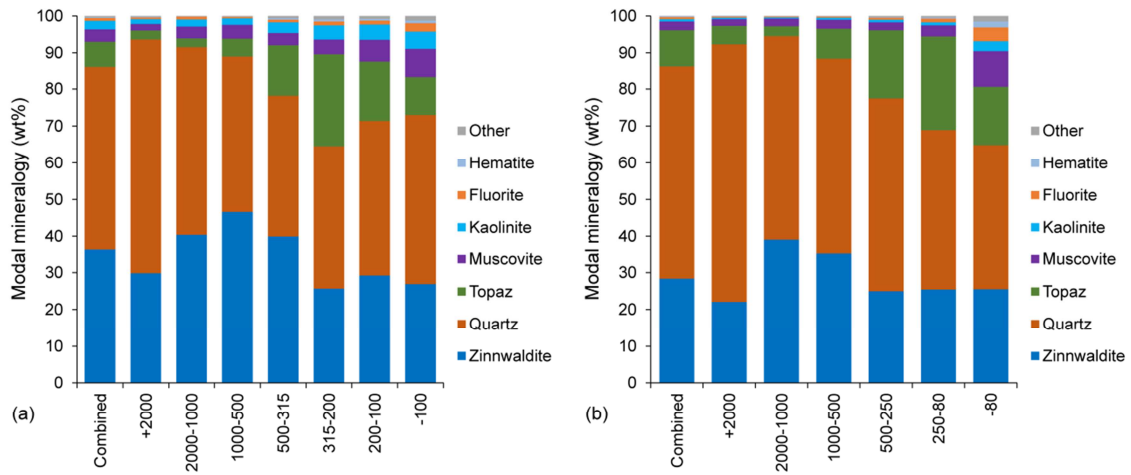


**Fig. 38:** Modal mineralogy of MLA measurements for the subsample from (a) conventional comminution and (b) high voltage pulse power fragmentation. The diagram shows as well the data of the educt ('combined') as the data for the different sieve fractions.

### 3.4.3 Mineral Locking and Mineral Association

Mineral locking and mineral association data as generated by MLA give valuable assistance to estimate the grade of associated minerals (e.g., gangue), which is important to optimize the mineral beneficiation process. The diagram of zinnwaldite mineral associations shows in general a decreasing amount of associated minerals respectively an increasing amount of non-associated zinnwaldite grains in smaller size fractions for both subsamples (Fig. 39). Zinnwaldite mineral grains that are not fully liberated are more associated with one mineral ('binary particles') than two or more minerals ('ternary+ particles') (for examples see Fig. 40).

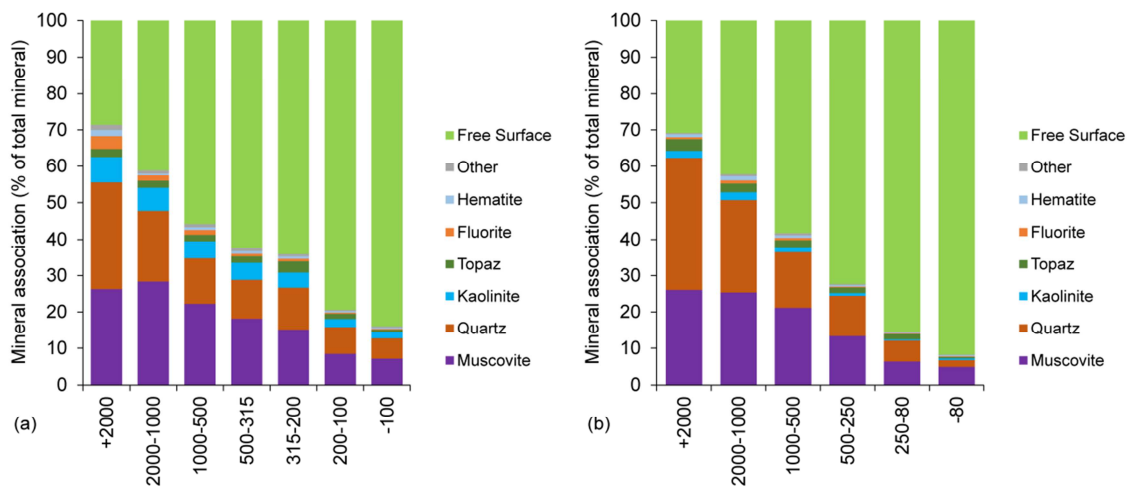


**Fig. 39:** Mineral association for zinnwaldite mineral grains in the different sieve fractions (a) from conventional comminution and (b) high voltage pulse power fragmentation.

The results of mineral association data reflect roughly the results of modal mineralogy with quartz, muscovite, topaz and kaolinite as the main minerals associated with zinnwaldite. It can be noted that the quartz-muscovite ratio in the zinnwaldite mineral association results ( $\leq 1$ ) is much lower than expected from the results of modal mineralogy (quartz-muscovite ratio:  $> 5$ ). This means that the muscovite-zinnwaldite grain boundary breakage is not as good as the quartz-zinnwaldite grain boundary breakage. This can be observed in both the conventional comminution subsample and the high voltage pulse power subsample and is explained by the overgrowth and replacement of zinnwaldite by muscovite in a younger greisenisation stage (Fig. 41).

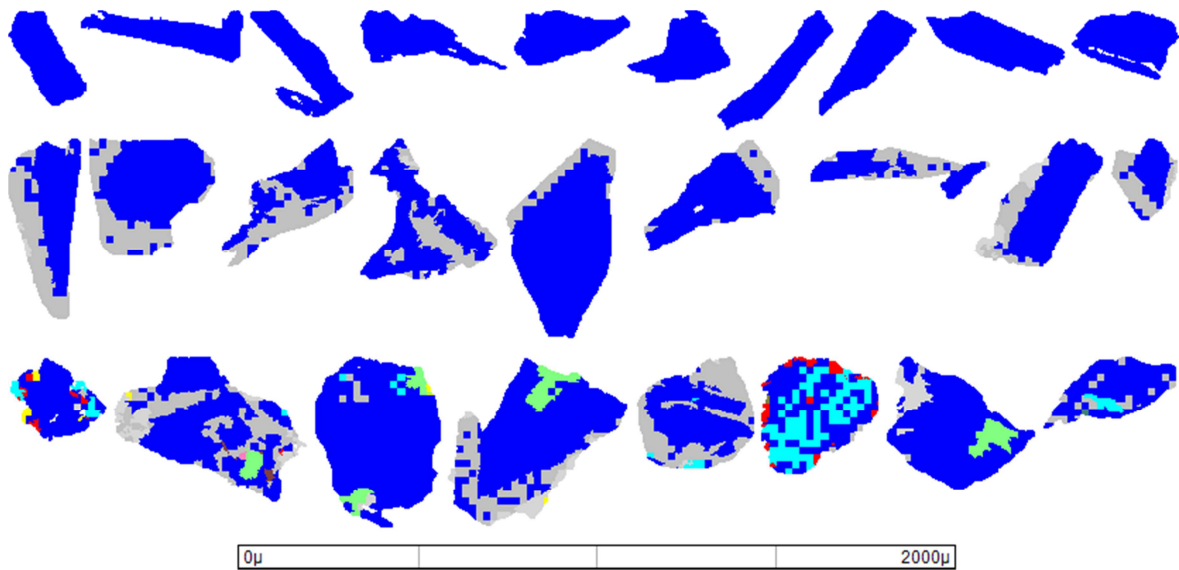


**Fig. 40:** Line-up of three groups of different zinnwaldite locking characteristics (Row 1 – liberated zinnwaldite grains; Row 2 – binary (with only one other phase) locked zinnwaldite grains; Row 3 – ternary and higher (with more than one phase) locked zinnwaldite grains) from the conventional comminution subsample.

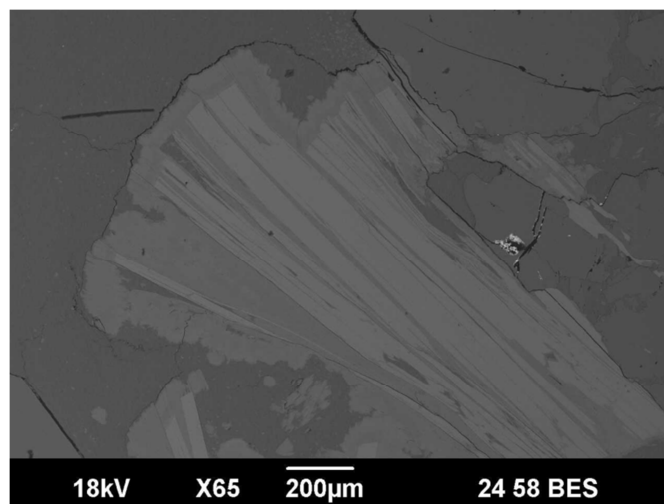


**Fig. 41:** Intense overgrowth and replacement of zinnwaldite (light grey; elongated) by muscovite (medium grey) in a younger greisenisation stage (BSE image from Atanasova (2012)).

### 3.4.4 Mineral Liberation

The mineral liberation by particle composition diagram for zinnwaldite-bearing particles shows not completely an increasing degree of liberation from smaller sieve fractions for both conventional comminution and high voltage pulse power subsamples (Fig. 42). This applies only for the three largest sieve fractions. The sieve fraction -500 to +315  $\mu\text{m}$  resp. -500 to +250  $\mu\text{m}$  shows, in contrast, a worse degree of liberation as compared to sieve fractions -1000 to +500  $\mu\text{m}$ , which is the best liberated fraction. The two smallest sieve fractions are again not as good liberated as sieve fraction -500 to +315  $\mu\text{m}$  resp. -500 to +250  $\mu\text{m}$ . All these apply for both conventional comminution and high voltage pulse power subsamples. The shape of the different curves is related to its starting point of the curve at the 100% liberation class. The curves with a small amount of particles in this class show a rapid increase in particles in the 90-95% liberation class. Curves with a higher starting point show a lower rise.

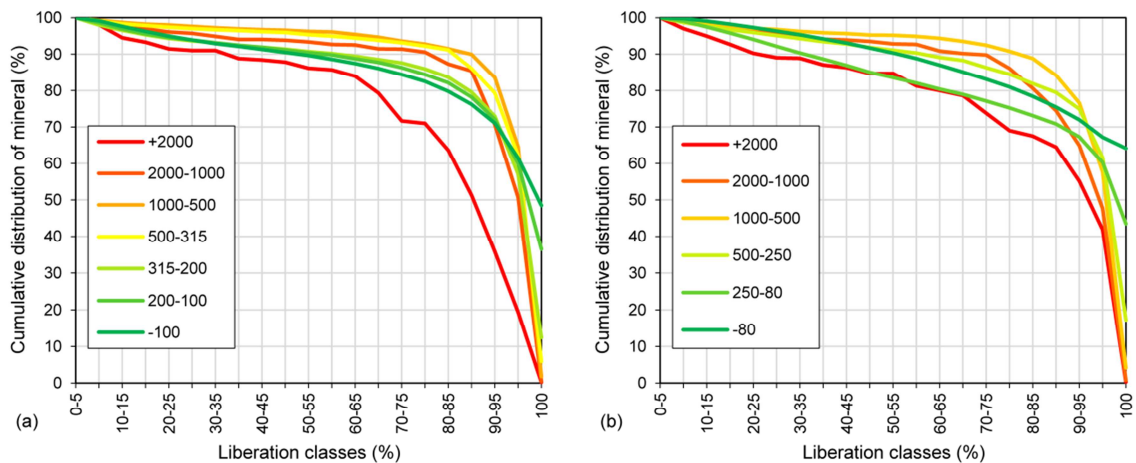


**Fig. 42:** Mineral liberation by particle composition for zinnwaldite mineral grains in different sieve fractions from (a) conventional comminution and (b) high voltage pulse power fragmentation subsamples.

### 3.4.5 Theoretical Grade Recovery

Theoretical grade-recovery curves are defined by the maximal expected recovery of a mineral at a given grade. These curves are related to the comminution size of the treatment process and determined from the liberation characteristics. It should be noted that theoretical grade-recovery curves are defined for the value minerals (e.g., zinnwaldite) and not based on a final product (e.g., metal or compound) to be recovered. Furthermore it is important to advise that the theoretical grade-recovery curves provided by the MLA are generated from 2D liberation measurements and therefore overestimate the true liberation by a certain amount (MinAssist Pty Ltd 2009).

The theoretical grade-recovery curves for zinnwaldite in Fig. 43 give reason to expect best results for zinnwaldite recovery in the sieve fraction -1000 to +500  $\mu\text{m}$  for both the conventional comminution subsample and the high voltage pulse power fragmentation subsample.

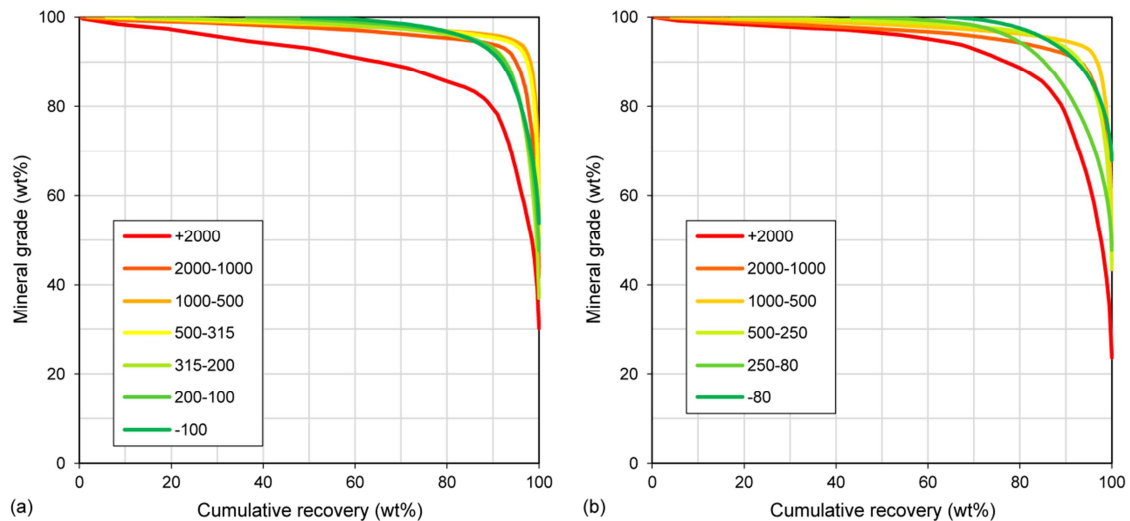


**Fig. 43:** Theoretical grade recovery curve for zinnwaldite mineral grains in different sieve fractions from (a) conventional comminution and (b) high voltage pulse power fragmentation subsamples.

### 3.5 Conclusions

It has been shown that for zinnwaldite-bearing materials from a greisen ore-type high recovery rates can be reached for both the high voltage pulse power fragmentation (SELFrag technology) and the conventional particle comminution. From the grade recovery curves it is obvious that optimal results for both processes could be achieved from the 1000-500  $\mu\text{m}$  size fraction. Smaller and larger size fractions show poorer results for the zinnwaldite recovery. In contrast, the results of the zinnwaldite mineral association show a continuous decrease in associated minerals and an increasing amount of liberated zinnwaldite grains by the decline of particle size fractions.

To further assess the quality of size and liberation/recovery data of this MLA study 3D measurements could be useful. This has been studied for the example of phosphate samples by X-ray micro-computer tomography, with better results in comparison to a 2D analysis (Miller et al. 2009).

Due to the method setting of this study it was not possible to conduct a direct comparison between the effectivity of the two comminution methods. However, a recent study by Wang et al. (2012) indicates on the example of sulphide ores and PGM ores, that high voltage pulse power fragmentation generates a coarser product with significantly less fines than the conventional mechanical comminution and that minerals of interest in the high voltage pulse power product are better liberated than in the conventional product. It should be considered, that various minerals can have a different behaviour (depending on e.g., electric conductivity, mineral cleavage, discontinuities in the material and much more) at the high voltage pulse power fragmentation. Hence, the results of single studies should not be transferred to another type of material without a reinvestigation. For a decision between different comminution techniques factors as throughput rates, processing time, energy costs or water consumption should be examined too as they will affect the processing efficiency and overall costs.



The present study demonstrates the capabilities of automated SEM-based image analysis systems, such as the Mineral Liberation Analyser (MLA), for the evaluation of industrial comminution processes. The obtained data provide valuable key information on quantitative mineralogy, mineral association, particle and mineral grain sizes, as well as mineral liberation and theoretical recovery data. Results illustrate that a MLA system can be used to constrain parameters relevant to assess comminution success in a fast and reproducible way.

### **3.6 Acknowledgements**

The authors would like to thank Thomas Zschoge from the Department of Mechanical Process Engineering and Mineral Processing (TU Bergakademie Freiberg) for supporting the conventional comminution as well as Thomas Mütze and Thomas Leißner from the same department for fruitful discussions and helpful suggestions. For instruction in sample processing by high voltage pulse fragmentation we thank Peter Segler from the Department of Geology (TU Bergakademie Freiberg). The preparation of polished grain mounts and the support during MLA measurement by Sabine Haser and Bernhard Schulz of the Department of Mineralogy, TU Bergakademie Freiberg is gratefully acknowledged. This study was supported by the Nordic Researcher Network on Process Mineralogy and Geometallurgy (ProMinNET) and was carried as part of a BMBF-funded research project (Hybride Lithiumgewinnung, Project No. 030203009).

## **Chapter 4: Characterisation of graphite by automated mineral liberation analysis (Sandmann *et al.*, 2014)**

### **4.1 Abstract**

The beneficiation of graphite is very costly and energy intensive and can does necessitate multiple processing steps, often including flotation. Products have to satisfy very stringent quality criteria. To decrease beneficiation costs a careful characterisation of feed and concentrate materials is needed. This study elucidates the additional benefit of methods of automated SEM-based image analysis, such as Mineral Liberation Analysis (MLA), in addition to ‘traditional’ methods (optical, XRD) for the analyses of graphite raw materials and processing products. Due to the physical and chemical properties of the mineral graphite, samples require delicate sample preparation as well as particular backscatter electron imaging calibration for automated image analysis. These are illustrated in this study. The results illustrate that SEM-based image analysis of graphite feeds and concentrates can provide accurate and reliable information for the graphite beneficiation process. This applies to both mineralogical characteristics and process relevant parameters.

### **4.2 Introduction**

Graphite, a crystalline form of native carbon with a sheet-like crystal structure (Rösler 1991) has a unique combination of physical properties, e.g. good thermal and electrolytic conductivity, outstanding lubrication properties, resistance against chemicals as well as temperature-change resistance. It is due to these properties that graphite has a wide range of industrial applications, including the production of graphene. The beneficiation of graphite is influenced by its crystallinity, flake size and the nature and distribution of associated gangue minerals (Acharya *et al.* 1996). It may comprise of a variety of processes, including crushing, grinding, screening, tabling, flotation, magnetic separation, and electrostatic separation (Andrews 1992). Beneficiation intricacy can vary from simple hand sorting and screening of high-grade ore to a multi-stage flotation process (Olson 2012). Since mineral beneficiation is both energy and cost intensive graphite raw materials and beneficiation products need to be characterised very carefully to optimize the beneficiation process chain. Currently, graphite raw materials are characterised using optical microscopy, X-ray powder diffraction, differential thermal analysis/thermogravimetry (DTA/TG), Raman spectroscopy, secondary ion mass spectrometry (SIMS) as well as chemical analysis (see, for example, Patil *et al.* (1997), Patnaik *et al.* (1999), Kwiecinska *et al.* (2010), and Volkova *et al.* (2011)). Whilst these analytical methods provide a host of relevant information, only optical microscopy will provide at least some information about mineral association, liberation or locking, all attributes relevant parameters to understand the success of beneficiation. However, optical microscopy is very time-consuming and thus expensive, with results often biased by the human factor. For many raw material types this situation has been greatly improved by the use of automated

SEM-based image analysis, for example with a Mineral Liberation Analyser (MLA) (Gu 2003, Fandrich *et al.* 2007) or a QEMSCAN system (Sutherland & Gottlieb 1991, Gottlieb *et al.* 2000, Pirrie *et al.* 2004).

Automated SEM-based image analysis has already been successfully applied to coal (Creelman & Ward 1996, Liu *et al.* 2005, van Alphen 2007, Moitsheki *et al.* 2010, O'Brien *et al.* 2011). However, its use has never been tested for graphite raw materials. This study thus explores the application of automated SEM-based image analysis for the characterisation of graphite raw materials and beneficiation products.

### 4.3 Sample preparation and analytical methods

Five crushed graphite samples were provided by the German-based AMG Mining AG for method development. These samples consisted of two crushed feed samples and three concentrate samples, which were each unsized. The samples originated from four different localities (Table 10). Prior to analysis no other data were furnished by AMG Mining for these samples.

**Table 10:** List of samples.

Sample	Origin	Type
FeedSB	Sri Lanka	Feed material
NPFeed5%C	Mozambique	Feed material
NPF175%C	Mozambique	Concentrate
Konz85B	Germany	Concentrate
LynxConc90	Zimbabwe	Concentrate

For automated SEM-based image analysis, polished sample surfaces of very high quality, as well as a very consistent backscattered electron (BSE) imaging condition that enables differentiation of different mineral particles and extraction of particles from the mounting medium, are needed. Epoxy resin typically used for grain mount sample preparation cannot be used for preparation of graphite bearing samples as the average atomic number (AAN) for graphite is very similar to that of epoxy resin. Thus the use of conventional epoxy would result in similar backscatter electron grey values for both, which, in turn, would render impossible the distinction of graphite from the mounting medium. Furthermore, graphite is a mineral that is exceptionally soft and with an excellent basal cleavage. Achieving well-polished surfaces and avoidance of smearing of graphite on the sample surface therefore requires different preparation procedures compared to coal samples (FEI Company 2009e). Sample preparation was carried out in the Department of Mineralogy, TU Bergakademie Freiberg. To attain a suitable contrast between graphite and mounting medium carnauba wax, having a lower AAN (and thus a lower BSE level) was used for the preparation of the samples according to a technical application note by FEI Company (2009e). The graphite-bearing samples were mixed with the carnauba wax in a ratio of 1:4 (graphite:wax) in 25 mm diameter plastic tubes. Then the samples were placed in an oven at 90 °C (melting point of carnauba wax: 84 °C) for about 2 hours until the wax was thoroughly melted, encasing the sample material, and the particles had sunk to the bottom of the tube. Afterwards the oven was set to 40 °C to reduce the temperature slowly to

control shrinkage and prevent cracking of the wax block. After cooling the sample blocks were removed from their tubes and were mounted with epoxy resin in the middle of 30 mm moulds to give the wax strength, stop it from breaking and provide a stable surface for the polishing process.

The formation of a thin graphite film, a few micrometres in thickness, across the entire sample surface was observed during the polishing of all samples. This film causes reduced contrast and brightness of the backscattered electron image, but has otherwise no detrimental impact as samples since SEM-based image analysis are usually covered by a conducting carbon layer. Because the exact thickness of the graphite film generated during polishing is not known, we addressed its presence by calibrating BSE image parameters using a quartz grain in the FEI's standard block for image calibration (FEI Company 2009e). It needs to be stressed that systematic errors can easily be brought in by sample preparation (Bachmann *et al.* 2012) and/or choice of analytical parameters. The occurrence or extent of such systematic errors can only be assessed by verification of analytical results using results obtained by independent, well-established analytical methods. For this purpose data were sourced from other analytical methods, with some of the information directly sourced from AMG Mining.

The polished grain mount specimens were carbon-coated (a few nanometres layer thickness) to provide a conductive coating for non-conducting minerals. Automated image analysis was carried out on a FEI MLA 600F system at the Department of Mineralogy, TU Bergakademie Freiberg. This system is based on a FEI Quanta 600F scanning electron microscope equipped with a field emission gun and two Bruker X-Flash SDD-EDS X-ray spectrometers. The instrument and image acquisition were controlled by the Mineral Liberation Analysis (MLA) software. Measurement modes used included 'XBSE\_STD' to collect mineral standards and 'GXMAP', i.e., grain X-ray mapping at a magnification of 200 times. The analytical working distance during the measurement was 10.9 mm, the emission current was 205  $\mu$ A, the beam current was 10 nA, and the overall electron beam accelerating voltage was 25 kV.

Quantitative X-ray powder diffraction (XRD) analysis was conducted by the mineralogical laboratory of the Department of Mineralogy, TU Bergakademie Freiberg on two of the samples (FeedSB and NPFeed5%C) using an URD 6 XRD device (Seifert/Freiberger Präzisionsmechanik) with Co- $K\alpha$  radiation (40 kV/30 mA). The irradiated length was kept constant at 15 mm and the samples were scanned with 2 $\theta$  steps of 0.02° in the range from 5-80° at step times of 2 s/step. Quantification of powder diffraction patterns was carried out using the Rietveld programs BGMN/AutoQuan (Taut *et al.* 1998).

Dry sieve classification data were supplied by AMG Mining AG, Kropfmühl. Silicon oil based laser diffraction was done at the Institute of Mechanical Process Engineering and Mineral Processing of the TU Bergakademie Freiberg using a Sympatec HELOS based on laser diffraction and a CUVETTE wet dispersing system. Prior to analysis the diluted suspension (graphite in low viscosity silicon oil) was dispersed by ultrasonication using a 200 W Bandelin sonotrode system for 4 min at 50% pulsation.

Loss on ignition as a method for measuring carbon content in graphite was conducted by AMG Mining AG, Kropfmühl. The sample size was 1 g per sample (dry weight), the ignition temperature 850 °C and the exposure time 20 minutes.

#### 4.4 Results and discussion

A cursory look at BSE images and extracted particle shapes shows that graphite mineral particles are very well resolved and grain outlines well recovered from BSE images collected (Fig. 44). Based on this impression, the results were processed to assess a comprehensive range of mineralogical and microfabric parameters relevant for beneficiation. These parameters were then, wherever possible, compared to data from alternative analytical tools. The most relevant of the parameters tested are presented and discussed below.

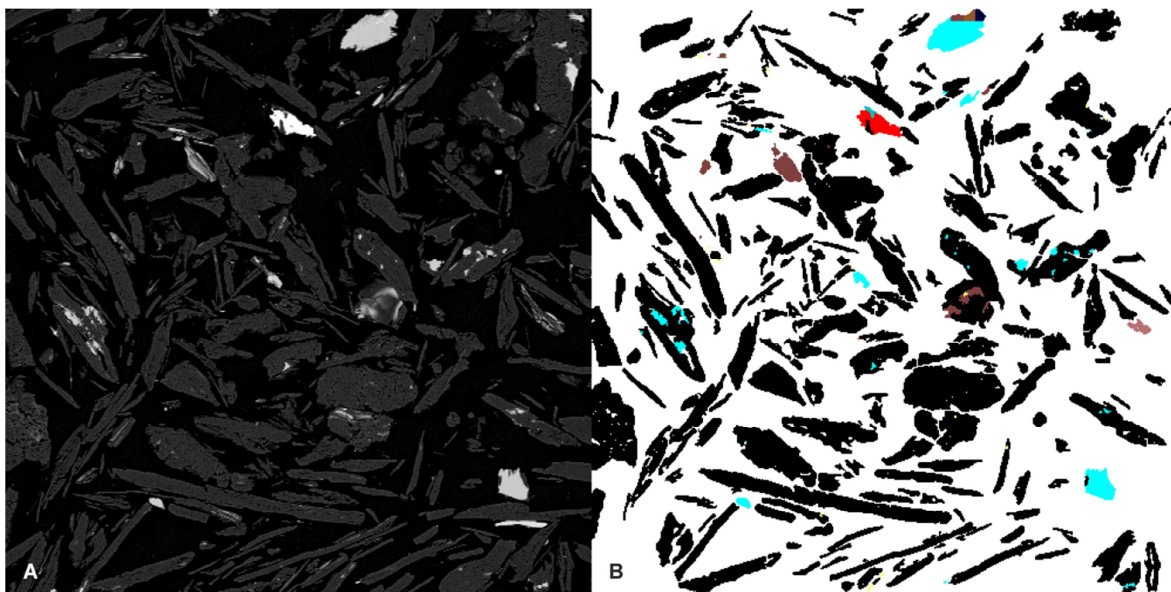


**Fig. 44:** (A) Backscatter electron (BSE) image of a MLA measurement frame of concentrate sample LynxConc90 mounted in carnauba wax (black - matrix of carnauba wax; dark grey - graphite; brighter grey tones - silicates) and (B) associated false colour image after background extraction and classification of minerals (graphite - black; quartz - blue; clay-minerals - brown; pyrite - red; muscovite - yellow) (size of frame: 500 x 500 pixels = 1.5 x 1.5 mm).

The MLA results showed that all five samples are principally composed of graphite and quartz, as well as feldspar and mica of variable composition (Fig. 45). Minor constituents include carbonates, chlorites and clay minerals. The complete mineral list for all samples comprises altogether 45 minerals. It should be noted that the minerals of the alunite group (including alunite, crandallite, jarosite, and natrojarosite), which occur with about 4 wt.% in sample Konz85B and about 1-2 wt.% in samples NPFeed5%C and NPFI75%C, are not primary constituents of the raw material. Instead, these minerals formed by the oxidation of sulphides, e.g. pyrrhotite and pyrite, during storage of these samples. Furthermore it is noted that each sample contains particular minerals characteristic of particular host rocks that point to the origin and geological context of the graphite raw material. Such minerals include pyroxenes, amphiboles and garnets in sample FeedSB. The presence of such a suite of gangue minerals points to an origin of graphite from charnockite, calc gneiss, or garnet-bearing gneiss. In sample LynxConc90, in contrast, sillimanite was identified suggesting that graphite was extracted from a sillimanite-bearing gneiss.

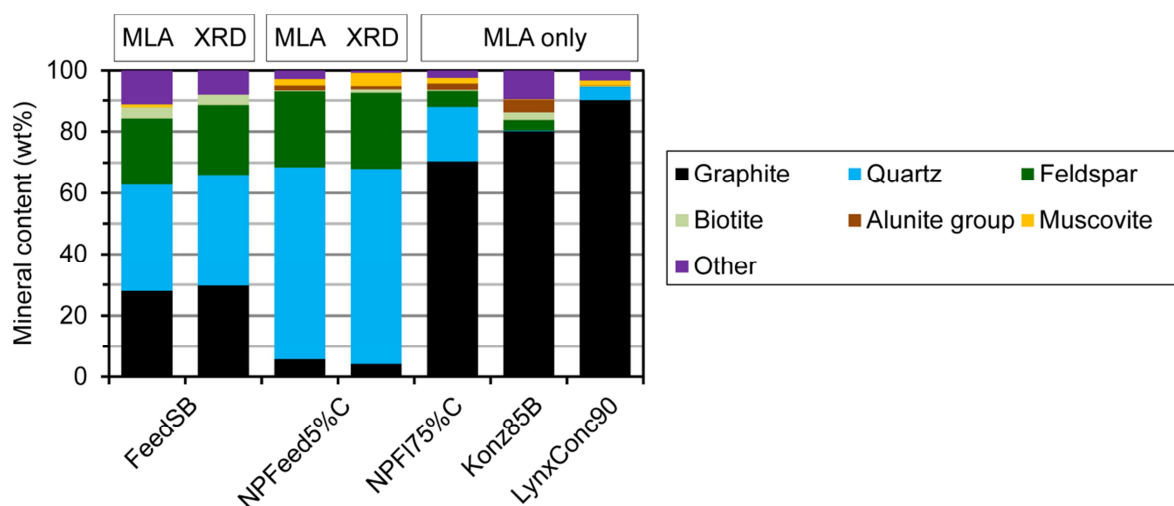


**Fig. 45:** Modal mineralogy of the five graphite samples studied based on MLA measurements and results of Rietveld analysis for comparison.

Modal mineralogies obtained by SEM-based image analysis for two feed samples (FeedSB, NPFeed5%C) contrasted with the results from quantitative X-ray powder diffraction analysis demonstrate an excellent agreement between the two analytical methods (see Fig. 45). Similarly, the elemental assay computed by the MLA software from the quantitative mineralogical data and stoichiometric mineral compositions can be compared to actual chemical assays (Table 11). In this case, the calculated carbon content is compared to the carbon concentration measured by the laboratory of the AMG Mining AG, Kropfmühl based on loss-on-ignition (LOI) determinations. Unfortunately no analytical error values for LOI analysis are available either in geochemical textbooks or in peer-reviewed articles. So it seems impossible to assess the carbon values calculated by MLA in comparison to the LOI determinations.

**Table 11:** Results of calculated elemental assay by MLA and carbon measurement with LOI method (all values are given in wt.%).

Element	FeedSB	NPFeed5%C	NPFI75%C	Konz85B	LynxConc90
MLA (calculated assay)					
C	28.2	5.7	70.4	80.1	90.2
Si	24.2	36.8	10.4	2.0	2.8
Al	3.9	3.9	1.3	0.9	0.8
Fe	2.7	0.9	1.0	5.9	0.6
K	2.1	2.3	0.8	0.6	0.2
Ca	1.7	0.3	0.1	0.3	0.0
Mg	0.7	0.1	0.1	0.3	0.0
O	35.0	47.2	14.3	6.7	4.6
S	0.2	0.3	0.3	2.0	0.2
Other	1.4	2.4	1.3	1.2	0.5
Total	100.0	100.0	100.0	100.0	100.0
LOI					
C	30.6	3.6	70.9	75.2	89.8

The results of the MLA particle size investigations show fairly similar size distributions for all samples (with P50 ca. 140-200  $\mu\text{m}$ ), except sample Konz85B, which appears to be finer-grained (P50 = 51  $\mu\text{m}$ ). A similar observation applies to the graphite mineral grain

size distributions (Fig. 46). It is to be noted that size data are based on the measured 2D surface of the particles and grains and were calculated from the MLA software using the equivalent circle diameter method.

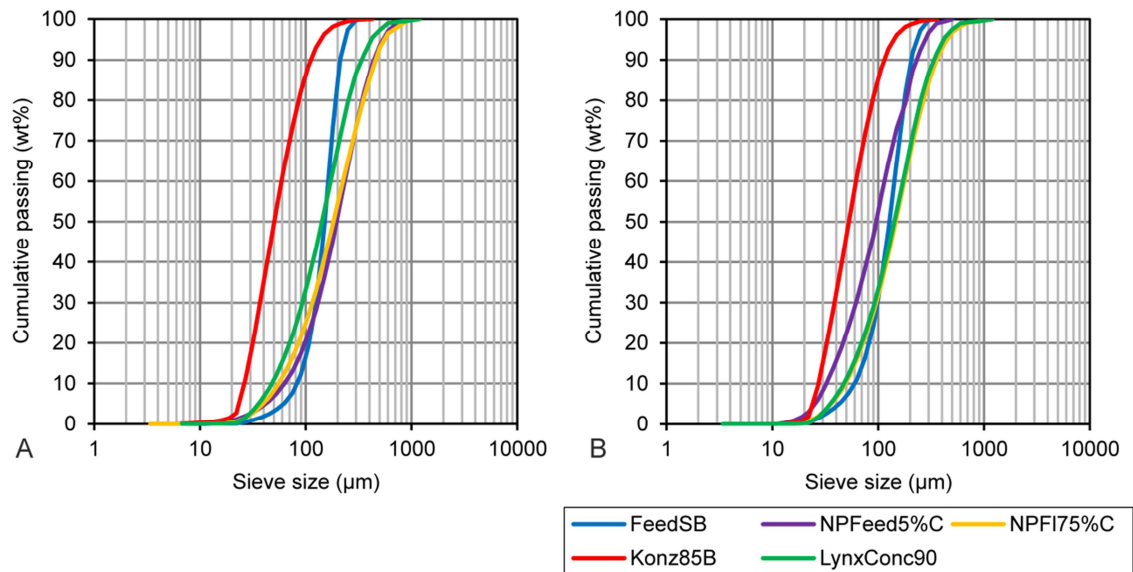


**Fig. 46:** (A) Cumulative particle size distribution and (B) cumulative graphite mineral grain size distribution.

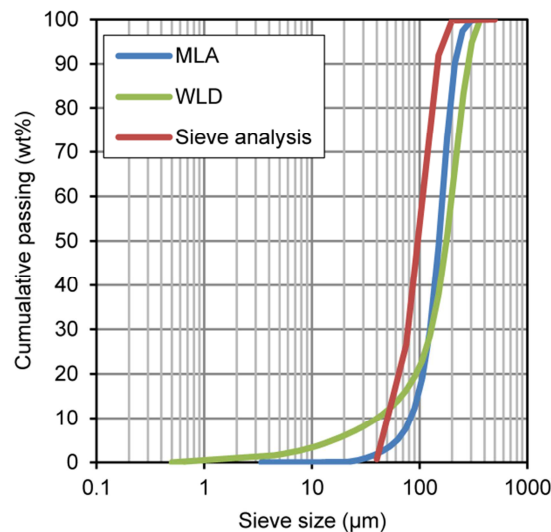


**Fig. 47:** Comparison of particle size distributions as determined by sieve classification, wet laser diffraction (WLD) and MLA for sample FeedSB (Note: comparative data for all samples are included in the supplementary data).

For comparison, particle size distributions were also assessed using dry sieve classification and wet laser diffraction. It has to be stressed that particles  $>315 \mu\text{m}$  could not be measured with the wet laser diffraction instrument used here. This coarse fraction was thus screened off prior to laser diffraction experiments. In general, the results of dry sieve classification yield a finer particle size distribution than wet laser diffraction across the central part of the particle size distribution curve (see example Fig. 47 and Supplementary Material). This is in good agreement with a study by Vlachos & Chang (2011) and is

attributed to particle shape attributes and their impact on the results of the analytical methods used. Furthermore it should be considered that particle sizes of very soft minerals, such as graphite, may well be affected by mechanical abrasion during sieve classification. It is also obvious that wet laser diffraction shows a much larger fraction of very fine particles than the two other methods. Given the physical properties of graphite, it appears likely that fine graphite-rich particles are effectively dispersed, and may be even decomposed, by the ultrasonic dispersion process and mechanical transport (Merkus 2009). Further explanations for the observed differences could be the classification of particles in the transfer from the sample dispersion unit to the measurement zone, instability of the dispersion or the inclusion of air bubbles. Sieve classification, as well as analysis by MLA, may well suffer from agglomeration of very fine particles.

For three of the five studied samples (FeedSB, Konz85B, LynxConc90) particle size distributions as determined by MLA are between those determined by sieve classification and laser diffraction. In contrast, the results for NPFeed5%C and NPFI75%C obtained by MLA show a somewhat coarser particle size distribution in comparison to the two other methods (Table 12). This is tentatively attributed to minor preferred orientation of the graphite flakes into the polished sample surface, an effect that may be particularly pronounced for graphite-rich samples. All in all, it is fair to conclude that MLA analysis provides a realistic assessment of particle size distributions of graphite feed and concentrate samples.

**Table 12:** P-values of the three different size distribution measurements for all five samples (MLA - mineral liberation analyser, WLD - wet laser diffraction, SC - dry sieve classification).

P-value		P10/ $\mu\text{m}$	P20/ $\mu\text{m}$	P50/ $\mu\text{m}$	P80/ $\mu\text{m}$	P90/ $\mu\text{m}$
FeedSB	MLA	82	108	152	193	212
	WLD	40	93	177	247	284
	SC	52	66	102	137	148
Konz85B	MLA	26	32	51	86	113
	WLD	12	25	72	141	185
	SC	-	-	-	-	-
LynxConc90	MLA	48	71	143	254	340
	WLD	42	76	180	-	-
	SC	-	45	118	197	267
NPFeed5%C	MLA	63	98	196	343	442
	WLD	5	13	96	-	-
	SC	-	41	128	218	292
NPFI75%C	MLA	55	85	183	350	459
	WLD	18	45	157	-	-
	SC	-	-	109	220	295

Unlike the parameters discussed above, quantitative mineral association and liberation data cannot be acquired with methods other than SEM-based image analysis – unless one uses optical microscopy, which is both very laborious and difficult for a mineral such as graphite which tends to obscure all associated mineral grains by forming thin coatings during sample preparation. Usage of SME-based image analysis thus yields very tangible information that can otherwise not be determined. The mineral association calculations show that quartz, feldspar and micas are the principal minerals associated with graphite in



all samples (Fig. 48). An exception is concentrate sample Konz85B. In this sample the secondary alunite group minerals are the most commonly attached to or intergrown with graphite. It is obvious that this is a phenomenon that would be irrelevant to beneficiation, since the alunite group minerals formed during sample storage.

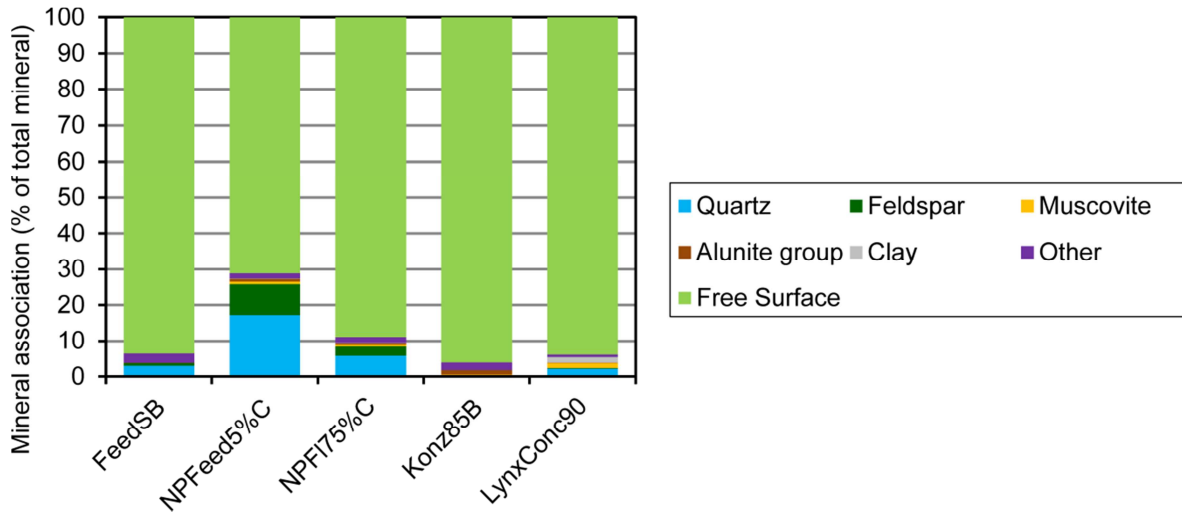


**Fig. 48:** Mineral association for graphite mineral grains.

Based on the results of the mineral association parameters in Fig. 48, about 90% of the total graphite mineral grain surface in the three concentrate samples is free surface. Even the two feed samples have very well exposed mineral surfaces, with FeedSB having more than 90% and NPFeed5%C having about 70% free surface of graphite mineral grains.

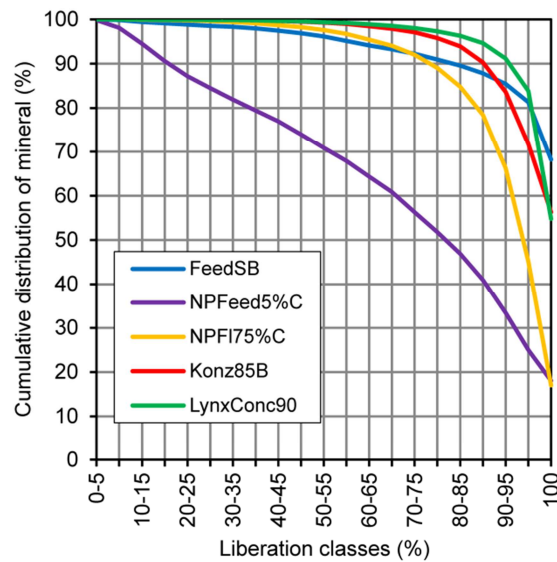


**Fig. 49:** Mineral liberation by free surface curve for graphite.

The mineral liberation by free surface curves for graphite (Fig. 49) for concentrate samples LynxConc90, Konz85B as well as feed sample FeedSB are marked by excellent liberation, in good agreement with the predominance of free surface. Similarly, the distinctly lower amount of free surface finds its expression in lower liberation of graphite in concentrate sample NPFI75%C. Feed sample NPFeed5%C, with a very low content of graphite, is also

marked by low graphite liberation. Liberation may be increased in both cases by further comminution. The mineral liberation by free surface curve is relevant for the flotation process as it gives information about the quality of the direct contact of the graphite to the flotation reagents. Calculated mineral grade recovery curves (Fig. 50) can be used to assess the maximum potential recovery at a given grade. This study clearly demonstrates that for all samples, except sample NPFeed5%C, high graphite recovery rates can be achieved at high mineral grades.

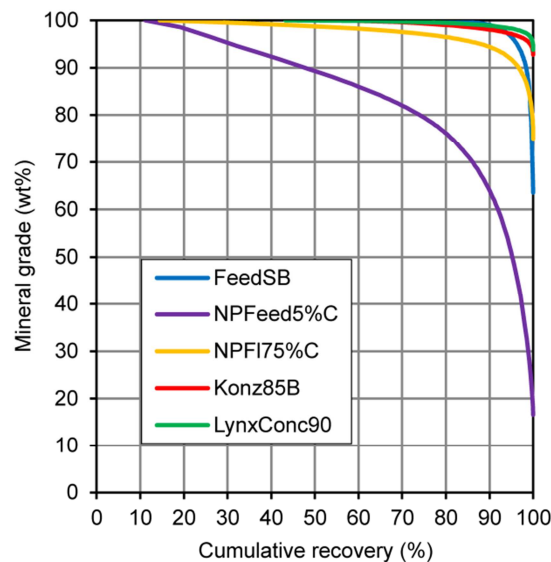


Fig. 50: Calculated mineral grade recovery curve for graphite.

## 4.5 Conclusions

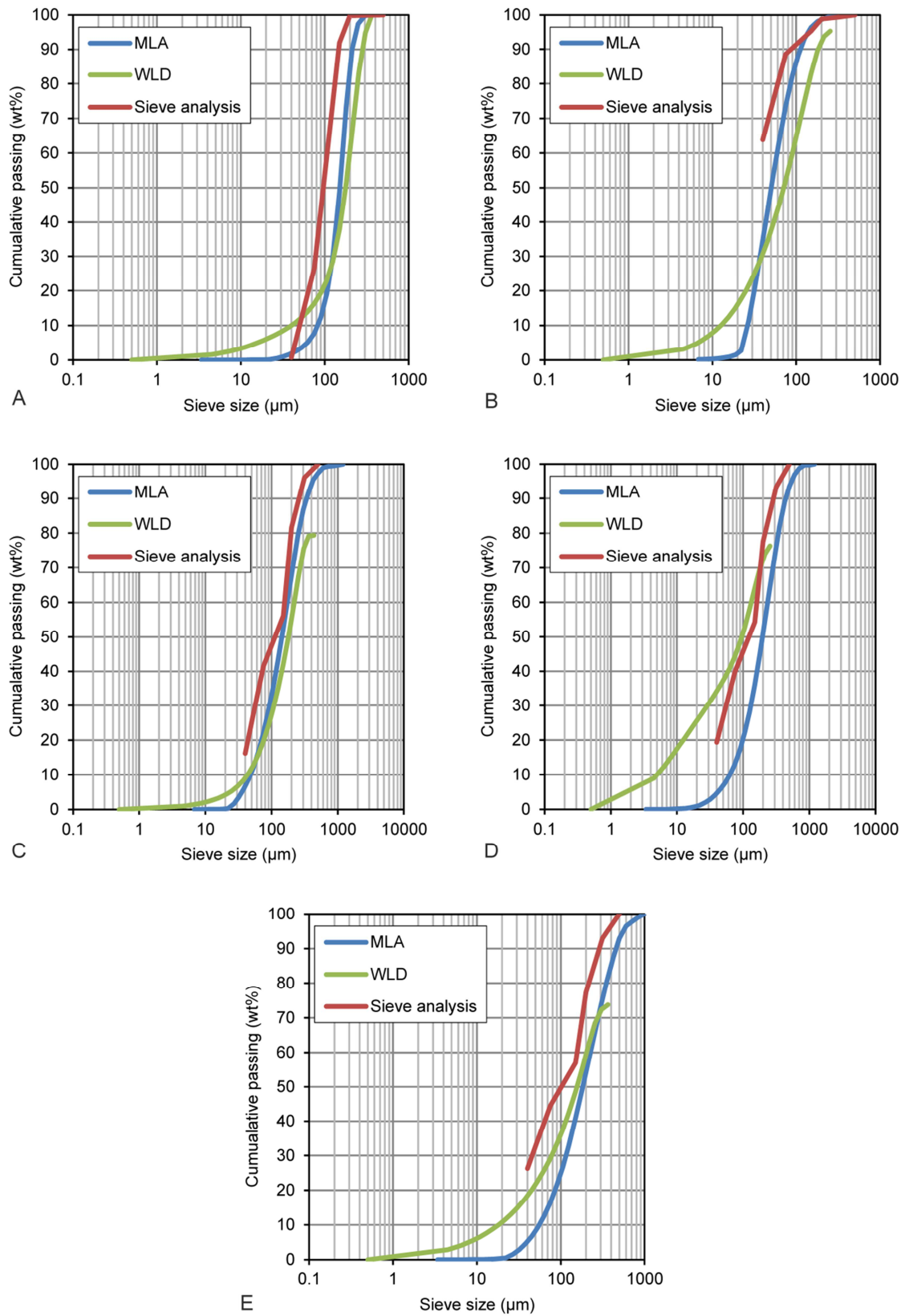
The present study reveals that automated SEM-based image analysis can be used effectively to characterise graphite raw materials and beneficiation products to predict and monitor the effects of mineral processing. The comparison of results with those obtained by well-established analytical methods yields good to excellent agreement with respect to quantitative mineralogy, carbon content, as well as particle size distribution. In addition, results of SEM-based image analysis provide access to tangible data on mineral grain size distribution, mineral association and liberation – information that cannot be obtained by other analytical tools currently available.

## 4.6 Acknowledgements

The authors would like to acknowledge the provision of sample material for this study as well as additional analyses by the AMG Mining AG (formerly Graphit Kropfmühl AG). Fiona Reiser from AMG Mining AG is thanked for providing further information on the samples and related literature as well as data of comparing analytical techniques and kindly reviewing of this study. We thank Bernhard Schulz from the Department of Mineralogy (TU Bergakademie Freiberg) for support during the MLA investigation and Martin

---

Rudolph (Helmholtz Institute Freiberg for Resource Technology) as well as Annet Kästner (Department of Mechanical Process Engineering and Mineral Processing, TU Bergakademie Freiberg) for the realisation of the laser diffraction analysis. Robert Möckel (Helmholtz Institute Freiberg for Resource Technology) is thanked for conducting the quantitative X-ray powder diffraction analysis. The authors thank an anonymous reviewer for thorough review. Special thanks are due to William John Rankin (co-editor) for his editorial handling and helpful comments to improve the submitted version of the manuscript. Discussions and support by the researchers of the Nordic Researcher Network on Process Mineralogy and Geometallurgy (ProMinNET) is gratefully acknowledged.

Supplement to Sandmann *et al.* 2014

Comparison of the MLA size distribution results with classical sieving analysis and wet laser diffraction (WLD) for the samples FeedSB (A), Konz85B (B), LynxConc90 (C), NPFeed5%C (D), NPFI75%C (E).

## **Chapter 5: Nature and distribution of PGE mineralisation in gabbroic rocks of the Lusatian Block, Saxony, Germany (Sandmann and Gutzmer, 2015)**

### **5.1 Abstract**

We have employed quantitative automated mineralogy using a Mineral Liberation Analyser to assess samples of gabbroic dykes of the Lusatian Block. These mafic dykes contain platinum-group elements – locally enriched with Cu and Ni sulphides – up to subeconomic concentrations of 0.4 ppm (4PGE+Au). In this study we analysed about 100 polished thin sections and polished blocks both with a mapping method and a search mode for bright phases in BSE images (sparse phase liberation analysis). The aim of the study was to obtain information regarding the occurrence of platinum-group minerals (PGM) and their relationship to base metal sulphides (BMS). Mineral groups found by sparse phase liberation analysis include several PGE-bearing and non-PGE-bearing tellurides, Pd bismuthides and antimonides, Pt arsenide as well as native gold and native bismuth. Mineral grain sizes of these trace minerals are in general below 10 µm. The results of the mineral association evaluation show that pyrrhotite is the main host for tellurides, native metals and platinum-group minerals. However, several other minerals show also a high degree of association with the PGM, most notably Ni-Co sulpharsenides, chalcopyrite, hydrothermal feldspar and chlorite. By using quantitative automated mineralogy we can clearly demonstrate that low-alteration, low-BMS gabbroic dyke samples contain no or only small amounts of PGM, whereas intense-alteration, high-BMS gabbroic dyke samples have elevated PGM contents. Furthermore, we show that for PGE concentrations < 1 ppm MLA analyses of just one polished thin section per sample show limitations with respect to the representativity of results for calculated element concentration, due to a combination of different limiting factors. Mineral liberation analysis reveals that PGM are much more widespread and abundant in the studied area compared to the results of previous careful light microscopic investigations and single grain electron probe micro analysis that resulted only in very few and isolated PGM grains to be identified.

### **5.2 Kurzfassung**

Für die vorliegende Studie wurde ein Mineral Liberation Analyser (MLA) genutzt, um mittels automatisierter quantitativer Mineralogie Proben von gabbroiden Gesteinsgängen des Lausitzer Blocks zu untersuchen. Diese Gesteinsgänge enthalten Platingruppen-elemente – teilweise angereichert in Cu- und Ni-Sulfiden – in unwirtschaftlichen Konzentrationen von bis zu 0,4 ppm (4PGE+Au). Die quantitativen Analysen erfolgten sowohl mit einer Abrasterungsmethode als auch mit einem speziellen Suchmodus. Das Ziel der Studie war es, Informationen über das Auftreten von Platingruppenmineralen und die Beziehungen zwischen ihnen und den assoziierten Buntmetallsulfiden (BMS) sowie die Art der gabbroiden Wirtsgesteine zu erhalten. Mineralgruppen, welche durch den Suchmodus

gefunden wurden, sind verschiedene PGE-führende und nicht-PGE-führende Telluride, Pd-Bismuthide und -Antimonide, Pt-Arsenide sowie gediegen Gold und gediegen Wismut. Die Mineralkorngrößen dieser Minerale liegen im Allgemeinen unter 10 µm. Die Ergebnisse der Mineralassoziationen zeigen, dass Pyrrhotin das Hauptwirtsmineral für einige Telluride, gediegene Metalle und Platingruppenminerale (PGM) ist. Allerdings zeigen auch einige andere Minerale einen höheren Grad der Assoziation mit den PGM, vor allem Ni-Co-Sulfarsenide, Chalkopyrit, hydrothermaler Plagioklas und Chlorit. Durch den Einsatz der automatisierten quantitativen Mineralogie können wir eindeutig aufzeigen, dass gering alterierte, gering BMS-führende gabbroide Gangproben keine oder nur geringe Gehalte an PGM führen, während stark alterierte, stark BMS-führende gabbroide Gangproben höhere PGM-Gehalte aufweisen. Darüber hinaus zeigen wir, dass für PGE-Konzentrationen <1 ppm MLA-Analysen von nur einem polierten Dünnschnitt pro Probe Einschränkungen in Bezug auf die Repräsentativität der Ergebnisse für die berechneten Elementkonzentration zeigen, was in einer Kombination von verschiedenen limitierenden Faktoren begründet ist. Es konnte weiterhin gezeigt werden, dass die Platingruppenminerale im Arbeitsgebiet viel weiter verbreitet sind und häufiger vorkommen als im Vergleich zu früheren Ergebnissen sorgfältig ausgeführter lichtmikroskopischer Untersuchungen und Einzelkorn-Elektronenstrahl-Mikroanalysen, die nur sehr wenige und isolierte PGM-Körner identifizieren konnten.

### 5.3 Introduction

At the beginning of the 20<sup>th</sup> century a small but nevertheless economic nickel-copper deposit was discovered in Sohland an der Spree (district of Äußerst-Mittel-Sohland) in the Lusatian Highlands, located near the German-Bohemian border (Beyer 1902, Beck 1902, 1903a, Dieseldorff 1903, Bergeat 1904). Ni-Cu sulphide mineralisation was closely associated with a mafic dyke and has characteristics typical of intrusion-related Ni-Cu-PGE mineralisation (Maier 2005). Between 1901 and 1920 the deposit was exploited by the Sohland-Rožany mine, a small underground operation that straddled the border between Germany and Bohemia. Cumulative production was about 500 tons (t) of Ni metal and about 200 t of Cu metal. In 1919 a chemical analysis of the ore provided evidence for significant noble metal contents (0.3 g/t Au, 7 g/t Ag, 0.1 g/t Pt) (Sächsisches Staatsarchiv 1919). In Bohemia, the Kunratice deposit, located about 6 km south of Sohland-Rožany is of similar origin and size to the Sohland-Rožany deposit, with copper mining since the 16<sup>th</sup> century and discontinuous Ni mining from 1897 to 1921. About 65 t of Ni metal and about 20 t of Cu metal were exploited from this deposit in the period from 1918-1921 (Vavřín & Frýda 1998). Further sites of Ni-Cu mineralisation have been reported associated with mafic intrusions in the area, but none of economic interest.

After a long dormant period the deposit and associated exploration potential was reassessed in the mid-1980s (Leeder & Krestin 1985, Nöldeke 1988, Nöldeke & Mettchen 1988). During this assessment the occurrence of Au, Ag, Pt, Pd and Rh in the ores of Sohland-Rožany was confirmed, and a tentative conclusion drawn that there may be

significant exploration potential for the discovery of magmatic Ni-Cu-PGE mineralisation in the area.

Because of the low-grade of the PGE mineralisation, the nature and distribution of platinum-group minerals (PGM) in the Ni-Cu ores of the Lusatian Block have remained poorly understood. Vavřín & Frýda (1998) described the occurrence of two Pd-bearing telluride minerals and sperrylite from the Kunratic deposit. Uhlig et al. (2001), in turn, evaluated the nature and distribution of the PGE mineralisation on the German side of the border. A large sample set from different sulphide-bearing mafic dykes in the area was studied (99 samples from 27 sample locations) for this purpose. Contents of up to 184 ppb Pt, up to 626 ppb Pd and up to 565 ppb Au were reported, but only a total of 5 PGE-bearing mineral grains were identified by optical and scanning electron microscopy. The actual identity of these five mineral grains remained a matter of speculation, as mineral chemistry was only recorded by energy-dispersive X-ray spectrometry (Kindermann et al. 2003). The results of the study by Uhlig et al. (2001) remained tentative as no sites for future exploration were clearly identified by the study. The most recent overview of the PGE mineralisation of the Bohemian Massif was given by Knésl & Ackerman (2005), but without adding any new information.

The source of the nickel-copper sulphide mineralisation is somewhat debatable since the discovery of the ores. Early investigations (Beck 1903a, b, Neumann 1904) suggested the sulphide mineralisation as magmatic segregation deposits and pointed out the similarity of this mineralisation to the Ni-Cu ores of the Sudbury district. A hydrothermal origin of the ores was favoured by Dickson (1906), Beck (1909, 1919), Berg (1939), Berg & Friedensburg (1944), Oelsner (1954), Fediuk et al. (1958), and Bautsch (1963). The later publications revert to the classification of the mineralisation as magmatic deposits (Rohde 1972, 1976, Bautsch & Rohde 1975, Kramer 1976, Kramer & Andrehs 1990, 2011, Pašava et al. 2001, Mücke 2012), however, with an influence of hydrothermal resp. autohydrothermal processes (Bautsch & Rohde 1975, Kramer 1976, Kramer & Andrehs 1990).

In this study, the mineralogy and textural associations of PGM in sulphide-mineralised and unmineralised gabbroic dyke samples from the Lusatian Block are examined using automated SEM-based image analysis. The results illustrate the nature and distribution of PGE mineralisation.

### **5.3.1 Geological setting**

The Lusatian Block, located in the eastern part of Germany, is bordered to the SW by the Elbe Fault Zone with the West Lusatian Fault and the Lusatian Thrust and to the NW by the Finsterwalde Fault Zone and the Doberlug Syncline (eastern part of the part of the Delitzsch-Torgau-Doberlug Synclinorium). To the NE Lusatia is bordered by the Inter-Lusatian Fault, the Görlitz Slate Belt/Görlitz Syncline and the Lusatian Main Fault. To the SE the Lusatian Block is separated to the Bohemian Massif by the Tertiary Eger Rift. (Krentz et al. 2000, Franke 2013)

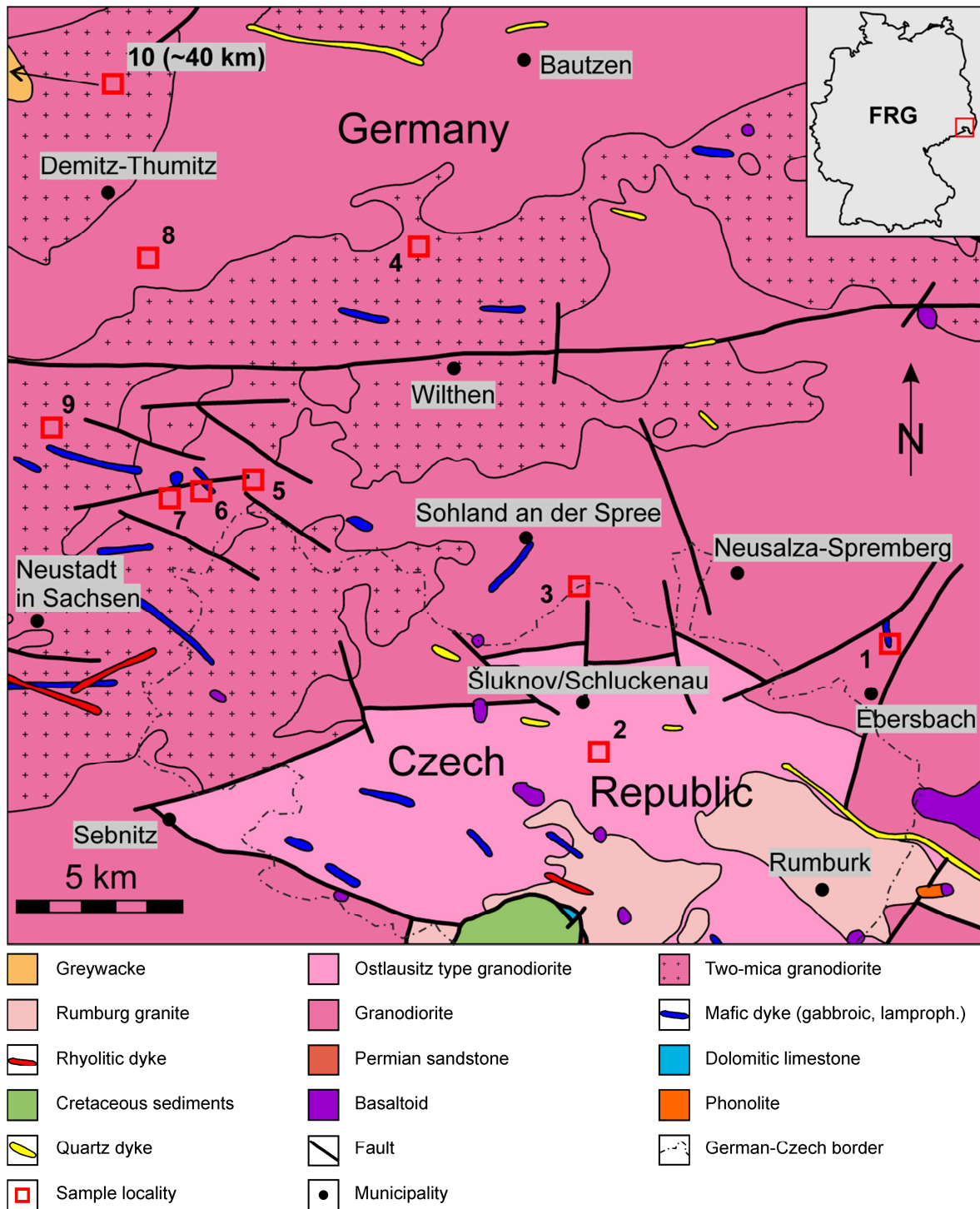


**Fig. 51:** Generalised geological map of the southern section of the Lusatian Block including position of sample localities (modified after Leonhardt (1995); numbers refer to Table 13; note: sample locality 10 is about 40 km east of this map section) and major municipalities (inset shows the position of the study area in eastern Germany).

The Lusatian Block, comprises of two large-scale granodiorite complexes (dominating the southern part of the block) which intruded into greywackes (dominating the northern part of the block). This Cadomian basement has been intruded by several granitic intrusions of various ages, as well as more than 1,000 dykes that form swarms of felsic to intermediate and mafic to ultramafic composition. According to Abdelfadil et al. (2010), Abdelfadil et al. (2013), and Kramer & Andrehs (2011), five age groups of mafic to ultramafic dykes



and sills can be distinguished, namely (I) Oligocene basalts and associated intrusives (24–34 Ma, K-Ar) (Pfeiffer & Suhr 2008), (II) Lower Cretaceous ultramafic alkaline lamprophyres (126 Ma, Ar-Ar) (Renno et al. 2003), (III) Carboniferous calc-alkaline lamprophyres (spessartites; 325–335 Ma, Ar-Ar) (Abdelfadil et al. 2013), (IV) alkaline basaltic dykes (pre-Variscan age) (Kramer 1988), (V) gabbroic rocks (microgabbros), from gabbro-norite, olivine-gabbro, to diorite (390–400 Ma, K-Ar and Pb-Pb) (Kramer et al. 1977, Kindermann et al. 2003) (Fig. 51).

The nickel-copper sulphide mineralisation is restricted to the Palaeozoic gabbroic rocks of group V, which can form dykes (predominantly WNW–ESE to NW–SE orientated) or stocks from some tens of meters to 100 m thickness (Kramer & Andrehs 2011). Since the discovery of the Ni-Cu ore the classification of these host rocks has changed somewhat and is still under discussion. In the first geological maps (Klemm 1890, Herrmann 1893) of the area as well as in the first publications (Beyer 1902, Beck 1902, 1903a, b, Neumann 1904) dealing with the newly discovered Ni-Cu sulphide mineralisation these host rocks are termed as diabase and hornblende-diabase – or even as proterobase (Herrmann 1893). Since the 1930s the terminology of the host rocks was changed to lamprophyre (Wernicke 1933, Berg 1939, Oelsner 1954, Löffler 1962, Bautsch 1963, Großer 1966, Rohde & Ullrich 1969, Rohde 1972, 1976). Until the mid-1970s, this term was retained. Since then, the host rocks are assigned by most authors to the gabbroic rocks, where the exact naming differs somewhat from gabbro (Kramer 1998, Kramer & Seifert 2000), microgabbro-microdiorite (Kramer et al. 1977, Kramer & Peschel 1987, Rösler et al. 1990, Kindermann 1999, Kindermann et al. 2003, Kramer & Andrehs 2011), gabbro-diorite (Löffler 1980), gabbro-norite to gabbro-diorite series (Heinrich 1993), gabbro-dolerite (Bautsch & Rohde 1975, Krestin 1987), dolerite (Kramer 1976) to diabase (Vavřín & Frýda 1998). The variability of names assigned is explained by compositional variability as well as non-systematic naming. In the very latest paper by Mücke (2012) the naming was changed back to lamprophyre, astonishingly, despite the fact that the geochemistry of the host rocks to Ni-Cu mineralisation does certainly not correspond to that of lamprophyre (see section ‘4.3. Whole rock geochemistry of investigated rocks’ in Abdelfadil et al. (2013)). For the purpose of this contribution, we apply the group name ‘gabbroic rocks’, based on the results of Uhlig et al. (2001).

These gabbroic rocks show ophitic textures as well as fine to coarse-grained hypidiomorphic textures and are predominantly composed of plagioclase and pyroxene (as well clinopyroxene as orthopyroxene). Olivine, amphibole, quartz, and biotite are not as frequent. Accessory minerals are apatite and zircon (Uhlig et al. 2001). According to Nöldeke (1988), and Fiedler (1999) sulphide mineralisation occurs as bleb-textured ore, triangular-acute angle-textured ore, scaffold-textured ore and massive sulphide ore. Following studies of Kramer et al. (1977), Löffler (1980), Heinrich (1993), Kindermann (1999), Uhlig et al. (2001), and Kramer & Andrehs (2011) a hydrothermal overprint of the gabbroic rocks of the Lusatian Block, likely related to greenschist metamorphism, has been established.

## 5.4 Approach and analytical methods

The current investigation was carried out using the entire set of 67 polished thin sections, 35 polished blocks of 40 mm diameter and 3 polished blocks of 1 inch diameter of the study of Uhlig et al. (2001). The samples originate from 10 different localities in the Lusatian Block (Table 13, Fig. 51). Samples represent gabbroic dykes (group V, see the above section) – and associated sulphide mineralisation (where present) as well as individual samples from the immediate country rocks surrounding the dykes. However, the latter are not part of this particular study. Uhlig et al. (2001) collected most samples from remaining stockpile material of historic mining at Sohland/Rožany, but also from active and abandoned quarries that exploit the gabbroic dykes for dimension stone, road-building material, railroad ballast as well as armourstone.

**Table 13:** Sample localities and number of samples (note: geographic coordinates are sourced from <http://www.openstreetmap.org>).

	<b>Municipality</b>	<b>Locality</b>	<b>No. of samples</b>	<b>Geographic coordinates</b>
1	Ebersbach/Sa.	Klunst quarry (active)	10	51.01492,14.59069
2	Kunratice u Šluknov (Schluckenau)	"Frisch Glück" mine in the 'Schweidrich' forest (U divého muže) (abandoned)	9	50.98581,14.46013
3	Sohland an der Spree/Rožany	"Sohlander Bergsegen" mine (abandoned)	40	51.03484,14.45130
4	Obergurig	Soraer Berg (Soraer Höhe/Kleiner Picho) quarry (active)	6	51.12441,14.38191
5	Neustadt in Sachsen	Hohwald, quarry in the forest district 15 (abandoned)	2	51.06223,14.31046
6	Neustadt in Sachsen	Hohwald, Grenzland I quarry (abandoned)	24	51.06221,14.28632
7	Neustadt in Sachsen	Hohwald, Valtengrund quarry (abandoned)	8	51.06127,14.27254
8	Schmölln-Putzkau	Tröbigauer Berg quarry (abandoned)	1	51.12691,14.26040
9	Neustadt in Sachsen	Oberottendorf quarry (active)	4	51.07687,14.22420
10	Ebersbach (bei Großhain)	Wetterberg quarry (active)	1	51.26572,13.64425

All samples were cleaned from old coatings and re-carbon-coated to provide an electrically conductive surface for non-conducting minerals prior to analysis. Automated SEM-based image analysis was carried out on a FEI MLA 650F system at the Department of Mineralogy, TU Bergakademie Freiberg. This high-speed automated mineralogy analyser (MLA) is based on a FEI Quanta 650F scanning electron microscope equipped with a field emission source and two Bruker XFlash® 5030 silicon drift energy dispersive X-ray detectors. The instrument and image acquisition are controlled by the automated Mineral Liberation Analysis (MLA) software (Gu 2003, Fandrich et al. 2007). The analytical working distance was 12 mm, the probe current 10 nA and the overall electron beam accelerating voltage 25 kV. Back scatter electron (BSE) image grey level calibration was set with epoxy resin as background (BSE grey value <25) and gold metal (pin in the standard block) as upper limit (BSE grey level value ~250).

Three MLA measurement modes were applied per sample (see Table 14 for measurement settings). Extended BSE liberation analysis method with automated standards collection (XBSE\_STD, (Fandrich et al. 2007)) was used to collect EDX spectra to develop the mineral reference database. X-ray modal analysis (XMOD, (Fandrich et al.

2007)) method was performed to obtain modal mineralogy data of the samples. The Sparse Phase Liberation analysis (SPL\_Lt\_MAP, (Fandrich et al. 2007)) method was used to search in particular for minerals with very high density, including the PGM. For this method a BSE grey level threshold was set from 150 to 255, so that only mineral grains falling in this particular BSE range were analysed. The same threshold was used for the mineral grain mapping of this measurement mode. XMOD and SPL\_Lt\_MAP measurement results were classified using a mineral standard database developed from the XBSE\_STD measurement EDX reference spectra list. The complete mineral reference list consists of about 110 entries. These were combined to about 60 mineral groups, to reduce complexity and to account for detection limits as well as the limitation of distinction of minerals of almost similar chemical composition by energy-dispersive X-ray spectroscopy. The final XMOD and SPL\_Lt\_MAP measurement data were exported and processed using MLA DataView software (Fandrich et al. 2007).

**Table 14:** Measurement settings (note: number of frames per thin section varies due to different sample sizes on the microscope slides; total measurement area varies therefore from about 700 mm<sup>2</sup> to about 1.200 mm<sup>2</sup>).

Measurement mode	Frame size (µm)	Frames per thin section	Frames per round block	BSE image resolution (µm)	Mapping resolution (µm)
XBSE_STD	1492x1492	308 to 558	385	2.98	-
XMOD	1492x1492	308 to 558	385	2.98	29.84
SPL_Lt_MAP	995x995	640 to 1150	897	0.99	5.97

## 5.5 Results

### 5.5.1 Modal mineralogy

The modal mineralogy of each gabbroic dyke sample was determined by XMOD measurements. For samples containing less than 50 per cent sulphides, appropriate lithological names were selected, after deduction of the sulphide content, following the nomenclature of the International Union of Geological Sciences Subcommittee on the Systematics of Igneous Rocks (IUGS) (Le Maitre et al. 1989, Le Bas & Streckeisen 1991). The QAPF diagrams, after Streckeisen (1976), and the triangular diagrams for the classification and nomenclature of gabbroic rocks based on the proportions of plagioclase, olivine, orthopyroxene, clinopyroxene and hornblende, after Streckeisen (1976), were used for this purpose. Samples having more than 50 per cent sulphides content were subdivided into massive (no silicate rock textures) or semi-massive sulphide (host rock textures locally recognizable) samples. 24 of the studied samples show a sulphide content of lower than 10 per cent and 31 samples have less than 50 per cent sulphides content.

It is noted that the magmatic silicate assemblage is altered in all samples, though alteration is of variable intensity and type. Intense chlorite-bearing alteration is most common. Due to the alteration intensity the exact rock attribution is sometimes debatable or even undeterminable as some of the samples are highly altered (such as sample HG3B, see Fig. 52b). Regarding the naming of the dyke-forming rocks in the recent and historic

literature it is obvious that the terminology ‘lamprophyre’ should not be used for these particular rocks. According to Woolley et al. (1996) “Lamprophyres are mesocratic to melanocratic igneous rocks, usually hypabyssal, with a panidiomorphic texture and abundant mafic phenocrysts of dark mica or amphibole (or both) with or without pyroxene, with or without olivine, set in a matrix of the same minerals, and with feldspar (usually alkali feldspar) restricted to the groundmass.” and Le Maitre et al. (2004) states “(2) they are porphyritic...

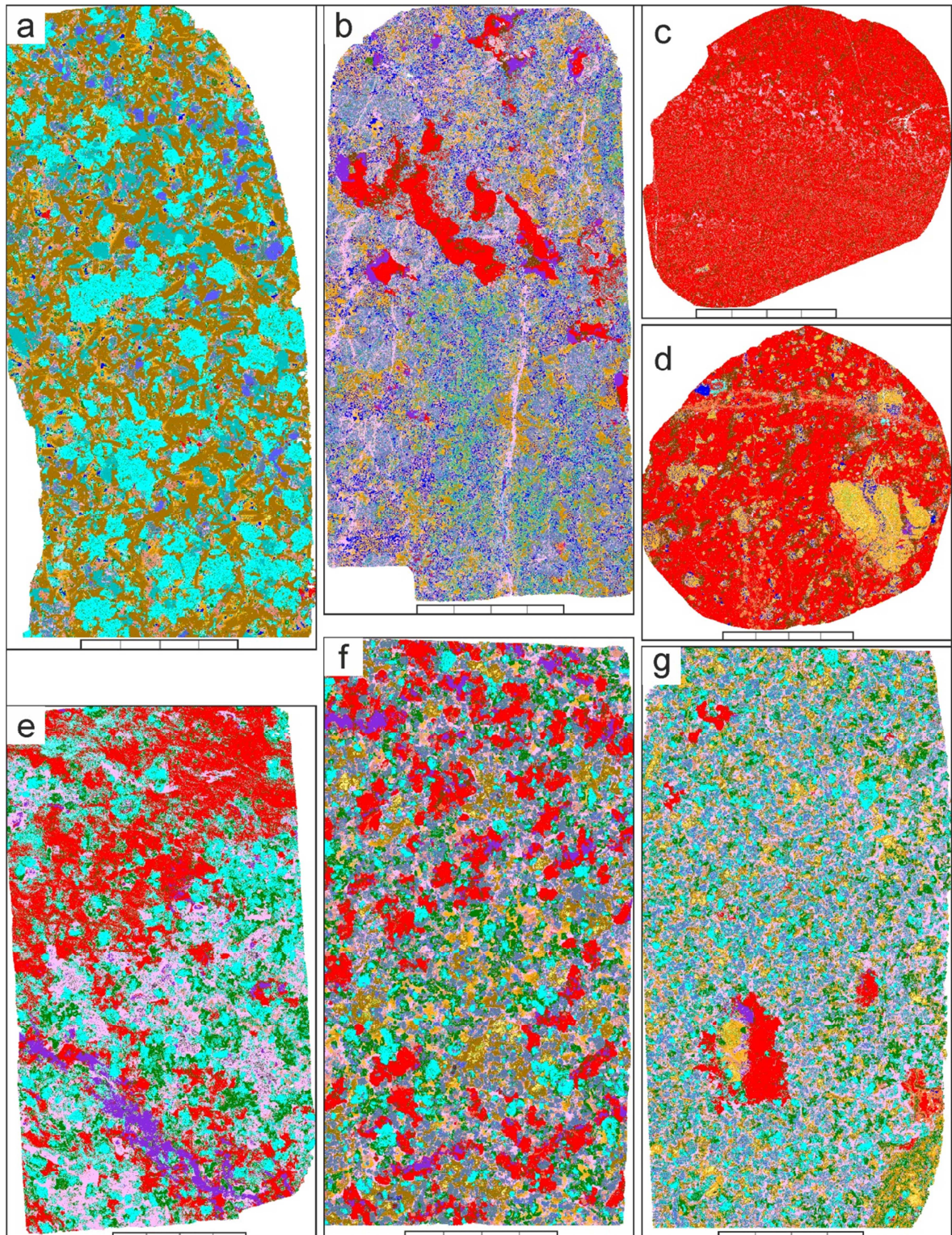




**Fig. 52:** MLA XMOD false colour mineral images of characteristic gabbroic rocks and base metal mineralisation (all scale bars are 10.000  $\mu\text{m}$  in width). **(a)** Pyroxene-hornblende-orthopyroxene-gabbro with incipient amphibole-chlorite-serpentine alteration (amphibole - green, chlorite - pink, serpentine - light slate grey) showing typical plagioclase laths (brownish) surrounded by pyroxene crystals (light bluish) and olivine (dark blue) (sample SS11, Kunratice). **(b)** Sulphide-bearing gabbroic-rock with highly intense chlorite-sericite-talc alteration (chlorite - pink, sericite - yellow, talc - bluish grey) showing relictic pyroxene (light bluish) and plagioclase (brownish) as well as partly remobilised sulphide mineralisation with pyrrhotite (red), chalcopyrite (blue violet) and Ni-Fe sulphide (dark brown) (sample HG3B, Grenzland). **(c)** Massive sulphide sample showing pyrrhotite (red), Ni-Fe sulphide (dark brown), magnetite (indian red), pyrite (flesh tones) and rare silicates (sample ESoh1-5, Sohland-Rožany). **(d)** Massive sulphide ore with pyrrhotite (red) and Ni-Fe sulphide (dark brown) as well as alkali feldspar (pale ochre), plagioclase (brownish) and quartz (blue). Pyrite (flesh tones) of younger origin fills a fissure in pyrrhotite. Chalcopyrite (blue violet) is remobilised and replaced next to the silicates (sample ESoh2-2, Sohland-Rožany). **(e)** Sulphide-bearing gabbroic-rock with intense chlorite-amphibole alteration (chlorite - pink, amphibole - green) showing relictic pyroxene (light bluish). Pyrrhotite (red) shows a semi-massive to scaffold texture. Ni-Fe sulphide (dark brown) is directly associated with pyrrhotite whereas younger-stage chalcopyrite (blue violet) cross-cut pyrrhotite (red) and gangue (sample ESoh5, Sohland-Rožany). **(f)** Sulphide-bearing pyroxene-hornblende-orthopyroxene-gabbro with intense serpentine-amphibole-chlorite-sericite alteration (serpentine - light slate grey, amphibole - green, chlorite - pink, sericite - yellow) shows a triangular-acute angle ore texture to scaffold ore texture. The base metal sulphides consist of pyrrhotite (red), chalcopyrite (blue violet) and Ni-Fe sulphide (dark brown) (sample ESoh4, Sohland-Rožany). **(g)** Sulphide-bearing pyroxene-hornblende-orthopyroxene-gabbro with intense chlorite-amphibole-serpentine-sericite alteration (chlorite - pink, amphibole - green, serpentine - light slate grey, sericite - yellow) shows a blebby to disseminated ore texture with pyrrhotite (red), Ni-Fe sulphide (dark brown), pyrite (flesh tones) and chalcopyrite (blue violet) (sample ESoh12, Sohland-Rožany).

(3) feldspars and/or feldspathoids, when present, are restricted to the groundmass". Mafic phenocrysts of biotite and/or amphibole are non-existent in a matrix of the same minerals in any of the PGM, Au, telluride or Bi-bearing samples of this study. Rather the plagioclase occurs as laths, most samples are medium- to coarse-grained ( $0.25 < 2$  mm resp.  $2 < 16$  mm (Gillespie & Styles 1999)) and show often an ophitic texture which is typical for gabbroic rocks and not for lamprophyres (Fig. 52a).

### 5.5.2 Base metal sulphide mineralogy

Based on the results of the MLA XMOD measurements it can be seen that the content of base metal sulphides (BMS; the term is in this study used to include pyrrhotite) ranges from 0 to 95 per cent in the entire set of gabbroic dyke samples. Pyrrhotite is the dominant BMS, while pyrite is related to secondary hydrothermal alteration processes and fills fractures in pyrrhotite (Fig. 52d). Two Fe-Ni sulphides, pentlandite and violarite, have been reported in the sample suite (Fiedler 1999, Kindermann 1999), but could not be distinguished by the MLA software, as the EDX spectra are rather similar. Based on the results of Fiedler (1999) and Kindermann (1999) it is obvious that violarite is rather rare and occurs as a product of hydrothermal alteration of pentlandite only. Therefore, only the

term pentlandite will be used here, acknowledging the fact that this includes a very minor amount of violarite. Chalcopyrite is another important BMS, it commonly appears remobilised (Fig. 52d and e). Four groups of ore textures (bleb-textured ore, triangular-acute angle-textured ore, scaffold-textured ore and massive sulphide ore) could be found in the samples of this study (Fig. 52d to g).

### 5.5.3 PGE mineralogy

Minerals matching the 150-255 BSE grey level range were identified by MLA in 103 of the 105 samples using the SPL\_Lt\_MAP measurement mode. These minerals include not only the PGM, but also monazite, xenotime, zircon, baddeleyite, chevkinite group minerals, U- and Th-bearing minerals, baryte, molybdenite, scheelite, galena, nickeline, loellingite, Ni-Co-Fe sulphides as well as Ni-Co-Fe sulpharsenides. In addition to PGM native Au, native Bi and a large range of tellurides were found. In the following only the last groups will be discussed. The PGM consist of Pd-Ni tellurides, Pd-Bi tellurides, Pd bismuthides, Pt tellurides, Pt arsenides, Rh sulpharsenides, while the non-PGE-bearing tellurides consist of Pb, Hg, Ag, Bi, Ni and Ni-Sb tellurides. The groups generated for PGMs/tellurides are listed in Table 15. It has to be noted that, due to the detection limits of the SEM, the identification especially of small mineral grains ( $< 1 \mu\text{m}$ ) remains tentative. Some minerals, such as 'PtBi telluride' or 'RhCoNi sulpharsenide' do not correspond in their chemical composition to any known mineral. The reason for this ambiguity is likely the minute size of these mineral grains, so that EDS yields mixed spectra.

Platinum-group minerals (PGM), native Au, native Bi and tellurides were found in 42 gabbroic dyke samples from 6 of 10 sample localities considered in Uhlig et al. (2001). The total number of mineral grains of PGM, native Au, native Bi and tellurides has been  $n=1315$ . Table 16 shows the occurrence of the mineral groups at the different localities. This table is subdivided in a 'precious-elements section' ( $n=349$ ), including PGMs and native Au, and an 'other-elements section' ( $n=966$ ), including the tellurides devoid of PGE as well as native Bi. As each locality represents a very different number of samples (e.g., Sohland-Rožany  $n=29$ , Soraer Berg  $n=2$ ) the relative modal abundance (RMA) in per cent was calculated for each locality. The sample locality Grenzland is the only one where the number of mineral grains in the 'precious section' is higher than the number of mineral grains in the 'other section'. It is quite evident that the number of PGM-bearing grains is rather low at three localities examined, namely Kunratice, Soraer Berg and Forest District 15. No PGMs were identified in samples from the locality Valtengrund.

A fairly high number of PGM were, in contrast, found at the localities Sohland-Rožany (for examples see Fig. 53) and Grenzland. At the locality Grenzland Pd-Ni tellurides are the most common PGMs, whereas Sohland-Rožany is dominated by Pt arsenides, as well as Pd-Bi and Pd-Ni tellurides and Kunratice is dominated by Pd-Bi tellurides and Pt arsenides. It can be seen that localities which show a high number of Pd-Bi telluride grains also have a high number of Bi telluride grains. The same applies to Pd-Ni tellurides and Ni tellurides. A few mineral groups occur only at the locality Sohland-Rožany, e.g., Pd antimonides, Rh sulpharsenides, Hg tellurides and Ni-Sb tellurides.

Mineral	Group	Formula	Ag	As	Bi	Co	Cu	Fe	Hg	Ir	Ni	Os	Pb	Pd	Pt	Rh	S	Sb	Te
medium_Pd Melonite	Pd-Ni telluride	[NiPdFeTe]*						1.6			14.2			4.9					79.3
high_Pd Melonite	Pd-Ni telluride	[NiPdBiTe_CuFe]*			13.9		2.1	1.9			11.7			6.9					63.6
Merenskyite	Pd-Bi telluride	(Pd,Pt)(Te,Bi) <sub>2</sub>			25.5						5.4			17.8					51.3
Testibiopalladite1	Pd-Bi telluride	PdTe(Sb,Te,Bi)_FeNi			24.7			1.5			1.4			23.3				18.2	30.8
Testibiopalladite2	Pd-Bi telluride	PdTe(Sb,Te,Bi)			15.1			2.2			0.3			24.9				26.5	31.0
Pd antimonide <sup>A</sup>	Pd antimonide	[PdSb_CoFeAsS]*		6.1		4.7		3.2			1.8			38.8			3.7	41.7	
Froodite <sup>#</sup>	Pd bismuthide	PdBi <sub>2</sub>			79.7									20.3					
PtBi telluride	Pt telluride	[PtBiTe_FeNi]*			16.7			14.2			3.9				28.7		7.4		29.2
Pt telluride	Pt telluride	[PtTe]*													60.0				40.0
Sperrylite <sup>#</sup>	Pt arsenide	PtAs <sub>2</sub>		43.4											56.6				
RhCoNi sulpharsenide	Rh sulpharsenide	[RhAsSCoNi]*		39.4		8.8		3.4		5.1	4.8					22.9	15.7		
RhOsIr sulpharsenide	Rh sulpharsenide	[RhOsIrAsS_Fe]*		12.9				9.3		11.6	0.5	21.7				24.9	19.0		
Altaite	Pb telluride	PbTe						1.5					58.1						40.5
Coloradoite_cpy	Hg telluride	HgTe_CuFe					3.2	3.2	54.4										39.2
Coloradoite_py	Hg telluride	HgTe_Fe						5.9	56.9										37.2
Hessite	Ag telluride	Ag <sub>2</sub> Te	61.6																38.5
Tsumoite	Bi telluride	BiTe_NiFe			58.0			1.3			1.0								39.6
Melonite	Ni telluride	NiTe <sub>2</sub>									22.4								77.6
Vavrinite	Ni-Sb telluride	Ni <sub>2</sub> SbTe <sub>2</sub>						0.3			25.1			0.3				23.8	50.6

**Table 15:** PGE- and/or Te-bearing minerals identified and their association with mineral groups, with mineral formula and elemental composition based on SEM analyses (note: # - elemental composition calculated from mineral formula; <sup>A</sup> potentially subburlyite ((Pd,Ni)Sb); \* 'formulas' in square brackets show only main the main elements of the particular mineral phase).

**Table 16:** Number of mineral grains found with SPL\_Lt\_MAP measurement mode and their relative modal abundance (RMA) per locality.

Locality	Kunratice		Sohland-Rožany		Soraer Berg		Forest District 15		Grenzland		Valtengrund	
	(n=3)		(n=29)		(n=2)		(n=2)		(n=5)		(n=1)	
Mineral	Total	RMA (%)	Total	RMA (%)	Total	RMA (%)	Total	RMA (%)	Total	RMA (%)	Total	RMA (%)
Pd-Ni telluride	1	0.8	38	4	2	50	-	-	77	52	-	-
Pd-Bi telluride	13	10	42	4	-	-	-	-	4	3	-	-
Pd antimonide	-	-	14	1	-	-	-	-	-	-	-	-
Pd bismuthide	-	-	1	0.1	-	-	1	3	-	-	-	-
Pt telluride	-	-	4	0.4	-	-	-	-	-	-	-	-
Pt arsenide	6	5	110	11	-	-	-	-	3	2	-	-
Rh sulpharsenide	-	-	1	0.1	-	-	-	-	-	-	-	-
Native gold	-	-	23	2	1	25	-	-	8	5	-	-
Pb telluride	-	-	155	16	-	-	24	63	15	10	5	19
Hg telluride	-	-	49	5	-	-	-	-	-	-	-	-
Ag telluride	-	-	10	1	-	-	6	16	4	3	-	-
Bi telluride	104	83	139	14	-	-	5	13	17	11	21	81
Ni telluride	1	0.8	258	27	1	25	-	-	21	14	-	-
Ni-Sb telluride	-	-	126	13	-	-	-	-	-	-	-	-
Native bismuth	-	-	3	0.3	-	-	2	5	-	-	-	-
Total	125	100	973	100	4	100	38	100	149	100	26	100

#### 5.5.4 PGM mineralisation and base metal sulphide mineralogy

Based on the comparison of base metal sulphide content and abundance of PGM and/or telluride grains it is obvious that samples having a BMS content below 1 weight% (n=16) show no or only a very low number of these particular mineral grains (Fig. 54a,b). Samples with a BMS content of higher than 1 weight% (n=42) show varying numbers of PGM and/or telluride grains. It can be concluded that the presence of base metal sulphide mineralisation in the gabbroic dykes is an important factor for the occurrence of PGM and tellurides.



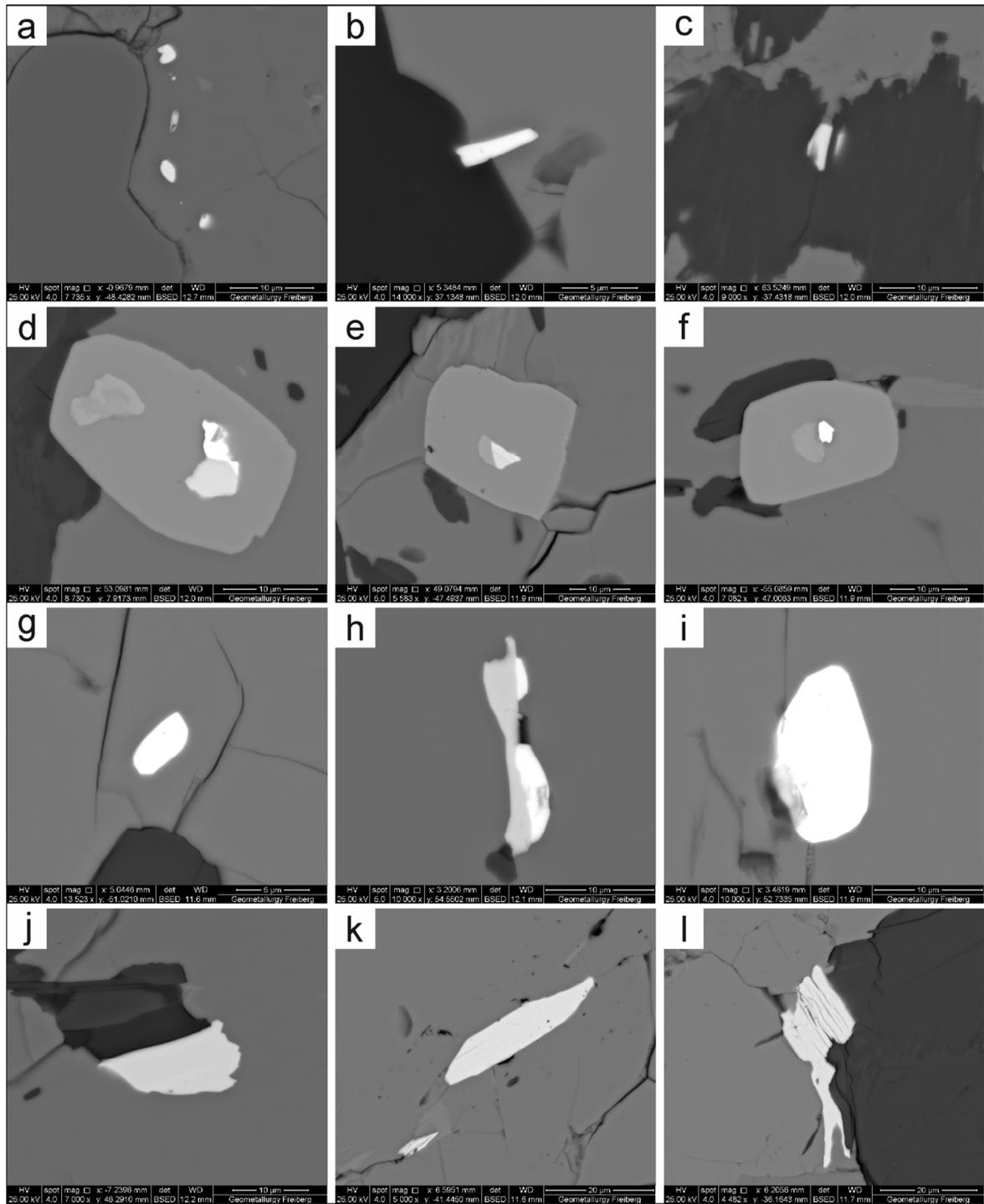


**Fig. 53:** Examples of high-resolution BSE images illustrating important characteristics of PGM, native gold and telluride grains (scale bars 10  $\mu\text{m}$  in width, except (b) and (g) 5  $\mu\text{m}$ , (k) and (l) 20  $\mu\text{m}$ ). (a) Four sperrylite grains (white, about 2-4  $\mu\text{m}$  in size) found by MLA measurement plus three grains (< 1  $\mu\text{m}$ ) too small for MLA SPL\_Lt measurement in pyrrhotite next to a magnetite grain (left) (sample ESoh1-3, locality Sohland-Rožany). (b) Sperrylite grain (white) at the contact between pyrrhotite (medium grey) and albite (dark grey) (sample ESoh2-2, locality Sohland-Rožany). (c) Two palladium-bearing melonite grains (white) in stilpnomelane (dark grey) next to pyrrhotite (medium grey) (sample ESoh1-1, locality Sohland-Rožany). (d) Testibiopalladite grain (middle right; bright grey adjacent to native gold) and native gold (middle right, white) as well as nickeline (middle left medium grey) in a cobaltite-gersdorffite series grain in a pyrrhotite matrix; silicates on the left edge are titanite (dark grey) and chlorite (darkest grey) (sample Sohld02, locality Sohland-Rožany). (e) Pd antimonide (possibly sudburyite; brightest grey) associated with testibiopalladite (somewhat darker) and nickeline (medium grey) in an alloclaste grain in a pyrrhotite matrix. In pyrrhotite several pentlandite “flames” occur. Darkest grey (left edge) is K-feldspar (sample Sohld09, locality Sohland-Rožany). (f) Native gold (white) associated with nickeline (medium grey) in a cobaltite-gersdorffite series

grain in a pyrrhotite matrix. In pyrrhotite a pentlandite “flame” and chlorite (darkest grey) occur (sample Sohld07, locality Sohland-Rožany). (g) Idiomorph altaite grain (white) in pyrrhotite (grey) next to chlorite (dark grey) (sample Sohld04, locality Sohland-Rožany). (h) Two coloradoite grains (white) associated with melonite (medium grey) in pyrrhotite next to a small chamosite grain (dark grey) (sample Sohld13, locality Sohland-Rožany). (i) Idiomorph Bi telluride grain (possibly tsumoite; white) in pyrrhotite (grey) (sample ESoh2-5, locality Sohland-Rožany). (j) Melonite grain (light grey) in a pyrrhotite matrix with pentlandite “flames”. Silicates are chlorite (dark grey) and stilpnomelane (darkest grey) (sample Sohld08, locality Sohland-Rožany). (k) Two vavřínite grains (light grey) in a pyrrhotite matrix (grey) with pentlandite “flames” (sample Sohld04, locality Sohland-Rožany). (l) Vavřínite grain (light grey) associated with pentlandite (left and top; medium grey), stilpnomelane (top right; darkest grey) and chlorite (bottom right; dark grey). Areas somewhat darker than pentlandite (bottom middle and top middle) are pyrrhotite (sample Sohld04, locality Sohland-Rožany).

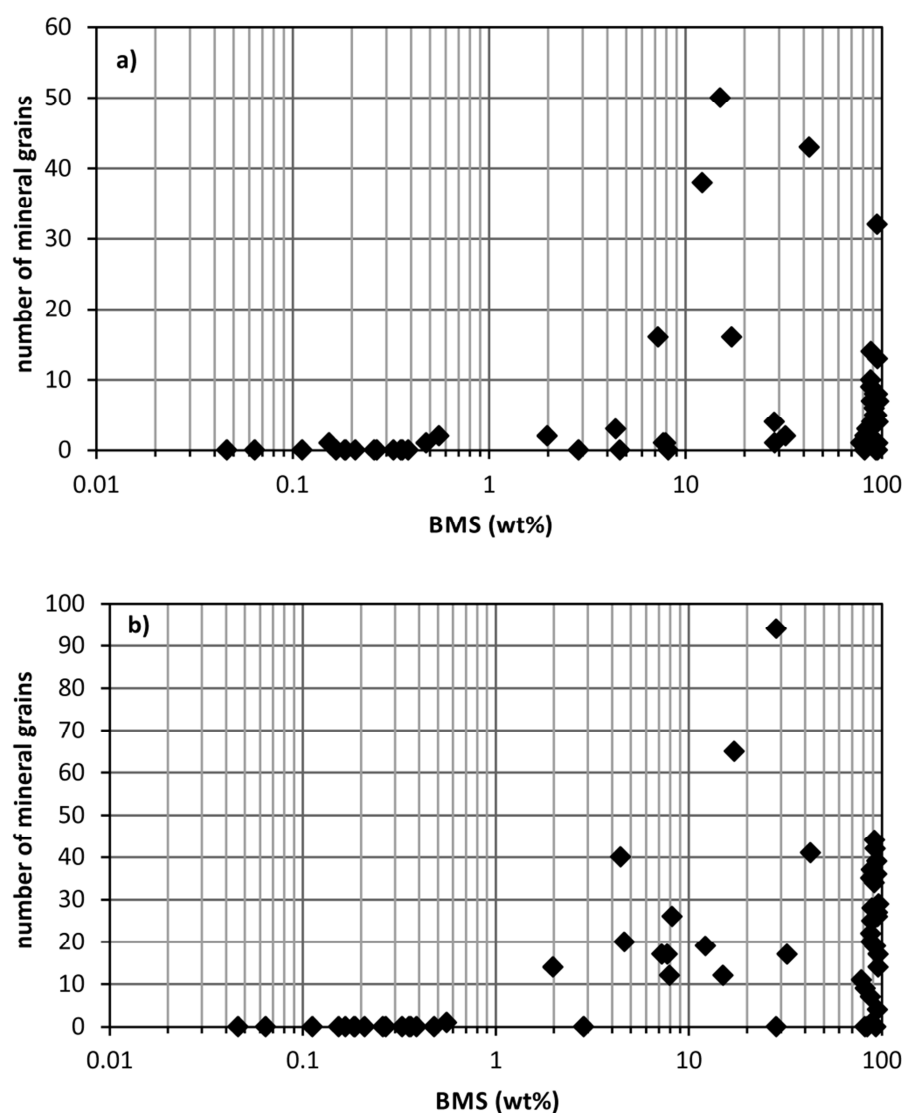


**Fig. 54:** (a) Comparison of base metal sulphide (BMS) content and number of PGM grains per sample. (b) Comparison of base metal sulphide (BMS) content and number of non-PGE-bearing telluride grains per sample.

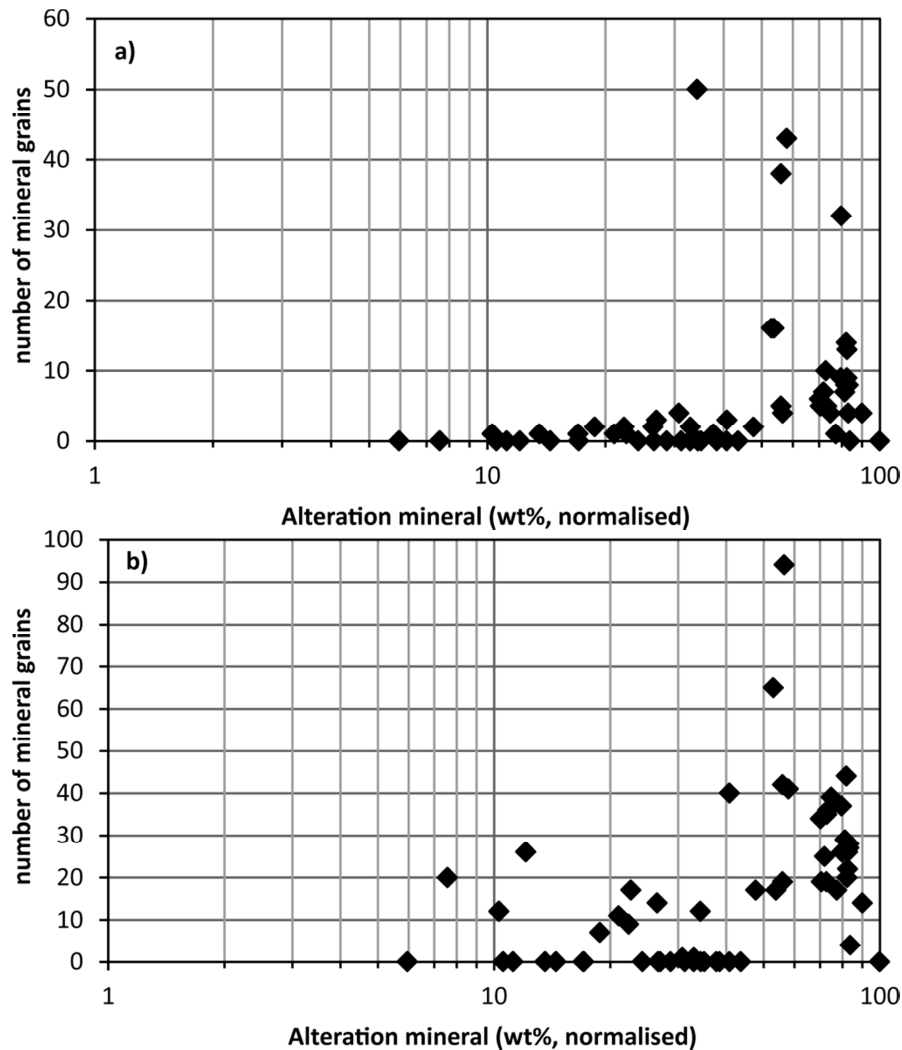


**Fig. 55:** (a) Comparison of total alteration (chlorite, serpentine, talc, sericite, stilpnomelane, amphibole, epidote, and carbonates) and number of PGM grains per sample. (b) Comparison of total alteration (chlorite, serpentine, talc, sericite, stilpnomelane, amphibole, epidote, and carbonates) and number of non-PGE-bearing telluride grains per sample. Alteration mineral content is calculated from MLA XMOD modal mineralogy normalised to 100% non-sulphides.

### 5.5.5 PGM mineralisation and alteration

Alteration indices based on geochemistry, such as the chlorite-carbonate-pyrite index (CCPI) described in Large et al. (2001) or the Ishikawa alteration index (AI) defined by Ishikawa et al. (1976) and specified in Large et al. (2001), both developed for the alteration of rocks associated with volcanic-hosted massive sulphide deposits) are not available for the studied rock suite. However, this is also not needed, as alteration indices using chemical element /oxide abundances are only needed as proxies for mineral abundances. In this study, we measured alteration mineral abundances directly and can thus apply these mineral abundances to estimate the alteration intensity. Alteration minerals included in this assessment include chlorite, serpentine, talc, sericite, stilpnomelane, amphibole, epidote and carbonates. Fig. 55 presents the relationship of PGM and telluride mineral grain count vs. total alteration mineral content (normalised to 100% non-sulphides) of the samples. Based on the comparison of PGM and alteration mineral content it can be seen that the highest number of PGM grains can be found in samples with normalised alteration content

between 40 and 90 wt.% (Fig. 55a). In contrast non-PGE-bearing telluride grains occur in samples ranging from 7 to 90 wt.% alteration content (Fig. 55b).

**Table 17:** Mineral grain sizes (in  $\mu\text{m}$ ) of the different mineral groups in total and per locality (note: the size calculation is based on the measured 2D surface area of the grains and calculated using the equivalent circle diameter; min. = minimum, percentile P50  $\hat{=}$  median, max. = maximum).

Locality	Mineral group	Min.	P50	Max.	Samples (n)	Mineral grains (n)
Total data set	Pd-Ni telluride	1.0	3.7	8.1	10	118
Kunratice	"	-	2.7	-	1	1
Sohland-Rožany	"	1.0	4.0	8.1	6	38
Soraer Berg	"	-	2.6	-	1	2
Grenzland	"	1.0	3.8	8.1	2	77
Total data set	Pd-Bi telluride	1.0	3.1	6.8	21	59
Kunratice	"	1.5	4.6	6.8	2	13
Sohland-Rožany	"	1.0	3.1	6.8	17	42
Grenzland	"	1.8	2.4	2.9	2	4
Sohland-Rožany	Pd antimonide	1.4	2.7	5.7	10	14
Sohland-Rožany	Pd bismuthide	-	3.2	-	1	1
Forest District 15	"	-	2.7	-	1	1
Sohland-Rožany	Pt telluride	1.8	3.1	5.7	4	4
Total data set	Pt arsenide	1.0	3.4	8.1	31	119
Kunratice	"	2.0	5.4	8.1	3	6
Sohland-Rožany	"	1.0	3.2	6.8	25	110
Grenzland	"	2.4	3.0	3.4	3	3
Sohland-Rožany	Rh sulpharsenide	-	2.2	-	1	1
Total data set	Native gold	1.0	2.5	4.8	11	32
Sohland-Rožany	"	1.0	2.6	3.4	8	23
Soraer Berg	"	-	2.7	-	1	1
Grenzland	"	1.4	2.4	4.8	2	8
Total data set	Pb telluride	1.0	3.3	6.8	24	199
Sohland-Rožany	"	1.0	2.8	6.8	19	155
Forest District 15	"	1.0	4.6	6.8	2	24
Grenzland	"	1.4	4.6	5.7	2	15
Valtengrund	"	2.4	6.9	8.1	1	5
Sohland-Rožany	Hg telluride	1.0	3.0	5.7	13	49
Total data set	Ag telluride	1.4	2.9	4.8	10	20
Sohland-Rožany	"	1.4	3.0	3.4	6	10
Forest District 15	"	1.4	3.5	4.8	2	6
Grenzland	"	1.4	2.0	2.4	2	4
Total data set	Bi telluride	1.0	4.7	22.0	16	286
Kunratice	"	1.4	9.4	22.0	2	104
Sohland-Rožany	"	1.0	4.4	11.4	8	139
Forest District 15	"	1.7	4.0	4.8	2	5
Grenzland	"	1.0	2.8	3.4	3	17
Valtengrund	"	2.0	5.2	9.6	1	21
Total data set	Ni telluride	1.0	4.0	11.4	27	281
Kunratice	"	-	1.6	-	1	1
Sohland-Rožany	"	1.0	4.4	11.4	22	258
Soraer Berg	"	-	2.2	-	1	1
Grenzland	"	1.0	2.1	3.4	3	21
Sohland-Rožany	Ni-Sb telluride	1.0	13.8	27.0	13	126
Total data set	Native bismuth	1.4	3.0	4.8	3	5
Sohland-Rožany	"	1.4	4.3	4.8	1	3
Forest District 15	"	-	2.3	-	2	2

### 5.5.6 Mineral grain sizes

The size distribution for mineral grains computed by the MLA software in this study is expressed as equivalent circle diameter. These size calculations are based on the measured surface area of a mineral grain. The results of the MLA grain size investigations show fairly similar size distributions for the majority of all mineral group totals, which show a median (P50) between 2.7  $\mu\text{m}$  and 4.7  $\mu\text{m}$  (Table 17). Bi telluride, Pd-Ni telluride, Ni telluride, Pt arsenide and Pd-Bi telluride grains tend to be slightly larger than the remaining mineral groups. However, the differences in P50 are only marginal. There are only very few grains larger than 10  $\mu\text{m}$ . The only exception to this is Ni-Sb telluride with a median of 13.8  $\mu\text{m}$  and a maximum size of 27  $\mu\text{m}$ . It applies to the most groups of minerals that there are only minor differences in the median (P50) between the different localities of a mineral group. It has to be noted that the minimum size of 1  $\mu\text{m}$  is an analytical minimum related to the capabilities of the SEM and the measurement settings (main cause the magnification used). Due to the limited number of mineral grains the size distribution is difficult to assess. For the mineral groups totals for Pt arsenide as well as Pb, Bi and Ni telluride, which have a higher number of mineral grains, it can be seen that the distribution is unimodal showing a positive skew. The Pd-Ni telluride grains show an approximately normal distribution. In contrast, the Ni-Sb telluride grains have a unimodal distribution with a negative skew.

### 5.5.7 Mineral association

The mineral association data computed by the MLA software describes the direct contact of a mineral of interest in relation to its associated minerals. The values are expressed as % association. Based on the results of mineral association parameters in Table 18 it can be seen that the greatest number of PGM and tellurides are associated with pyrrhotite. An example for this is Pt arsenide with 37% association with pyrrhotite and 14% association with Ni-Fe sulphide considering all 119 grains of this mineral group. However, looking at individual localities the preferences are somewhat different. The PGM and telluride grains of the localities Grenzland and Valtengrund show only a minor association with pyrrhotite. Additional to pyrrhotite other minerals associated with PGM and tellurides to a greater extent include Ni-Co sulpharsenides (especially for associations of Pd-Bi telluride, Pd antimonide, native Au, and Ag telluride), chalcopyrite (especially association of Ag telluride), hydrothermal plagioclase, and chlorite. It can be seen that the degree of mineral associations to plagioclase is very variable, even within individual localities. In contrast, the mineral associations with chlorite are more constant but on a lower level.

The association of Pd-Bi telluride is heterogeneous. Whereas at the locality Sohland-Rožany the Pd-Bi tellurides are mainly associated with Ni-Co-Fe sulpharsenide (37%), pyrrhotite (8%) and chlorite (20%), they show a strong association to pyroxene (63%), chlorite (13%) and chalcopyrite (10%) at Kunratice. Pb telluride grains show a heterogeneous association with strong relationship to pyrrhotite in Sohland-Rožany (68%), but are mainly associated with plagioclase at Forest District 15 (63%), Grenzland (48%)

**Table 18:** Mineral association (expressed as % association) of PGM, native Au, telluride and native bismuth grains found by MLA measurement.

	Mineral group	Bi telluride	Ni-Fe sulphide	Ni-Co-Fe sulpharsenide	Pyrrhotite	Pyrite	Chalcopyrite	Ilmenite
Total data set	Pd-Ni telluride	0	6	4	23	0	2	0
Kunratice	"	0	0	0	0	0	0	0
Sohland-Rožany	"	0	1	6	25	0	1	0
Soraer Berg	"	0	39	0	61	0	0	0
Grenzland	"	0	5	0	9	0	6	0
Total data set	Pd-Bi telluride	0	2	30	7	0	5	1
Kunratice	"	0	2	0	4	0	10	0
Sohland-Rožany	"	0	3	37	8	0	2	2
Grenzland	"	0	0	0	0	0	21	0
Sohland-Rožany	Pd antimonide	0	3	77	3	0	0	0
Total data set	Pd bismuthide	0	0	0	0	0	0	27
Sohland-Rožany	"	0	0	0	0	0	0	54
Forest District 15	"	0	0	0	0	0	0	0
Sohland-Rožany	Pt telluride	0	25	0	65	0	0	0
Total data set	Pt arsenide	0	14	1	37	0	7	0
Kunratice	"	0	0	0	18	0	64	0
Sohland-Rožany	"	0	17	2	40	0	1	0
Grenzland	"	0	0	0	29	0	0	0
Sohland-Rožany	Rh sulpharsenide	0	0	0	100	0	0	0
Total data set	Native gold	0	0	33	0	0	0	1
Sohland-Rožany	"	0	0	46	0	0	0	0
Soraer Berg	"	0	0	0	0	0	0	0
Grenzland	"	0	0	0	0	0	0	5
Total data set	Pb telluride	1	7	2	54	0	4	0
Sohland-Rožany	"	0	8	2	68	0	4	0
Forest District 15	"	1	0	0	2	0	0	0
Grenzland	"	0	3	0	0	0	5	2
Valtengrund	"	12	14	0	0	0	11	0
Sohland-Rožany	Hg telluride	0	2	7	44	0	9	0
Total data set	Ag telluride	0	0	21	7	0	44	0
Sohland-Rožany	"	0	0	34	12	0	32	0
Forest District 15	"	0	0	0	0	0	76	0
Grenzland	"	0	0	0	0	0	50	0
Total data set	Bi telluride	0	6	0	9	16	7	3
Kunratice	"	0	3	0	18	0	8	1
Sohland-Rožany	"	0	10	0	12	33	6	2
Forest District 15	"	0	0	0	0	0	13	10
Grenzland	"	0	3	0	3	0	6	5
Valtengrund	"	0	0	0	1	0	0	0
Total data set	Ni telluride	0	13	1	64	2	7	0
Kunratice	"	0	100	0	0	0	0	0
Sohland-Rožany	"	0	9	1	73	2	3	0
Soraer Berg	"	0	0	0	100	0	0	0
Grenzland	"	0	18	0	4	0	40	2
Sohland-Rožany	Ni-Sb telluride	0	18	3	56	0	5	0
Total data set	Native bismuth	0	0	0	0	0	0	0
Sohland-Rožany	"	0	0	0	0	0	0	0
Forest District 15	"	0	0	0	0	0	0	0

**Table 18:** (continued).

	Mineral group	Quartz	Alkali feldspar	Plagioclase	Pyroxene	Amphibole	Biotite	Chlorite
Total data set	Pd-Ni telluride	9	0	0	1	2	2	27
Kunratice	"	0	0	0	0	0	0	0
Sohland-Rožany	"	5	0	0	0	3	0	35
Soraer Berg	"	0	0	0	0	0	0	0
Grenzland	"	28	1	0	4	1	9	31
Total data set	Pd-Bi telluride	4	3	0	7	2	3	20
Kunratice	"	6	0	0	63	2	0	13
Sohland-Rožany	"	2	3	0	0	2	0	20
Grenzland	"	12	0	0	0	0	26	23
Sohland-Rožany	Pd antimonide	0	0	0	0	0	0	0
Total data set	Pd bismuthide	0	0	50	0	9	0	0
Sohland-Rožany	"	0	0	0	0	17	0	0
Forest District 15	"	0	0	100	0	0	0	0
Sohland-Rožany	Pt telluride	4	0	0	0	0	0	6
Total data set	Pt arsenide	0	6	1	5	1	2	8
Kunratice	"	0	0	0	13	0	0	0
Sohland-Rožany	"	0	7	1	1	1	3	10
Grenzland	"	0	0	0	33	4	0	0
	Rh							
Sohland-Rožany	sulpharsenide	0	0	0	0	0	0	0
Total data set	Native gold	11	4	10	8	1	1	9
Sohland-Rožany	"	0	0	0	10	1	1	13
Soraer Berg	"	0	0	100	0	0	0	0
Grenzland	"	63	22	5	0	0	0	0
Total data set	Pb telluride	0	1	11	0	2	4	8
Sohland-Rožany	"	0	1	0	0	0	3	8
Forest District 15	"	0	4	63	3	17	4	2
Grenzland	"	0	0	48	0	9	12	17
Valtengrund	"	0	0	49	0	0	14	0
Sohland-Rožany	Hg telluride	1	2	0	1	1	0	10
Total data set	Ag telluride	7	0	0	3	2	0	5
Sohland-Rožany	"	0	0	0	0	0	0	9
Forest District 15	"	0	0	0	14	11	0	0
Grenzland	"	33	0	0	0	0	0	0
Total data set	Bi telluride	3	1	15	9	6	5	9
Kunratice	"	7	0	5	28	6	5	10
Sohland-Rožany	"	0	2	0	6	10	5	8
Forest District 15	"	0	0	53	0	0	4	8
Grenzland	"	10	0	13	11	0	8	11
Valtengrund	"	3	0	76	0	5	0	10
Total data set	Ni telluride	2	0	0	1	1	0	2
Kunratice	"	0	0	0	0	0	0	0
Sohland-Rožany	"	0	0	0	1	1	0	1
Soraer Berg	"	0	0	0	0	0	0	0
Grenzland	"	14	0	0	2	0	4	9
Sohland-Rožany	Ni-Sb telluride	1	0	0	0	0	0	7
Total data set	Native bismuth	0	0	33	9	15	40	0
Sohland-Rožany	"	0	0	0	26	45	19	0
Forest District 15	"	0	0	50	0	0	50	0

Table 18: (continued).

	Mineral group	Stilpnomelane	Carbonate	Other	Total	Samples (n)	Mineral grains (n)
Total data set	Pd-Ni telluride	8	10	7	100	10	118
Kunratice	"	0	100	0	100	1	1
Sohland-Rožany	"	13	0	9	100	6	38
Soraer Berg	"	0	0	0	100	1	2
Grenzland	"	0	0	6	100	2	77
Total data set	Pd-Bi telluride	6	2	10	100	21	59
Kunratice	"	0	0	0	100	2	13
Sohland-Rožany	"	6	3	11	100	17	42
Grenzland	"	7	0	10	100	2	4
Sohland-Rožany	Pd antimonide	0	0	17	100	10	14
Total data set	Pd bismuthide	0	0	14	100	2	2
Sohland-Rožany	"	0	0	29	100	1	1
Forest District 15	"	0	0	0	100	1	1
Sohland-Rožany	Pt telluride	0	0	0	100	4	4
Total data set	Pt arsenide	7	1	10	100	31	119
Kunratice	"	0	5	0	100	3	6
Sohland-Rožany	"	9	0	8	100	25	110
Grenzland	"	0	0	33	100	3	3
	Rh						
Sohland-Rožany	sulpharsenide	0	0	0	100	1	1
Total data set	Native gold	0	0	22	100	11	32
Sohland-Rožany	"	0	0	30	100	8	23
Soraer Berg	"	0	0	0	100	1	1
Grenzland	"	0	0	5	100	2	8
Total data set	Pb telluride	0	0	4	100	24	199
Sohland-Rožany	"	0	0	5	100	19	155
Forest District 15	"	0	2	1	100	2	24
Grenzland	"	0	1	3	100	2	15
Valtengrund	"	0	0	0	100	1	5
Sohland-Rožany	Hg telluride	19	0	5	100	13	49
Total data set	Ag telluride	3	2	6	100	10	20
Sohland-Rožany	"	3	3	7	100	6	10
Forest District 15	"	0	0	0	100	2	6
Grenzland	"	6	0	11	100	2	4
Total data set	Bi telluride	0	1	11	100	16	286
Kunratice	"	0	0	8	100	2	104
Sohland-Rožany	"	0	0	8	100	8	139
Forest District 15	"	0	6	6	100	2	5
Grenzland	"	0	0	30	100	3	17
Valtengrund	"	0	0	4	100	1	21
Total data set	Ni telluride	1	0	7	100	27	281
Kunratice	"	0	0	0	100	1	1
Sohland-Rožany	"	1	1	8	100	22	258
Soraer Berg	"	0	0	0	100	1	1
Grenzland	"	0	0	6	100	3	21
Sohland-Rožany	Ni-Sb telluride	9	0	1	100	13	126
Total data set	Native bismuth	0	0	3	100	3	5
Sohland-Rožany	"	0	0	10	100	1	3
Forest District 15	"	0	0	0	100	2	2



and Valtengrund (49%). Bi telluride grains show very different associations, ranging from pyrrhotite (for example Kunratice 18%) and pyrite (Sohland-Rožany 33%) to several silicates in all localities (e.g., Kunratice 28% with pyroxene, Valtengrund 76% with plagioclase). In contrast Ni telluride grains are mostly associated with pyrrhotite (63% of total grains), except of additional chalcopyrite in Grenzland locality (40%). It is worth mentioning that the different telluride groups can be associated among themselves to a minor degree as it can be seen in Table 18 for Pb tellurides of the location Valtengrund which show 10% association with Bi telluride.

### 5.5.8 Palladium and platinum elemental department

The elemental distribution/departement is computed by the MLA software and shows in which minerals the elements occur and their relative abundances (per element) – based on the mineral composition allocated in the MLA mineral reference database and the modal composition of the sample. The elemental distribution of palladium regarding its host mineral is variable between the different localities (Table 19). In Kunratice, Sohland-Rožany and Soraer Berg the largest amount of the element Pd occurs in Pd-Bi tellurides. In the Grenzland locality the majority of Pd can be found in Pd-Ni tellurides. In contrast to Pd platinum is in all localities, were this element was found, almost entirely limited to Pt arsenide. Rhodium was found in Rh sulpharsenide only.

**Table 19:** Relative department of (A) palladium, (B) platinum, and (C) rhodium to mineral groups.

(A)	Kunratice	Sohland-Rožany	Soraer Berg	Forest District 15	Grenzland
n (sample)	2	26	1	1	3
n (grain)	14	479	3	1	102
Pd-Ni telluride	0.4	5.0	89.0	0	62.1
Pd-Bi telluride	98.9	31.0	0.0	0	35.4
Pd antimonide	0	14.5	0	0	0
Pd bismuthide	0	3.8	0	100	0
Ni telluride	0.7	35.6	11.0	0	2.5
Ni-Sb telluride	0	9.9	0	0	0
Total	100	100	100	100	100

(B)	Kunratice	Sohland-Rožany	Grenzland
n (sample)	3	25	3
n (grain)	6	114	3
Pt telluride	0	4.4	0
Pt arsenide	100	95.6	100
Total	100	100	100

(C)	Sohland-Rožany
n (sample)	1
n (grain)	1
Rh sulpharsenide	100

**Table 20:** Pt, Pd and Au bulk-rock estimates (in ppb) calculated by the MLA software per locality (note: min. = sample minimum, max. = sample maximum, mean = arithmetic mean, s.d. = standard deviation).

Locality	Kunratice (n=3)			Sohland-Rožany (n=29)			Soraer Berg (n=2)			Forest District 15			Grenzland (n=5)		
	min.	max.	mean s.d.	min.	max.	mean s.d.	min.	max.	mean s.d.	min.	max.	mean s.d.	min.	max.	mean s.d.
Pt (ppb)	10	48	22 18 <0.4	410	39	78 <0.4	<0.4	<0.4	<0.4	-	<0.4	<0.4	8	3	3
Pd (ppb)	<0.4	41	14 19 <0.4	47	14	13 <0.4	0.5	0.4	0.2	1	<0.4	33	12	13	13
Au (ppb)	<0.4	<0.4	<0.4	54	6	14 <0.4	5	3	2	<0.4	<0.4	62	13	24	24

### 5.5.9 Calculated bulk-rock PGE content

Bulk rock ('assay') values are calculated by the MLA software based on the modal analysis and the mineral compositions as well as the densities allocated in the MLA mineral reference database. The Pt, Pd and Au values are computed from the SPL\_Lt\_MAP measurement mode and this reflects only the area of the sample which falls into the BSE grey level range of 150 to 255. To obtain the estimated bulk-rock values for the entire sample the SPL area values for Pt, Pd and Au were set into relation to the total surface area measured for each sample. These total area values were calculated from the XMOD measurement mode. For the samples for which no distinct Pd, Pt or Au-bearing

minerals were identified by the SPL\_Lt\_MAP measurement mode an estimated detection limit of 0.4 ppb has been set, based on the lowest value observed in these computations. The results of this study show that both Au and Pt-Pd values are rather variable in all localities where mineral species containing significant concentrations of these metals were identified (Table 20). However, it can be seen that in the samples of the localities Kunratice and Sohland-Rožany the mean Pt content is higher than in the samples from Soraer Berg, Forest District 15 and Grenzland. The localities Kunratice, Sohland-Rožany and Grenzland show a higher Pd content than the localities Soraer Berg, Forest District 15. The Au content is much higher in the Grenzland locality than in all other localities.

## 5.6 Discussion

For an understanding of the genesis of PGE mineralisation not only the total content and distribution of the PGE, but also its exact mineralogy and association are of relevance (Gervilla & Kojonen 2002, Augé & Lerouge 2004, Li et al. 2004). Ni-Cu deposits associated with mafic and ultramafic magmatic rocks are, of course, the dominant source of PGE, with many examples known (Naldrett 2004). The mineralogy of these deposits is highly complex, with more than 100 minerals known to occur (Cabri 2002). However, there are some general trends that have been recognised. The ores of the Bushveld complex, South Africa (Cawthorn 1999, Naldrett et al. 2009, Naldrett et al. 2012) and Noril'sk-Talnakh, Russia (Naldrett 1992, Naldrett et al. 1992, Naldrett et al. 1995) are generally thought to be of primary magmatic origin, while those of Pechenga, Russia (Distler et al. 1990) and parts of the Sudbury complex, Canada (Carter et al. 2001) are strongly affected by hydrothermal remobilisation. This classification is supported by data including sulphur isotope geochemistry, elemental geochemistry, and mineral characteristics of the deposits.

In comparison the deposits mentioned above and the hydrothermal metamorphic characteristics of the gabbroic dykes of this study it is likely that the wide distribution of the PGM and telluride grains is the result of hydrothermal remobilisation and replacement processes during greenschist metamorphism. Among others, this is supported by the facts that (a) chalcopyrite appears in many samples remobilised and relocated and that (b) some PGM and tellurides show associations with rock-forming silicates (e.g., plagioclase) and alteration minerals (e.g., chlorite). However, a certain relationship to pyrrhotite cannot be negated, which seems to be an indication of the primary magmatic origin, as no remobilisation characteristics are visible. This applies especially to Pt arsenide, Ni telluride and Ni-Sb telluride. The source of tellurium for the genesis of the tellurides remains somewhat debatable. Hattori et al. (2002) illustrated that primitive mantle sulphides can contain up to 17 ppm Te, whereas the bulk primitive mantle average is only 0.012 ppm Te (McDonough & Sun 1995). Data compiled by Zemmann & Leutwein (1974) show that the tellurium content in sedimentary rock types is rather low (for example, greywackes and shales 0.1-1 ppm Te), and even lower for the average crustal abundance (0.001 ppm Te). Hence, the most likely explanation for the source of Te is the release of the tellurium from the primary sulphides during the hydrothermal remobilisation process similar as suggested by Distler et al. (1990) for platinoids.

	this study <sup>#</sup>			Uhlig et al. (2001)			Relative difference (Uhlig et al. = 100%)			BMS (wt.%)	this study				
	Pt	Pd	Au	Pt	Pd	Au	Pt	Pd	Au		Pt arsenide	Pd-Ni telluride	Pd-Bi telluride	Pd bismuthide	native Au
	(ppb)	(ppb)	(ppb)	(ppb)	(ppb)	(ppb)	(%)	(%)	(%)		(n)	(n)	(n)	(n)	(n)
ESoh2-1/98	6	4	b.d.l.							87.3	1		1		
ESoh2-2/98	22	b.d.l.	b.d.l.							82.2	2				
ESoh2-3/98	24	b.d.l.	b.d.l.	35.2*	20.9*	53*	56	6	-	84	3				
ESoh2-4/98	22	b.d.l.	b.d.l.							89.1	4				
ESoh2-5/98	25	1	b.d.l.							78.3	1				
ESoh-11/98	b.d.l.	1	54	19	28.9	57	-	3	94	32.3			1	1	
Sohland	b.d.l.	0.5	b.d.l.	145	320	69	-	0.1	-	94.9					
FA15H-1/98H	b.d.l.	1	b.d.l.	26.1	42.7	44	-	3	-	7.7				1	
HGI-15/98	4	b.d.l.	b.d.l.	2.5	12.1	13	159	-	-	28.4	1				
HG-3/99A	b.d.l.	23	62	68.2	166	75	-	14	82	12.2		29	2	7	
HG-3/99B	3	33	2	70.4	156	84	5	21	3	15.0	1	48		1	
HG-6/99	8	b.d.l.	b.d.l.	12.1	26.4	44	66	-	-	7.9	1				
SB-2/99	b.d.l.	1	b.d.l.	11.6	21.8	28	-	2	-	0.6		2			
SS-2/98	48	41	b.d.l.	19.5	28.2	22	245	144	-	17.2	4	1	11		

**Table 21:** Comparison of Pt, Pd, Au values calculated by MLA analysis in this study and values given from Uhlig et al. (2001) (NIS Fire Assay-ICP/MS) as well as calculated relative difference (Uhlig et al. 2001 = 100%). For evaluation the BMS content as well as the number of Pt, Pd and Au-bearing mineral grains for each sample are given (note: b.d.l. – below detection limit, # estimated detection limit is 0.4 ppb; \* bulk sample ESoh2/98).

### 5.6.1 Comparison of calculated PGE content with assay data

NiS Fire Assay-ICP/MS data (Actlabs, Canada) of Pt, Pd and Au reported by Uhlig et al. (2001) for ten selected samples. These assay data are compared to our calculated bulk rock estimates (Table 21). It is important to note that of the total 10 samples for which geochemical and mineralogical data are available, only 5 samples were found to contain Pt-bearing PGM grains in the polished surface studied by MLA. The same applies for native Au grains (found only in 3 samples out of 10). Pd-bearing PGM values are more comparable as they could be found by MLA in 8 of 10 samples.

Furthermore, it should be noted that the calculated Pt, Pd, and Au data result from a few mineral grains per sample only (Pt: 1 to 4 Pt arsenide grains, Pd: 1 to 48 Pd-bearing mineral grains, Au: 1 to 7 native Au grains; see Table 21). Comparing the calculated Pt, Pd, and Au values with the numbers of the geochemical analyses given by Uhlig et al. (2001) it can be seen that only a few samples show relatively similar values, but most show as well lower as higher values. Additionally, in several samples no Pt, Pd or Au-bearing mineral grains could be found by MLA analysis whereas geochemical analysis by Uhlig et al. (2001) shows values from 12 to 145 ppb Pt, 12 to 26 ppb Pd and 13 to 69 ppb Au for these particular samples. No correlation could be observed between the relative differences to Uhlig et al. (2001) and total BMS content of the samples.

These observed differences are attributed to a combination of factors. The first that may be invoked is the nugget effect, i.e., the highly irregular distribution of PGM and Au - and the small surface area studied for every sample by MLA. However, given the large number of samples studied it would be expected that calculated PGE contents would have the chance to deviate both positively and negatively from the chemical assay. This is essentially not observed here, as the calculated value is in all but one examples well below the chemical assay result (Table 21).

A second cause for significant deviation could be the occurrence of PGE substituted into the lattice of BMS. According to a compilation in Daltry & Wilson (1997) the maximum recorded platinum content in pyrrhotite is 0.52 wt.% and in pentlandite is 1.90 wt.%. The maximum recorded palladium content in pyrrhotite is 0.61 wt.%, in pentlandite is 3.30 wt.% and in chalcopyrite is 0.16 wt.%. This PGE enrichment in BMS is also supported by several recent laser ablation ICP-MS studies (Barnes et al. 2006, Godel & Barnes 2008, Dare et al. 2011, Piña et al. 2012, Osbahr et al. 2013). As there is no exact mineral chemistry data available for the BMS from the Lusatian Block this may indeed be a very likely source of the observed differences. Even for the samples with low BMS content (for instance SB-2/99 or HG-6/99) the BMS content is still sufficient to host a possible Pt or Pd content in pyrrhotite and/or pentlandite of up to several 10,000 ppb by using the mentioned above maximum recorded Pt and Pd contents in pyrrhotite and pentlandite for calculation.

Of some importance may also be the varying mineral chemistry of some of the PGM. This is particularly likely for melonite ( $\text{NiTe}_2$ ) and merenskyite ( $(\text{Pd,Te})(\text{Te,Bi})_2$ ), which form a solid solution series. As the MLA did not measure the elemental composition of each single mineral grain but compares the elemental spectra and uses the general elemental composition given in the mineral reference table for each particular mineral

species here also differences can occur. Furthermore it could be seen by observation of single high-resolution BSE images that Pt, Pd and Au-bearing minerals occur as inclusions < 1  $\mu\text{m}$  additionally to the mineral grains found by the MLA SPL measurements, for which the BSE image resolution was limited to about 1  $\mu\text{m}$  due to the technical restrictions of the MLA technique (see Fig. 53a). However, it is deemed unlikely that the occurrence of such minute grains will make a significant difference to the calculated data. In summary we can conclude that for PGE concentrations < 1 ppm and a probably strong influence of the “nugget effect” MLA analyses of just one polished thin section are not able to reflect the “real” PGE concentration and distribution in a sample. Considering that, a larger area would have to be analysed to obtain congruent values.

## 5.7 Conclusions

This study illustrates that quantitative mineralogy by automated image analysis is a fast and reliable tool to characterise the nature of PGE mineralisation in magmatic environments – even at very low concentrations. However, it also documents the limitations with respect to the representativity of results. The mineral abundance of PGM, native Au, and non-PGE-bearing tellurides is higher in the samples of semi-massive and massive sulphide mineralisation, which occurs in gabbroic dykes, than in the silicate-rich samples of the dyke rocks. Most mineral grains containing stoichiometric concentrations of noble metals are smaller than 10  $\mu\text{m}$ . No significant differences between different mineral groups or different localities were observed. The close association to base metal sulphides, observed by Uhlig et al. (2001), can be confirmed. This suggests a primary magmatic genesis of the PGM. Pt arsenide and Rh sulpharsenide are regarded as being of primary magmatic origin. Effects of remobilisation, tentatively attributed to a metamorphic-hydrothermal overprint, are evident in all samples. This is illustrated by the association of some PGM (tellurides, antimonides and bismuthides) and non-PGE-bearing tellurides with alteration silicates as well as remobilised chalcopyrite and Ni-Co sulpharsenides. Primary magmatic sulphides (such as pyrrhotite and pentlandite) are identified as the likely source of tellurium required to form secondary tellurides. The remobilisation process is similar to that documented in several prominent magmatic Ni-Cu-PGE districts, such as Pechenga, Russia, parts of the Sudbury Complex, Canada or Las Aguilas, Argentina.

## 5.8 Acknowledgments

We thank Andreas Kindermann (Treibacher Schleifmittel Zschornowitz GmbH) for providing access to all samples as well as additional information about samples and sample localities. Michael Leh (Naturforschende Gesellschaft der Oberlausitz e. V., FG Geologie/Mineralogie Bautzen) is thanked for guidance in the field and valuable suggestions. We acknowledge support by Christin Kehrer (Geoscientific Collections, TU Bergakademie Freiberg) in compiling the overview of archived materials of the study of Uhlig et al. (2001) and allowing the access to counter samples for comparative studies. The authors thank Bernd Lehmann and Volker Steinbach for thorough review and constructive comments which have greatly improved the quality of the manuscript. We thank Andreas Hoppe for his editorial handling and helpful comments.

## Chapter 6: Summary and Conclusions

The aim of this research study was to develop new methods for different fields of application in automated mineralogy. As the focus of this discipline is not any longer only on ore mineral processing applications it is important to supply techniques for new fields of application as described in chapter 1. Importantly, results obtained by automated mineralogy methods need to be validated by alternative analytical methods before they should be implemented. This has been a major drawback of the application of automated mineralogy, as results remain untested. The research articles published for this thesis contribute here in different ways.

### Summary of Research Papers

*Paper 1* (chapter 3) dealing with the characterisation of lithium-bearing zinnwaldite micas shows that SEM-based image analyses can contribute in the characterisation of silicate mineral assemblages in a fast and accurate way. It has been shown that industrial mineral products derived from comminution processes can benefit from the capabilities of automated SEM-based image analysis systems, such as MLA, in the same way as ore beneficiation intermediate and products. This study clearly illustrates that the MLA can provide quantitative mineral data for industrial silicate minerals of the same quality as other analytical methods.

This is aptly illustrated too by the characterisation of graphite raw materials and processing products in *Paper 2* (chapter 4). Despite the fact that numerous articles related to automated quantitative analyses of coal and related products are available since the late 1980s this is the first research paper which covers the automated SEM-based quantitative analysis of graphite. The study shows clearly that due to its special physical and chemical properties samples containing graphite need a sophisticated sample preparation methodology and an adapted BSE image calibration for MLA measurement. The results of the study document that automated SEM-based image analysis, such as MLA, is an accurate and reliable tool to attain mineralogical information and process-relevant data for graphite beneficiation. However, this should be always complemented by other analytical methods such as quantitative X-ray powder diffraction. Furthermore, it is shown that particle size characterisation by MLA is in relative good agreement with other measurement methods as wet laser diffraction and dry sieve classification.

The results of a study, published in *Paper 3* (chapter 5), on about 100 polished thin sections and polished round blocks on the nature and distribution of PGE-bearing minerals and the relationship of PGMs, base metal sulphides and gabbroic host rocks may provide an indication for the scope of developing mineralogical - rather than geochemical - vectors towards mineralisation. Here, the MLA contributes mineral quantification, mineral grain size characterisation and mineral association information at a detailed level that can otherwise not be obtained. By this study, it is shown that automated SEM-based image analysis can provide valuable data for the characterisation of trace minerals relevant for petrological studies. This can lead to a potential development of a new type of mineralogical vectors which may well become useful exploration tools.

### **MLA Calculated Elemental Assay/Modal Mineralogy Results and Comparisons**

It is best practice to compare modal mineralogy results and derived therefrom calculated elemental assay data obtained by MLA measurements with quantitative analytical methods. Unfortunately, no bulk chemical assay data were available for comparisons of calculated elemental assay data obtained from the MLA measurements of the three studies of this thesis. Only for one study comparative data on the PGE content of gabbroic rocks and associated ores of the Lusatian Block (*Paper 3*, see chapter 5) were available. As illustrated in the corresponding paper calculated PGE assay data obtained from MLA analysis showed major differences to chemical PGE assay data due to several factors such as nugget effect, PGE substitution into BMS and the varying mineral chemistry of some of the PGM. (see chapter 5.6.1). However, a variety of other studies such as Benvie (2007), Pascoe et al. (2007), Ryösä et al. (2008), Spicer et al. (2008), Donskoi et al. (2011), Ayling et al. (2012), Huminicki et al. (2012), Boni et al. (2013), Jones et al. (2013), Lund et al. (2013), Richards et al. (2013), Smythe et al. (2013), Anderson et al. (2014), Donskoi et al. (2014), and Santoro et al. (2014) showed that a good comparability between chemical assays and calculated assays obtained from automated SEM-based image analysis is no exception. Even though some particular samples in the studies mentioned above showed major differences this is not the rule. Some of these differences can be caused among others by chemical variations within a mineral group or different measurement “areas/volumes”. As already mentioned, MLA uses an average chemical composition for each mineral listed in the mineral reference database and a complex mineralogy may cause here issues. “The pitfalls of the method are related to the user: the data are only as good as the mineralogist or geologist performing the evaluation.” stated Hoal et al. (2009a) in relation to the SEM-based QEMSCAN methodology but this sentence is true for the MLA technique too. Coarse-grained heterogeneous particles or heterogeneous thin sections can differ in their modal composition measured by automated mineralogy from, for example, well homogenised samples analysed by QXRD as the heterogeneous analysed sections would show a very low representativity for the entire sample due to its coarser characteristics. Such issues can be reduced by the analyses of several blocks of such a sample to increase the total number of analysed particles and hence to improve the reliability. In *Paper 2* (chapter 4) it can be seen that modal mineralogy data obtained by SEM-based image analysis and QXRD show only minor differences and compare very well. In average the divergences for the main phases are here in the range of 1-6% relative difference.

An advantage of automated SEM-based image analysis in contrast to QXRD is a much lower mineral detection limit. As the detection limit of the QXRD is about 0.1-1 wt.% (Koninklijke Philips N.V. 2013, PANalytical B.V. 2014) the identification of most of the minor mineral phases (trace minerals) is not possible by this analytical method. Another benefit of automated SEM-based image analysis in comparison with QXRD is the possibility to determine particle sizes and mineral grain sizes. Furthermore, textural information can be extracted by SEM-based image analysis which is not possible by QXRD as the samples have to be micronised here for analysis.



### Size Characterisation by MLA and Comparisons

In the research articles of this study it has been shown that particle size/mineral grain size characterisation by automated SEM-based image analysis systems, such as MLA, can provide a valuable addition or alternative to classical size analyses methods as dry sieving and laser diffraction. The size characterisation by automated systems is principally dependent on the BSE image resolution of the hardware platform and the chosen magnification of the analysis. Even if a modern SEM hardware platform supports an image resolution down into the nanometre range automated SEM-based image analysis systems are optimised for rapid measurements (high EDX count rates). This limits the BSE image resolution to about 0.5  $\mu\text{m}$  per pixel. A measurement magnification of 300 x at a 500x500 pixel area would result in an about 1  $\mu\text{m}$ /pixel image resolution and a magnification of 200 x at a 1000x1000 pixel area in an about 3  $\mu\text{m}$ /pixel image resolution. As the SEM-based image analysis is a size characterisation by area it shares the same problem with dry sieving, i.e., the influence of shape (King 1984, Sutherland 2007). Elongated particles can be under-represented (Brandes & Hirata 2009, Vlachos & Chang 2011). Therefore, an accurate sample homogenisation and random-orientated particle mounting in the mounting media is crucial to obtain reliable measurement results. Due to effects of sectioning (exposed surfaces of the minerals) a sufficient amount of particles is necessary to obtain size data with a low bias. Since the late 1970s several studies (Grant et al. 1979, Pong et al. 1983, King 1984, Jackson et al. 1988, Fregeau-Wu et al. 1990, 1992, Lastra et al. 1998, Kahn et al. 2002, Chernet & Marmo 2003, Sutherland 2007, Taşdemir 2008, Taşdemir et al. 2011, Evans & Napier-Munn 2013) investigated the effects of size measurements by image analysis.

In comparison with dry sieve analysis MLA analyses of graphites show somewhat larger particle sizes as illustrated in *Paper 2* (chapter 4). This could be related to the softness of graphite and a mechanical abrasion during sieve classification. Furthermore, it cannot be completely excluded that a minor preferred orientation of graphite flakes into the polished sample surface exist as well as agglomerations of finer particles occur, which could not be resolved by the chosen image magnification of the MLA measurement. In comparison with wet laser diffraction MLA analyses of graphite show in general a much smaller fraction of very fine particles. This could be related to a number of factors, such as dispersion or decomposition of graphite particles by the ultrasonic dispersion process and mechanical transport, instability of the dispersion, inclusion of air bubbles or classification of particles in the transfer from the sample dispersion unit to the measurement zone (Merkus 2009). It is generally accepted that a direct comparability of different methods of particle size characterisation cannot be achieved due to their different methodological approaches (Allen 2003, Merkus 2009). Unfortunately, no published research articles dealing with the comparison of particle size characterisation by automated mineralogy and other methods exist as of this writing. However, in general it is most likely that particle sizes and mineral grain sizes of materials embedded in solid mounting media were size-underestimated by image-based analysis due to stereological effects (Allen 2003, Gu et al. 2012). Nevertheless, it can be concluded that size data obtained by MLA are realistic and can be used as alternative and/or in addition to size data obtained by other methods. It should be remembered that size characterisation by MLA has an important advantage over

the other methods of size characterisation. While the latter give only “bulk” results MLA can report size data for every single mineral species inside a bulk sample.

Size data are by default reported by MLA Dataview reporting software in equivalent circle diameter, but can be changed in this software to equivalent ellipse minor axis (more realistic for elongated particles) or maximum diameter (more realistic for very irregular shaped particles). As all relevant size and shape properties for both particles and mineral grains are stored in a database by the MLA software, the user can even extract custom size and shape information (e.g., particle polygon length, convex hull length, Paris factor, area delta factor or form index).

Regarding the determination of mineral grain sizes in polished thin sections and polished blocks it has to be noted that size data of connected mineral grains of similar mineral species cannot be determined at a normal image magnification as they show the same BSE grey value and thus cannot be segmented (see section 2.1.3 for segmentation functionality). By using a higher magnification during the measurement sometimes grain boundaries are visible as somewhat darker lines which may be used to separate the grains.

### **Guideline for Method Development**

In the following section a guideline for accurate method development for automated mineralogy analysis is given. In general, it is best practise to perform every step in a careful manner and to document every procedure.

The correct way of sampling is described above (see section 2.2) and includes accurate planning as well as random and representative sampling.

The sample preparation procedure (see section 2.2) has to be very accurate with respect to type and properties of the sample material. Sample preparation test series will help to find the best way for the preparation of new types of sample materials.

The choice of the measurement mode (see section 2.1.4) must be in accordance with the objective of the analysis. The type of sample material shall be clear to avoid the choice of an unsuitable measurement mode.

The pre-measurement calibrations and measurement set-up must be handled very accurately and clearly geared to the type of sample material and the objective of the study. Pre-measurement tests of a small number of frames can reveal issues. The careful build-up of the mineral reference list may be supported by other analytical data (EMPA, LA-ICP-MS) and/or the analysis of pure reference minerals.

An advanced mineral classification can help to eliminate mineral classification issues. Careful image screening will reveal problems and help to improve the quality of the results.

The analysis results have to be assessed very carefully and the errors analysis shall be supported by comparability tests using additional analytical methods (size characterisation, chemical assay, QXRD, and much more). Duplicate and replicate analysis will help to determine the accuracy and precision of the measurement.

### **Recommendations for Further Development of the MLA Technique**

It has to be noted that each method has not only advantages but also challenges. The automated SEM-based image analysis is in comparison to other analytical techniques a relatively novel method and has still room for improvements. This comprises as well MLA Measurement software, MLA Mineral Reference Editor and MLA Image Processing software. A first point for improvements in the measurement software would be the optimisation of the BSE image calibration. Here, a semi-automated three point calibration as available in FEI's QEMSCAN software could replace the previous manual BSE image calibration. In addition, a BSE image grey value optimisation feature would be advantageous to allow a better image contrast for particular samples. Another point related to improvements in the measurement software would be the extension of the automated mineral reference standard collection to mapping measurement modes like GXMAP and search modes like SPL (see section 2.1.4). This would optimise the mineral reference standard collection in particular related to minerals of relatively similar average atomic numbers respectively BSE grey values and tiny mineral grains of interest. Even the measurements itself could be optimised. The centroid X-ray acquisition point-based measurement modes should be provided with a kind of homogeneity check in which the similar composition of a mineral grain of a uniform BSE grey value is proved. For X-ray mapping modes a buffer zone at the grain boundaries should be implemented to prevent the unnecessary collection of mixed spectra directly on these boundaries.

The mineral reference editor can be improved by taking the elemental variability of the minerals into consideration for the spectra matching. Hardly any mineral has a strict chemical composition but large ranges in elemental variations (often several wt.%) are common. In addition, there should be the possibility to create mineral solid solution series to allow substitution in particular elements (e.g., Mg for Fe). Hence only end member spectra would be stored in the reference library and the software computes the intermediate members. A last point to mention in this section is the construction of an extensive mineral standard library stock as this is critical to improve the quality of the mineral reference standard library. Here "certified" minerals are essential, which means that reference mineral standards should be collected from reference standard blocks which have to be checked for homogeneity and their elemental composition have to be analysed by electron probe microanalysis (EPMA). As a result of this the reference standard collection during measurement could be all but omitted.

Regarding image processing and measurement an improvement of the automated de-agglomeration function is desirable (see section 2.3). Here, it is important to optimise the handling of particular mineral grains such as micas. Another point for improvements for the classification process in image processing would be the automated detection of mixed spectra respectively the involved single spectra. Important for better image handling would be the extension of existing image data management tools like filtering, sorting or separation and the implementation of new image data management tools like segmentation, overlaying, contouring, thresholding, and so on. In addition measurement and statistic tools would be very useful.

Last but not least an advanced sample changer is desirable as a rapid analysis time is only worth half as much if the replacement of samples and pumping down of the system

to a good vacuum takes a long time. Currently samples holders for FEI's Quanta hardware platform are available for 8 x 4 cm round blocks, 14 x 3 cm round blocks, 13 x 1 inch round blocks and 12 x thin sections. As an example for improvement sample changer systems such as for XRD or XRF instruments can be considered.

### **Recommendations for Further Applications of Automated Mineralogy**

As described in the introduction section automated SEM-based image analysis systems are used in wide fields of application currently, ranging from industry-driven fields like mineral processing, the petroleum industry, and coal and fly ash characterisation to more science-driven fields like environmental mineralogy, soil science, general geoscience, archaeology, planetary geology, and forensic geoscience. Nevertheless, there are still a plenty of fields of application left where automated systems are uncommon or rare to find at this time but have potential. One of these is the recycling industry. Often it is very difficult to separate the different metals in a composite material of electronic waste ("designer minerals") (Worrell & Reuter 2014a, b). In addition, "designer minerals" are much more complex and diverse in their composition as natural minerals (Worrell & Reuter 2014a, b). Here, automated systems can provide a valuable contribution to analyse the products of recycling beneficiation and metal recovery. Another industrial-based field of application may be the quality control of products which require a supreme purity such as specialty glasses and optical glasses or wafer in electronics. Automated systems may even analyse plastics although they consist mainly of carbon and oxygen but were often added with fillers and colorants such as rutile, chromium oxide, strontium aluminate, zinc oxide, quartz, and chalk (Muccio 1991, 1999) which can be identified by automated SEM-based image analysis. An emerging field of application for automated mineralogy is the determination of source areas of weathering in sedimentology (provenance studies). Automated systems can also provide valuable assistance in disciplines such as palaeontology, micropalaeontology, palynology, palaeoclimatology, and glacial geology.

Additionally to the expansion into new fields of application for automated SEM-based image analysis a better linkage of the existing fields of application is desirable. Automated data interpretation systems could provide valuable assistance for instance for the fields of mining and mineral processing. Furthermore, a better extraction of statistical data could help to improve the quality of the generated information.

In conclusion, it can be stated that automated SEM-based image analysis systems like MLA are powerful analytical tools to complement other well established analytical techniques with valuable quantitative and comprehensive data. This comprises as well quantitative mineral analysis, elemental analysis, size analysis, textural analysis, mineral association and mineral locking analysis, and liberation analysis. It is illustrated that MLA technique is a methodology which is able to generate a significant saving of time and labour in relation to the usage of other analytical methods (e.g. optical methods) while handling vast amounts of data. A large number of samples containing a vast number of particles/mineral grains can be analysed fully automated. In addition, this study has shown that the data provided by MLA analyses are both robust and reliable, even when dealing with very difficult materials such as graphite. This is despite the fact that no internationally

certified reference materials are available for external instrument calibration. However, almost every type of sample material providing a sufficient degree of chemical variability for distinction can be analysed, whereby the very low detection limit allows identifying and characterising mineral grains/phases occurring as traces in the sample material. The full graphical presentation of the analysed materials is a further very valuable benefit which only few analytical methods can deliver. The high-resolution images allow observing unique features such as sample texture. Due to an operator independent measurement unbiased data can be gathered in contrast to point counting by optical microscopy. However, skilled mineralogy experts are and will be required for mineral identification, reference mineral database generation as well as data assessment, interpretation, and reporting (Schouwstra & Smit 2011).

## Bibliography

- Abdelfadil, K.M., Romer, R.L., Seifert, T. & Lobst, R. (2010): Geochemistry and petrology of alkaline basalt and ultramafic lamprophyre dikes from Lusatia (Lausitz) Germany. – *Mineral. Spec. Pap.*, 37: 17-18.
- Abdelfadil, K.M., Romer, R.L., Seifert, T. & Lobst, R. (2013): Calc-alkaline lamprophyres from Lusatia (Germany)—Evidence for a repeatedly enriched mantle source. – *Chem. Geol.*, 353: 230-245. doi:10.1016/j.chemgeo.2012.10.023
- Acharya, B.C., Rao, D.S., Prakash, S., Reddy, P.S.R. & Biswal, S.K. (1996): Processing of low grade graphite ores of Orissa, India. – *Miner. Eng.*, 9 (11): 1165-1169. doi:10.1016/0892-6875(96)00110-0
- Agorhom, E.A., Skinner, W. & Zanin, M. (2013): Influence of gold mineralogy on its flotation recovery in a porphyry copper-gold ore. – *Chem. Eng. Sci.*, 99: 127-138. doi:10.1016/j.ces.2013.05.037
- Agron-Olshina, N., Gottlieb, P. & Creelman, R.A. (1992): The characterisation of mineral matter in coal and fly ashes using QEM\*SEM. 121st SME Annual Meeting and Exhibit, February 24-27, 1992, Phoenix, AZ, USA: 1-11.
- Ahmad, M. & Haghighi, M. (2012): Mineralogy and petrophysical evaluation of Roseneath and Murteee shale formations, Cooper Basin, Australia using QEMSCAN and CT-scanning. SPE Asia Pacific Oil and Gas Conference and Exhibition 2012: Providing a Bright Future, APOGCE 2012, 22-24 October, Perth, WA, Australia: 559-572.
- Airo, A. (2010): Biotic and abiotic controls on the morphological and textural development of modern microbialites at Lago Sarmiento, Chile. PhD Thesis, Stanford University, Stanford, CA, USA.
- Alkuwairan, M.Y. (2012): Polygenetic dolomite in subtidal sediments of northern Kuwait Bay, Kuwait. PhD Thesis, Colorado School of Mines, Golden, CO, USA.
- Allan, R.W. & Lynch, A.J. (1983): Characterization of the behavior of composite particles in a lead-zinc flotation circuit. – *Part. Sci. Technol.*, 1 (2): 155-164. doi:10.1080/02726358308906362
- Allen, T. (2003): *Powder Sampling and Particle Size Determination*. 660 p., Amsterdam, The Netherlands (Elsevier).
- ALS Limited (2015): *Mineralogy Capabilities - Facility and Services*. <http://www.alsglobal.com/en/Our-Services/Minerals/Geochemistry/Capabilities/Mineralogy-Services>. Accessed 8 January 2015.
- Andersen, J., Rollinson, G. & Dawson, D. (2012): Use of automated scanning electron microscopy (QEMSCAN®) to characterise the texture and mineralogy of medieval and post-medieval pottery from Somerset. *Insight from Innovation: New Light on Archaeological Ceramics*, 19-21 October 2012, Southampton, UK: 1 p.
- Anderson, K.F.E., Wall, F., Rollinson, G.K. & Moon, C.J. (2014): Quantitative mineralogical and chemical assessment of the Nkout iron ore deposit, Southern Cameroon. – *Ore Geol. Rev.*, 62: 25-39. doi:10.1016/j.oregeorev.2014.02.015
- Andrews, P.R.A. (1992): Beneficiation of Canadian graphite ores. A review of processing studies at CANMET. – *CIM Bull.*, 85 (960): 76-83.
- Ardila, J. & Clerke, E.A. (2014): *Khuff C Carbonate Mineralogy Data at Multiple Sample Scales*. SPWLA 55th Annual Logging Symposium, 18-22 May 2014, Abu Dhabi, United Arab Emirates: 14 p.
- Armitage, P.J., Faulkner, D.R., Worden, R.H., Aplin, A.C., Butcher, A.R. & Iliffe, J. (2011): Experimental measurement of, and controls on, permeability and permeability anisotropy of caprocks from the CO<sub>2</sub> storage project at the Krechba Field, Algeria. – *J. Geophys. Res. B Solid Earth*, 116 (B12): 18 p. doi:10.1029/2011JB008385
- Armitage, P.J., Worden, R.H., Faulkner, D.R., Aplin, A.C., Butcher, A.R. & Espie, A.A. (2013): Mercia mudstone formation caprock to carbon capture and storage sites: Petrology and petrophysical characteristics. – *J. Geol. Soc.*, 170 (1): 119-132. doi:10.1144/jgs2012-049

- Armitage, P.J., Worden, R.H., Faulkner, D.R., Aplin, A.C., Butcher, A.R. & Iliffe, J. (2010): Diagenetic and sedimentary controls on porosity in Lower Carboniferous fine-grained lithologies, Krechba field, Algeria: A petrological study of a caprock to a carbon capture site. – *Mar. Pet. Geol.*, 27 (7): 1395-1410. doi:10.1016/j.marpetgeo.2010.03.018
- Ashton, T., Ly, C.V., Spence, G. & Oliver, G. (2013a): Application of Real-Time Well-Site Tools for Enhanced Geosteering, Reservoir and Completions Characterization. Unconventional Resources Technology Conference (URTEC), 12-14 August 2013, Denver, CO, USA: 10 p.
- Ashton, T., Ly, C.V., Spence, G. & Oliver, G. (2013b): Drilling completion and beyond, RoqSCAN case study from the Barnett/Chester Play. – *Oilfield Technology*, 6 (4): 63-68.
- Ashton, T., Ly, C.V., Spence, G. & Oliver, G. (2013c): Portable technology puts real-time automated mineralogy on the well site. SPE Western Regional / Pacific Section AAPG Joint Technical Conference 2013: Energy and the Environment Working Together for the Future, 19-25 April 2013, Monterey, CA, USA: 484-494.
- ASPEX Corporation (2006): History.  
<https://web.archive.org/web/20060318170216/http://www.aspecorp.com/html/about/history.html>. Accessed 22 November 2014.
- ASPEX Corporation (2011): ASPEX – Bringing Real Control to Quality Control.  
<https://web.archive.org/web/20111228101622/http://www.aspecorp.com/Solutions/SEMS.aspx>. Accessed 22 November 2014.
- Atanasova, P. (2012): Mineralogy, Geochemistry and Age of Greisen Mineralization in the Li-Sn(-W) Deposit Zinnwald, Eastern Erzgebirge, Germany. Master Thesis, Technische Universität Bergakademie, Freiberg, Germany.
- Augé, T. & Lerouge, C. (2004): Mineral-chemistry and stable-isotope constraints on the magmatism, hydrothermal alteration, and related PGE - (base-metal sulphide) mineralisation of the Mesoarchaeon Baula-Nuasahi Complex, India. – *Miner. Deposita*, 39 (5-6): 583-607. doi:10.1007/s00126-004-0428-x
- Austin, L.G., Sutherland, D.N. & Gottlieb, P. (1993): An analysis of SAG mill grinding and liberation tests. – *Miner. Eng.*, 6 (5): 491-507. doi:10.1016/0892-6875(93)90177-O
- Australian Broadcasting Corporation (2014): Global mining in a 'crisis of confidence' as debt soars, profits plunge. <http://www.abc.net.au/news/2014-06-05/global-mining-slump-sees-profits-plunge/5502572>. Accessed 23 November 2014.
- AXT Pty Ltd (2014): TIMA – SEM-Based Automated Minerals Analyser.  
<http://www.axt.com.au/tescan-integrated-minerals-analyser-tima/>. Accessed 22 November 2014.
- Ayling, B., Rose, P. & Petty, S. (2011): Using QEMSCAN® to characterize fracture mineralization at the Newberry Volcano EGS Project, Oregon: A pilot study. Geothermal Resources Council Annual Meeting 2011, Geothermal 2011, 23-26 October, San Diego, CA, USA: 301-305.
- Ayling, B., Rose, P., Petty, S., Zemach, E. & Drakos, P. (2012): QEMSCAN® (Quantitative Evaluation of Minerals by Scanning Electron Microscopy): capability and application to fracture characterization in geothermal systems. Thirty-Seventh Workshop on Geothermal Reservoir Engineering, January 30 - February 1, 2012, Stanford, California, USA: 596-606.
- Bachmann, K., Haser, S., Seifert, T. & Gutzmer, J. (2012): Preparation of grain mounds of heterogeneous mineral concentrates for automated mineralogy – An Example of Li-bearing Greisen from Zinnwald, Saxony, Germany. – *Schr. Dtsch. Ges. Geowiss.*, 80, Abstracts of Lectures and Posters GeoHannover 2012, October 1-3: 395.
- Barbery, G. (1974): Determination of particle size distribution from measurements on sections. – *Powder Tech.*, 9 (5-6): 231-240. doi:10.1016/0032-5910(74)80047-1
- Barbery, G. (1985): Mineral liberation analysis using stereological methods: a review of concepts and problems. 2nd International Congress on Applied Mineralogy in the Minerals Industry, February 22-25, 1984, Los Angeles, California, USA: 171-190.
- Barbery, G. (1992): Latest Developments in the Interpretation of Section Measurements for Liberation-Practical Aspects. – *Can. Metall. Q.*, 31 (1): 1-10. doi:10.1179/cm.1992.31.1.1

- Barbery, G., Huyet, G. & Gateau, C. (1981): Liberation analysis by means of image analysers: theory and applications. XIII International Mineral Processing Congress, June 4-9, 1979, Warsaw, Poland: 568-599.
- Barnes, S.J., Cox, R.A. & Zientek, M.L. (2006): Platinum-group element, Gold, Silver and Base Metal distribution in compositionally zoned sulfide droplets from the Medvezky Creek Mine, Noril'sk, Russia. – *Contrib. Mineral. Petrol.*, 152 (2): 187-200. doi:10.1007/s00410-006-0100-9
- Baum, W., Lotter, N.O. & Whittaker, P.J. (2004): Process mineralogy - A new generation for ore characterization and plant optimization. 2004 SME Annual Meeting, 23-25 2004, Denver, CO, USA: 73-77.
- Baumann, L., Kuschka, E. & Seifert, T. (2000): Lagerstätten des Erzgebirges. 300 p., Stuttgart, Germany (ENKE im Georg Thieme Verlag).
- Bautsch, H.-J. (1963): Über die Sulfide in den Lamprophyren der Lausitz und ihre genetische Ableitung. – *Geologie*, 12 (3): 362-364.
- Bautsch, H.-J. & Rohde, G. (1975): Die Paragenese der Metallchalkogenide in den Gabbrodoleriten der Lausitz. – *Freib. Forschungsh.*, C 308: 73-98.
- Beamond, T.W. (1970): Automatic pulse-height tracking for an electron probe microanalyser. – *J. Phys. E Sci. Instrum.*, 3 (10): 826-827. doi:10.1088/0022-3735/3/10/423
- Beck, R. (1902): Ueber eine neue Nickelerzlagerstaette in Sachsen. – *Z. Prakt. Geol.*, 10: 41-43, 379-381.
- Beck, R. (1903a): Die Nickelerzlagerstätte von Sohland a. d. Spr. und ihre Gesteine. – *Z. Dtsch. Geol. Ges.*, 55: 296-330.
- Beck, R. (1903b): Lagerstätten von nickelhaltigem Magnetkies am Schweidrich bei Schluckenau in Nordostböhmen und bei Sohland in der sächsischen Lausitz. In: Beck, R. (ed) *Lehre von den Erzlagerstätten*. 2nd revised edn. Verlag von Gebrüder Borntraeger, Berlin, Germany, 46-47.
- Beck, R. (1909): Lagerstätten von nickelhaltigem Magnetkies und Kupferkies in Lausitzer Diabasen. In: Beck, R. (ed) *Lehre von den Erzlagerstätten*. 3rd revised edn. Verlag von Gebrüder Borntraeger, Berlin, Germany, 81-86.
- Beck, R. (1919): Über die sogenannten Röhrchenerze am Schweidrich bei Schluckenau. – *Z. Prakt. Geol.*, 27: 5-7.
- Benzie, B. (2007): Mineralogical imaging of kimberlites using SEM-based techniques. – *Miner. Eng.*, 20 (5): 435-443. doi:10.1016/j.mineng.2006.12.017
- Berg, G. (1939): Aplite, Lamprophyre und Erze. – *Z. Prakt. Geol.*, 47 (5): 81-85.
- Berg, G. & Friedensburg, F. (1944): Nickel und Kobalt. Die Metallischen Rohstoffe - ihre Lagerungsverhältnisse und ihre wirtschaftliche Bedeutung, 6. Heft. 280 p., Stuttgart, Germany (Ferdinand Enke Verlag).
- Bergeat, A. (1904): Nickelhaltiger Magnetkies (und Kupferkies) gebunden an Gesteine der Gabbrofamilie und deren metamorphe Abkömmlinge. a) Vorkommen gebunden an mehr oder weniger unveränderte intrusive Gabbros und gabbroähnliche Gesteine jüngeren Alters. In: Bergeat, A. (ed) *Die Erzlagerstätten*. Unter Zugrundelegung der von Alfred Wilhelm Stelzner hinterlassenen Vorlesungsmanuskripte und Aufzeichnungen, 1. Hälfte. Verlag von Arthur Felix, Leipzig, Germany, 42-44.
- Bernstein, S., Frei, D., McLimans, R.K., Knudsen, C. & Vasudev, V.N. (2008): Application of CCSEM to heavy mineral deposits: Source of high-Ti ilmenite sand deposits of South Kerala beaches, SW India. – *J. Geochem. Explor.*, 96 (1): 25-42. doi:10.1016/j.gexplo.2007.06.002
- Beyer, O. (1902): Die erste Erzlagerstätte der Oberlausitz. – *Wiss. Beil. Leipz. Ztg.*, Nr. 19 (Donnerstag, den 13. Februar): 73-75.
- Bishop, J.K.B. & Biscaye, P.E. (1982): Chemical characterization of individual particles from the nepheloid layer in the Atlantic Ocean. – *Earth Planet. Sci. Lett.*, 58 (2): 265-275. doi:10.1016/0012-821X(82)90199-6
- Blaskovich, R.J. (2013): Characterizing waste rock using automated quantitative electron microscopy. Master Thesis, University of British Columbia, Vancouver, BC, Canada.



- Bluhm, H., Frey, W., Giese, H., Hoppé, P., Schultheiß, C. & Sträßner, R. (2000): Application of pulsed HV discharges to material fragmentation and recycling. – *IEEE Trans. Dielectr. Electr. Insul.*, 7 (5): 625-636. doi:10.1109/94.879358
- Bolduan, H., Lächelt, A. & Malasek, F. (1967): Zur Geologie und Mineralisation der Lagerstätte Zinnwald (Cinovec). – *Freib. Forschungsh.*, C 218: 35-52.
- Boni, M., Rollinson, G., Mondillo, N., Balassone, G. & Santoro, L. (2013): Quantitative mineralogical characterization of karst bauxite deposits in the southern apennines, Italy. – *Econ. Geol.*, 108 (4): 813-833. doi:10.2113/econgeo.108.4.813
- Both, R.A. & Stumpf, E.F. (1987): Distribution of silver in the Broken Hill orebody (Australia). – *Econ. Geol.*, 82 (4): 1037-1043. doi:10.2113/gsecongeo.82.4.1037
- Botha, P.W.S.K., Wentworth, S.J., Butcher, A.R., Horsch, H. & McKay, D. (2009): Automated particle analysis of Apollo 17 regolith: quantitative insights into the composition and textures of glass spheres from the shorty crater sampling site. 2009 GSA Annual Meeting, 18-21 October 2009, Portland, Oregon, USA: 266.
- Brandes, H.G. & Hirata, J.G. (2009): An automated image analysis procedure to evaluate compacted asphalt sections. – *Int. J. Pavement Eng.*, 10 (2): 87-100. doi:10.1080/10298430801916866
- Brown, M. & Dinham, P. (2007): Benchmark quality investigation on automated mineralogy. *Automated Mineralogy 2007*, September 1-2, Brisbane, QLD, Australia: 10 p.
- Bruker AXS (2010a): XFlash<sup>®</sup> 5010 Detector. <https://web.archive.org/web/20101124101949/http://bruker-axs.com/xflash-5010.html>. Accessed 22 November 2014.
- Bruker AXS (2010b): XFlash<sup>®</sup> 5030 Detector. <https://web.archive.org/web/20101124094834/http://bruker-axs.com/xflash-5030.html>. Accessed 22 November 2014.
- Bruker Nano GmbH (2011): QUANTAX User Manual. 199 p. unpublished work
- Burne, R.V., Moore, L.S., Christy, A.W., Troitzsch, U., King, P.L., Carnerup, A.M. & Joseph Hamilton, P. (2014): Stevensite in the modern thrombolites of Lake Clifton, Western Australia: A missing link in microbialite mineralization? – *Geology*, 42 (7): 575-578. doi:10.1130/G35484.1
- Burtman, V., Fu, H. & Zhdanov, M.S. (2014): Experimental Study of Induced Polarization Effect in Unconventional Reservoir Rocks. – *Geomater.*, 4 (04): 117-128. doi:10.4236/gm.2014.44012
- Bushell, C. (2011): A new SEM-EDS based automated mineral analysis solution for PGM-bearing ores and flotation products. – *Miner. Eng.*, 24 (12): 1238-1241. doi:10.1016/j.mineng.2011.02.018
- Butcher, A.R. (2010): A practical guide to some aspects of mineralogy that affect flotation. In: Greet, C.J. (ed) *Flotation Plant Optimisation: A Metallurgical Guide to Identifying and Solving Problems in Flotation Plants*. Spectrum Series, vol 16. The Australasian Institute of Mining and Metallurgy, Carlton, Victoria, Australia, 83-93.
- Butcher, A.R. & Botha, P.W.S.K. (2007): Case Study: Well lithotyping from cuttings Basker-5, Gippsland Basin. *Intellection Pty Ltd*, Brisbane, QLD, Australia: 6 p.
- Butcher, A.R., Cropp, A.L.F.R., French, D.H. & Azzi, M. (2005): Source characterisation of atmospheric particles using automated scanning electron microscopy (QEMSCAN<sup>™</sup>). 17th International Clean Air & Environment Conference, 3-6 May 2005, Hobart, Tasmania, Australia: 5 p.
- Butcher, A.R., Gravestock, D.I., Gottlieb, P., Cubitt, C. & Edwards, G.V. (2000): A New Way To Analyse Drill Cuttings: A Case Study From Debaranie – 1, Cooper Basin, South Australia. – *APPEA J.*, 40: 774-775.
- Byers, R.L., Davis, J.W., White, E.W. & McMillan, R.E. (1971): A computerized method for size characterization of atmospheric aerosols by the scanning electron microscope. – *Environ. Sci. Tech.*, 5 (6): 517-521. doi:10.1021/es60053a003
- Cabri, L.J. (2002): The geology, geochemistry, mineralogy and mineral beneficiation of platinum-group elements. *CIM Special Volume 54*. 852 p., Montreal, Quebec, Canada (Canadian Institute of Mining, Metallurgy and Petroleum).

- Carl Zeiss AG (2014a): Products - Scanning Electron Microscopes - Mineralogic Systems. [http://www.zeiss.com/microscopy/en\\_de/products/scanning-electron-microscopes/mineralogic-systems.html](http://www.zeiss.com/microscopy/en_de/products/scanning-electron-microscopes/mineralogic-systems.html). Accessed 22 November 2014.
- Carl Zeiss AG (2014b): ZEISS Mineralogic Mining - ZEISS Launches Mineral Analysis Solution for Mining Industry. [http://www.zeiss.com/corporate/en\\_de/media-forum/press-releases.html?id=E4C44C2A9C746059C1257D1C00299182](http://www.zeiss.com/corporate/en_de/media-forum/press-releases.html?id=E4C44C2A9C746059C1257D1C00299182). Accessed 22 November 2014.
- Carter, W.M., Watkinson, D.H. & Jones, P.C. (2001): Post-magmatic remobilization of platinum-group elements in the Kelly Lake Ni-Cu sulfide deposit, Copper Cliff Offset, Sudbury. – *Explor. Min. Geol.*, 10 (1-2): 95-110. doi:10.2113/10.1-2.95
- Casuccio, G.S., Janocko, P.B., Lee, R.J., Kelly, J.F., Dattner, S.L. & Mgebroff, J.S. (1983): The use of computer controlled scanning electron microscopy in environmental studies. – *J. Air Pollut. Contr. Assoc.*, 33 (10): 937-943. doi:10.1080/00022470.1983.10465674
- Cawthorn, R.G. (1999): Platinum-group element mineralization in the Bushveld Complex - a critical reassessment of geochemical models. – *S. Afr. J. Geol.*, 102 (3): 268-281.
- Celik, I.B., Can, N.M. & Sherazadishvili, J. (2011): Influence of process mineralogy on improving metallurgical performance of a flotation plant. – *Miner. Process. Extr. Metall. Rev.*, 32 (1): 30-46. doi:10.1080/08827508.2010.509678
- Chernet, T. & Marmo, J. (2003): Direct comparison on mechanical and digital size analyses of Kemi Chromite, Finland. – *Miner. Eng.*, 16 (11, Supplement 1): 1245-1249. doi:10.1016/j.mineng.2003.05.002
- Chin, K., Pearson, D. & Ekdale, A.A. (2013): Fossil Worm Burrows Reveal Very Early Terrestrial Animal Activity and Shed Light on Trophic Resources after the End-Cretaceous Mass Extinction. – *PLoS ONE*, 8 (8): e70920. doi:10.1371/journal.pone.0070920
- Creelman, R.A., Greenwood-Smith, R., Gottlieb, P. & Paulson, C.A.J. (1986): The characterisation of mineral matter in coal and the products of coal combustion using QEM\*SEM. 2nd Australian Coal Science Conference, 1-2 December, 1986, Newcastle, NSW, Australia: 215-221.
- Creelman, R.A. & Ward, C.R. (1996): A scanning electron microscope method for automated, quantitative analysis of mineral matter in coal. – *Int. J. Coal Geol.*, 30 (3): 249-269. doi:10.1016/0166-5162(95)00043-7
- Cropp, A.L.F.R., Butcher, A.R., French, D.H., Gottlieb, P., O'Brien, G. & Pirrie, D. (2003): Automated measurement of coal and mineral matter by QEMSCAN - a new mineralogical tool based on proven QEM\*SEM technology. *Applied Mineralogy 03: International Applied Mineralogy Symposium*, 17-18 March 2003, Helsinki, Finland: 2 p.
- CSIRO (2004): *CSIRO Annual Report 2003-04*. Commonwealth Scientific and Industrial Research Organisation, Canberra, ACT, Australia: 216 p.
- CSIRO (2008): *Technology for rapid mineralogical analysis*. <http://www.csiro.au/Organisation-Structure/Flagships/Minerals-Down-Under-Flagship/Processing/QEMSCAN.aspx>. Accessed 22 November 2014.
- Dal Martello, E., Bernardis, S., Larsen, R.B., Tranell, G., Di Sabatino, M. & Arnberg, L. (2012): Electrical fragmentation as a novel route for the refinement of quartz raw materials for trace mineral impurities. – *Powder Tech.*, 224: 209-216. doi:10.1016/j.powtec.2012.02.055
- Daltry, V.D.C. & Wilson, A.H. (1997): Review of platinum-group mineralogy: Compositions and elemental associations of the PG-minerals and unidentified PGE-phases. – *Mineral. Petrol.*, 60 (3-4): 185-229. doi:10.1007/BF01173709
- Dare, S.A.S., Barnes, S.J., Prichard, H.M. & Fisher, P.C. (2011): Chalcophile and platinum-group element (PGE) concentrations in the sulfide minerals from the McCreedy East deposit, Sudbury, Canada, and the origin of PGE in pyrite. – *Miner. Deposita*, 46 (4): 381-407. doi:10.1007/s00126-011-0336-9
- Dickson, C.W. (1906): Genetic relations of nickel-copper ores, with special reference to the deposits at St. Stephen, N.B., and Sohland, Germany. – *J. Can. Min. Inst.*, 9: 236-260.
- Dieseldorff, A. (1903): Berichtigung einiger Angaben des Herrn R. BECK über „Die Nickelerzlagerstätte von Sohland a. d. Spree und ihre Gesteine.“. – *Z. Dtsch. Geol. Ges.*, 55: 43-48.

- Dinger, D.R. & White, E.W. (1976): Analysis of Polished Sections as a Method for the Quantitative 3-D Characterization in Particulate Materials. 9th Annual Scanning Electron Microscopy Symposium, April 5-9, 1976, IITRI, Chicago, Illinois, USA: 409-416.
- Distler, V.V., Fillmonova, A.A., Grokhovskaya, T.L. & Laputina, I.P. (1990): Platinum-Group Elements in the Copper-Nickel Ores of the Pechenga Ore Field. – *Int. Geol. Rev.*, 32 (1): 70-83. doi:10.1080/00206819009465756
- Donskoi, E., Manuel, J.R., Austin, P., Poliakov, A., Peterson, M.J. & Hapugoda, S. (2011): Comparative study of iron ore characterisation by optical image analysis and QEMSCAN™. IRON ORE Conference 2011, 11-13 July, Perth, WA, Australia: 213-222.
- Donskoi, E., Manuel, J.R., Austin, P., Poliakov, A., Peterson, M.J. & Hapugoda, S. (2014): Comparative study of iron ore characterisation using a scanning electron microscope and optical image analysis. – *Trans. Inst. Min. Metall. B: Appl. Earth Sci.*, 122 (4): 217-229. doi:10.1179/1743275814Y.0000000042
- Egerton, R.F. (2005): Physical principles of electron microscopy: An introduction to TEM, SEM, and AEM. 202 p., New York (Springer). doi:10.1007/b136495
- Evans, C.L. & Napier-Munn, T.J. (2013): Estimating error in measurements of mineral grain size distribution. – *Miner. Eng.*, 52: 198-203. doi:10.1016/j.mineng.2013.09.005
- Exell, R.H.B. (2001): PRACTICAL MATHEMATICS - Error Analysis. <http://www.jgsee.kmutt.ac.th/exell/PracMath/ErrorAn.htm>. Accessed 22 September 2014.
- Fandrich, R., Gu, Y., Burrows, D. & Moeller, K. (2007): Modern SEM-based mineral liberation analysis. – *Int. J. Miner. Process.*, 84 (1-4): 310-320. doi:10.1016/j.minpro.2006.07.018
- Fandrich, R.G., Bearman, R.A., Boland, J. & Lim, W. (1997): Mineral liberation by particle bed breakage. – *Miner. Eng.*, 10 (2): 175-187. doi:10.1016/S0892-6875(96)00144-6
- Fandrich, R.G., Schneider, C.L. & Gay, S.L. (1998): Two stereological correction methods: Allocation method and kernel transformation method. – *Miner. Eng.*, 11 (8): 707-715. doi:10.1016/S0892-6875(98)00057-0
- Fediuk, F., Losert, J., Röhlich, P. & Šilar, J. (1958): Geologické poměry území podél lužické poruchy ve šluknovském výběžku. – *Rozpr. Česk. Akad. Věd, Řada Mat. Přír. Věd.*, 68 (9): 1-42.
- FEI Company (1996): Form 8-K Current Report Filed Nov 22, 1996. <http://investor.fei.com/secfiling.cfm?filingID=893877-96-405&CIK=914329>. Accessed 22 November 2014.
- FEI Company (1997): Form 8-K Current Report Filed Mar 5, 1997. <http://investor.fei.com/secfiling.cfm?filingID=893877-97-160&CIK=914329>. Accessed 22 November 2014.
- FEI Company (2001): FEI's Quanta(TM) SEM Series Offers Flexible, Automated Solutions For Structural Diagnostics on any Material. <http://investor.fei.com/releasedetail.cfm?ReleaseID=255455>. Accessed 14 June 2014.
- FEI Company (2009a): FEI Acquires JKTech Mineral Liberation Analysis Business. <http://investor.fei.com/releasedetail.cfm?ReleaseID=389583>. Accessed 14 June 2014.
- FEI Company (2009b): FEI Company Expands Presence in Automated Mineralogy Market. <http://investor.fei.com/releasedetail.cfm?ReleaseID=357467>. Accessed 14 June 2014.
- FEI Company (2009c): Product Data - Quanta™ 650 FEG. [https://web.archive.org/web/20100225222213/http://www.fei.com/uploadedFiles/DocumentsPrivate/Content/2009\\_03\\_Quanta650FEG\\_ds.pdf](https://web.archive.org/web/20100225222213/http://www.fei.com/uploadedFiles/DocumentsPrivate/Content/2009_03_Quanta650FEG_ds.pdf). Accessed 22 November 2014.
- FEI Company (2009d): The Quanta FEG 250 / 450 / 650 User Operation Manual. 234 p. unpublished work
- FEI Company (2009e): Technical Application Note: Application of Coal Preparation for SEM & MLA Measurement. 6 p. unpublished work
- FEI Company (2010): MLA 3.0 User Guide. 41 p. unpublished work
- FEI Company (2011a): MLA System User Training Course. 380 p. unpublished work
- FEI Company (2011b): Product Data - MLA 650F Automated, Quantitative Petrographic Analyzer. <https://web.archive.org/web/20130409133141/http://www.fei-natural-resources.com/uploadedFiles/DocumentsPrivate/Content/MLA650F-DS-0036-12-11-eng.pdf>. Accessed 22 November 2014.
- FEI Company (2011c): Technical Application Note: De-agglomeration. 4 p. unpublished work

- FEI Company (2011d): Technical Application Note: MLA Sample Preparation Procedure. 18 p. unpublished work
- FEI Company (2012): FEI Buys ASPEX Corporation. <http://investor.fei.com/releasedetail.cfm?ReleaseID=637983>. Accessed 22 November 2014.
- FEI Company (2014a): Products - Quanta SEM. <http://www.fei.com/products/sem/quanta-products/?ind=MS>. Accessed 22 November 2014.
- FEI Company (2014b): Products - SEM. <http://www.fei.com/products/sem/>. Accessed 22 November 2014.
- Ferrara, G., Preti, U. & Meloy, T.P. (1989): Inclusion shape, mineral texture and liberation. – *Int. J. Miner. Process.*, 27 (3-4): 295-308. doi:10.1016/0301-7516(89)90070-7
- Fiedler, F. (1999): *Erzpetrographische Untersuchungen an Mikrogabbros der Lausitzer Antiklinalzone/Sachsen*. Student Research Project (Studienarbeit), TU Bergakademie, Freiberg, Germany.
- Folkedahl, B.C., Steadman, E.N., Brekke, D.W. & Zygarlicke, C.J. (1994): Inorganic phase characterization of coal combustion products using advanced SEM techniques. *The Impact Of Ash Deposition On Coal Fired Plants: Engineering Foundation Conference*, June 20-25, 1993, Solihull, UK: 399-407.
- Ford, F.D., Wercholz, C.R. & Lee, A. (2011): Predicting process outcomes for sudbury platinum-group minerals using grade-recovery modeling from mineral liberation analyzer (MLA) data. – *Can. Mineral.*, 49 (6): 1627-1642. doi:10.3749/canmin.49.6.1627
- François-Bongarçon, D. & Gy, P. (2002): Critical aspects of sampling in mills and plants: A guide to understanding sampling audits. – *J. S. Afr. Inst. Min. Metall.*, 102 (8): 481-484.
- Franke, D. (2013): *Regionale Geologie von Ostdeutschland – Ein Wörterbuch*. [www.regionalgeologie-ost.de](http://www.regionalgeologie-ost.de). Accessed 12 June 2013.
- Fregeau-Wu, E., Pignolet-Brandom, S. & Iwasaki, I. (1990): In Situ Grain Size Determination of Slow-Cooled Steelmaking Slags with Implications to Phosphorus Removal for Recycle. *Process Mineralogy IX: applications to mineral beneficiation, metallurgy, gold, diamonds, ceramics, environment, and health : proceedings of International Symposium on Applied Mineralogy (MAC-ICAM-CAM) held at Montreal, Quebec, Canada on May 14 to 17, 1989, and of the Process Mineralogy Symposium held at Las Vegas, Nevada, February 27 to March 2, 1989*: 429-439.
- Fregeau-Wu, E., Pignolet-Brandom, S. & Iwasaki, I. (1992): In situ grain size distribution determination and liberation modeling of slow-cooled steelmaking slags: implications for phosphorus removal. – *Miner. Metall. Process.*, 9 (2): 85-91.
- Frei, D., Knudsen, C., McLimans, R.K. & Bernstein, S. (2005): Fully automated analysis of chemical and physical properties of individual mineral species in heavy mineral sands by computer controlled scanning electron microscopy (CCSEM). *2005 Heavy Minerals Conference, HMC 2005, 16-19 October, Jacksonville, FL, USA*: 103-108.
- French, D. & Ward, C.R. (2009): The application of advanced mineralogical techniques to coal combustion product characterisation. *3rd World of Coal Ash, WOCA Conference, May 4-7, 2009, Lexington, KY, USA*: 28 p.
- Fröhlich, S., Redfern, J., Petitpierre, L., Marshall, J.D., Power, M. & Grech, P.V. (2010): Diagenetic evolution of incised channel sandstones: Implications for reservoir characterisation of the lower carboniferous marar formation, ghadames basin, western Libya. – *J. Pet. Geol.*, 33 (1): 3-18. doi:10.1111/j.1747-5457.2010.00461.x
- Frost, M.T., O'Hara, K., Suddaby, P., Grant, G., Reid, A.F., Wilson, A.F. & Zuiderwyk, M. (1976): A description of two automated control systems for the electron microprobe. – *X-Ray Spectrom.*, 5 (4): 180-187. doi:10.1002/xrs.1300050403
- Fugro Robertson (2011): *RoqSCAN – Real Time Rock Properties*. <https://web.archive.org/web/20120323024838/http://www.fugro-robertson.com/scripts/filehandler.asp?fp=roqscan.pdf>. Accessed 22 November 2014.
- Fugro Robertson Ltd (2011): Fugro enters into an exclusive agreement with Carl Zeiss to jointly develop and distribute Roqscan™. <http://www.fugro.com/media-centre/news/fulldetails/2011/04/01/fugro-enters-into-an-exclusive-agreement-with-carl-zeiss-to-jointly-develop-and-distribute-roqscan-tm>. Accessed 22 November 2014.

- Galbreath, K., Zygarlicke, C., Casuccio, G., Moore, T., Gottlieb, P., Agron-Olshina, N., Huffman, G., Shah, A., Yang, N., Vleeskens, J. & Hamburg, G. (1996): Collaborative study of quantitative coal mineral analysis using computer-controlled scanning electron microscopy. – *Fuel*, 75 (4): 424-430. doi:10.1016/0016-2361(95)00277-4
- Garagan, M.J. (2014): Textural and spatial relationship between platinum-group elements and alteration assemblages in the Afton porphyry system, Kamloops, British Columbia. Bachelor (Hons) Thesis, Saint Mary's University, Halifax, N.S., Canada.
- Gasparon, M., Ciminelli, V.S.T., Cordeiro Silva, G., Dietze, V., Grefalda, B., Ng, J.C. & Nogueira, F. (2014): A new method for arsenic analysis in Atmospheric Particulate Matter. 5th International Congress on Arsenic in the Environment (As 2014), 11-16 May, Buenos Aires, Argentina: 167-171.
- Gay, S.L. (1995): Stereological equations for phases within particles. – *J. Microsc.*, 179 (3): 297-305. doi:10.1111/j.1365-2818.1995.tb03645.x
- Gay, S.L. (1999): Numerical verification of a non-preferential-breakage liberation model. – *Int. J. Miner. Process.*, 57 (2): 125-134. doi:10.1016/S0301-7516(99)00011-3
- Gay, S.L. & Morrison, R.D. (2006): Using Two Dimensional Sectional Distributions to Infer Three Dimensional Volumetric Distributions - Validation using Tomography. – *Part. Part. Syst. Charact.*, 23 (3-4): 246-253. doi:10.1002/ppsc.200601056
- Gervilla, F. & Kojonen, K. (2002): The platinum-group minerals in the upper section of the Keivitsansarvi Ni-Cu-PGE deposit, Northern Finland. – *Can. Mineral.*, 40 (2): 377-394. doi:10.2113/gscanmin.40.2.377
- Ghosal, S., Ebert, J.L. & Self, S., A. (1993): Chemical Composition and Size Distributions for Fly Ashes. – Preprint. Paper. Am. Chem. Soc. Div. Fuel Chem., 38 (4): 1195-1202.
- Gillespie, M.R. & Styles, M.T. (1999): BGS Rock Classification Scheme - Volume 1 - Classification of igneous rocks. BGS Rock Classification Scheme, 2nd edn. British Geological Survey, Nottingham: 52 p.
- Godel, B. & Barnes, S.J. (2008): Image analysis and composition of platinum-group minerals in the J-M reef, stillwater complex. – *Econ. Geol.*, 103 (3): 637-651. doi:10.2113/gsecongeo.103.3.637
- Gomez, C.O., Rowlands, N., Finch, J.A. & Wilhelmy, J.-F. (1988): A specimen preparation procedure for automated image analysis. *Process Mineralogy VIII*, January 25-28, 1988, Phoenix, Arizona, USA: 359-367.
- Good, T.R. & Ekdale, A.A. (2014): Paleocology and taphonomy of trace fossils in the eolian Upper Triassic/Lower Jurassic Nugget Sandstone, northeastern Utah. – *PALAIOS*, 29 (8): 401-413. doi:10.2110/palo.2014.013
- Goodall, W.R. & Butcher, A.R. (2007): The use of QEMSCAN® in practical gold deportment studies. *World Gold 2007*, 22-24 October, Cairns, QLD, Australia: 221-228.
- Goodall, W.R. & Scales, P.J. (2007): An overview of the advantages and disadvantages of the determination of gold mineralogy by automated mineralogy. – *Miner. Eng.*, 20 (5): 506-517. doi:10.1016/j.mineng.2007.01.010
- Goodall, W.R., Scales, P.J. & Butcher, A.R. (2005): The use of QEMSCAN and diagnostic leaching in the characterisation of visible gold in complex ores. – *Miner. Eng.*, 18 (8): 877-886. doi:10.1016/j.mineng.2005.01.018
- Goonan, T.G. (2012): Lithium use in batteries. U.S. Geological Survey Circular 1371.
- Görz, H., White, E.W., Johnson Jr., G.G. & Pearson, M.W. (1972): CESEMI studies of Apollo 14 and 15 fines. *Third Lunar Science Conference*, January 10-13, 1972, Houston, TX, USA: 3195-3200.
- Görz, H., White, E.W., Roy, R. & Johnson Jr., G.G. (1971): Particle size and shape distributions of lunar fines by CESEMI. *Second Lunar Science Conference*, January 11-14, 1971, Houston, TX, USA: 2021-2025.
- Gottlieb, P. (2008): The Revolutionary Impact of Automated Mineralogy on Mining and Mineral Processing. *XXIV International Mineral Processing Congress*, 24-28 September 2008, Beijing, China: 165-174.
- Gottlieb, P., Agron-Olshina, N., Ho-Tun, E. & Sutherland, D.N. (1989): The automatic measurement of mineral matter in coal. *ICAM '89, International Workshop on Image Analysis Applied to Mineral and Earth Sciences*, May 1989, Ottawa, Canada: 133-140.

- Gottlieb, P., Agron-Olshina, N. & Sutherland, D.N. (1990): The characterisation of mineral matter in coal and fly ash. 4th Australian Coal Science Conference, December 3-5, 1990, Brisbane, QLD, Australia: 339-346.
- Gottlieb, P., Wilkie, G., Sutherland, D., Ho-Tun, E., Suthers, S., Perera, K., Jenkins, B., Spencer, S., Butcher, A. & Rayner, J. (2000): Using quantitative electron microscopy for process mineralogy applications. – *JOM*, 52 (4): 24-25. doi:10.1007/s11837-000-0126-9
- Govindaraju, K., Rubeska, I. & Paukert, T. (1994): 1994 Report on Zinnwaldite ZW-C analysed by ninety-two GIT-IWG member-laboratories. – *Geostand. Newsl.*, 18 (1): 1-42. doi:10.1111/j.1751-908X.1994.tb00502.x
- Gräfe, M., Landers, M., Tappero, R., Austin, P., Gan, B., Grabsch, A. & Klauber, C. (2011): Combined application of QEM-SEM and hard X-ray microscopy to determine mineralogical associations and chemical speciation of trace metals. – *J. Environ. Qual.*, 40 (3): 767-783. doi:10.2134/jeq2010.0214
- Grammatikopoulos, T., Mercer, W., Gunning, C. & Prout, S. (2011): Quantitative characterization of the REE minerals by QEMSCAN from the Nechalacho Heavy Rare Earth Deposit, Thor Lake Project, NWT, Canada. *SGS Minerals Services*: 11 p.
- Grant, G., Hall, J.S., Reid, A.F. & Zuiderwyk, M. (1976): Multicompositional particle characterization using the SEM-microprobe. 9th Annual Scanning Electron Microscopy Symposium, April 5-9, 1976, IITRI, Chicago, Illinois, USA: 401-408.
- Grant, G., Hall, J.S., Reid, A.F. & Zuiderwyk, M.A. (1977): Characterization of particulate and composite mineral grains by on-line computer processing of SEM images. *APCOM 77*, 15th International Symposium on the Application of Computers and Operations Research in the Mineral Industries, 4-8 July 1977, Brisbane, QLD, Australia: 159-170.
- Grant, G., Miller, P., Reid, A.F. & Zuiderwyk, M.A. (1981): Feature extraction and population distribution from complex ore particles by QEM/SEM image analysis. *Contemporary Stereology*. 3rd European Symposium for Stereology, June 22-27, 1981, Ljubljana, Yugoslavia: 233-238.
- Grant, G. & Reid, A.F. (1980): A fast and precise boundary tracing algorithm. – *Mikrosk.*, 37: 455-457.
- Grant, G. & Reid, A.F. (1981): An efficient algorithm for boundary tracing and feature extraction. – *Comput. Graph. Image Process.*, 17 (3): 225-237. doi:10.1016/0146-664X(81)90003-4
- Grant, G., Reid, A.F. & Zuiderwyk, M.A. (1979): Simplified size and shape description of ore particles as measured by automated SEM. *International Conference on Powder and Bulk Solids Handling and Processing*, 15-17 May 1979, Philadelphia, Pennsylvania, USA: 168-175.
- Gregory, M.J., Lang, J.R., Gilbert, S. & Hoal, K.O. (2013): Geometallurgy of the Pebble porphyry copper-gold-molybdenum deposit, Alaska: Implications for gold distribution and paragenesis. – *Econ. Geol.*, 108 (3): 463-482. doi:10.2113/econgeo.108.3.463
- Großer, P. (1966): Differentiation in Lamprophyren der Lausitz. – *N. Jahrb. Mineral. Abhand.*, 105 (2): 133-160.
- Gu, Y. (1998): Rapid mineral liberation analysis using the JKMRC/Philips MLA. *Mineralogy for Mineral Processing Engineers Workshop, Minerals Processing '98*, 6-7 August, Cape Town, South Africa: 14 p.
- Gu, Y. (2003): Automated scanning electron microscope based mineral liberation analysis. – *J. Miner. Mater. Charact. Eng.*, 2 (1): 33-41. doi:10.4236/jmmce.2003.21003
- Gu, Y., Schouwstra, R. & Wang, D. (2012): A comparison between 2D and 3D particle size measurements. *Process Mineralogy '12*, 7-9 November 2012, Cape Town, South Africa: 4 p.
- Gu, Y., Schouwstra, R.P. & Rule, C. (2014): The value of automated mineralogy. – *Miner. Eng.*, 58: 100-103. doi:10.1016/j.mineng.2014.01.020
- Gu, Y. & Sugden, T. (1995): A highly integrated SEM-EDS-IP system for automated quantitative mineral analysis. *Third Biennial Symposium on SEM Imaging and Analysis: Applications and Techniques*, February 15-17, 1995, Melbourne, VIC, Australia: 53-54.
- Gupta, R.P., Wall, T.F., Kajigaya, I., Miyamae, S. & Tsumita, Y. (1998): Computer-controlled scanning electron microscopy of minerals in coal-implications for ash deposition. – *Prog. Energy Combust. Sci.*, 24 (6): 523-543. doi:10.1016/S0360-1285(98)00009-4

- Gy, P.M. (1979): Sampling of Particulate Materials: Theory and Practice. Developments in Geomathematics, 4. 431 p., Amsterdam, Netherlands (Elsevier Scientific).
- Haberlah, D., Dosseto, A., Butcher, A.R. & Hrstka, T. (2010): South Australian loess-palaeosol sequences spanning the last glacial cycle. 19th World Congress of Soil Science, 1-6 August 2010, Brisbane, QLD, Australia.
- Haberlah, D., Strong, C., Pirrie, D., Rollinson, G.K., Gottlieb, P., Botha, P.W.S.K. & Butcher, A.R. (2011): Automated petrography applications in Quaternary science. – *Quat. Australas.*, 28 (2): 3.
- Hall, J.S. (1977): Composite Mineral Particles: Analysis by Automated Scanning Electron Microscopy. Doctoral Thesis, University of Queensland, Brisbane, QLD, Australia.
- Harb, J.N., Slater, P.N. & Marchek, J.E. (1993): Mineral Associations in Pulverized Coal. – Preprint. Paper. Am. Chem. Soc. Div. Fuel Chem., 38 (4): 1189-1194.
- Harrowfield, I.R., MacRae, C.M. & Simmonds, P.F. (1988): The automated scanning electron microscope as a tool for gold microprospecting. 23rd Annual Conference of the Microbeam Analysis Society, 8-12 August 1988, Milwaukee, Wisconsin, USA: 481-482.
- Hattori, K.H., Arai, S. & Clarke Barrie, D.B. (2002): Selenium, tellurium, arsenic and antimony contents of primary mantle sulfides. – *Can. Mineral.*, 40 (2): 637-650.  
doi:10.2113/gscanmin.40.2.637
- Heinrich, C. (1993): Hydrothermalmetamorphose und Geochemie der Lausitzer Gabbro-Diorit-Serie. PhD Thesis, Universität (TH) Fridericiana, Karlsruhe, Germany.
- Heinrich, K.F.J. (1966): Electron probe microanalysis by specimen current measurement. IV Congrès International sur l'Optique des Rayons X et la Microanalyse, September 7-10, 1965, Orsay, France: 159-167.
- Henley, K.J. (1983): Ore-dressing mineralogy - a review of techniques, applications and recent developments. ICAM 81: Proceedings of the First International Congress on Applied Mineralogy, June 1981, Johannesburg, South Africa: 175-200.
- Henley, K.J. (1989): Ore-dressing mineralogy update - a review of developments since ICAM 81. Mineralogy-Petrology Symposium '89 (MINPET), February 1989, Sydney, NSW, Australia: 61-75.
- Herrmann, O. (1893): Erläuterungen zur geologischen Specialkarte des Königreichs Sachsen, Section Schirgiswalde-Schluckenau, Blatt 70. 37 p., Leipzig, Germany (Engelmann).
- Hiemstra, S.A. (1985): The Role of Applied Mineralogy in Ore Beneficiation as Illustrated by Case Histories. 2nd International Congress on Applied Mineralogy in the Minerals Industry, February 22-25, 1984, Los Angeles, California, USA: 9-20.
- Hill, G.S., Rowlands, N. & Finch, J.A. (1987): Data correction for two-dimensional liberation studies. Process Mineralogy VII: Applications to Mineral Beneficiation Technology and Mineral Exploration, with Special Emphasis on Disseminated Carbonaceous Gold Ores, February 23-27, 1987, Denver, Colorado, USA: 617-632.
- Hirsch, D. (2012): How to make a thin section.  
<http://geology.wvu.edu/dept/faculty/hirschd/other/thinsections/>. Accessed 15 January 2015.
- Hoal, K., Stammer, J., Appleby, S., Gregory, M., Woodhead, J. & Ross, J. (2009a): Impacts of Quantitative Mineral Characterization on Processing. In: Malhotra, D., Taylor, P., Spiller, E., LeVier, M. (eds): Recent Advances in Mineral Processing Plant Design. Society for Mining, Metallurgy, and Exploration, Littleton, CO, USA, 79-84.
- Hoal, K.O., Appleby, S.K., Stammer, J.G. & Palmer, C. (2009b): SEM-based quantitative mineralogical analysis of peridotite, kimberlite, and concentrate. – *Lithos*, 112 (Supplement 1): 41-46. doi:10.1016/j.lithos.2009.06.009
- Hoal, K.O., Stammer, J.G., Appleby, S.K., Botha, J., Ross, J.K. & Botha, P.W. (2009c): Research in quantitative mineralogy: Examples from diverse applications. – *Miner. Eng.*, 22 (4): 402-408. doi:10.1016/j.mineng.2008.11.003
- Hoare, T. (2007): Fingerprinting soil using mineralogy. – *Aust. Vitic.*, 4 (September/October): 30-33.
- Hrstka, T. (2008): Preliminary Results on the Reproducibility of Sample Preparation and QEMSCAN® Measurements for Heavy Mineral Sands Samples. 9th International

- Congress for Applied Mineralogy, ICAM 2008, 8-10 September, Brisbane, QLD, Australia: 107-111.
- Huminicki, M.A.E., Sylvester, P.J. & Shaffer, M. (2007): Three-dimensional quantitative mineralogical modelling of the Voisey's Bay Ni-Cu-Co Ovoid deposit: confirming the mineralogical model using MLA techniques. *Automated Mineralogy 2007*, September 1-2, Brisbane, QLD, Australia: 12 p.
- Huminicki, M.A.E., Sylvester, P.J., Shaffer, M., Wilton, D.H.C., Evans-Lamswood, D. & Wheeler, R.I. (2012): Systematic and integrative ore characterization of massive sulfide deposits: An Example from voisey's bay Ni-Cu-Co Ovoid Orebody, Labrador, Canada. – *Explor. Min. Geol.*, 20 (1): 53-86.
- Hynes, R.G., French, D.H. & Azzi, M. (2007): Chemical characterisation of fine particles in the Sydney Basin. 14th International Union of Air Pollution Prevention and Environmental Protection Associations (IUAPPA) World Congress 2007, 18th Clean Air Society of Australia and New Zealand (CASANZ) Conference, 9-13 September 2007, Brisbane, QLD, Australia: 1-5.
- ICAM (2000): INTERNATIONAL COUNCIL FOR APPLIED MINERALOGY - CONSTITUTION 2000. <http://www.bgr.de/icam/constitution2000.htm>. Accessed 22 November 2014.
- Intellection Pty Ltd (2008): News Room - sift. <https://web.archive.org/web/20080820201300/http://intellection.com.au/sift.html>. Accessed 22 November 2014.
- IP Australia (2014): ATMOSS - Australian Trade Mark On-line Search System. [http://pericles.ipaustralia.gov.au/atmoss/falcon.application\\_start](http://pericles.ipaustralia.gov.au/atmoss/falcon.application_start). Accessed 22 November 2014.
- Ishikawa, Y., Sawaguchi, T., Iwaya, S. & Horiuchi, M. (1976): Delineation of prospecting targets for Kuroko deposits based on modes of volcanism of underlying dacite and alteration halos. – *Min. Geol.*, 26 (136): 105-117. doi:10.11456/shigenchishitsu1951.26.105
- Jackson, B.R., Gottlieb, P. & Sutherland, D.N. (1988): A method for measuring and comparing the mineral grain sizes of ores of different origins. 3rd Mill Operators' Conference, 9-12 May 1988, Cobar, NSW, Australia: 61-65.
- Jackson, B.R., Reid, A.F. & Wittenberg, J.C. (1984): Rapid production of high quality polished sections for automated image analysis of minerals. – *Proc. Australas. Inst. Min. Metall.*, 289: 93-97.
- Jeanrot, P. (1980): Digital analysis of chemical informations with automatic S.E.M. – *Mikrosk.*, 37: 453-454.
- Jeanrot, P., Landes, D. & Boxo, P. (1978): Automatisation du microscope électronique à balayage en vue de l'analyse quantitative d'images élémentaires. – *J. Microsc. Spectrosc. Électron.*, 3: 157-164.
- JEOL Ltd. (2014): JEOL Products. <http://www.jeol.co.jp/en/products/>. Accessed 22 November 2014.
- JKMRC (1999): MLA bureau opens for business. [https://web.archive.org/web/19990910165138/http://www.jkmrc.uq.edu.au/news/recentnews/990604\\_mla/990604\\_mla.htm](https://web.archive.org/web/19990910165138/http://www.jkmrc.uq.edu.au/news/recentnews/990604_mla/990604_mla.htm). Accessed 22 November 2014.
- JKTech Pty Ltd (2001): UQ facility identifies new revenue stream for the minerals industry. <https://web.archive.org/web/20010408174814/http://www.jktech.com.au/news/mlalaunch01/mlalaunch01.htm>. Accessed 22 November 2014.
- JKTech Pty Ltd (2007): MLA Celebrates 10 Years!! – *MLA Today*, June 2007: 3.
- JKTech Pty Ltd (2008): Newsletters. [https://web.archive.org/web/20081122025933/http://www.jktech.com.au/News\\_Publications/newsletters.htm](https://web.archive.org/web/20081122025933/http://www.jktech.com.au/News_Publications/newsletters.htm). Accessed 22 November 2014.
- Jones, G.C., Becker, M., van Hille, R.P. & Harrison, S.T.L. (2013): The effect of sulfide concentrate mineralogy and texture on Reactive Oxygen Species (ROS) generation. – *Appl. Geochem.*, 29: 199-213. doi:10.1016/j.apgeochem.2012.11.015
- Jones, M.P. (1977): Automatic image analysis. In: Zussman, J. (ed) *Physical Methods of Determinative Mineralogy*. 2nd edn. Academic Press, London, UK, 167-199.



- Jones, M.P. (1987a): Applied Mineralogy: a quantitative approach. 259 p., London, UK (Graham & Trotman).
- Jones, M.P. (1987b): Image Analysis - Theory. In: Jones, M.P. (ed) Applied Mineralogy: a quantitative approach. Graham & Trotman, London, UK, 70-80.
- Jones, M.P. (1987c): Sampling of mineralogical materials. In: Jones, M.P. (ed) Applied Mineralogy: a quantitative approach. Graham & Trotman, London, UK, 13-26.
- Jones, M.P. & Barbery, G. (1976): Stereology and the automatic linear analysis of mineralogical materials. Fourth International Congress For Stereology, September 4-9, 1975, Gaithersburg, Maryland, USA: 189-192.
- Jones, M.P. & Gavrilovic, J. (1968): Automatic searching unit for the quantitative location of rare phases by electron-probe X-ray microanalysis. – Trans. Inst. Min. Metall. B: Appl. Earth Sci., 77 (744): B137-143.
- Jones, M.P. & Gavrilovic, J. (1969): The application of scanning electron beam anomalous transmission patterns in mineralogy. – Mineral. Mag., 37 (286): 270-274.
- Jones, M.P. & Shaw, J.L. (1974): Automatic measurement and stereological assessment of mineral data for use in mineral technology. Tenth International Mineral Processing Congress, 1973, April 2-14, London, UK: 737-756.
- Kahn, H., Mano, E.S. & Tassinari, M.M.M.L. (2002): Image Analysis Coupled With A SEM-EDS Applied To The Characterization Of A Zn-Pb Partially Weathered Ore. – J. Miner. Mater. Charact. Eng., 1 (1): 1-9.
- Kahn, H., Ulsen, C., Franca, R.R., Hawlitschek, G. & Contessotto, R. (2014): Quantificação das fases constituintes de agregados reciclados por análise de imagens automatizada. – HOLOS, 2014 (3): 44-52. doi:10.15628/holos.2014.1787
- Kelly, N., Appleby, S.K. & Mahan, K. (2010): Mineralogical and textural characterization of metamorphic rocks using an automated mineralogy approach. 2010 GSA Annual Meeting, 31 October - 3 November 2010, Denver, CO, USA 48.
- Kelm, U., Avendaño, M., Balladares, E., Helle, S., Karlsson, T. & Pincheira, M. (2014): The use of water-extractable Cu, Mo, Zn, As, Pb concentrations and automated mineral analysis of flue dust particles as tools for impact studies in topsoils exposed to past emissions of a Cu-smelter. – Chem. Erde - Geochem., 74 (3): 365-373. doi:10.1016/j.chemer.2013.12.001
- Kerrick, D.M., Eminhizer, L.B. & Villaume, J.F. (1973): The Role of Carbon Film Thickness in Electron Microprobe Analysis. – Am. Mineral., 58 (9-10): 920-925.
- Keulen, N., Frei, D., Bernstein, S., Hutchison, M.T., Knudsen, C. & Jensen, L. (2008): Fully automated analysis of grain chemistry, size and morphology by CCSEM: Examples from cement production and diamond exploration. – Geol. Surv. Den. Greenl. Bull., 15: 93-96.
- Keulen, N., Frei, D., Riisager, P. & Knudsen, C. (2012): Analysis of heavy minerals in sediments by Computer-Controlled Scanning Electron Microscopy (CCSEM): principles and applications. In: Sylvester, P. (ed) Short-Course Volume 42. Mineralogical Association of Canada (MAC), St. John's, NL, Canada, 167-184.
- Kindermann, A. (1999): Basitgänge und Ni-Cu-Sulfidmineralisationen der Lausitzer Antiklinalzone: petrologische und geochemische Untersuchungen. Diploma Thesis (Diplomarbeit), TU Bergakademie, Freiberg, Germany.
- Kindermann, A., Fiedler, F., Seifert, T. & Uhlig, S. (2003): Platinmetall-Führung der Ni-Cu-Sulfidmineralisationen im Bereich der Lausitzer Antiklinalzone. – Z. Angew. Geol., 49 (2): 43-47.
- King, R.P. (1978): Determination of particle size distribution from measurements on sections. – Powder Tech., 21 (1): 147-150. doi:10.1016/0032-5910(78)80117-X
- King, R.P. (1979): A model for the quantitative estimation of mineral liberation by grinding. – Int. J. Miner. Process., 6 (3): 207-220. doi:10.1016/0301-7516(79)90037-1
- King, R.P. (1982): Determination of the distribution of size of irregularly shaped particles from measurements on sections or projected areas. – Powder Tech., 32 (1): 87-100. doi:10.1016/0032-5910(82)85009-2
- King, R.P. (1984): Measurement of particle size distribution by image analyser. – Powder Tech., 39 (2): 279-289. doi:10.1016/0032-5910(84)85045-7
- King, R.P. (1994): Comminution and liberation of minerals. – Miner. Eng., 7 (2-3): 129-140. doi:10.1016/0892-6875(94)90059-0

- King, R.P. & Schneider, C.L. (1993): An Effective SEM-Based Image Analysis System for Quantitative Mineralogy. – *KONA Powder Part. J.*, 11: 165-177.  
doi:10.14356/kona.1993019
- King, R.P. & Schneider, C.L. (1998a): Mineral liberation and the batch comminution equation. – *Miner. Eng.*, 11 (12): 1143-1160. doi:10.1016/S0892-6875(98)00102-2
- King, R.P. & Schneider, C.L. (1998b): Stereological correction of linear grade distributions for mineral liberation. – *Powder Tech.*, 98 (1): 21-37. doi:10.1016/S0032-5910(98)00013-8
- Klemm, G. (1890): Erläuterungen zur geologischen Specialkarte des Königreichs Sachsen, Section Neustadt-Hohwald, Blatt 69. 36 p., Leipzig, Germany (Engelmann).
- Klopper, L., Strydom, C.A. & Bunt, J.R. (2012): Influence of added potassium and sodium carbonates on CO<sub>2</sub> reactivity of the char from a demineralized inertinite rich bituminous coal. – *J. Anal. Appl. Pyrol.*, 96: 188-195. doi:10.1016/j.jaap.2012.04.005
- Knappett, C., Pirrie, D., Power, M.R., Nikolakopoulou, I., Hilditch, J. & Rollinson, G.K. (2011): Mineralogical analysis and provenancing of ancient ceramics using automated SEM-EDS analysis (QEMSCAN®): A pilot study on LB I pottery from Akrotiri, Thera. – *J. Archaeol. Sci.*, 38 (2): 219-232. doi:10.1016/j.jas.2010.08.022
- Knésl, I. & Ackerman, L. (2005): PGE mineralisation of the Bohemian Massif, Czech Republic: An overview. 10th International Platinum Symposium 'Platinum-Group Elements - from Genesis to Beneficiation and Environmental Impact', August 8-11, 2005, Oulu, Finland: 408-411.
- Knudsen, C., Frei, D., Rasmussen, T., Rasmussen, E.S. & McLimans, R. (2005): New methods in provenance studies based on heavy minerals: An example from Miocene sands in Jylland, Denmark. – *Geol. Surv. Den. Greenl. Bull.*, 7: 29-32.
- Koninklijke Philips N.V. (2013): X-Ray Diffraction (XRD) - Technical Note.  
<http://www.innovationservices.philips.com/sites/default/files/materials-analysis-xrd.pdf>. Accessed 03 September 2014.
- Koolschijn, M.A.P. (2012): The use of cuttings in shale gas play assessment; The Sbaa basin (Algeria) as case study. Master thesis, Universiteit Utrecht, Utrecht, The Netherlands.
- Kormos, L.J., Oliveira, J., Whittaker, P.J. & Lipten, E. (2008): Characterisation of the Antamina bornite zone for process mineralogy modelling. *Automated Mineralogy 2008*, August 27-28, Brisbane, QLD, Australia: 11 p.
- Králová, V. & Motl, D. (2014): Automated mineral analysis focused on large sample sets. 2014 SME Annual Meeting and Exhibit: Leadership in Uncertain Times, SME 2014, 23-26 February, Salt Lake City, UT, USA: 593-594.
- Králová, V., Motl, D. & Klíma, J. (2012a): New Automated Mineralogy Solution for Process Mineralogical Analyses. *Process Mineralogy '12*, 7-9 November 2012, Cape Town, South Africa: 10 p.
- Králová, V., Motl, D. & Kynický, J. (2012b): TIMA – TESCAN Integrated Mineral Analyzer: New approach for rapid evaluation of critical elements ore samples. *Deposits of critical metals and related carbonatite-alkaline rock systems*, September 4-7, 2012, Peking, China: 8.
- Kramer, W. (1976): Zur Petrologie und metallogenetischen Bedeutung der Dolerite (Lamprophyre) des Lausitzer Massivs. – *Z. Geol. Wiss.*, 4 (7): 975-994.
- Kramer, W. (1988): Magmengenetische Aspekte der Lithosphärenentwicklung : geochemisch-petrologische Untersuchung basaltoider variszischer Gesteinsformationen sowie mafischer und ultramafischer Xenolithe im nordöstlichen Zentraleuropa. *Schriftenreihe für geologische Wissenschaften*, Heft 26. 136 p., Berlin (Akademie-Verlag).
- Kramer, W. (1998): Mafische Kleinintrusionen im Grundgebirge Sachsens - Größere Konsequenzen für Petrologie, Metallogenie & Tektonik. – *Z. Geol. Wiss.*, 26 (1-2): 171-182.
- Kramer, W. & Andrehs, G. (1990): Geochemie und Mineralogie der Gabbroide der Oberlausitz. – *Ber. Dtsch. Mineral. Ges.*, 1990 (1): 140.
- Kramer, W. & Andrehs, G. (2011): Basische Gangintrusionen im Oberlausitzer Bergland, Ostsachsen. – *Ber. Naturforsch. Ges. Oberlausitz*, 19: 21-46.
- Kramer, W., Müller, B. & Peschel, A. (1977): Zur tektonischen und substantiellen Charakteristik der Basite des Lausitzer Antiklinoriums und deren Altersbeziehungen. – *Z. Geol. Wiss.*, 5 (1): 95-100.

- Kramer, W. & Peschel, A. (1987): Erkenntnisentwicklung zum Problem basischer phanerozoischer Intrusiva der Lausitz. – Abh. Ber. Naturkundemus. Görlitz, 60 (2): 19-28.
- Kramer, W. & Seifert, W. (2000): Mafische Xenolithe und Magmatite im östlichen Saxothuringikum und westlichen Lugikum: Ein Beitrag zum Krustenbau und zur regionalen Geologie. – Z. Geol. Wiss., 28 (1-2): 133-156.
- Krentz, O., Walter, H., Brause, H., Hoth, K., Berger, H.-J., Kemnitz, H., Lobst, R., Kozdrój, W., Cymerman, Z., Opletal, M., Štěpánka, M., Valečka, J., Prouza, V., Kachlík, V. & Cajz, V. (2000): Geologische Karte Lausitz - Jizera - Karkonosze. 1 : 100 000. Sächsisches Landesamt für Umwelt und Geologie, Freiberg, Germany; Pánstwowy Instytut Geologiczny, Warszawa, Poland; Český geologický ústav, Praha, Czech Republic
- Krestin, E.M. (1987): Classification of copper-nickel deposits and examples in Central Europe. – Freib. Forschungsh., C 425: 78-92.
- Kwieceńska, B., Suárez-Ruiz, I., Paluszkiwicz, C. & Rodrigues, S. (2010): Raman spectroscopy of selected carbonaceous samples. – Int. J. Coal Geol., 84 (3–4): 206-212. doi:10.1016/j.coal.2010.08.010
- Kwitko-Ribeiro, R. (2012): New Sample Preparation Developments to Minimize Mineral Segregation in Process Mineralogy. 10th International Congress for Applied Mineralogy (ICAM), 1-5 August 2011, Trondheim, Norway: 411-417.
- Lang, C., Hiscock, M., Liipo, J. & Otterstroem, H. (2013): Automated Mineral Liberation Analysis on a Multipurpose SEM. – Acta Mineral. Sin., 2013 (S1): 15.
- Langmi, H.W. & Watt, J. (2003): Evaluation of computer-controlled SEM in the study of metal-contaminated soils. – Mineral. Mag., 67 (2): 219-231. doi:10.1180/0026461036720096
- Large, R.R., Gemmill, J.B., Paulick, H. & Huston, D.L. (2001): The Alteration Box Plot: A Simple Approach to Understanding the Relationship between Alteration Mineralogy and Lithogeochemistry Associated with Volcanic-Hosted Massive Sulfide Deposits. – Econ. Geol., 96 (5): 957-971. doi:10.2113/gsecongeo.96.5.957
- Laslett, G.M., Sutherland, D.N., Gottlieb, P. & Allen, N.R. (1990): Graphical assessment of a random breakage model for mineral liberation. – Powder Tech., 60 (2): 83-97. doi:10.1016/0032-5910(90)80135-L
- Lastra, R. (2007): Seven practical application cases of liberation analysis. – Int. J. Miner. Process., 84 (1-4): 337-347. doi:10.1016/j.minpro.2006.07.017
- Lastra, R. & Petruk, W. (2014): Mineralogical Characterization of Sieved and Un-Sieved Samples. – J. Miner. Mater. Charact. Eng., 2 (1): 40-48. doi:10.4236/jmmce.2014.21007
- Lastra, R., Petruk, W. & Wilson, J. (1998): Image-analysis techniques and applications to mineral processing. In: Cabri, L.J., Vaughan, D.J. (eds): Modern approaches to ore and environmental mineralogy, Short Course Series, 27. Mineralogical Association of Canada, Ottawa, Ontario, Canada, 327-366.
- Lätti, D. & Adair, B.J.I. (2001): An assessment of stereological adjustment procedures. – Miner. Eng., 14 (12): 1579-1587. doi:10.1016/S0892-6875(01)00176-5
- Lätti, D., Doyle, J. & Adair, B.J.I. (2001): A QEM\*SEM study of a suite of pressure leach products from a gold circuit. – Miner. Eng., 14 (12): 1671-1678. doi:10.1016/S0892-6875(01)00185-6
- Laukkanen, J. & Lehtinen, M. (2005): Mineralogisiin tutkimuksiin Australiassa kehitettyjen SEM-EDS-ohjelmistokokonaisuuksien soveltuvuus GTK: n tutkimustarpeisiin. Geological Survey of Finland (GTK), Outokumpu, Finland: 92 p.
- Le Bas, M.J. & Streckeisen, A.L. (1991): The IUGS systematics of igneous rocks. – J. Geol. Soc., 148 (5): 825-833. doi:10.1144/gsjgs.148.5.0825
- Le Maitre, R.W., Bateman, P., Dudek, A., Keller, J., Lameyre, J., Le Bas, M.J., Sabine, P.A., Schmid, R., Sorensen, H., Streckeisen, A., Woolley, A.R. & Zanettin, B. (1989): A classification of igneous rocks and glossary of terms : recommendations of the International Union of Geological Sciences Subcommittee on the Systematics of Igneous Rocks. 193 p., Oxford, UK (Blackwell).
- Le Maitre, R.W., Streckeisen, A., Zanettin, B., Le Bas, M.J., Bonin, B., Bateman, P., Bellieni, G., Dudek, A., Efremova, S., Keller, J., Lameyre, J., Sabine, P.A., Schmid, R., Sorensen, H. & Woolley, A.R. (2004): Igneous Rocks: A Classification and Glossary of Terms, Recommendations of the International Union of Geological Sciences Subcommittee on

- the Systematics of Igneous Rocks. 2nd edn. 236 p., Cambridge, UK (Cambridge University Press).
- Lebiedzki, J., Burke, K.G., Troutman, S., Johnson, G.G. & White, E.W. (1973): New methods for quantitative characterization of multiphase particulate materials including thickness measurements. 6th Annual Scanning Electron Microscope Symposium, April 23-27, 1973, IITRI, Chicago, Illinois, USA: 121-128.
- Lee, R.J. & Fisher, R.M. (1980): Quantitative characterization of particulates by scanning and high voltage electron microscopy. Special Section on Particle Analysis, 13th Annual Conference of the Microbeam Analysis Society, June 22, 1978, Ann Arbor, MI, USA: 63-82.
- Leeder, O. & Krestin, E.M. (1985): Mafischer Magmatismus und Cu-Ni-Vererzungen im S-Teil des Lausitzer Blocks. Ministerium für Hoch- und Fachschulwesen der DDR - unpublished report.
- Leigh, G.M., Lyman, G.J. & Gay, S.L. (1997): Computer-based examination of self-contained, flexible stereological correction procedures. – *Powder Tech.*, 92 (2): 101-110. doi:10.1016/S0032-5910(97)03220-8
- Leigh, G.M., Lyman, G.J. & Gottlieb, P. (1996): Stereological estimates of liberation from mineral section measurements: A rederivation of Barbary's formulae with extensions. – *Powder Tech.*, 87 (2): 141-152. doi:10.1016/0032-5910(95)03080-8
- Leigh, G.M., Sutherland, D.N. & Gottlieb, P. (1993): Confidence limits for liberation measurements. – *Miner. Eng.*, 6 (2): 155-161. doi:10.1016/0892-6875(93)90129-B
- Leißner, T., Mütze, T., Bachmann, K., Rode, S., Gutzmer, J. & Peuker, U.A. (2013): Evaluation of mineral processing by assessment of liberation and upgrading. – *Miner. Eng.*, 53: 171-173. doi:10.1016/j.mineng.2013.07.018
- Lemmens, H.J., Butcher, A.R. & Botha, P.W.S.K. (2010): FIB/SEM and automated mineralogy for core and cuttings analysis. SPE Russian Oil and Gas Technical Conference and Exhibition 2010, 26-28 October, Moscow, Russia: 881-884.
- Lemmens, H.J., Butcher, A.R. & Botha, P.W.S.K. (2011): FIB/SEM and SEM/EDX: A new dawn for the sem in the Core Lab? – *Petrophysics*, 52 (6): 452-456.
- Leonhardt, D. (1995): Geologische Übersichtskarte des Freistaates Sachsen 1 : 400 000. Karte ohne känozoische Sedimente. 3rd edn. Sächsisches Landesamt für Umwelt und Geologie, Freiberg, Germany
- Li, C., Ripley, E.M., Merino, E. & Maier, W.D. (2004): Replacement of base metal sulfides by actinolite, epidote, calcite, and magnetite in the UG2 and Merensky reef of the Bushveld Complex, South Africa. – *Econ. Geol.*, 99 (1): 173-184. doi:10.2113/gsecongeo.99.1.0173
- Liipo, J., Lang, C., Burgess, S., Otterström, H., Person, H. & Lamberg, P. (2012): Automated mineral liberation analysis using INCA Mineral. Process Mineralogy '12, 7-9 November 2012, Cape Town, South Africa: 7 p.
- Lin, D., Lastra, R. & Finch, J.A. (1999): Comparison of stereological correction procedures for liberation measurements by use of a standard material. – *Trans. Inst. Min. Metall. C: Miner. Process. Extr. Metall.*, 108 (SEPT/DEC): C127-C136.
- Liu, Y., Gupta, R., Sharma, A., Wall, T., Butcher, A., Miller, G., Gottlieb, P. & French, D. (2005): Mineral matter–organic matter association characterisation by QEMSCAN and applications in coal utilisation. – *Fuel*, 84 (10): 1259-1267. doi:10.1016/j.fuel.2004.07.015
- Löffler, H.K. (1962): Petrologische Studien an einem Gangkreuz Lausitzer Lamprophyre bei Niederfriedersdorf. – *Ber. Geol. Ges. DDR*, 6: 72-84.
- Löffler, H.K. (1980): Die eruptiven und metamorphen Gesteine des Lausitzer Blocks; Teil 1. Petrologie der basischen Magmatite des intrusiven Stocks vom Valtengrund am Hohwald/Oberlausitz. – *Z. Geol. Wiss.*, 8 (11): 1421-1448.
- Lotter, N.O., Kowal, D.L., Tuzun, M.A., Whittaker, P.J. & Kormos, L. (2003): Sampling and flotation testing of Sudbury Basin drill core for process mineralogy modelling. – *Miner. Eng.*, 16 (9): 857-864. doi:10.1016/S0892-6875(03)00207-3
- Lotter, N.O., Whittaker, P.J., Kormos, L., Stickling, J.S. & Wilkie, G.J. (2002): The development of process mineralogy at Falconbridge Limited and application to the Raglan Mill. – *CIM Bull.*, 95 (1066): 85-92.

- Lund, C., Lamberg, P. & Lindberg, T. (2013): Practical way to quantify minerals from chemical assays at Malmberget iron ore operations - An important tool for the geometallurgical program. – *Miner. Eng.*, 49: 7-16. doi:10.1016/j.mineng.2013.04.005
- Ly, C.V., Nelson, D.R., Biondo, A. & Mason, K. (2007): Application of QEMSCAN for the interpretation of textures and minerals in extra terrestrial materials. *Automated Mineralogy 2007*, 1-2 September, Brisbane, QLD, Australia.
- Ly, C.V., Oliver, G.M., Spence, G., Centurion, S., Jackson, C.E., Hearn, F.P. & Palomarez, V. (2014): Cross Correlation of Logging Data With SEM-Based Mineralogical and Textural Well Data: A New Tool for Optimized Completion Design. *SPE Russian Oil and Gas Exploration & Production Technical Conference and Exhibition*, 14-16 October 2014, Moscow, Russia: 8 p.
- Lynch, A. (2011): The Legend of P9 – The First 20 Years. Julius Kruttschnitt Mineral Research Centre. <https://www.jkmrc.uq.edu.au/Portals/0/The%20Legend%20of%20P9.pdf>. Accessed 14.06.2014.
- Lynch, K., Spear, J.R. & Munakata Marr, J. (2013): Microbial Diversity in Hypersaline Sediments of the Great Salt Lake Desert. *2013 GSA Annual Meeting in Denver: 125th Anniversary of GSA*, 27-30 October 2013, Denver, CO, USA: 138.
- MacDonald, M., Adair, B., Bradshaw, D., Dunn, M. & Latti, D. (2012): Learnings from five years of on-site MLA at Kennecott Utah Copper Corporation. *10th International Congress for Applied Mineralogy, ICAM 2011*, 1-5 August, Trondheim, Norway: 419-426.
- Mackenzie, R.A.D. & Smith, G.D.W. (1990): Focused ion beam technology. A bibliography. – *Nanotechnol.*, 1 (2): 163-201. doi:10.1088/0957-4484/1/2/007
- Maier, W.D. (2005): Platinum-group element (PGE) deposits and occurrences: Mineralization styles, genetic concepts, and exploration criteria. – *J. Afr. Earth Sci.*, 41 (3): 165-191. doi:10.1016/j.jafrearsci.2005.03.004
- Mainwaring, P.R. & Petruk, W. (1987): Automatic Electron Microprobe Image Analysis: Applications to Mineral Processing. *International Symposium Workshop on Particulate and Multiphase Processes*, 16th Annual Meeting of the Fine Particle Society, April 22-26, 1985, Miami Beach, Florida, USA: 433-442.
- Marketwire L.P. (2014): ZEISS Launches Digital Petrophysics Solution for Oil and Gas Industry. <http://www.marketwired.com/press-release/zeiss-launches-digital-petrophysics-solution-for-oil-and-gas-industry-1945082.htm>. Accessed 22 November 2014.
- Marquez, X., Gagigi, T., Finlay, S.J., Solling, T. & Bounoua, N. (2014): 3D Imaging of the Pore Network in the Shuaiba Reservoir, Al Shaheen Field. *International Petroleum Technology Conference 2014: Unlocking Energy Through Innovation, Technology and Capability*, IPTC 2014, 19-22 January, Doha, Qatar: 3898-3913.
- Martens, A.E., Morton, R.R.A. & McCarthy, C.J. (1978): The application of advanced image analysis techniques. In: Chermant, J.-L. (ed) *Quantitative Analysis of Microstructures in Materials Science, Biology and Medicine*. Riederer-Verlag, Stuttgart, Germany, 426-432.
- Matjie, R.H., French, D., Ward, C.R., Pistorius, P.C. & Li, Z. (2011): Behaviour of coal mineral matter in sintering and slagging of ash during the gasification process. – *Fuel Process. Tech.*, 92 (8): 1426-1433. doi:10.1016/j.fuproc.2011.03.002
- Matson, W.L., McKinstry, H.A., Johnson Jr, G.G., White, E.W. & McMillan, R.E. (1970): Computer processing of SEM images by contour analyses. – *Pattern Recogn.*, 2 (4): 303-306, IN341,307-312. doi:10.1016/0031-3203(70)90020-8
- McDonough, W.F. & Sun, S.-S. (1995): The composition of the Earth. – *Chem. Geol.*, 120 (3-4): 223-253. doi:10.1016/0009-2541(94)00140-4
- McGladrey, A.J. (2014): The Integration of Physical Rock Properties, Mineralogy and Geochemistry for the Exploration of Large Hypogene Zinc Silicate Deposits: A Case Study Of The Vazante Zinc Deposits, Minas Gerais, Brazil. Master Thesis, Queen's University, Kingston, Ontario, Canada.
- Meloy, T.P., Preti, U. & Ferrara, G. (1987): Liberation - Volume and mass lockedness profiles derived - Theoretical and practical conclusions. – *Int. J. Miner. Process.*, 20 (1-2): 17-34. doi:10.1016/0301-7516(87)90014-7

- Merkus, H.G. (2009): Particle Size Measurements - Fundamentals, Practice, Quality. Particle Technology Series, Volume 17. 548 p., London, UK (Springer). doi:10.1007/978-1-4020-9016-5
- Messent, B.E.J. & Farmer, L.E. (2008): Basker Field, Gippsland Basin: Assessing reservoir connectivity with the aid of complementary technologies. PESA Eastern Australasian Basins Symposium III, 14-17 September, 2008, Sydney, NSW, Australia: 29-44.
- Miller, J.D., Lin, C.L., Hupka, L. & Al-Wakeel, M.I. (2009): Liberation-limited grade/recovery curves from X-ray micro CT analysis of feed material for the evaluation of separation efficiency. – *Int. J. Miner. Process.*, 93 (1): 48-53. doi:10.1016/j.minpro.2009.05.009
- Miller, P.R., Reid, A.F. & Zuiderwyk, M.A. (1982): QEM\*SEM image analysis in the determination of modal assays, mineral associations and mineral liberation. XIV International Mineral Processing Congress, October 17-23, 1982, Toronto, Ontario, Canada: VIII-3.1-VIII-3.20.
- MinAssist Pty Ltd (2009): What is a theoretical grade-recovery curve? An example. <http://www.minassist.com.au/blog/what-is-a-theoretical-grade-recovery-curve-an-example/>. Accessed 12 June 2013.
- Minnis, M.M. (1984): An automatic point-counting method of mineralogical assessment. – *Bull. Am. Assoc. Petrol. Geol.*, 68 (6): 744-752.
- Miranda, P. & Seal, T. (2008): MLA: Current projects at the center for advanced mineral and metallurgical processing. Hydrometallurgy 2008: 6th International Symposium, 17-21 August 2008, Phoenix, AZ, USA: 455-461.
- Mkhatshwa, S.F. (2012): Assessment of the mineralogical variability of the A1, UE1A, and A5-reefs at Cooke Section, Rand Uranium, using MLA-based automated mineralogy. Master Thesis, University of Johannesburg, Johannesburg, South Africa.
- Mngoma, L. (2012): A gold, uranium and thorium deportment analysis of Witwatersrand ore from Cooke section, Rand Uranium Randfontein. Master Thesis, University of Johannesburg, Johannesburg, South Africa.
- Moen, K. (2006): Quantitative Measurements of Mineral Microstructures: Development, implementation and use of methods in applied mineralogy. Doctoral theses, Norwegian University of Science and Technology, Trondheim, Norway.
- Moen, K., Malvik, T., Breivik, T. & Hjelen, J. (2006): Particle texture analysis in process mineralogy. XXIII International Mineral Processing Congress, IMPC 2006, 3-8 September, Istanbul, Turkey: 242-246.
- Moitsheki, L.J., Matjie, R.H., Baran, A., Mooketsi, O.I. & Schobert, H.H. (2010): Chemical and mineralogical characterization of a South African bituminous coal and its ash, and effect on pH of ash transport water. – *Miner. Eng.*, 23 (3): 258-261. doi:10.1016/j.mineng.2009.11.019
- Molhave, K. (2006): Electron Scattering in Solid Samples. OpenSource Handbook of Nanoscience and Nanotechnology. [http://en.wikibooks.org/w/index.php?title=Nanotechnology/Electron\\_microscopy&oldid=2711390](http://en.wikibooks.org/w/index.php?title=Nanotechnology/Electron_microscopy&oldid=2711390).
- Mondillo, N., Balassone, G., Boni, M. & Rollinson, G. (2011): Karst bauxites in the Campania Apennines (southern Italy): A new approach. – *Period. Mineral.*, 80 (3): 407-432. doi:10.2451/2011PM0028
- Morris, A. (1990): Morpho-Chemical Analysis. The Use of Computers in Electron Microscopy, 7 December 1990, London, UK: 1 p.
- Morrison, R. & Dungalison, M. (2011): Metallurgical accounting, control and simulation. In: Wills, B.A., Napier-Munn, T.J. (eds): *Wills' Mineral Processing Technology: An Introduction To The Practical Aspects Of Ore Treatment And Mineral Recovery*. 7th edn. Butterworth-Heinemann, Oxford, UK, 39-89.
- Muccio, E.A. (1991): *Plastic Part Technology*. 304 p., Materials Park, OH (ASM International).
- Muccio, E.A. (1999): *Decoration and Assembly of Plastic Parts*. 253 p., Materials Park, OH (ASM International).
- Mücke, A. (2012): Das Nickelvorkommen von Sohland an der Spree: Die Mineralien des lamprophyrischen Ganggesteins, der Vererzung und deren Genese. – *Aufschluss*, 63 (2-3): 141-172.

- Mwase, J.M., Petersen, J. & Eksteen, J.J. (2012): Assessing a two-stage heap leaching process for Platreef flotation concentrate. – *Hydrometall.*, 129-130: 74-81.  
doi:10.1016/j.hydromet.2012.09.007
- Nabity, J., Campbell, L.A., Zhu, M. & Zhou, W. (2007): E-beam nanolithography integrated with scanning electron microscope. In: Zhou, W., Wang, Z.L. (eds): *Scanning Microscopy for Nanotechnology: Techniques and Applications*. Springer, New York, USA, 120-151.  
doi:10.1007/978-0-387-39620-0\_5
- Naldrett, A.J. (1992): A model for the Ni-Cu-PGE ores of the Noril'sk region and its application to other areas of flood basalt. – *Econ. Geol.*, 87 (8): 1945-1962.  
doi:10.2113/gsecongeo.87.8.1945
- Naldrett, A.J. (2004): *Magmatic Sulfide Deposits: Geology, Geochemistry and Exploration*. 728 p., Heidelberg, Germany (Springer).
- Naldrett, A.J., Fedorenko, V.A., Lightfoot, P.C., Kuniyov, V.I., Gorbachev, N.S., Doherty, W. & Johan, Z. (1995): Ni-Cu-PGE deposits of Noril'sk region, Siberia: their formation in conduits for flood basalt volcanism. – *Trans. Inst. Min. Metall. B: Appl. Earth Sci.*, 104: B18-B36.
- Naldrett, A.J., Lightfoot, P.C., Fedorenko, V., Doherty, W. & Gorbachev, N.S. (1992): Geology and geochemistry of intrusions and flood basalts of the Noril'sk region, USSR, with implications for the origin of the Ni-Cu ores. – *Econ. Geol.*, 87 (4): 975-1004.  
doi:10.2113/gsecongeo.87.4.975
- Naldrett, A.J., Wilson, A., Kinnaird, J. & Chunnett, G. (2009): PGE tenor and metal ratios within and below the Merensky Reef, Bushveld Complex: Implications for its genesis. – *J. Petrol.*, 50 (4): 625-659. doi:10.1093/petrology/egp015
- Naldrett, A.J., Wilson, A., Kinnaird, J., Yudovskaya, M. & Chunnett, G. (2012): The origin of chromitites and related PGE mineralization in the Bushveld Complex: New mineralogical and petrological constraints. – *Miner. Deposita*, 47 (3): 209-232. doi:10.1007/s00126-011-0366-3
- Neumann, B. (1904): Die Nickelerzvorkommen an der sächsisch-böhmischen Grenze. – *Berg- und hüttenmänn. Ztg.*, 63 (13): 177-180.
- Newman, O.M.G., Jackson, B.R. & Wilkie, G.J. (1989): QEM\*SEM analysis of metallurgical residues in ocean sediments. SME Annual Meeting, February 27 - March 2, 1989, Las Vegas, Nevada, USA: 16 p.
- Nicholls, J. & Stout, M.Z. (1986): Electron beam analytical instruments and the determination of modes, spatial variations of minerals and textural features of rocks in polished section. – *Contrib. Mineral. Petrol.*, 94 (3): 395-404. doi:10.1007/BF00371447
- Nie, J., Peng, W., Pfaff, K., Möller, A., Garzanti, E., Andò, S., Stevens, T., Bird, A., Chang, H., Song, Y., Liu, S. & Ji, S. (2013): Controlling factors on heavy mineral assemblages in Chinese loess and red clay. – *Palaeogeogr. Palaeoclimatol. Palaeoecol.*, 381-382: 110-118.  
doi:10.1016/j.palaeo.2013.04.020
- Nitters, G. & Hagelaars, A.M.P. (1990): Careful planning and sophisticated laboratory support : The key to improved acidisation results. European Petroleum Conference - EUROPEC 90, 21-24 October, 1990, The Hague, Netherlands: 289-306.
- Nöldeke, W. (1988): *Einschätzung Rohstoffführung Grundgebirgseinheiten S-Teil DDR, Maßstab 1:100000; Lausitzer Scholle - Elbezone (LEZ)*. Zentrales Geologisches Institut (ZGI) der DDR - unpublished final report.
- Nöldeke, W. & Mettchen, H.-J. (1988): *Höflichkeitseinschätzung der an die Dolerite der Oberlausitz gebundenen Ni-Cu-Mineralisationen*. Zentrales Geologisches Institut (ZGI) der DDR - unpublished report.
- O'Driscoll, B., Butcher, A.R. & Latypov, R. (2014): New insights into precious metal enrichment on the Isle of Rum, Scotland. – *Geol. Today*, 30 (4): 134-141. doi:10.1111/gto.12059
- O'Brien, G., Gu, Y., Adair, B.J.I. & Firth, B. (2011): The use of optical reflected light and SEM imaging systems to provide quantitative coal characterisation. – *Miner. Eng.*, 24 (12): 1299-1304. doi:10.1016/j.mineng.2011.04.024
- Oelsner, O.W. (1954): *Bemerkungen zur Genese der Magnetkies-Pentlandit-Lagerstätte Sohland/Spree*. – *Freib. Forschungsh.*, C 10: 33-45.

- Oghazi, P., Pålsson, B. & Tano, K. (2009): Applying traceability to grinding circuits by using Particle Texture Analysis (PTA). – *Miner. Eng.*, 22 (7-8): 710-718. doi:10.1016/j.mineng.2009.01.017
- Oliver, G. (2012): RoqSCAN Technology Puts Real-time Automated Mineralogy on the Well Site. AAPG/EAGE/SPE Shale Gas Workshop, 15-17 October 2012, Muscat, Oman: 2 p.
- Oliver, G.M., Ly, C.V., Speence, G. & Rael, H. (2013): A new approach to measuring rock properties data from cores & cuttings for reservoir & completions characterization: An example from the Bakken formation. SPE Reservoir Characterisation and Simulation Conference and Exhibition: New Approaches in Characterisation and Modelling of Complex Reservoirs, RCSC 2013, 16-18 September, Abu Dhabi, UAE: 115-118.
- Olson, W.D. (2012): Graphite. – *U.S. Geol. Surv. Miner. Yearb.* 2010: 32.31-32.10.
- Osbahr, I., Klemd, R., Oberthür, T., Brätz, H. & Schouwstra, R. (2013): Platinum-group element distribution in base-metal sulfides of the Merensky Reef from the eastern and western Bushveld Complex, South Africa. – *Miner. Deposita*, 48 (2): 211-232. doi:10.1007/s00126-012-0413-8
- Oxford Instruments plc (2012): Oxford Instruments launches new product for Mineral Liberation Analysis. <http://www.oxford-instruments.com/news/2012/june/oxford-instruments-launches-new-product-for-minera>. Accessed 22 November 2014.
- Oxford Instruments plc (2014): Mineral Liberation Analysis. <http://www.oxford-instruments.com/products/microanalysis/solutions/mineral-liberation>. Accessed 22 November 2014.
- Paine, M.D., Anand, R.R., Aspandiar, M., Fitzpatrick, R.R. & Verrall, M.R. (2005): Quantitative heavy-mineral analysis of a Pliocene beach placer deposit in southeastern Australia using the autogeosem. – *J. Sediment. Res.*, 75 (4): 742-759. doi:10.2110/jsr.2005.060
- Pal, A.R., Bharati, S., Krishna, N.V.S., Das, G.C. & Pal, P.G. (2012): The effect of sintering behaviour and phase transformations on strength and thermal conductivity of disposable tundish linings with varying compositions. – *Ceram. Int.*, 38 (4): 3383-3389. doi:10.1016/j.ceramint.2011.12.049
- PANalytical B.V. (2014): Technology background - Phase quantification <http://www.panalytical.com/Technology-background/Phase-quantification.htm>. Accessed 3 September 2014.
- Pašava, J., Vavřín, I. & Jelínek, E. (2001): Distribution of PGE in rocks and Ni-Cu ores of the Rožany and Kunratic deposits (Lusatian massif, Bohemian Massif). In: Piestrzyński, A. (ed) *Mineral Deposits at the Beginning of the 21st Century: Proceedings of the Joint Sixth Biennial SGA-SEG Meeting, Kraków, Poland, 26-29 August 2001*. A.A. Balkema, Lisse, Netherlands, 627-630.
- Pascoe, R.D., Power, M.R. & Simpson, B. (2007): QEMSCAN analysis as a tool for improved understanding of gravity separator performance. – *Miner. Eng.*, 20 (5): 487-495. doi:10.1016/j.mineng.2006.12.012
- Patil, M.R., Shivakumar, K.S., Prakash, S. & Bhima Rao, R. (1997): Estimation of the liberation size of graphite in a schistose rock and its response to beneficiation. – *Miner. Metall. Process.*, 14 (4): 41-44.
- Patnaik, N., Patil, R., Saktivelu, R. & Bhima Rao, R. (1999): Thermal and Structural Study of Low Grade Graphite Ore From Shivaganga, India — Its Implications in Beneficiation Process. – *J. Therm. Anal. Calorim.*, 57 (2): 541-549. doi:10.1023/A:1010132511670
- Penberthy, C.J. (2001): The effect of mineralogical variation in the UG2 chromitite on recovery of platinum-group elements. PhD Thesis, University of Pretoria, Pretoria, South Africa.
- Penberthy, C.J. & Oosthuizen, E.J. (1992): The use of an integrated SEM-EDS image-analysis system in an applied mineralogy environment. – *Quantimet News Rev.*, 6: 6-7.
- Petruk, W. (1976): The Application of Quantitative Mineralogical Analysis of Ores to Ore Dressing. – *CIM Bull.*, 69 (767): 146-153.
- Petruk, W. (1986): The MP-SEM-IPS image analysis system. CANMET report (Canada Centre for Mineral and Energy Technology), vol 87-1E. Department of Energy, Mines and Resources, Canada, Ottawa, Ontario: 28 p.
- Petruk, W. (1988a): Automatic Image Analysis for Mineral Beneficiation. – *J. Met.*, 40 (4): 29-31. doi:10.1007/BF03259018



- Petruk, W. (1988b): Capabilities of the microprobe Kontron image analysis system: Application to mineral beneficiation. – *Scanning Microsc.*, 2 (3): 1247-1256.
- Petruk, W. (2000): *Applied Mineralogy in the Mining Industry*. 288 p., Amsterdam, New York (Elsevier).
- Petruk, W. & Lastra, R. (2008): Instrument developments and applications of applied mineralogy. 9th International Congress for Applied Mineralogy, ICAM 2008, Brisbane, QLD: 453-458.
- Pfeiffer, L. & Suhr, P. (2008): Tertiärer Vulkanismus. In: Pälchen, W., Walter, H. (eds): *Geologie von Sachsen – Geologischer Bau und Entwicklungsgeschichte*. E. Schweizerbart'sche Verlagsbuchhandlung (Nägele u. Obermiller), Stuttgart, Germany, 486-498.
- Pierson, J.T. (2014): Assessing nutrient loads from in-situ fertilizer amendments in Willard Spur. Master Thesis, The University of Utah, Salt Lake City, UT, USA.
- Piña, R., Gervilla, F., Barnes, S.J., Ortega, L. & Lunar, R. (2012): Distribution of platinum-group and chalcophile elements in the Aguablanca Ni-Cu sulfide deposit (SW Spain): Evidence from a LA-ICP-MS study. – *Chem. Geol.*, 302-303: 61-75.  
doi:10.1016/j.chemgeo.2011.02.010
- Pirrie, D. (2009): Forensic geology in serious crime investigation. – *Geol. Today*, 25 (5): 188-192.  
doi:10.1111/j.1365-2451.2009.00729.x
- Pirrie, D., Butcher, A.R., Power, M.R., Gottlieb, P. & Miller, G.L. (2004): Rapid quantitative mineral and phase analysis using automated scanning electron microscopy (QemSCAN); potential applications in forensic geoscience. – *Geol. Soc. Spec. Publ.*, 232: 123-136.  
doi:10.1144/gsl.sp.2004.232.01.12
- Pirrie, D., Power, M.R., Rollinson, G.K., Wiltshire, P.E.J., Newberry, J. & Campbell, H.E. (2009a): Automated SEM-EDS (QEMSCAN®) Mineral Analysis in Forensic Soil Investigations: Testing Instrumental Reproducibility. In: Ritz, K., Dawson, L., Miller, D. (eds): *Criminal and Environmental Soil Forensics*. Springer, Dordrecht ; London, 411-430.  
doi:10.1007/978-1-4020-9204-6\_26
- Pirrie, D. & Rollinson, G.K. (2011): Unlocking the applications of automated mineral analysis. – *Geol. Today*, 27 (6): 226-235. doi:10.1111/j.1365-2451.2011.00818.x
- Pirrie, D., Rollinson, G.K. & Power, M.R. (2009b): Role of automated mineral analysis in the characterisation of mining-related contaminated land. – *Geosci. South West Engl.*, 12 (2): 162-170.
- Pirrie, D., Rollinson, G.K., Power, M.R. & Webb, J. (2013): Automated forensic soil mineral analysis; testing the potential of lithotyping. – *Geol. Soc. Spec. Publ.*, 384: 47-64.  
doi:10.1144/SP384.17
- Pong, T.C., Haralick, R.M., Craig, J.R., Yoon, R.H. & Choi, W.Z. (1983): The application of image analysis techniques to mineral processing. – *Pattern Recogn. Lett.*, 2 (2): 117-123.
- Potter-McIntyre, S.L. (2013): Biogeochemical signatures in iron (oxyhydr)oxide diagenetic precipitates: chemical, mineralogical and textural markers. PhD Thesis, University of Utah, Salt Lake City, UT, USA.
- Pudmenzky, C., Butcher, A., Love, B. & McTainsh, G.H. (2007): QEMSCAN™ application in Aeolian geomorphology. *Automated Mineralogy 2007*, 1-2 September, Brisbane, QLD, Australia.
- Redwan, M. & Rammlmair, D. (2012): Understanding Micro-Environment Development in Mine Tailings Using MLA and Image Analysis. 10th International Congress for Applied Mineralogy (ICAM), 1-5 August 2011, Trondheim, Norway: 589-596.
- Redwan, M., Rammlmair, D. & Meima, J.A. (2012): Application of mineral liberation analysis in studying micro-sedimentological structures within sulfide mine tailings and their effect on hardpan formation. – *Sci. Total Environ.*, 414: 480-493.  
doi:10.1016/j.scitotenv.2011.10.038
- Reed, S.J.B. (1968): Probe current stability in electron-probe microanalysis. – *J. Phys. E Sci. Instrum.*, 1 (2): 136-139. doi:10.1088/0022-3735/1/2/412
- Reed, S.J.B. (2005): *Electron Microprobe Analysis and Scanning Electron Microscopy in Geology*. 2nd edn. 212 p., New York (Cambridge University Press).  
doi:10.1017/CBO9780511610561

- Reichelt, R. (2007): Scanning Electron Microscopy. In: Hawkes, P.W., Spence, J.C.H. (eds): Science of Microscopy. Springer, New York, USA, 133-272. doi:10.1007/978-0-387-49762-4\_3
- Reid, A.F., Gottlieb, P., MacDonald, K.J. & Miller, P.R. (1985): QEM\*SEM image analysis of ore minerals : volume fraction, liberation, and observational variances. 2nd International Congress on Applied Mineralogy in the Minerals Industry, February 22-25, 1984, Los Angeles, California, USA: 191-204.
- Reid, A.F. & Zuiderwyk, M.A. (1975): An interface system for minicomputer control of instruments and devices suitable for control of the mechanical and electronic devices of instrument and data collection systems, and specifically applied to the control of a microprobe analyser. Commonwealth Scientific and Industrial Research Organization, Division of Mineral Chemistry, Investigation report 115. 12 p., Port Melbourne, VIC, Australia (CSIRO, Division of Mineral Chemistry).
- Reid, A.F. & Zuiderwyk, M.A. (1983): QEM\*SEM: automated image analysis and stereological applications to mineral processing and ore characterization. – *Acta Stereol.*, 2 (1): 205-208.
- Renno, A.D., Hacker, B.R. & Stanek, K.P. (2003): An Early Cretaceous (126 Ma) ultramafic alkaline lamprophyre from the Quarry Klunz (Ebersbach, Lusatia, Germany). – *Z. Geol. Wiss.*, 31 (1): 31-36.
- Richards, J.M., Naude, G., Theron, S.J. & McCullum, M. (2013): Petrological characterization of coal: An evolving science. – *J. S. Afr. Inst. Min. Metall.*, 113 (11): 865-875.
- Rickman, D., Wentworth, S.J., Schrader, C.M., Stoesser, D., Botha, P., Butcher, A., Horsch, H.E., Benedictus, A., Gottlieb, P. & McKay, D. (2008): New insights into the composition and texture of lunar regolith using ultrafast automated electron-beam analysis. 2008 Joint Meeting of The Geological Society of America, Soil Science Society of America, American Society of Agronomy, Crop Science Society of America, Gulf Coast Association of Geological Societies with the Gulf Coast Section of SEPM, 5-9 October 2008, Houston, TX, USA: 552.
- Rieuwerts, J.S., Mighanetara, K., Braungardt, C.B., Rollinson, G.K., Pirrie, D. & Azizi, F. (2014): Geochemistry and mineralogy of arsenic in mine wastes and stream sediments in a historic metal mining area in the UK. – *Sci. Total Environ.*, 472: 226-234. doi:10.1016/j.scitotenv.2013.11.029
- Riley, S.J., Creelman, R.A., Warner, R.F., Greenwood-Smith, R. & Jackson, B.R. (1989): The potential in fluvial geomorphology of a new mineral identification technology (QEM\*SEM). – *Hydrobiol.*, 176-177 (1): 509-524. doi:10.1007/BF00026586
- Robinson, B.W., Hitchen, G.J. & Verrall, M.R. (2000): The AutoGeoSEM: A programmable fully-automatic SEM for rapid grain-counting and heavy-mineral characterisation in exploration. Modern Approaches to Ore and Environmental Mineralogy, MSF Mini-Symposium, 11-17 June 2000, Espoo, Finland: 71-74.
- Rodrigues, S., Kwitko-Ribeiro, R., Collins, S., Esterle, J. & Jaime, P. (2013): Coal characterization by QEMSCAN: the study case of Bowen Basin, Queensland, Australia. 10th Australian Coal Science Conference, November 18-19, 2013, Brisbane, QLD, Australia: 5 p.
- Rohde, G. (1972): Über Pentlanditgemischungen in Pyrrhotinen aus Lausitzer Lamprophyren. – *Ber. Dtsch. Ges. Geol. Wiss. B Mineral. Lagerstättenforsch.*, 16 (2): 265-269.
- Rohde, G. (1976): Zur Petrogenese von Pyrrhotinparagenesen in Lausitzer Lamprophyren. – *Jahrb. Geol.*, 5-6 (1969/1970): 277-306.
- Rohde, G. & Ullrich, H.-J. (1969): Über einige Erzminerale in Pyrrhotinparagenesen verschiedener Lausitzer Lamprophyre. – *Ber. Dtsch. Ges. Geol. Wiss. B Mineral. Lagerstättenforsch.*, 14 (4): 315-326.
- Rollinson, G.K., Andersen, J.C.O., Stickland, R.J., Boni, M. & Fairhurst, R. (2011): Characterisation of non-sulphide zinc deposits using QEMSCAN®. – *Miner. Eng.*, 24 (8): 778-787. doi:10.1016/j.mineng.2011.02.004
- Rösler, H.J. (1991): Lehrbuch der Mineralogie. 5th edn. 844 p., Leipzig, Germany (Dt. Verl. für Grundstoffindustrie).
- Rösler, H.J., Schmädicke, E. & Bothe, M. (1990): Mineralogisch-geochemische Untersuchungen an einer epidotführenden Gangzone im Basit des Steinbruches Grenzland in der Lausitz. – *Abh. Staatl. Mus. Mineral. Geol. Dresden*, 37: 125-131.

- Ross, J., Appleby, S.K., Hoal, K. & Botha, P. (2009): Quantitative mineralogical study of ore domains at Bingham Canyon, Utah, USA. SME Annual Meeting and Exhibit and CMA's 111th National Western Mining Conference 2009, 22-25 February, Denver, CO, USA: 685-689.
- Rossi, M.E. & Deutsch, C.V. (2014): Data Collection and Handling. In: Rossi, M.E., Deutsch, C.V. (eds): Mineral Resource Estimation. Springer Science & Business Media, Dordrecht, Heidelberg, New York, London, 67-96. doi:10.1007/978-1-4020-5717-5\_5
- Ryösa, E., Wikström, J., Lindblom, B., Rutqvist, E., Benedictus, A. & Butcher, A. (2008): Investigation of minerals and iron oxide alterations in olivine pellets excavated from the LKAB Experimental Blast Furnace. 9th International Congress for Applied Mineralogy, ICAM 2008, 8-10 September, Brisbane, QLD, Australia: 545-555.
- Sächsisches Staatsarchiv (1919): Bergarchiv Freiberg, Akte OBA-F I Nr. 506.
- Sala, M. (1999): Geochemische und mineralogische Untersuchungen an alterierten Gesteinen aus dem Kuppelbereich der Lagerstätte Zinnwald (Osterzgebirge). PhD Thesis, Technische Universität Bergakademie, Freiberg, Germany.
- Santoro, L., Boni, M., Rollinson, G.K., Mondillo, N., Balassone, P. & Clegg, A.M. (2014): Mineralogical characterization of the Hakkari nonsulfide Zn(Pb) deposit (Turkey): The benefits of QEMSCAN®. – *Miner. Eng.*, 69: 29-39. doi:10.1016/j.mineng.2014.07.002
- Scheu, C. & Kaplan, W.D. (2012): Introduction to Scanning Electron Microscopy. In: Dehm, G., Howe, J.M., Zweck, J. (eds): In-Situ Electron Microscopy: Applications in Physics, Chemistry and Materials Science. Wiley-VCH, Weinheim, Germany, 1-37. doi:10.1002/9783527652167.ch1
- Schimmoller, B.K., Hucko, R.E., Stanley Jacobsen, P. & Killmeyer, R.P. (1995): A Comparison of Centrifugal Float-Sink Testing with Alternative Methods for Determining Grade-Yield Curves of Fine Coal. – *Coal Prep.*, 16 (3-4): 119-134. doi:10.1080/07349349508905247
- Schmandt, D., Broughton, D., Hitzman, M.W., Plink-Bjorklund, P., Edwards, D. & Humphrey, J. (2013): The Kamo copper deposit, democratic republic of Congo: Stratigraphy, diagenetic and hydrothermal alteration, and mineralization. – *Econ. Geol.*, 108 (6): 1301-1324. doi:10.2113/econgeo.108.6.1301
- Schneider, C.L., Neumann, R. & Alcover-Neto, A. (2004): Automated, Adaptive Thresholding Procedure for Mineral Sample Images Generated by BSE Detector. 8th International Congress on Applied Mineralogy, ICAM 2004, 19-22 September, Sao Paulo, Brazil: 103-106.
- Schouwstra, R.P. & Smit, A.J. (2011): Developments in mineralogical techniques - What about mineralogists? – *Miner. Eng.*, 24 (12): 1224-1228. doi:10.1016/j.mineng.2011.02.002
- Schwoeble, A.J., Dalley, A.M., Henderson, B.C. & Casuccio, G.S. (1988): Computer-controlled SEM and microimaging of fine particles. – *J. Met.*, 40 (8): 11-14. doi:10.1007/BF03258113
- Schwoeble, A.J., Lentz, H.P., Mershon, W.J. & Casuccio, G.S. (1990): Microimaging and off-line microscopy of fine particles and inclusions. – *Mater. Sci. Eng. A*, 124 (1): 49-54. doi:10.1016/0921-5093(90)90334-Y
- Sciortino, M., Muinonen, J., Korczak, J. & St-Jean, A. (2013): Geometallurgical modelling of the Dumont Deposit. The Second AusIMM International Geometallurgy Conference (GeoMet 2013), 30 September - 2 October, Brisbane, QLD, Australia: 93-100.
- Scott, P.W., Ealey, P.J. & Rollinson, G.K. (2011): Bog iron ore from Lowland Point, St Keverne, Lizard, Cornwall. – *Geosci. South West Engl.*, 12 (4): 260-268.
- Šegvić, B., Süssenberger, A., Ugarković, M. & Moscariello, A. (2014): Mineralogy and cultural heritage – introducing QEMSCAN® automated technology to the study of ancient artefacts. 12th Swiss Geoscience Meeting, 21-22 November 2014, Fribourg, Switzerland: 89-90.
- Seibel, O. (1975): Kartierung ausgewählter Profile im Grubenbereich Zinnwald unter besonderer Berücksichtigung paragenetischer und struktureller Aspekte von Granithochlagen. Master Thesis (Diplomarbeit), Bergakademie, Freiberg, Germany.
- Severin, K.P. (2004): Energy dispersive spectrometry of common rock forming minerals. 225 p., Dordrecht, The Netherlands (Kluwer Academic Publishers).

- Shaffer, M. & Huminicki, M.A.E. (2007): Using silicon-drift x-ray detector technology for quantifying coarse-grain pentlandite-chalcopyrite associations in situ. *Automated Mineralogy 2007*, September 1-2, Brisbane, QLD, Australia: 7 p.
- Siame, E. & Pascoe, R.D. (2011): Extraction of lithium from micaceous waste from china clay production. – *Miner. Eng.*, 24 (14): 1595-1602. doi:10.1016/j.mineng.2011.08.013
- Sikazwe, O.N., Hagni, A.M. & Hagni, R.D. (2008): Refractory copper ore from Nchanga, Zambia: A materials characterization study. *SME Annual Meeting and Exhibit 2008: "New Horizons - New Challenges"*, 24-27 February 2008, Salt Lake City, UT, USA: 100-107.
- Simons, B., Pirrie, D., Rollinson, G.K. & Shail, R.K. (2011): Geochemical and mineralogical record of the impact of mining on the Teign Estuary, Devon, UK. – *Geosci. South West Engl.*, 12 (4): 339-350.
- Sliwinski, J., Le Strat, M. & Dublonko, M. (2009): New Quantitative Method for Analysis of Drill Cuttings and Core for Geologic, Diagenetic and Reservoir Evaluation. *CSPG/CSEG/CWLS GeoConvention 2009*, May 4-8, 2009, Calgary, Alberta, Canada: AAPG Search and Discovery Article #90171.
- Smith, A.J.B., Gutzmer, J., Beukes, N.J., Reinke, C. & Bau, M. (2008): Rare earth elements (REE) in banded iron formations - Link between geochemistry and mineralogy. *9th International Congress for Applied Mineralogy, ICAM 2008*, 8-10 September, Brisbane, QLD, Australia: 651-658.
- Smythe, D.M., Lombard, A. & Coetzee, L.L. (2013): Rare Earth Element deportment studies utilising QEMSCAN technology. – *Miner. Eng.*, 52: 52-61. doi:10.1016/j.mineng.2013.03.010
- Sok, R.M., Varslot, T., Ghous, A., Latham, S., Sheppard, A.P. & Knackstedt, M.A. (2010): Pore scale characterization of carbonates at multiple scales: Integration of micro-CT, BSEM, and FIBSEM. – *Petrophysics*, 51 (6): 379-387.
- Sølling, T.I., Mogensen, K. & Gerwig, T. (2014): On diverse applications of QEMSCAN in the oil and gas industry (and beyond). *International Symposium of the Society of Core Analysts*, 8-11 September, 2014, Avignon, France: 1-6.
- Speirs, J.C., McGowan, H.A. & Neil, D.T. (2008): Polar eolian sand transport: Grain characteristics determined by an automated scanning electron microscope (QEMSCAN®). – *Arctic Antarct. Alp. Res.*, 40 (4): 731-743. doi:10.1657/1523-0430(07-029)[SPEIRS]2.0.CO;2
- Spencer, S.J. & Sutherland, D.N. (2000): Stereological correction of mineral liberation grade distributions estimated by single sectioning of particles. – *Image Anal. Stereol.*, 19 (3): 175-182. doi:10.5566/ias.v19.p175-182
- Spicer, E., Verryn, S.M.C. & Deysel, K. (2008): Analysis of heavy mineral sands by quantitative X-ray powder diffraction and mineral liberation analyser - Implications for process control. *9th International Congress for Applied Mineralogy, ICAM 2008*, 8-10 September, Brisbane, QLD, Australia: 165-172.
- Springer, G. (1982): Automated Detection of Unrecovered Minerals in Mill Wastes by Electron Microprobe. *Process Mineralogy II: Applications in Metallurgy, Ceramics, and Geology. Proceedings of a Symposium held at the AIME Annual Meeting, February 14-18, 1982, Dallas, TX, USA: 69-75.*
- Stewart, A.D. & Anand, R.R. (2014): Anomalies in insect nest structures at the Garden Well gold deposit: Investigation of mound-forming termites, subterranean termites and ants. – *J. Geochem. Explor.*, 140: 77-86. doi:10.1016/j.gexplo.2014.02.011
- Stewart, P.S.B. & Jones, M.P. (1980): Determining the amounts and compositions of composite (middling) particles. *XII International Mineral Processing Congress*, 28 August - 3 September, 1977, Sao Paulo, Brazil: 90-116.
- Stjernberg, J., Lindblom, B., Wikström, J., Antti, M.L. & Odén, M. (2010): Microstructural characterization of alkali metal mediated high temperature reactions in mullite based refractories. – *Ceram. Int.*, 36 (2): 733-740. doi:10.1016/j.ceramint.2009.10.018
- Straszheim, W.E. & Markuszewski, R. (1989): Association of mineral matter with the organic coal matrix. – *Preprint. Paper. Am. Chem. Soc. Div. Fuel Chem.*, 34 (3): 648-655.
- Streckeisen, A. (1976): To each plutonic rock its proper name. – *Earth. Sci. Rev.*, 12 (1): 1-33. doi:10.1016/0012-8252(76)90052-0

- Sustainable Minerals Institute (2006): Annual Report. Sustainable Minerals Institute, Brisbane, Queensland, Australia: 70 p.
- Sutherland, D. (2007): Estimation of mineral grain size using automated mineralogy. – *Miner. Eng.*, 20 (5): 452-460. doi:10.1016/j.mineng.2006.12.011
- Sutherland, D.N. (1989): Batch flotation behaviour of composite particles. – *Miner. Eng.*, 2 (3): 351-367. doi:10.1016/0892-6875(89)90004-6
- Sutherland, D.N. & Gottlieb, P. (1991): Application of automated quantitative mineralogy in mineral processing. – *Miner. Eng.*, 4 (7-11): 753-762. doi:10.1016/0892-6875(91)90063-2
- Sutherland, D.N., Gottlieb, P. & Butcher, A.R. (1999): The use of light element X-ray detectors in automated mineral phase analysis. *Chemeca 99: Chemical Engineering: Solutions in a Changing Environment*, 26-29 September 1999, Newcastle, NSW, Australia: 487-492.
- Sutherland, D.N., Gottlieb, P., Jackson, B.R., Wilkie, G.K. & Stewart, P. (1988): Measurement in section of particles of known composition. – *Miner. Eng.*, 1 (4): 317-326. doi:10.1016/0892-6875(88)90021-0
- Sutherland, D.N., Gottlieb, P., Wilkie, G.K. & Johnson, C.R. (1991): Assessment of ore processing characteristics using automated mineralogy. XVII International Mineral Processing Congress, September 23-28, 1991, Dresden, Germany: 353-362.
- Swift, A.M., Anovitz, L.M., Sheets, J.M., Cole, D.R., Welch, S.A. & Rother, G. (2014): Relationship between mineralogy and porosity in seals relevant to geologic CO<sub>2</sub> sequestration. – *Environ. Geosci.*, 21 (2): 39-57. doi:10.1306/eg.03031413012
- Sylvester, P. (2012): Use of the Mineral Liberation Analyzer (MLA) for Mineralogical Studies of Sediments and Sedimentary Rocks. In: Sylvester, P. (ed) *Short-Course Volume 42. Mineralogical Association of Canada (MAC), St. John's, NL, Canada*, 1-16.
- Taşdemir, A. (2008): Evaluation of grain size distribution of unbroken chromites. – *Miner. Eng.*, 21 (10): 711-719. doi:10.1016/j.mineng.2008.01.010
- Taşdemir, A., Özdağ, H. & Önal, G. (2011): Image analysis of narrow size fractions obtained by sieve analysis - an evaluation by log-normal distribution and shape factors. – *Physicochem. Probl. Miner. Process.*, 46: 95-106.
- Tattam, A. (2003): QEMSCAN bosted by new company. – *Process*, October: 3.
- Taut, T., Kleeberg, R. & Bergmann, J. (1998): Seifert Software: The new Seifert Rietveld Program BGMN and its Application to Quantitative Phase Analysis. – *Mater. Struct. Chem. Biol. Phys. Tech.*, 5 (1): 57-64.
- Taylor, I.F. & Gottlieb, P. (1986): Design of a high speed data acquisition interface for VAX computers. *Proceedings of the Digital Equipment Computer Users Society*: 105-109.
- Taylor, J.R. (1997): An introduction to error analysis. The study of uncertainties in physical measurements. 2nd edn. 327 p., Sausalito, California, USA (University Science Books).
- Taylor, S.R. & McLennan, S.M. (1995): The geochemical evolution of the continental crust. – *Rev. Geophys.*, 33 (2): 241-265. doi:10.1029/95RG00262
- TESCAN, a.s. (2012): TESCAN Introduces the TIMA Mineralogy Solution. <http://www.tescan.com/en/news/tescan-introduces-tima-mineralogy-solution>. Accessed 22 November 2014.
- TESCAN, a.s. (2014): Products - TIMA3 LM. <http://www.tescan.com/en/products/tima>. Accessed 22 November 2014.
- Thaulow, N. & White, E.W. (1972): General method for dispersing and disaggregating particulate samples for quantitative SEM optical microscopic studies. – *Powder Tech.*, 5 (6): 377-379. doi:10.1016/0032-5910(72)80043-3
- Tilyard, P.A. (1978): Bougainville Copper, Ltd., flotation circuit: recent improvements and current investigations. – *Trans. Inst. Min. Metall. C: Miner. Process. Extr. Metall.*, 87: C6-C15.
- Tonžetić, I., Duncan, M. & Bramdeo, S. (2014): The autosem ore characterisation of conglomeratic and banded iron formations. – *Miner. Eng.*, 61: 54-65. doi:10.1016/j.mineng.2014.03.007
- Tracor Northern (1981): Quantitative Metallography. – *Anal. Chem.*, 53 (4): 613A-613A. doi:10.1021/ac00227a801
- Troutman, S., Johnson, G.G.M., White, E.W. & Lebedzik, J. (1974): Automated Quantitative SEM Characterization of Complex Particulate Shapes. – *Am. Lab.*, 6: 31-38.

- Tsikouras, B., Pe-Piper, G., Piper, D.J.W. & Schaffer, M. (2011): Varietal heavy mineral analysis of sediment provenance, Lower Cretaceous Scotian Basin, eastern Canada. – *Sediment. Geol.*, 237 (3-4): 150-165. doi:10.1016/j.sedgeo.2011.02.011
- Uhlig, S., Kindermann, A., Seifert, T., Fiedler, F. & Herzig, P. (2001): Platinmetall-Führung der Ni-Cu-Sulfidmineralisationen im Bereich der Lausitzer Antiklinalzone. *Berichte zur Lagerstätten- und Rohstoffforschung*, vol 45. Bundesanstalt für Geowissenschaften und Rohstoffe, Hannover, Germany: 68 p.
- Ulsen, C., Kahn, H., de França, R.R., Uliana, D. & Campbell, F.S. (2012): Microstructural Characterization of Fine Recycled Aggregates by SEM-MLA. 10th International Congress for Applied Mineralogy (ICAM), 1-5 August 2011, Trondheim, Norway: 725-732.
- van Alphen, C. (2005): Factors influencing fly ash formation and slag deposit formation (slagging) on combusting a south african pulverised fuel in a 200 MWe boiler. PhD Thesis, University of the Witwatersrand, Johannesburg, South Africa.
- van Alphen, C. (2007): Automated mineralogical analysis of coal and ash products - Challenges and requirements. – *Miner. Eng.*, 20 (5): 496-505. doi:10.1016/j.mineng.2006.12.013
- Van der Merwe, F. (2011): MLA-based mineralogical investigation of PGE mineralisation at Lonmin's Akanani platinum group metal project, northern limb of the Bushveld Complex. Master Thesis, University of Johannesburg, Johannesburg, South Africa.
- Vavřín, I. & Fryda, J. (1998): Pt-Pd-As-Te mineralizace na ložiskách měďnato-niklových rud z Kunratic a Rožan na Šluknovsku. – *Věst. Čes. geol. úst.*, 73 (2): 177-180.
- Viljoen, R.M., Smit, J.T., Du Plessis, I. & Ser, V. (2001): The development and application of in-bed compression breakage principles. – *Miner. Eng.*, 14 (5): 465-471. doi:10.1016/S0892-6875(01)00034-6
- Vlachos, N. & Chang, I.T.H. (2011): Graphical and statistical comparison of various size distribution measurement systems using metal powders of a range of sizes and shapes. – *Powder Metall.*, 54 (4): 497-506. doi:10.1179/003258910X12707304455022
- Volkova, S., Il'icheva, O. & Kuznetsov, O. (2011): X-ray study of the graphite-bearing rocks from the Pestpaksha ore occurrence and structural features of graphite. – *Lithol. Miner. Resour.*, 46 (4): 363-368. doi:10.1134/S0024490211040092
- von Ardenne, M. (1937): *Elektronenmikroskop oder Elektronen-Rastermikroskop*. vol 765083.
- Voordouw, R.J., Gutzmer, J. & Beukes, N.J. (2010): Zoning of platinum group mineral assemblages in the UG2 chromitite determined through in situ SEM-EDS-based image analysis. – *Miner. Deposita*, 45 (2): 147-159. doi:10.1007/s00126-009-0265-z
- Vuthaluru, H.B. & French, D. (2008): Ash chemistry and mineralogy of an Indonesian coal during combustion. Part 1 Drop-tube observations. – *Fuel Process. Tech.*, 89 (6): 595-607. doi:10.1016/j.fuproc.2007.12.002
- Walker, D.A., Paktunc, A.D. & Villeneuve, M.E. (1989): Automated image analysis applications: Characterisation of (1) platinum-group minerals and (2) heavy mineral separates. ICAM '89, International Workshop on Image Analysis Applied to Mineral and Earth Sciences, May 1989, Ottawa, Canada: 94-105.
- Wandler, A.V., Davis, T.L. & Singh, P.K. (2012): An Experimental and Modeling Study on the Response to Varying Pore Pressure and Reservoir Fluids in the Morrow A Sandstone. – *Int. J. Geophys.*, 2012: Article ID 726408. doi:10.1155/2012/726408
- Wang, E., Shi, F. & Manlapig, E. (2011): Pre-weakening of mineral ores by high voltage pulses. – *Miner. Eng.*, 24 (5): 455-462. doi:10.1016/j.mineng.2010.12.011
- Wang, E., Shi, F. & Manlapig, E. (2012): Mineral liberation by high voltage pulses and conventional comminution with same specific energy levels. – *Miner. Eng.*, 27-28: 28-36. doi:10.1016/j.mineng.2011.12.005
- Weißflog, C., Gutzmer, J. & Magnus, M. (2011): Preparation of a polished reference block for the identification of copper ores. 11th Society of Geology Applied to Mineral Deposits Biennial Meeting, Let's Talk Ore Deposits, 26-29 September 2011, Antofagasta, Chile: 965-966.
- Wen Qi, G., Parentich, A., Little, L.H. & Warren, L.J. (1992): Selective flotation of apatite from iron oxides. – *Int. J. Miner. Process.*, 34 (1-2): 83-102. doi:10.1016/0301-7516(92)90017-Q

- Wernicke, F. (1933): Magnetkiesparagenesen von sächsischen Lagerstätten. – *Z. Krist. Miner. Petrogr. Abt. B, Miner. petrogr. Mitt.*, 44 (6): 463-469. doi:10.1007/BF02939085
- Whateley, M.K.G. & Scott, B.C. (2006): Evaluation Techniques. In: Moon, C.J., Whateley, M.K.G., Evans, A.M. (eds): *Introduction to mineral exploration*. 2nd edn. Blackwell Publishing, Malden, MA, USA, 199-252.
- White, E.W., Görz, H., Johnson Jr, G.G. & McMillan, R.E. (1970): Particle size distributions of particulate aluminas from computer-processed SEM images. 3rd Annual Scanning Electron Microscope Symposium, April 28-30, 1970, IITRI, Chicago, Illinois, USA: 49-64.
- White, E.W., Mayberry, K. & Johnson Jr, G.G. (1972): Computer analysis of multi-channel SEM and X-ray images from fine particles. – *Pattern Recogn.*, 4 (2): 173-192, IN111,193. doi:10.1016/0031-3203(72)90027-1
- White, E.W., McKinstry, H.A. & Johnson Jr, G.G. (1968): Computer Processing of SEM Images. Scanning Electron Microscope Symposium, IITRI, Chicago, Illinois, USA: 95-103.
- Wigley, F., Williamson, J. & Gibb, W.H. (1997): The distribution of mineral matter in pulverised coal particles in relation to burnout behaviour. – *Fuel*, 76 (13): 1283-1288. doi:10.1016/S0016-2361(97)00139-7
- Wilde, A., Otto, A., Jory, J., MacRae, C., Pownceby, M., Wilson, N. & Torpy, A. (2013): Geology and Mineralogy of Uranium Deposits from Mount Isa, Australia: Implications for Albitite Uranium Deposit Models. – *Minerals*, 3 (3): 258-283. doi:10.3390/min3030258
- Williamson, B.J., Rollinson, G. & Pirrie, D. (2013): Automated mineralogical analysis of PM10: New parameters for assessing PM toxicity. – *Environ. Sci. Tech.*, 47 (11): 5570-5577. doi:10.1021/es305025e
- Wills, B.A. & Napier-Munn, T.J. (2011): *Wills' Mineral Processing Technology: An Introduction To The Practical Aspects Of Ore Treatment And Mineral Recovery*. 7th edn. 444 p., Oxford, UK (Butterworth-Heinemann).
- Wilton, D.H.C. & Winter, L. (2012): SEM–MLA (Scanning Electron Microscope – Mineral Liberation Analyzer) Research on Indicator Minerals in Till and Stream Sediments – An Example from the Exploration for Awaruite in Newfoundland and Labrador. In: Sylvester, P. (ed) *Short-Course Volume 42. Mineralogical Association of Canada (MAC)*, St. John's, NL, Canada, 265-283.
- Woolley, A.R., Bergman, S.C., Edgar, A.D., Le Bas, M.J., Mitchell, R.H., Rock, N.M.S. & Scott Smith, B.H. (1996): Classification of lamprophyres, lamproites, kimberlites, and the kalsilitic, melilitic, and leucitic rocks. – *Can. Mineral.*, 34 (2): 175-186.
- Worrell, E. & Reuter, M.A. (2014a): Chapter 1 - Recycling: A Key Factor for Resource Efficiency. In: Worrell, E., Reuter, M.A. (eds): *Handbook of Recycling*. Elsevier, Boston, 3-8. doi:10.1016/B978-0-12-396459-5.00001-5
- Worrell, E. & Reuter, M.A. (2014b): Chapter 2 - Definitions and Terminology. In: Worrell, E., Reuter, M.A. (eds): *Handbook of Recycling*. Elsevier, Boston, 9-16. doi:10.1016/B978-0-12-396459-5.00002-7
- Young, C., Dahlgren, E., Nordwick, S., Graham, J. & Lambson, R. (2012): Beneficiation Of Terrestrial Resources For The Production Of Lunar Simulant Separates. SME Annual Meeting, February 19-22, 2012, Seattle, WA, USA: 1-5.
- Young, R.J. (1993): Micro-machining using a focused ion beam. – *Vacuum*, 44 (3-4): 353-356. doi:10.1016/0042-207X(93)90182-A
- Yu, H., Marchek, J.E., Adair, N.L. & Harb, J.N. (1994): Characterization of minerals and coal/mineral associations in pulverized coal. Engineering Foundation Conference on the Impact of Ash Deposition on Coal Fired Plants, June 20-25, 1993, Solihull, UK: 361-372.
- Zamalloa, M., Utigard, T.A. & Lastra, R. (1995): Quantitative mineralogical characterization of roasted Ni-Cu concentrates. – *Can. Metall. Q.*, 34 (4): 293-301. doi:10.1016/0008-4433(95)00025-S
- Zemann, J. & Leutwein, F. (1974): Tellurium. In: Wedepohl, K.H. (ed) *Handbook of Geochemistry*, Vol. II/4. Springer-Verlag, Berlin-Heidelberg, Germany, 52-A-51 - 52-O-51.
- Zijp, M.H.A.A., Nelskamp, S., Schavemaker, Y.A., Ten Veen, J.H. & Ter Heege, J.H. (2013): Multidisciplinary approach for detailed characterization of shale gas reservoirs: A

Netherlands showcase. Offshore Technology Conference, OTC Brasil 2013 - From North to South: A Wealth of Opportunities, 29-31 October 2013, Rio de Janeiro, Brazil: 898-907.